University of Bath

UNIVERSITY OF
BATH

PHD

Intramolecular hydroamination of aminoalkenes with group 2 precatalysts: mechanistic insights and ligand design

Arrowsmith, Merle

Award date:
2011

Awarding institution:
University of Bath

[Link to publication](#)

Intramolecular hydroamination of aminoalkenes with group 2 precatalysts: mechanistic insights and ligand design.

Merle Arrowsmith

A thesis submitted for the degree of Doctor of Philosophy

University of Bath

Department of Chemistry

March 2011

List of publications resulting from this PhD

1. *Suppression of Schlenk Equilibration and Heavier Alkaline Earth Alkyl Catalysis: a Dearomatization Strategy.* (Chapter 4.2)

   Arrowsmith, M.; Hill, M. S.; Kociok-Köhn, G. *Organometallics;* Publication Date (Web): February 24, **2011**; DOI: 10.1021/om200028m.

2. *Cation Charge Density and Precatalyst Selection in Group 2-Catalyzed Aminoalkene Hydroamination.* (Chapter 2.2 - 2.4)

   Arrowsmith, M.; Crimmin, M. R.; Barrett, A. G. M.; Hill, M. S; Kociok-Köhn. G.; Procopiou, P. A., *Organometallics*; Publication Date (Web): February 23, **2011**; DOI: 10.1021/om101063m.

3. *Dearomatization and C-H Deprotonation with Heavier Group 2 Alkyls: Does Size Matter?* (Chapter 4.1)

   Arrowsmith, M.; Hill, M. S.; Kociok-Köhn, G. *Organometallics* **2010**, *29*, 4203-4206.

4. *Intramolecular Hydroamination of Aminoalkenes by Calcium and Magnesium Complexes: A Synthetic and Mechanistic Study.*

   Crimmin, M. R.; Arrowsmith, M.; Barrett, A. G. M.; Casely, I. J.; Hill, M. S.; Procopiou, P. A. *Journal of the American Chemical Society* **2009**, *131*, 9670-9685.

5. *Tris(imidazolin-2-ylidene-1-yl)borate Complexes of the Heavier Alkaline Earths: Synthesis and Structural Studies.* (Chapter 3.2)

   Arrowsmith, M.; Heath, A.; Hill, M. S.; Hitchcock, P. B.; Kociok-Köhn, G. *Organometallics* **2009**, *28*, 4550-4559.

6. *A Hydride-Rich Magnesium Cluster.*

   Arrowsmith, M.; Hill, M. S.; MacDougall, D. J.; Mahon, M. F. *Angewandte Chemie – International Edition* **2009**, *48*, 4013-4016.

7. *Bis(imidazolin-2-ylidene-1-yl)borate Complexes of the Heavier Alkaline Earths: Synthesis and Studies of Catalytic Hydroamination.* (Chapter 3.1)

   Arrowsmith, M.; Hill, M. S.; Kociok-Köhn, G. *Organometallics* **2009**, *28*, 1730-1738.

Table of contents

<u>Acknowledgements</u>

First of all I would like to thank my supervisor, Mike Hill, for the fantastic opportunity he gave me to do this PhD, for his enthusiasm and his inspiring love of research, and simply for being the best supervisor I could imagine.

I particularly would like to thank Gabriele Kociok-Köhn for her patient efforts in selecting crystals suitable for X-ray crystallography even from the most unlikely samples, and for many a nice chat in German while waiting for the results of cell unit checks. I am also indebted to John Lowe for teaching me the use of the 400 MHz NMR spectrometer for kinetics and variable temperature experiments.

A big thank you to the members of the Hill group over the last three years, in particular Dugald MacDougall for his help on many occasions (and his Scottish sense of humour) and Mark Crimmin for teaching me Schlenk technique; not to forget Steve Richards, Sarah Lomas, Ben Wickham, Tom Wildsmith, Tom Robinson, David Liptrot and Marina Hodgson who have made working in the lab such a pleasure, as well as the Molloy and Johnson groups for highly entertaining group meetings.

I am so grateful for my family supporting me all along and patiently listening to my ramblings about calcium catalysis, crystal structures and the like, especially my granddad, Opa Rolf, who passed away six months ago. Special thanks also go to my loving husband, Rory, with whom I had the privilege to share and discuss many ideas relating to this PhD.

I also want to thank the members of Station Hill Baptist Church in Chippenham, in particular my house group, the worship team, the pastoral care group, and my best friends, Kathinka and Claire, for their continued prayerful, practical and loving support and for the wonderful family they've been to me for the past three years.

Finally, this research is dedicated to my Saviour and Lord, Jesus Christ, for the amazing intricacies of His creation which He has given me a glimpse of through my research. To Him be all the Glory!

Declaration

The work described in this thesis was conducted by the author at the University of Bath between October 2007 and November 2010. It represents the author's original and independent work, except where specific reference is made to the contrary. Neither the whole nor any part of this thesis has been submitted previously in support of a degree at any other university. It does not exceed the prescribed limit, including tables, references and appendices.

Abstract

Long relegated to the background by the pre-eminence of magnesium-based, stoichiometric Grignard reagents, a distinct chemistry of the heavier alkaline earth metals, calcium, strontium and barium, is only now starting to emerge. As similarities have been drawn between the large, electropositive, redox-inert and d^0 alkaline earth Ae^{2+} dications and the Ln^{3+} cations of the lanthanide series, a growing group 2-mediated catalytic chemistry has developed over the last decade, including polymerisation reactions, heterofunctionalisation reactions of multiple bonds and some rare examples of dehydrocoupling reactions. Among these catalytic reactions the magnesium- and calcium-catalysed intramolecular hydroamination of aminoalkenes has attracted particular interest. Mechanistic studies have demonstrated many parallels with the lanthanide-mediated catalytic cycle based upon successive σ-bond metathesis and insertion steps.

In the first part of this thesis, further investigations into the hydroamination/cyclisation reaction have demonstrated the prominent role of the charge density of the catalytic group 2 cation (M = Mg, Ca, Sr, Ba), the beneficial influence of stabilising spectator ligands, and the importance of the choice of the reactive co-ligand for efficient catalyst initiation. Kinetic analyses of reactions monitored by NMR spectroscopy have given new insight into activation energies, entropic effects, substrate and product inhibition, and kinetic isotope effects, leading to a review of the previously suggested lanthanide-mimetic mechanism.

In a second part, this study seeks to address two of the main challenges posed by the intramolecular hydroamination reaction in particular, and heavier alkaline earth-catalysed reactions in general:

(i)   The need to design new monoanionic spectator ligands capable of stabilising heteroleptic heavier alkaline earth complexes and preventing deleterious Schlenk-type ligand redistribution processes in solution;

(ii) The stabilisation of highly reactive heteroleptic group 2 alkyl functionalities for fast, irreversible catalyst initiation and novel reactivity.

Abbreviations

9-BBN = 9-borabicyclo[3.3.1]nonane
[18]crown-6 = 1,4,7,10,13,16-hexaoxacyclooctadecane
A$^-$ = anion
Ad = adamantyl
Ae = alkaline earth metal
Anal. Calc. = calculated elemental analysis data
Ar = aromatic hydrocarbon substituent
ATI = aminotroponiminate
avg. = average
BIAN = bis(imino)acenaphthene
BINOL = 1,1'-binaphthyl-2,2'-diol
Bn = benzyl
Boc = *tert*-butyloxycarbonyl
Box = bis(oxazoline)
b.p. = boiling point
br. = broad
Bu = butyl
cat = catalyst
CL = caprolactone
COD = 1,5-cyclooctadiene
COSY = correlation spectroscopy
Cp = cyclopentadienyl
Cp* = 1,2,3,4,5-pentamethylcyclopentadienyl
Cp'' = 2,3,4,5-tetramethylcyclopentadienyl
CSI-MS = cold-spray ionisation mass spectrometry
Cy = cyclohexyl
DAB = 1,4-diaza-1,3-butadiene
DFT = density functional theory
dipp = 2,6-di-*iso*-propylphenyl
DME = dimethyl ether
DMF = dimethylformamide
ee = enantiomeric excess
eq. = equivalents
ESI-MS = electrospray ionisation mass spectrometry
Et = ethyl
hex = hexane
HMBC = heteronuclear multiple bond coherence
HMPA = hexamethylphosphoramide
HMQC = heteronuclear multiple quantum coherence
IAN = isoquinoline 2-aminonaphthalene
Im = imidazole

ⁱPr = *iso*-propyl

IR = infrared

KIE = kinetic isotope effect

L = monoanionic spectator ligand

LA = lactide

Ln = lanthanide

M = metal centre / molar

MAO = methylalumoxane

Me = methyl

Mes = mesityl = 2,4,6-trimethylphenyl

MMA = methyl methacrylate

MO = molecular orbital

m.p. = melting point

NBO = natural bond orbital

NHC = N-heterocyclic carbene

NMR = nuclear magnetic resonance

ORTEP = Oak Ridge Thermal Ellipsoid Plot

PDI = polydispersity index

Ph = phenyl

PLA = poly(lactide)

PMMA = poly(methyl methacrylate)

ppm = parts *per* million

PTFE = poly(tetrafluoroethylene)

PyBox = pyridine-2,6-bis(oxazoline)

pyr = pyridine

pz = pyrazolyl

R = alkyl or aryl substituent

RNA = ribonucleic acid

rt = room temperature

S = solvent

sub = substrate

T = temperature

^tBu = *tert*-butyl

Tf = triflate

THF = tetrahydrofuran

TMSS = tetrakis(trimethylsilyl)silane

tol = toluene

Tp = tris(pyrazolyl)

TS = transition state

X = σ-bonded monoanionic substituent or halide

Y = σ-bonded monoanionic substituent

1   Introduction

1.1   Background

More than a century after Grignard's seminal work on his eponymous reagents, which won him the Nobel Prize in 1912,[1] the organometallic chemistry of the alkaline earth metals is still largely dominated by stoichiometric organomagnesium reagents.[2] Despite early efforts to obtain the analogous heavier alkaline earth alkyl or aryl halides,[3] the extremely air- and moisture-sensitive nature of these thermally unstable compounds long prevented the development of a related calcium, strontium or barium chemistry. It is therefore remarkable that Westerhausen and co-workers recently succeeded in isolating and structurally characterising a whole series of calcium aryl halides despite their tendency to decompose through ether cleavage even at temperatures below -35 $^{\circ}$C.[4, 5] Although more reactive calcium alkyl halide analogues, as well as related strontium and barium aryl halides, have yet to be structurally characterised, the heavier alkaline earth metals, and especially calcium, have been freed from their limitations as "heavy Grignard reagents" by the emergence, over the last decade, of a rapidly expanding catalytic group 2 chemistry.

Upon descending the group, the divalent alkaline earth cations display a striking 88% increase in ionic radius from magnesium to barium (six-coordinate radii: Mg^{2+}, 0.72 Å; Ca^{2+}, 1.00 Å; Sr^{2+}, 1.18 Å; Ba^{2+}, 1.35 Å)[6] accompanied by a marked decrease in electronegativity.[7] As a result metal-ligand bonding becomes increasingly ionic and non-directional. Furthermore, with the exception of a handful of outstanding, recent examples of subvalent Mg(I) and Ca(I) compounds displaying metal-metal bonds stabilised by either bulky ligands or extended π-systems,[8] the vast majority of complexes of the alkaline earth metals are redox inactive and found in their 2+ oxidation state, thus achieving a d^0 electronic configuration. Consequently comparisons have often been made with the properties of lanthanide cations which are generally found in their principal 3+ oxidation state. Similarly to the alkaline earth metals, Ln^{3+} complexes are characterised by their d^0 configuration, redox inactivity and ionic metal-ligand bonding resulting from high electropositivity and little polarisability.[9] Moreover, the f-orbitals, which remain shielded by the $5s^2 5p^6$ outer shell electrons, do not intervene in complex formation. Parallels have also been drawn between the size of the

Ca^{2+} dication and the ionic radii of the largest lanthanide cations (six-coordinate radii: La^{3+}, 1.03 Å; Nd^{3+}, 0.98 Å; Sm^{3+}, 0.96 Å).[6] Both lanthanide and alkaline earth metal cations interact preferentially with hard ligands and exhibit strong oxophilic character. As a consequence the same problems initially encountered with the synthesis of lanthanide complexes also apply to heavier group 2 compounds; for example, simple homoleptic species commonly display low solubility in organic solvents, and kinetic instability must be countered by the use of sterically demanding anionic ligands.

These structurally-based analogies have naturally led to the proposal of similar reactivity for lanthanide and alkaline earth complexes. Since the 1980s lanthanide complexes of the form L$_2$LnX (L = monoanionic spectator ligand, e.g. cyclopentadienyl; X = monoanionic substituent, e.g. alkyl, amide, phosphide, hydride, etc.) have been widely used in a variety of catalytic transformations based on two simple mechanistic pathways: (a) the σ-bond metathesis or protonolysis of the monoanionic substituent X and (b) the insertion of unsaturated bonds into the Ln-X σ-bond (Scheme 1).[10]

Scheme 1. Stoichiometric reactivity of lanthanide complexes: (a) σ-bond metathesis and (b) insertion.
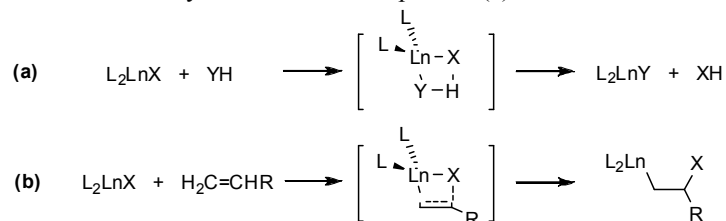
Incorporated into catalytic cycles, these two reactions pathways have enabled a vast number of synthetic reactions ranging from the inter- and intramolecular heterofunctionalisation of carbon-carbon multiple bonds (hydroamination, hydrophosphination, hydroalkoxylation, hydrosilylation, hydroboration, etc.) to the polymerisation of alkenes.[11] A general catalytic cycle for these lanthanide-mediated reactions is presented in Figure 1. Activation of the precatalyst occurs through either reversible or irreversible σ-bond metathesis, followed by the rate-determining insertion of the unsaturated bond which proceeds *via* a four-membered cyclic transition state. The resulting, highly reactive lanthanide alkyl species is then protonated to liberate the functionalised product and regenerate the active catalyst. Highly encumbered ligands are of importance for the kinetic stabilisation of the active species in order to avoid ligand redistribution towards unreactive homoleptic complexes or dimerisation, both leading to a decrease in reactivity. Highly substituted and *ansa*-bridged

cyclopentadienyl ligands have proved spectator ligands of choice for many of these transformations.[12] In recent years, the focus has shifted towards a wide variety of sterically demanding, chiral non-cyclopentadienyl ligands for stereoselective catalysis.[13] Reduced access to the metal centre as a consequence of steric hindrance of the ligand, however, may cause a decrease in reactivity by impeding the insertion step, especially if the unsaturated bond is highly substituted. Catalytic activity is also generally inhibited by the presence of Lewis donor solvents, such as THF, which may block potential coordination sites for substrate access or, if product and substrate present a similar pK_a, lead to competitive product coordination and/or reversible protonolysis.

Figure 1. General catalytic cycle for the lanthanide-mediated heterofunctionalisation of carbon-carbon double bonds.
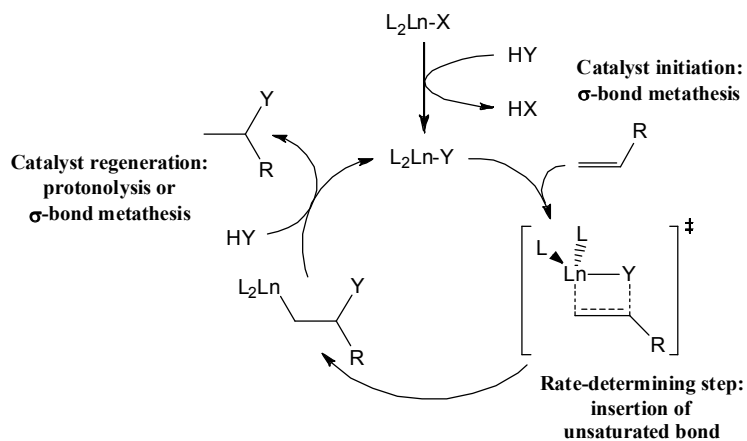
Owing to the similarities between lanthanide (III) and heavier group 2 complexes, the latter have long been treated as merely "lanthanide mimetic". Indeed the last decade has shown that group 2 complexes of the form LAeX (L = monoanionic spectator ligand, e.g. β-diketiminate; X = amide, alkyl, phosphide, oxide, hydride, etc.) undergo σ-bond metathesis and insertion reactions identical to those of lanthanide species, and these have been successfully incorporated into an ever wider range of catalytic processes, often analogous to those encountered in lanthanide chemistry (Figure 2).[14]

Figure 2. Proposed catalytic cycle for the alkaline earth-mediated heterofunctionalisation of carbon-carbon double bonds.
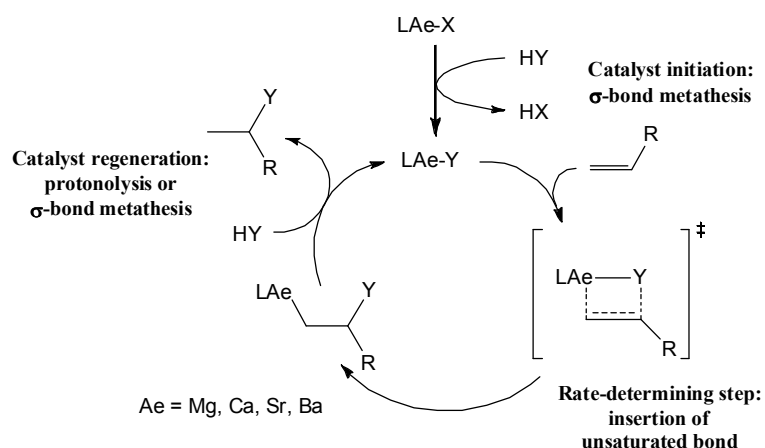
Calcium and its heavier group 2 congeners are also finding a unique place in organometallic chemistry due to a number of important factors differentiating them from their lanthanide counterparts. The 88% increase in size down the group from Mg^{2+} to Ba^{2+} contrasts markedly with the 17% range of the lanthanide contraction from La^{3+} to Lu^{3+}. Similarly, Pauling electronegativity decreases by 35% from magnesium to barium, whereas only a 15% increase is observed from lanthanum to lutetium. While the larger Ae^{2+} dications display higher polarisability, their increasingly diffuse charge induces a decrease in their polarising capacity. As a consequence, despite the many parallels that can be drawn especially between magnesium or calcium and the lanthanide systems, a much wider scope of largely unexploited reactivity might be expected from complexes of the heavier alkaline earth metals. Furthermore, from an economical and sustainability point of view, the availability of calcium as the fifth most abundant element in the earth's crust (4.15 weight %)[15] and the relative abundance of the other alkaline earth metals compared with the rare earth metals make research into this nascent area of chemistry even more desirable. This is best illustrated by the cost comparison of alkaline earth versus lanthanide starting materials in Figure 3. Finally, with the increasing interest in the production of biocompatible polymers for medicinal applications, the use of perfectly biocompatible calcium or magnesium polymerisation precatalysts might solve the problem of having to remove potentially toxic trace metals from these materials.

Figure 3. Comparison between the cost of alkaline earth and rare earth starting materials.[16]
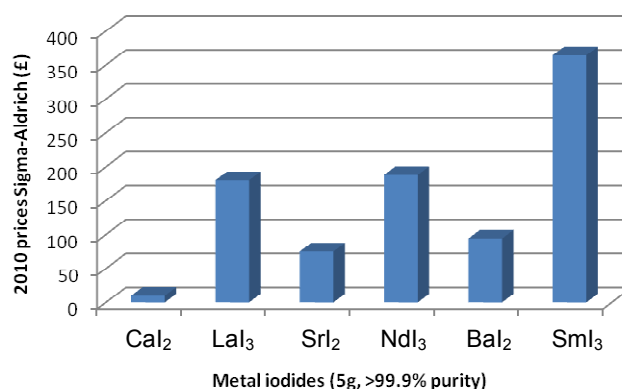
This introduction aims to provide an overview of the whole extent of heavier alkaline earth-mediated catalysis (M = Mg, Ca, Sr, Ba), including polymerisation reactions, heterofunctionalisation of multiple bonds and σ-bond coupling reactions with well-defined homoleptic and heteroleptic group 2 precatalysts. Key stoichiometric σ-bond metathesis and insertion reactions will be examined in parallel to provide useful mechanistic insight into the catalytic processes. Recent and related advances in organic asymmetric Lewis acid-catalysed carbon-carbon bond formation relying on chiral alkaline earth alkoxides formed *in situ* will also be discussed briefly.

1.2 Catalysis with group 2 complexes

Whereas heterogeneous alkaline earth oxide and alkoxide catalysts have been studied for a few decades and have found various industrial applications, often in combination with other metals (Li, Al, etc.),[17] homogeneous catalysis with group 2 complexes is still in its infancy. Whether based on homoleptic precatalysts of the form AeX_2 (X = NR_2, OR, R) or on heteroleptic compounds of the form LAeX (X = NR_2, OR, R, H) where L is a sterically demanding, monoanionic, generally polydentate spectator ligand, these catalytic transformations can be broken down into a series of σ-bond metathesis (or protonolysis) and insertion steps.

1.2.1 The Schlenk equilibrium: a problem for well-defined single-site catalysis.

As homoleptic alkaline earth compounds of the form AeX_2 may often be polymeric or insoluble in hydrocarbon solvents research has focused on designing sterically demanding, lipophilic, monoanionic ligands to stabilise and solubilise group 2 amide, alkoxide, alkyl or hydride functionalities in heteroleptic complexes of the form LAeX. Due to the weakening of the metal-ligand bonds down the group, however, the larger alkaline earth metal centres present an increasing problem of ligand exchange equilibria. Similarly to the dynamic behaviour of RMgX Grignard reagents exemplified in the Schlenk equilibrium, heteroleptic LAeX complexes tend to irreversibly redistribute towards the kinetically stabilised homoleptic AeL_2 and AeX_2 species (Scheme 2). While the former are catalytically inactive, the latter, although potentially reactive, are often insoluble or may cause a dramatic change in catalytic activity and selectivity. Such Schlenk-type equilibria are especially problematic when dealing with LAeX complexes for potentially enantioselective catalysis, where L is a chiral spectator ligand.[18] In most cases, while the heteroleptic magnesium and calcium analogues can be readily isolated in good purity and show no or little ligand lability in solution up to high temperatures, the related strontium and barium complexes, if isolable, are usually found in solution equilibrium with the homoleptic species, even at room temperature.[19] Another common problem is the dimerisation of heteroleptic species bearing small monoanionic co-ligands, which may impede catalytic reactions by blocking vacant coordination sites.

Scheme 2. Schlenk-type ligand redistribution equilibria for alkaline earth β-diketiminate amide complexes.
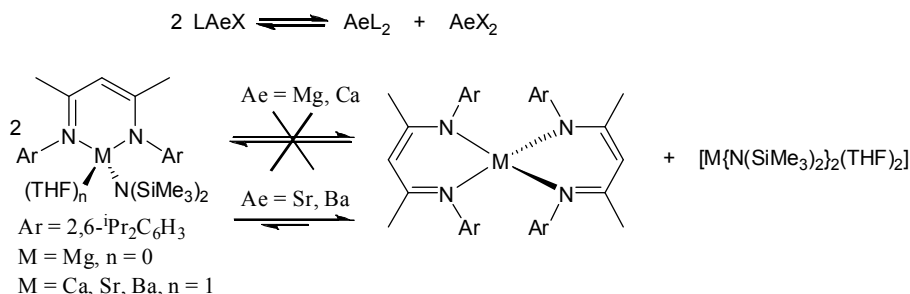
While early research focused on sterically hindering cyclopentadienyl ligands to overcome this problem, the resulting half-sandwich calcium amide, acetylide, halide or borohydride complexes, although heteroleptic in the solid state, often remained prone to Schlenk-type ligand redistribution in solution, and thus exhibited limited use as

precatalysts.[20] As the synthesis of heteroleptic strontium or barium metallocenes proved rather elusive, more recent attention has shifted towards monoanionic non-cyclopentadienyl ligands bearing bulky substituents which may be easily tuned for steric, electronic, and potentially chiral effects. A landmark in this area was the isolation in 2004 by Chisholm and co-workers of the heteroleptic calcium β-diketiminate and tris(pyrazolyl)borate complexes **2**, **3** and **4** and their application to the ring-opening polymerisation of lactides (Figure 4).[21] Since then the β-diketiminate ligand has been successfully employed to stabilise a wide variety of heteroleptic magnesium, calcium and strontium complexes bearing even small functionalities (F, OH, NH_2, CN, H, etc.).[22] It is therefore not surprising that heteroleptic amide and hydride complexes based on this particular ligand have so far been used in the majority of alkaline earth-catalysed reactions, together with heteroleptic tris(pyrazolyl)borate, aminotroponiminate and triazenide group 2 amide complexes, as well as fluorenyl-supported benzyl complexes (Figure 4).

Figure 4. Examples of heteroleptic alkaline earth precatalysts.

1 M = Mg, X = Me, n = 0
2 M = Ca, X = N(SiMe_3)_2, n = 1

3 X = N(SiMe_3)_2,
4 X = O-2,6^iPr_2C_6H_3

5 M = Ca
6 M = Sr

8a-d R = CMe_3, CMe_2Ph, CMePh_2,
C(Me)(4-^tBuC_6H_4)_2

7
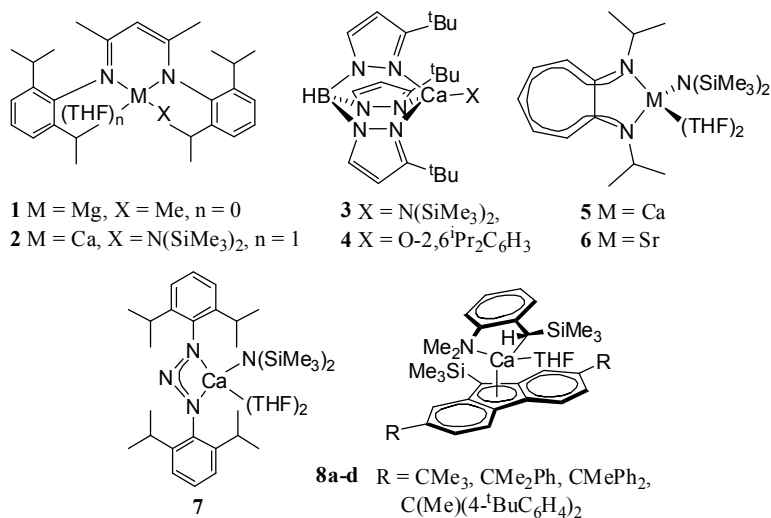
1.2.2 Polymerisation

Polymerisation of polar monomers

The catalytic synthesis of polymers with either mechanical or medicinal applications, such as poly(methyl methacrylate) (PMMA) or poly(lactide) (PLA), requires the catalyst to be either entirely removable from the finished product or, if this is not the

case, at least non-coloured or biocompatible. Biocompatible magnesium and calcium catalysts are therefore highly desirable for these transformations. The earliest polymerisation studies with homogeneous alkaline earth catalysts date back as far as the early 1970s. In 1974, Lindsell and co-workers reported the highly syndiotactic polymerisation of MMA with bis(cyclopentadienyl) calcium precatalysts, albeit in very poor yield (8%).[23] Although attempts by M. S. Chisholm's group to reproduce the tacticity reported in this early study failed, they introduced the use of more soluble [(Cp*)$_2$Ca(THF)$_2$] precatalysts to obtain high yields of essentially atactic PMMA.[24] Later studies by Schumann with similar homoleptic and heteroleptic Mg, Ca, Sr and Ba precatalysts allowed fast and near quantitative polymerisation of functionalised methacrylate monomers and the formation of block-copolymers.[25] More recently, the use of heteroleptic β-diketiminato magnesium enolate dimer **9** by Dove *et al.* (Scheme 3) provided fast, living and highly syndioselective polymerisation of PMMA (*rr* = 96%).[26]

Scheme 3. Syndioselective polymerisation of MMA.
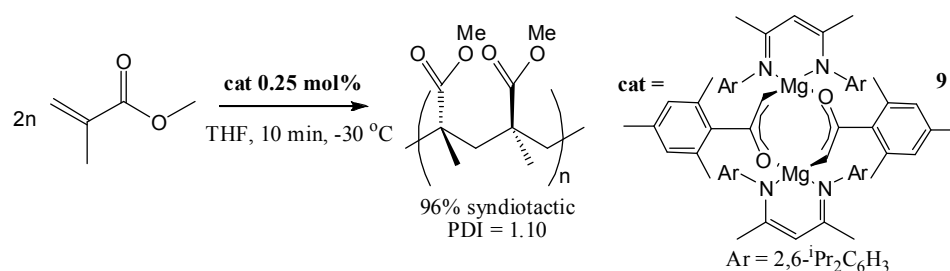
Until recently the most efficient catalysts for the polymerisation of cyclic esters such as lactide (LA), ε-caprolactone (ε-CL) and trimethylene carbonate (TMC) were based upon zinc, as well as other transition and main group metals. Over the last decade, however, research has turned increasingly and with great success towards biocompatible alkaline earth-based catalysts for these polymerisation reactions. As early as 1996, CaH$_2$ was reported to promote the copolymerisation of L-LA and poly(ethylene glycol).[27] Calcium and magnesium acetylacetonate complexes, as well as dibutylmagnesium were also used to catalyse the ring-opening copolymerisation of both L-LA and ε-CL with glycolide.[28] The resulting polymers were found to be entirely compatible with brain tissue. In 2001 Feijin and Westerhausen investigated the potential of commercially available [Ca(OMe)$_2$] as well as alkoxide species generated *in situ* from more soluble [Ca{N(SiMe$_3$)$_2$}$_2$(THF)$_2$], showing the latter to be efficient precatalysts for the living polymerisation of both ε-CL and L-LA, without racemisation.[29] The resulting polymers

displayed narrow polydispersities, enabling the formation of block-copolymers. Since then a growing number of heteroleptic monomeric, dimeric and even trimeric calcium amide, alkoxide and magnesium alkyl species, as well as several group 2 complexes bearing bis(phenolate) ligands have been tested for the polymerisation and copolymerisation of L-LA and ε-CL, as shown in Scheme 4.[30] To date only one example of barium-catalysed ring-opening polymerisation of L-LA and ε-CL has been reported.[31] For the polymerisation of TMC and its copolymerisation with L-LA, Darensbourg studied the use of tridentate and tetradentate Schiff base derivatives of calcium and magnesium such as **11**.[32]

Scheme 4. Polymerisation of L-lactide and ε-caprolactone with examples of group 2 precatalysts.

Stereocontrolled polymerisation of *rac*-lactide was first achieved by Chisholm and co-workers using the tris(pyrazolyl)borate calcium amide and phenoxide complexes **3** and **4**.[21] Conversions > 90% with a heterotacticity of 90% were obtained in less than one minute in THF at room temperature, in the presence of 0.5 mol% of **4** (Scheme 5). According to Chisholm *et al.* this was "probably the most reactive and stereoselective catalyst reported to date." Similarly high heteroselectivity could be obtained with a *β*-diketiminato magnesium methoxide catalyst.[33]

Scheme 5. Stereoselective polymerisation of *rac*-lactide with calcium tris(pyrazolyl)borate complex **4**.

The Union Carbide catalyst [(NH$_2$)Ca(O^{i}Pr)] has also been shown to promote the ring-opening polymerisation of propylene oxide, while 3-(S)-iso-propylmorpholine-2,5-dione may be polymerised with CaH$_2$ in the presence of poly(ethylene oxide).[34] Although several attempts to design bimetallic calcium and magnesium catalysts for the copolymerisation of cyclohexene oxide and CO$_2$ have been described, the only successful system was reported by Xiao et al. whose bimetallic magnesium complex, **14**, proved efficient for this reaction, even at CO$_2$ pressures as low as 1 bar (Scheme 6).[35]

Scheme 6. Copolymerisation of cyclohexene oxide and CO$_2$ with a bimetallic magnesium catalyst, **14**.
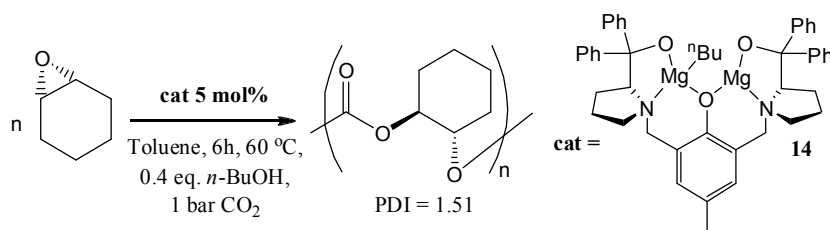
In all the above-mentioned studies catalyst activities were shown to be dependent on the metal centre used, with turnover frequencies always in the order of Ca > Mg > Zn when analogues of all three metals were compared.[36] In general, reactions are living, first-order in monomer, and do not exhibit any induction period. Catalyst activation is usually achieved by σ-bond metathesis (protonolysis) of a group 2 amide or alkyl precursor with an alcohol, phenol or enolisable ketone (Scheme 7). This first step is well documented in the literature.[26, 37-39]

Scheme 7. Examples of catalyst activation through σ-bond metathesis of a magnesium alkyl and a calcium amide precursor with an enolisable ketone and a phenol respectively.[26]
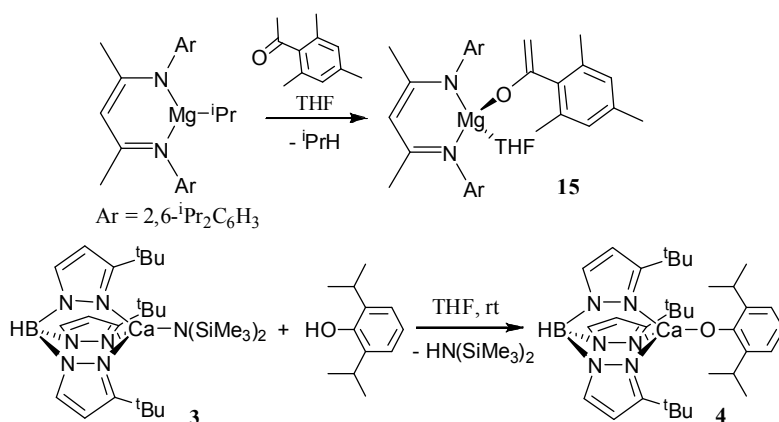
Subsequent propagation proceeds *via* multiple insertion steps of the ester function of the substrate into the metal-alkoxide bond of the active catalyst. In support of this

mechanism, Mingos and co-workers already reported in the 1990s the stoichiometric insertion of carbonyl sulphide and carbon dioxide into the M-O bonds of alkaline earth bis(alkoxide) species.[40] More recent attempts by Harder and Roesky to insert carbon dioxide into the Ca-O bond of heteroleptic calcium hydroxide dimer **16** resulted in the irreversible protonation of the β-diketiminate ligand accompanied by slow precipitation of calcium carbonate according to the reaction pathway proposed in Scheme 8.[38]

Scheme 8. Insertion of CO_2 into a Ca-O bond, followed by decomposition into $[Ca(CO_3)_2]$.

$Ar = 2,6\text{-}^iPr_2C_6H_3$ **16**
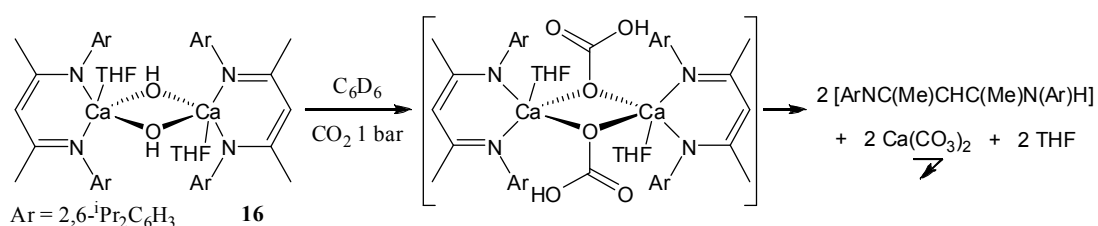
Polymerisation of styrene

The polymerisation of alkenes by large group 2 metal centres requires conjugation of the alkene monomer. In 2000 Weeber *et al.* reported the first dibenzylbarium catalyst for the polymerisation of styrene.[41] The reaction, however, was neither living nor stereoselective, and presented a slow initiation as well as high ligand lability of the catalyst, as result of the highly diffuse charge density of the large Ba^{2+} centre. Efforts by Harder and co-workers thereafter focused on more readily manipulated calcium initiators based on the chiral bidentate (2-NMe$_2$-α-Me$_3$Si-benzyl) ligand, such as complex **17** (Scheme 9).[42]

Scheme 9. Synthesis of heteroleptic benzylcalcium initiators by σ-bond metathesis for the stereoselective polymerisation of styrene.

8a-d R = CMe$_3$, CMe$_2$Ph, CMePh$_2$, C(Me)(4-^{t}BuC$_6$H$_4$)$_2$
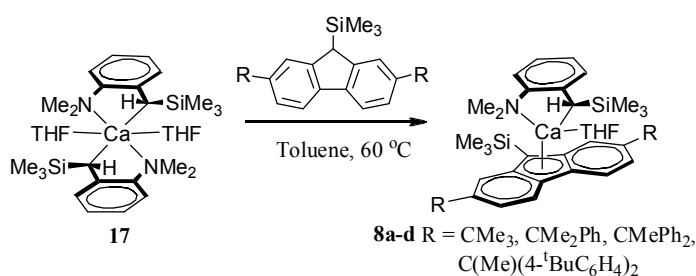
Although very active for the living anionic polymerisation reaction, the homoleptic, diastereomeric precatalyst **17** produced largely atactic polystyrene due to racemisation in solution. The heteroleptic versions **8a-d** obtained by σ-bond metathesis between **17** and a number of heavily substituted fluorenes (Scheme 9), however, allowed the production of polymers with up to 94% syndiotacticity in dyads from neat styrene at 20 °C (Scheme 10).[43] Stereoselectivity was found to increase with the steric bulk of the fluorenyl substituents.

Scheme 10. Syndioselective polymerisation of styrene.
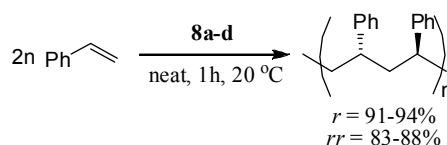
In all cases, broad molecular weight distributions, arising from slow catalyst initiation, prevented the synthesis of block-copolymers. The reaction mechanism is thought to involve pre-coordination of the alkene, as the presence of coordinated THF deactivates the precatalyst. Following slow catalyst initiation by σ-bond metathesis of the alkene with the benzyl ligand, propagation proceeds *via* multiple insertions of styrene into the metal-alkyl bond. In relation to this, Harder and co-workers have shown that the reaction of $[Ba(CH_2Ph)_2(THF)_2]$ with 1,1-diphenylethene yields quantitative insertion of the alkene into the Ba-C bonds to form $[Ba\{C(Ph)_2CH_2CH_2Ph\}_2(THF)_2]$ which was characterised by ^1H NMR spectroscopy (Scheme 11).[41]

Scheme 11. Insertion of 1,1-diphenylethene into a barium-benzyl bond.
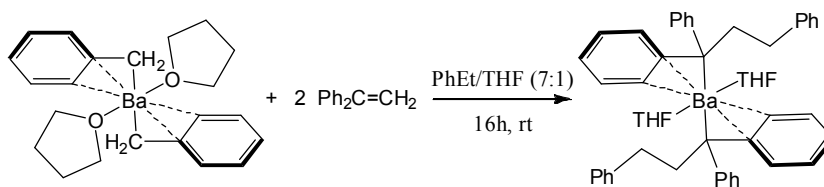
Oligomerisation reactions

A small number of oligomerisation reactions mediated by heavier group 2 complexes has been reported. In 2007 Hill and co-workers showed that the dimerisation of a variety of aldehydes into esters, also known as Tishchenko reaction, could be catalysed

by the simple homoleptic alkaline earth bis(bis(trimethylsilylamide)) complexes (Figure 5).[44] Catalyst activities were in the order of Ca > Sr > Ba. Given that the reaction involves the formal reduction of one aldehyde molecule and the oxidation of another, and that group 2 Ae^{2+} cations are redox inactive, the catalytic process necessarily involves a hydride transfer between aldehydes. Quenching of the catalytic reaction with benzaldehyde in the early stages showed that catalyst initiation generates a calcium alkoxide intermediate with liberation of a benzamide through a Meerwein-Ponndorf-Verley-type reduction of the aldehyde. This is followed by insertion of the second aldehyde equivalent into the metal-alkoxide bond and hydride transfer to another equivalent of coordinated aldehyde to regenerate the catalyst and liberate the ester. Preliminary results showed the reaction could also be applied to the polymerisation of dialdehydes into polyesters.

Figure 5. Tishchenko reaction with homoleptic group 2 amides and proposed mechanism.
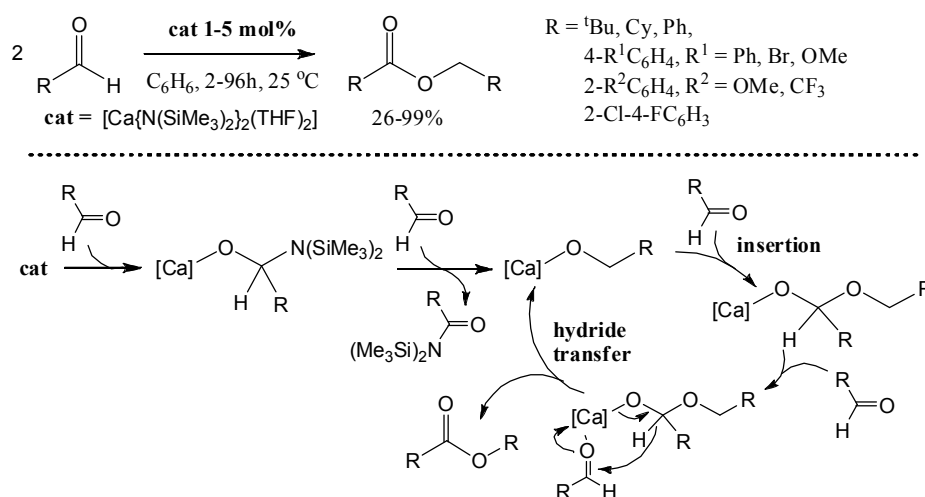
Harder and co-workers showed that the catalytic trimerisation of phenyl- and cyclohexyl isocyanate can be achieved with calcium methandiide complex **18** at room temperature (Scheme 12).[45] Thanks to the very slow reaction rate of the cyclohexyl substrate, the double insertion intermediate **19**, which also proved active as a catalyst, could be isolated and crystallographically characterised.

Scheme 12. Trimerisation of isocyanates.
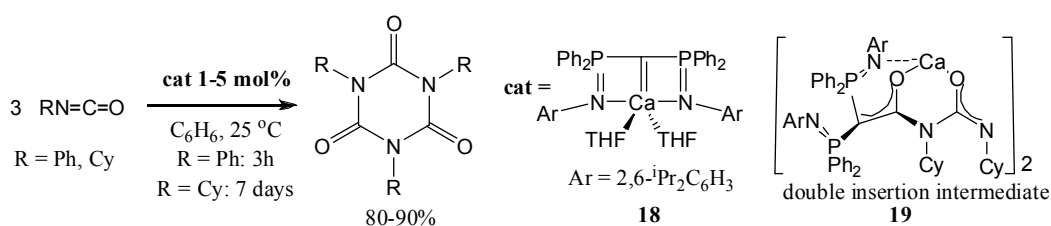
More recently Hill and co-workers reported the unexpected catalytic dimerisation of 3-methoxypropyne into the 2,3,4-hexatriene [MeOCH$_2$CH=C=C=CHCH$_2$OMe] in the presence of heteroleptic calcium β-diketiminate and triazenide complexes **2** and **7** (Scheme 13).[46] Since the dimerisation of terminal alkynes with transition metal and lanthanide catalysts most often results in the formation of the more stable enyne products,[47] the exclusive production of the substituted hexatriene in this case is quite remarkable.

Scheme 13. Dimerisation of 3-methoxypropyne and proposed acetylide-butatriene diyl equilibrium.
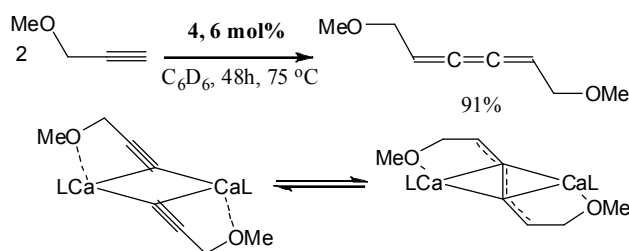
Catalyst initiation *via* σ-bond metathesis between the terminal alkyne and the alkaline earth amide precursor has been well documented in numerous stoichiometric reactions yielding both homoleptic and heteroleptic group 2 acetylides (Scheme 14).[48, 49] The reaction is then thought to proceed *via* a dimeric μ-(Z)-butatriene diyl bridging unit as has been shown to exist with group 3 and 4f elements.[50] Carbon-carbon bond formation is further driven by the asymmetric bridging mode and coordination of the ether moiety to the highly electropositive calcium centres, which reduces charge repulsion between the terminal acetylide carbons (Scheme 13).

Scheme 14. Synthesis of homoleptic and heteroleptic group 2 acetylides by σ-bond metathesis.

$$[M\{N(SiMe_3)_2\}_2(THF)_2] \ + \ 2 \quad RC\equiv CH \xrightarrow[- \ 2 \ HN(SiMe_3)_2]{\substack{[18]crown\text{-}6, \\ THF, \ -80 \ ^oC}} RC\equiv\!\!-\!\!\cdots M \cdots\!\!-\!\!\equiv CR$$

M = Ca, Sr, Ba
R = SiPh$_3$

Ar = 2,6-^{i}Pr$_2$C$_6$H$_3$
R = ^{n}Bu, ^{t}Bu, 4-MeC$_6$H$_4$, Ph
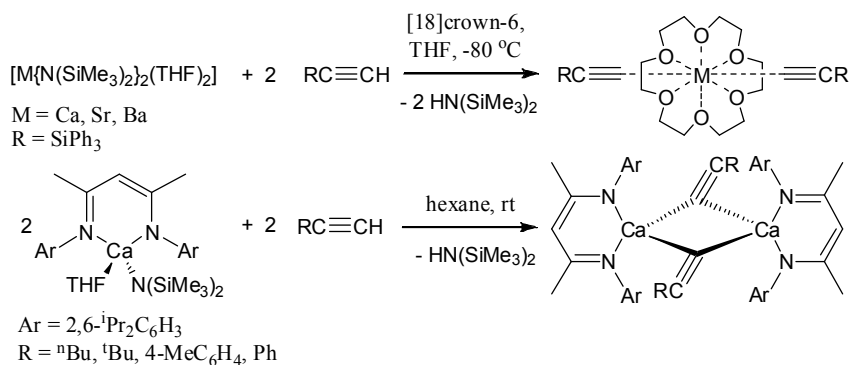
1.2.3 Heterofunctionalisation of unsaturated bonds

Intra- and intermolecular hydroamination of unsaturated bonds

Achiral and chiral lanthanide complexes, pioneered by Marks and co-workers in the early 1990s, are among the most efficient catalysts for the intramolecular hydroamination/cyclisation of aminoalkenes, -alkynes, -dienes and -allenes.[51] In 2005 Crimmin *et al.* published the first report of the calcium-mediated intramolecular hydroamination of a number of aminoalkenes, based on Chisholm's β-diketiminato calcium amide complex **2**. Catalytic activity proved to be comparable to the best of the conventional group 3 and lanthanide systems.[52] Reactions proceeded at high rates under mild conditions (25-60 ^{o}C) with moderate catalyst loadings (10-20 mol%) and produced substituted pyrrolidines and piperidines in high yields without apparent ligand redistribution to the homoleptic calcium species. Later, a study on an extensive range of aminoalkene substrates showed that the ease of cyclisation decreases with ring-size, following Baldwin's guidelines for ring-closure (Scheme 15). While pyrrolidines could be obtained at room temperature and with low catalyst loadings (2-10 mol%) in near quantitative yields within a few minutes, the formation of piperidines and hexahydroazepines required longer periods of time (up to 5.5 days), higher catalyst loadings (10-20 mol%) and sometimes prolonged heating at 80 ^{o}C. Bulky geminal substituents in the β-position of the amine facilitated cyclisation by favouring reactive conformations of the insertion transition state (Thorpe-Ingold effect), while internal substitution of the alkene moiety significantly hindered the reaction. None of the β-diketiminate precatalysts could achieve the hydroamination of substrates with internal

alkenes under the reported reaction conditions. Whereas prochirality in the β-position of the amine did not lead to diastereoselectivity, the α-substituted aminoalkenes 1-amino-1-methyl-4-pentene and 1-amino-1-phenyl-4-pentene underwent diastereoselective hydroamination favouring the *trans*-geometry of the pyrrolidine with a diastereomeric excess of 78% for calcium precatalyst **2**. The smaller magnesium metal centre of precatalyst **1** afforded significantly higher selectivity (84% diastereomeric excess). Similar preference for the *trans*-conformation of the product had already been observed in the case of analogous lanthanide-catalysed hydroamination, with smaller Ln^{3+} centres affording increased diastereoselectivity, induced by a tighter conformation of the transition state.[53] Although significantly more active than its magnesium counterpart **1**, the use of calcium complex **2** was limited by its propensity to deleterious Schlenk-like ligand redistribution equilibria at high temperature, alkene isomerisation side reactions of 1-amino-5-hexene substrates, and its incapacity to cyclise 1-amino-2,2-diphenyl-6-heptene into the resulting hexahydroazepine. In contrast, this latter reaction could be achieved with magnesium precatalyst **1**, albeit very slowly and at high temperature (5.5 days, 80 ºC, 88% yield).[54]

Scheme 15. Intramolecular hydroamination of aminoalkenes with heteroleptic Mg and Ca precatalysts.

R^1, R^2 = H, Me, Ph, -(C_6H_{10})-
R^1 = allyl, R^2 = Me
R^3 = H, Me; R^4 = H, Me; R^5 = H, allyl
n = 1, 2, 3

60-100%
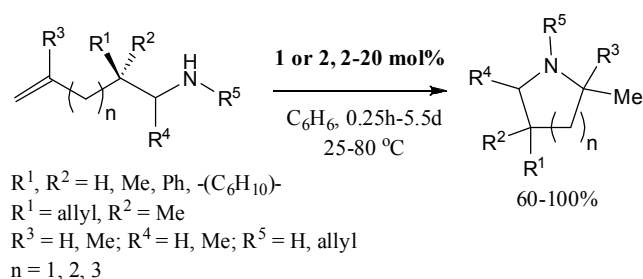
The individual steps of the originally proposed catalytic cycle were investigated with a series of stoichiometric reactions. Whereas σ-bond metathesis between complexes **1** or **2** and a number of secondary and primary amines (Scheme 16A) was shown to be fast and irreversible, yielding new isolable group 2 amide species, a stoichiometric reaction between calcium amide precatalyst **2** and benzylamine resulted in a quantifiable equilibrium, with a ΔG^o (298 K) value of -11.4 kJ.mol^{-1} indicating fast but reversible catalyst initiation (Scheme 16B).[55-57] Other, less acidic amines such as tert-butylamine and cyclohexylamine were found to displace the adducted THF molecule to form amine adducts (Scheme 16C), thus providing a model for pre-coordination of the aminoalkene and potential substrate inhibition during catalysis. Kinetic experiments with variable

substrate concentrations at constant catalyst concentration also revealed the importance of substrate and product inhibition, as had already been demonstrated in analogous lanthanide-based reactions.[58] The presence of THF also significantly slowed down reaction rates.

Scheme 16. Transamination reactions with group 2 amides.

Ar = 2,6-^{i}Pr$_2$C$_6$H$_3$

M = Mg, X = Bu, n = 0

M = Ca, X = N(SiMe$_3$)$_2$, n = 1

M = Mg, Ca; R^1 = H, R^2 = -(CH$_2$)$_2$OMe,

M = Mg; R^1 = R^2 = -(CH$_2$)$_5$-, -CH$_2$C(Ph)$_2$CH$_2$CH(Me)-

M = Ca; R^1 = H, R^2 = 2,6-^{i}Pr$_2$C$_6$H$_3$,

R^1 = R^2 = Ph.
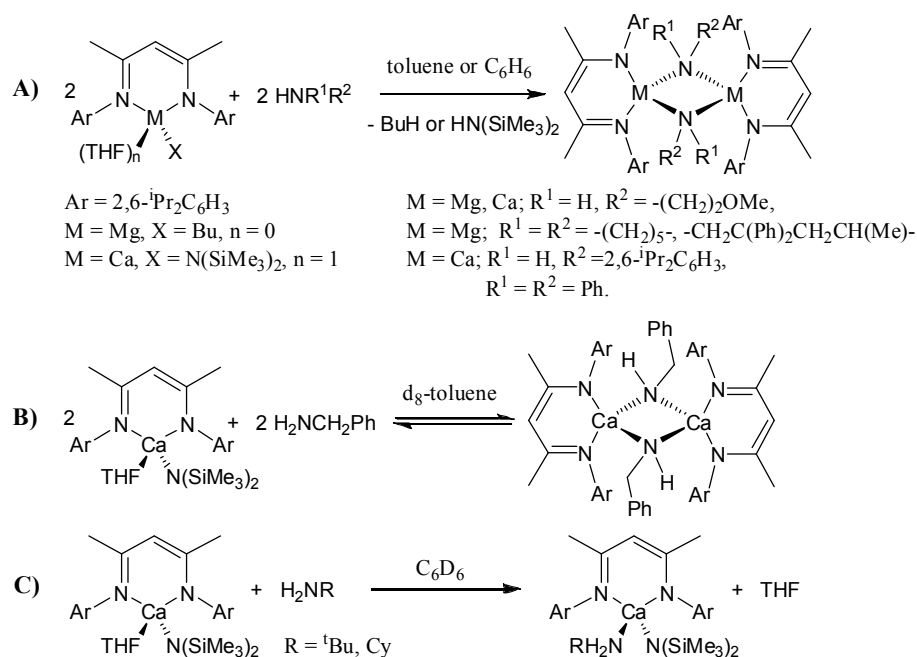
Catalytic hydroamination of deuterated substrates pointed towards a short-lived alkyl intermediate resulting from the intramolecular insertion of the terminal alkene into the metal-amide bond. These findings resulted in the proposal of two distinct catalytic cycles depending on the nature of the precatalyst (Figure 6).[54]

Figure 6. Proposed catalytic cycles for the intramolecular hydroamination of aminoalkenes with reversible or irreversible catalyst initiation.
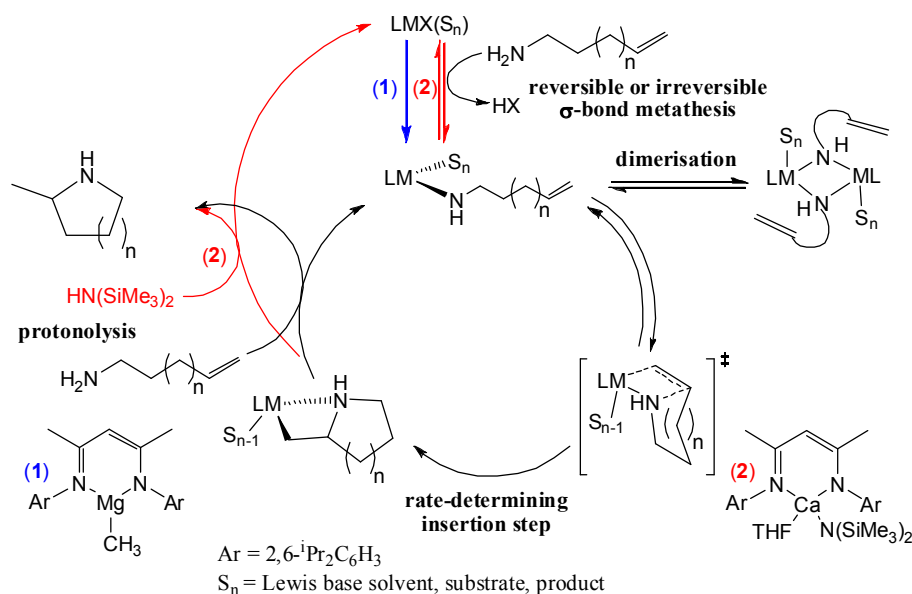
Heteroleptic calcium and strontium amide complexes bearing triazenide and aminotroponiminate spectator ligands have also been used in the hydroamination of aminoalkenes with similar results, despite their propensity to redistribute to homoleptic complexes.[59-61] It is, however, notable that the aminotroponiminate-stabilised calcium and strontium species **5** and **6** (Figure 4) reported by Roesky allow the facile cyclisation of 1-amino-2,2-dimethyl-5-phenyl-4-pentene and 1-amino-7-phenyl-6-hexyne at room temperature (Scheme 17). These are the first examples of group 2-catalysed hydroamination of aminoolefins with terminal substituents on the olefin moiety. In all cases, the calcium precatalysts produced higher turnover frequencies than their strontium counterparts. The tendency for ligand redistribution towards the homoleptic species, especially with the larger strontium centre, however, did not allow a more quantitative comparison of the effect of ionic radii on the rate of catalysis. Initial attempts by Buch *et al.* to achieve stereocontrolled intramolecular hydroamination by using a chiral (*S*)-(Ph-Box)-supported calcium amide precatalyst have only yielded extremely low enantioselectivities (ee < 10%), mainly due to Schlenk-type ligand redistribution equilibria leading to a catalytically inactive, homoleptic calcium (*S*)-(Ph-Box) complex and achiral [Ca{N(SiMe$_3$)$_2$}$_2$(THF)$_2$].[18] The latter was also proposed to be catalytically active. In 2009, Hultzsch and co-workers reported a chiral diamidobinaphthyl magnesium complex for the hydroamination/cyclisation of aminoalkenes, for which enantiomeric excess was limited to 14% due to ligand

exchange by protonation.[62] The most efficient systems to date, based on chiral tris(oxazolinyl)borate ligands, are still limited to enantioselectivities of 18% and 36% for calcium and magnesium respectively.[63]

Scheme 17. Intramolecular hydroamination of terminally substituted aminoalkenes and -alkynes.
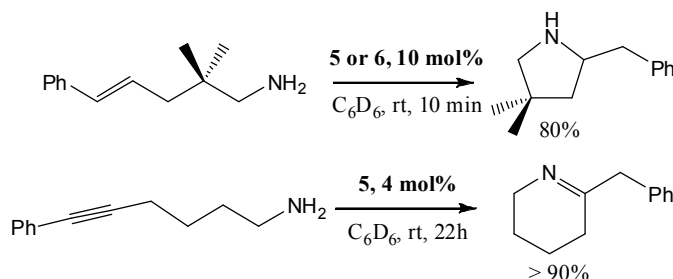
In 2008 group 2-mediated hydroamination was extended to the catalytic synthesis of guanidines and ureas from carbodiimides and isocyanates respectively, using heteroleptic calcium complex **2** and the homoleptic $[M\{N(SiMe_3)_2\}_2(THF)_n]$ series (M = Ca, Sr, Ba; n = 0, 2) as precatalysts (Scheme 18).[64] In both cases strontium yielded significantly higher turnover frequencies than calcium, although this was not quantitatively investigated. Catalysis with barium, however, was much slower and usually accompanied by the precipitation of insoluble products which, although not characterised, were thought to be polymeric and catalytically inactive species.

Scheme 18. Catalytic hydroamination of carbodiimides and isocyanates.
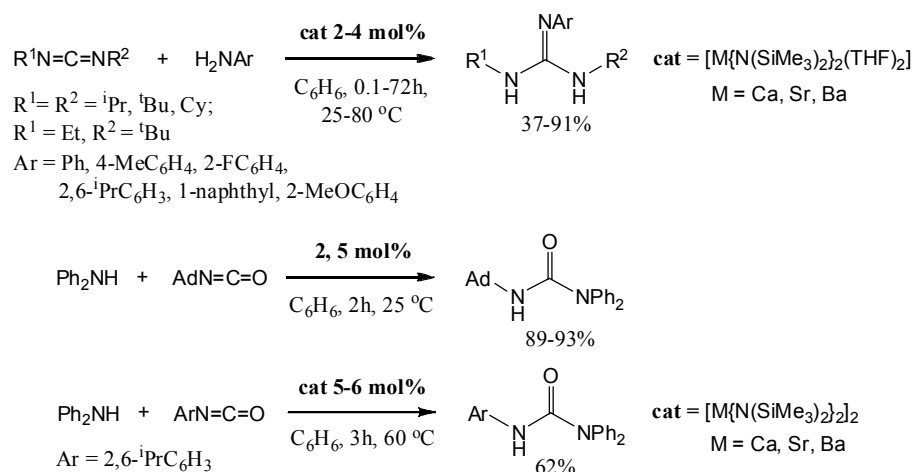
Stoichiometric reactions allowed the isolation of both heteroleptic and homoleptic guanidinate insertion products and a heteroleptic calcium urea complex as catalytically

active intermediates, demonstrating that catalysis occurs *via* an amide-carbodiimide or amide-isocyanate coordination-insertion mechanism (Scheme 19).

Scheme 19. Insertion of carbodiimides and isocyanates into alkaline earth-amide bonds.
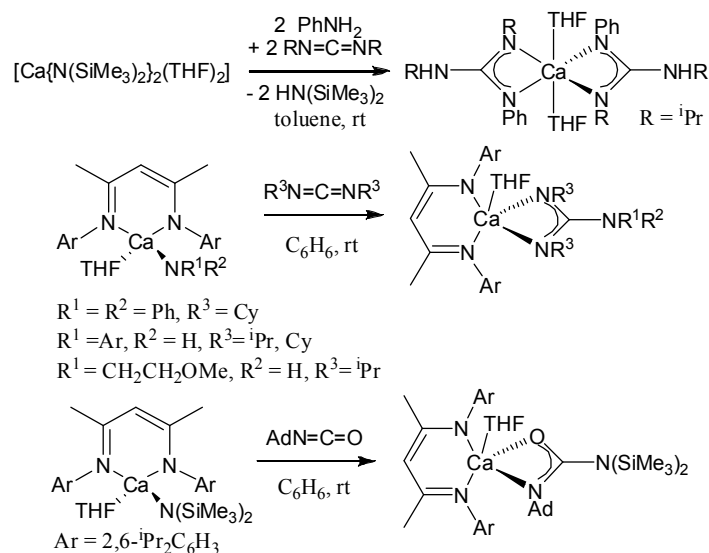
In 2009 Barrett *et al.* reported the first example of intermolecular hydroamination of activated alkenes with heavier alkaline earth complexes under mild conditions (5 mol% catalyst loading, 60 $^{\circ}$C) with excellent *anti*-Markovnikov regioselectivity (Scheme 20).[65] This time the homoleptic strontium precatalyst displayed higher catalytic activities than its calcium counterpart.

Scheme 20. Intermolecular hydroamination of activated alkenes.
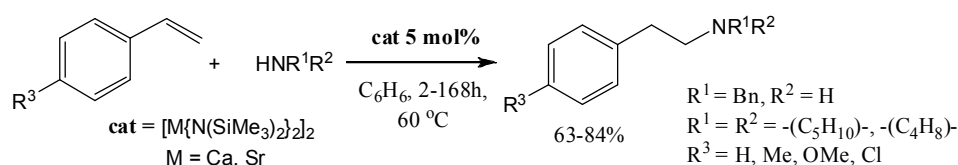
Kinetic data showed that, although the activation energy for strontium was higher than for calcium, this was counterbalanced by a significantly less negative value of the entropy of activation for strontium, mirroring a much looser four-membered insertion transition state, and giving the larger metal cation a clear entropic advantage under the reported reaction conditions. A computational study of a model ethene-ammonia system catalysed by a simplified alkaline earth *β*-diketiminato amide complex confirmed previous experimental findings from the intramolecular hydroamination of

aminoalkenes, by showing that calcium provided much lower activation barriers than magnesium for both the alkene insertion and final protonolysis steps (Figure 7).

Figure 7. Computational study of the intermolecular hydroamination of ethene with ammonia by heteroleptic group 2 precatalysts.
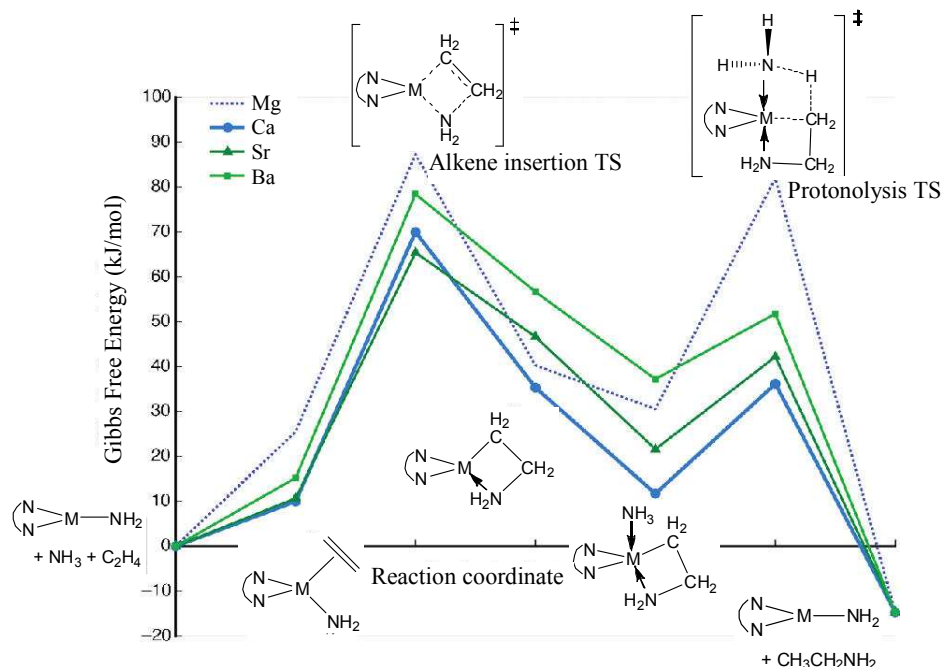
In relation to this theoretical study, it is notable that Harder and co-workers managed to stabilise a small amide functionality by reacting heteroleptic calcium amide **2** with NH$_3$(g) under very mild conditions at room temperature under a pressure of 1 bar (Scheme 21), a result which augurs well for the potential of group 2-mediated intermolecular hydroamination of alkenes with ammonia.

Scheme 21. Synthesis of a heteroleptic calcium amide complex by σ-bond metathesis with ammonia.
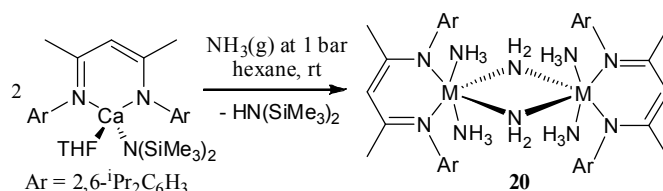
Intermolecular hydrophosphination of unsaturated bonds

Although lanthanocenes have been applied to the intramolecular hydrophosphination/cyclisation of phosphinoalkenes,[66] reports on the intermolecular

organolanthanide-catalysed version of this reaction remain limited.[67] Based upon the success of the intramolecular hydroamination of aminoalkenes with group 2 precatalysts, Hill and co-workers reported in 2007 the use of heteroleptic calcium complex **2** for the intermolecular hydrophosphination of unhindered activated alkenes and alkynes with diphenylphosphine, with activities comparable to those reported for late transition metal catalysts.[68] Addition of the phosphine across the carbon-carbon double bond was both regioselective, with a marked preference for the *anti*-Markovnikov product, and stereoselective, with nearly exclusive *syn*-addition as shown by the (*Z*) geometry of the product resulting from the hydrophosphination of 1,2-diphenylethyne (Scheme 22).

Scheme 22. Intermolecular hydrophosphination of activated alkenes and alkynes.
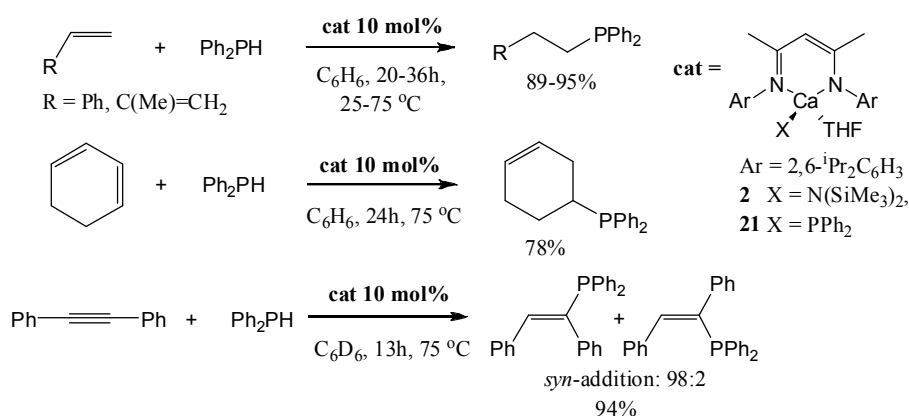
Initiation of the precatalyst occurs *via* σ-bond metathesis to generate the heteroleptic calcium diphenylphosphide complex **21**, which is itself catalytically active.[68] The chemistry of stoichiometric σ-bond metathesis between phosphines and group 2 amides has been well established by Westerhausen and co-workers since the 1990s and led to the isolation of numerous homoleptic alkaline earth phosphides (Scheme 23).[69]

Scheme 23. Synthesis of homoleptic and heteroleptic alkaline earth phosphides by protonolysis.
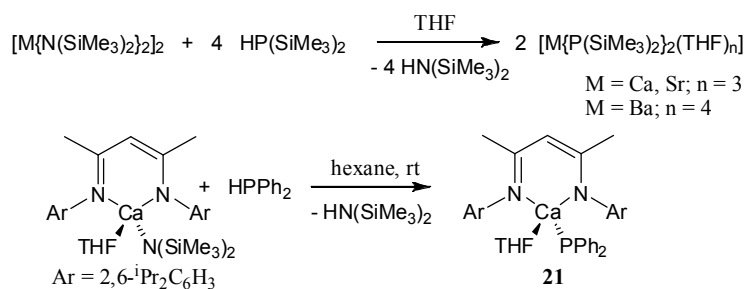
The active catalyst then undergoes concerted insertion of the alkene or alkyne into the calcium-phosphorus bond, which leads to the observed *syn*-stereoselectivity. In accordance with this mechanism, Westerhausen *et al.* described the stoichiometric insertion of one equivalent of diphenylbutadiyne into one of the Mg-P bonds of [Mg{P(SiMe₃)₂}₂(THF)₄] to yield the heteroleptic insertion product displayed in Scheme 24.[70]

Scheme 24. Insertion of diphenylbutadiyne into an Mg-P bond.
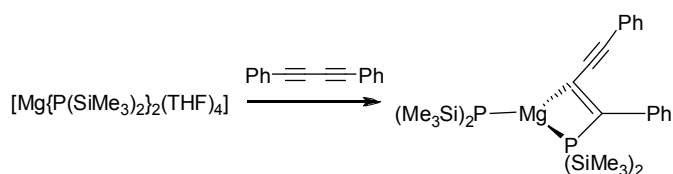
Attempts by Hill and co-workers to use homoleptic [Ca{N(SiMe₃)₂}₂(THF)₂] under these reaction conditions met with limited success due to formation of homoleptic calcium diphosphide species which are highly insoluble in benzene. Later, however, Westerhausen reported that homoleptic [Ca(PPh₂)₂] efficiently catalyses the *syn*-addition of diphenylphosphine to both diphenylethyne and diphenylbutadiyne in THF, in which the catalyst is soluble (Figure 8).[71]

Figure 8. Hydrophosphination of alkynes using [Ca(PPh₂)₂] and proposed mechanism.
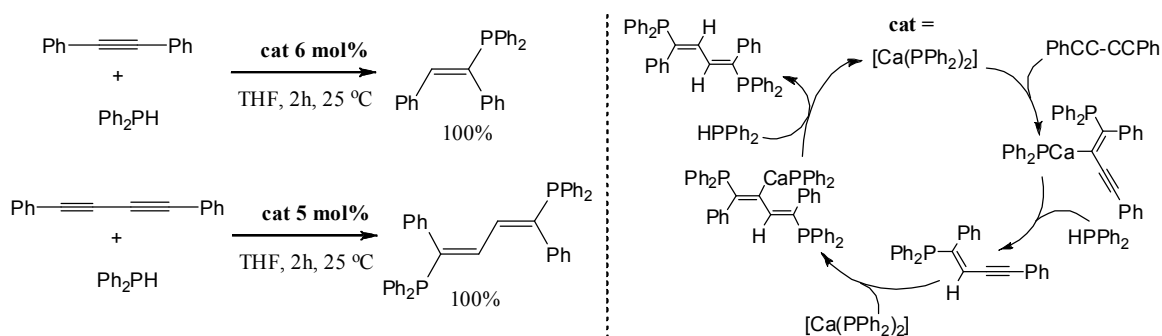
As for the hydroamination reaction, this reactivity could be extended to other unsaturated substrates, such as carbodiimides.[72] Although heteroleptic calcium complex **2** was found to catalyse the reaction, the less hindered homoleptic heavier group 2 bis(amides) [M{N(SiMe₃)₂}₂(THF)₂] (M = Ca, Sr, Ba) and the unsolvated [Ca{N(SiMe₃)₂}₂]₂ proved more active precatalysts. Although no kinetic studies could be undertaken due to extremely fast reaction rates, it appeared that the larger strontium and barium metal centres were more efficient than their calcium counterpart.

Hydrophosphination of both symmetric and unsymmetric carbodiimides with diarylphosphines proceeded at room temperature with low catalyst loadings to give the analogous phosphaguanidine in high yield (Figure 9). Hydrophosphination of sterically demanding 1,3-di-*tert*-butylcarbodiimide could not be achieved. Furthermore, dicyclohexylphosphine did not react with any of the carbodiimide substrates under the reported reaction conditions. In this latter case, the decreased acidity of the dialkylphosphine compared to the diarylphosphines was reasoned to prevent catalyst initiation. As for the hydroamination of carbodiimides, the reaction proceeds *via* insertion of the carbodiimide into the metal-phosphide bond (Scheme 25). Interestingly, addition of one equivalent of phosphine to the isolated calcium phosphaguanidinate insertion product **22** did not lead to *σ*-bond metathesis. Addition of a further equivalent of carbodiimide, however, resulted in liberation of the free phosphaguanidine. The authors explained this by invoking the Curtin-Hammett principle, arguing that the intermediate, **22**, and diphenylphosphine are in equilibrium with a small amount of the phosphaguanidine and calcium phosphide complex, which in turn reacts readily with the carbodiimide to achieve catalytic turnover. A catalytic cycle based on mostly reversible processes is outlined in Figure 9.

Figure 9. Hydrophosphination of carbodiimides and proposed mechanism.
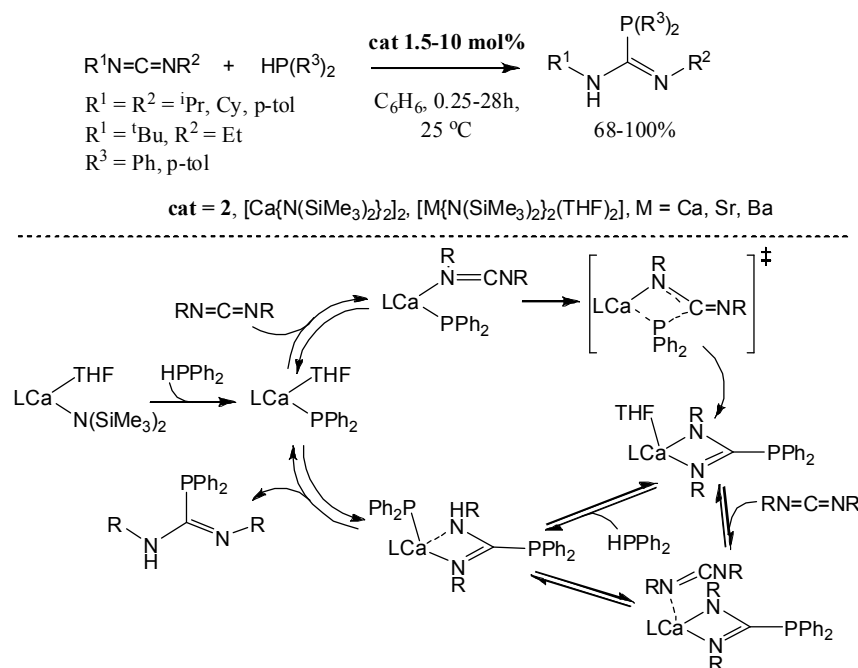
Following this, Westerhausen also reported that the homoleptic calcium phosphide complex [Ca(PPh$_2$)$_2$(THF)$_4$] undergoes insertion with carbodiimides to form a homoleptic calcium bis(phosphaguanidinate) species, which in turn displays only very limited catalytic activity.[73]

Scheme 25. Stoichiometric synthesis of the calcium phosphaguanidinate insertion intermediate.
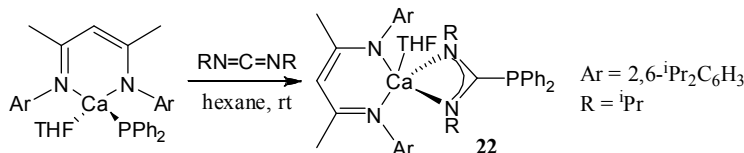
Intermolecular hydroacetylenation of carbodiimides

In 2009 Hill and co-workers reported the stoichiometric insertion of carbodiimides into the calcium-carbon bond of heteroleptic calcium acetylides (Scheme 26).[49]

Scheme 26. Stoichiometric insertion of carbodiimides into a heteroleptic calcium acetylide complex.
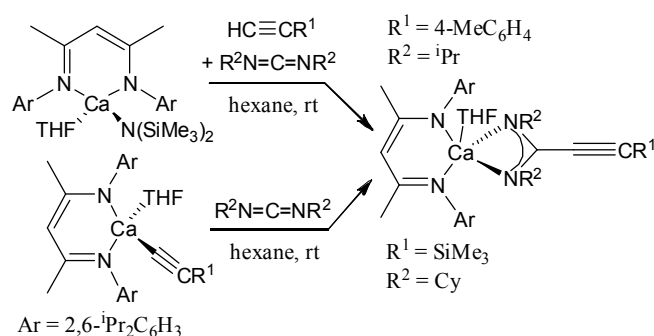
Based upon the precedent of lanthanide-mediated hydroacetylenation, the authors showed in a preliminary experiment that 5 mol% of calcium complex **2** catalyse the hydroacetylenation of 1,3-di-*iso*-propylcarbodiimide with phenylacetylene at 80 °C over a period of 14h (Scheme 27). NMR experiments, however, showed that the *β*-diketiminate ligand is protonated by the acetylene under the reaction conditions, making it unlikely that either the heteroleptic amide, acetylide or insertion products shown above are catalytically active species.

Scheme 27. Catalytic calcium-mediated hydroacetylenation of a carbodiimide.

35
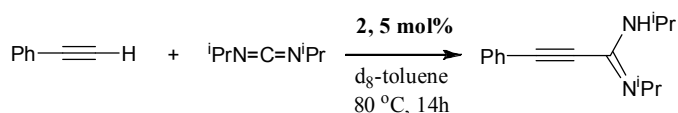
Intermolecular hydrosilylation of unsaturated bonds

In 2006, Buch and Harder described the regioselective hydrosilylation of activated alkenes with homoleptic calcium and strontium benzyl precatalysts **17** and **23** under mild reaction conditions (0.5-10 mol% catalyst loading, 25-50 °C, 0.1-48h).[74] The larger strontium metal centre displayed higher turnover frequencies than its smaller calcium counterpart. Despite these dibenzyl species also being active as anionic styrene polymerisation initiators, clean conversion to the silylated alkene was observed in each case. Regioselectivity could be effectively influenced by the choice of solvent: in apolar benzene exclusive formation of the Markovnikov product was observed, whereas in polar THF only the *anti*-Markovnikov product was obtained (Scheme 28). Reactions in diethyl ether yielded a mixture of isomers in the presence of the calcium precatalyst, but only the terminally silylated product was obtained with strontium.

Scheme 28. Regioselective hydrosilylation of activated alkenes.
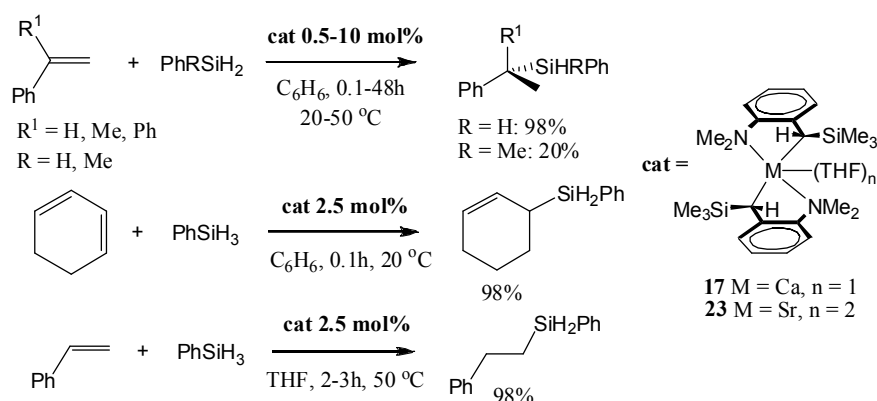
In both polar and apolar solvents catalyst initiation occurs through σ-bond metathesis of the dibenzyl precatalyst with the silane to form a transient, highly reactive, heteroleptic group 2 hydride intermediate which, although it could not be isolated, is thought to form hydride-rich clusters in solution. The successful isolation of heteroleptic calcium complex **24** and its magnesium analogue, obtained from the reaction of β-diketiminato magnesium and calcium complexes **1** and **2** with phenylsilane, as well as the synthesis of a hydride-rich Mg_4H_6 cluster, **25**, from a similar reaction of a carbene-supported magnesium bis(amide), strongly support this mechanism (Scheme 29).[75, 76] Commercially available CaH_2, however, did not catalyse the hydrosilylation of alkenes, even if freshly and finely ground.

Scheme 29. Synthesis of magnesium and calcium hydride complexes by σ-bond metathesis with PhSiH₃.
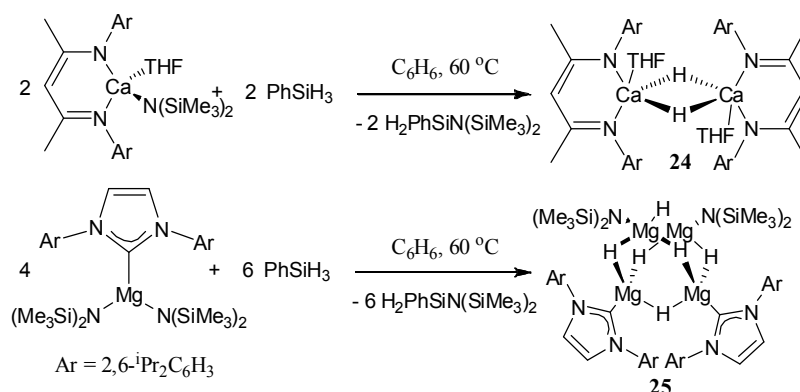
In the case of apolar solvents, the reaction then proceeds through conventional insertion of the alkene into the metal-hydride bond to form the most stable alkyl intermediate, which then undergoes σ-bond metathesis with another equivalent of silane to reform the metal hydride and the silylated Markovnikov product (Figure 10, **(A)**). In the case of polar solvents, the authors made a case for a catalytic cycle proceeding *via* a charge separated ion pair of the form $[LM]^+[PhSiH_4]^-$ which then converts into a group 2 silanide complex (Figure 10, **(B)**). Due to steric factors alkene insertion into the metal-silicon bond would therefore yield the *anti*-Markovnikov product, thus accounting for the observed regioisomer. Although this second catalytic cycle provides a justification for the influence of the solvent on regioselectivity, evidence for the charge-separated ion pair or silanide intermediate in THF, as well as for concomitant H_2 release, has yet to be reported. Therefore the possibility of a polarity-influenced transition state for the σ-bond metathesis between the group 2 alkyl intermediate and the silane in the first catalytic cycle can not be discounted.

Figure 10. Proposed catalytic cycles for the hydrosilylation of alkenes in apolar **(A)** and polar **(B)** solvents.

37
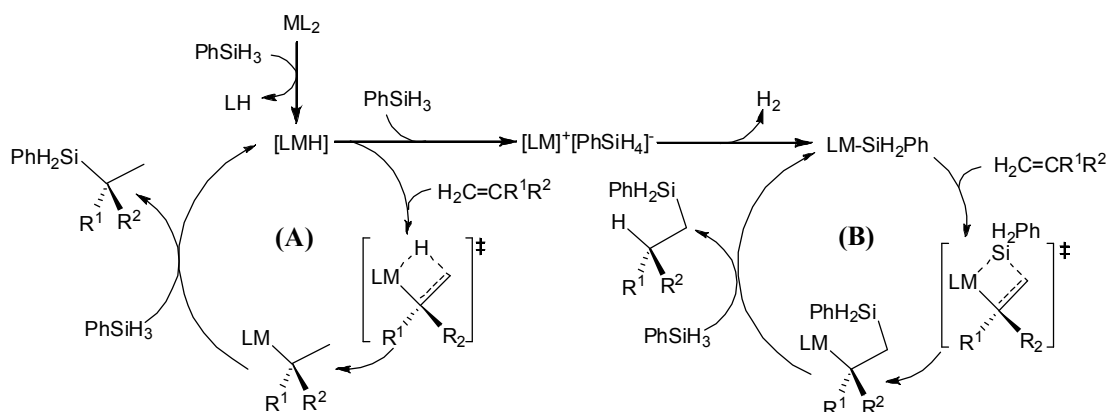
Both the homoleptic dibenzyl calcium complex **17** and the molecular calcium hydride complex **24** were also reported to promote the catalytic hydrosilylation of ketones.[77] Reactions proceeded under mild conditions (1-5 mol% catalyst loading, 20-50 ^{o}C) and yielded almost exclusively the dialkoxysilane, independent of the initial ratio between silane and ketone (Scheme 30). Whereas the stoichiometric insertion of ketones into the metal-hydride bond to form calcium alkoxide species **26a-e** was always accompanied by a substantial amount of enolisation (Scheme 31), enolisation products were virtually absent under catalytic conditions, suggesting that silylation of the alkoxide species is faster than enolisation.

Scheme 30. Catalytic hydrosilylation of ketones.

$R^1 = R^2 = Ph, Bn, -(C_5H_{10})-, -(C_9H_{14})-$
$R^1 = Ph, R^2 = Me$
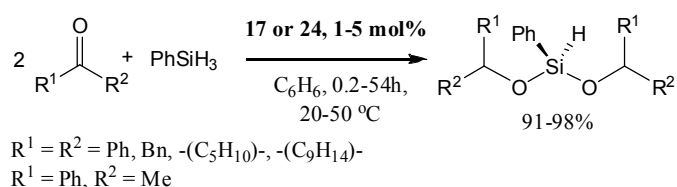
Since the isolated calcium alkoxide species did not react in turn with phenylsilane, it was argued that catalysis does not proceed *via* a calcium alkoxide intermediate. Rather, and although reactions were carried out in apolar benzene, Spielmann and Harder put forward a catalytic cycle based entirely upon charge separated ion pairs, with reactions occurring exclusively at the hypervalent anionic silicon centres. Nonetheless, since the isolated calcium alkoxide compounds **26a-e** were found to be active catalysts for the reaction, it is possible that, according to the Curtin-Hammett principle, the alkoxide species and silane are in equilibrium with a small amount of the free alkoxysilane and the calcium hydride complex **24**, which in turn reacts readily with excess ketone to achieve catalytic turnover.

Scheme 31. Stoichiometric insertion of ketones into the heteroleptic calcium hydride complex **24**.

26a $R^1 = R^2 = Ph$, 0% enolisation
26b $R^1 = R^2 = Bn$, 32% enolisation
26c $R^1 = R^2 = -(CH_2)_5-$, 35% enolisation
26d $R^1 = R^2 = -(C_9H_{14})-$, <1% enolisation
26e $R^1 = Me, R^2 = Ph$, 15% enolisation
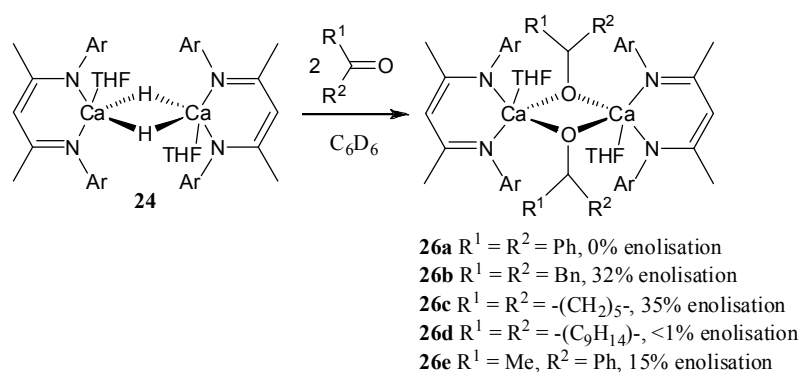
Hydrogenation of activated alkenes

Based upon their success at catalysing the hydrosilylation of conjugated alkenes, Spielmann and Harder described in 2008 the catalytic hydrogenation of alkenes with molecular calcium hydride **24** and the dibenzylcalcium and -strontium complexes **17** and **23**.[78] Reactions proceeded under relatively mild conditions (2.5-5 mol% catalyst loading, 20-60 $^{\circ}$C, 20 bar H_2) and gave the mono-hydrogenated product in moderate to high yields (Scheme 32). As for the hydrophosphination and hydrosilylation reactions, reactivity was limited to activated alkenes such as 1,1-diphenylethene, styrene, α-methylstyrene and cyclohexadiene.

Scheme 32. Catalytic hydrogenation of conjugated alkenes.
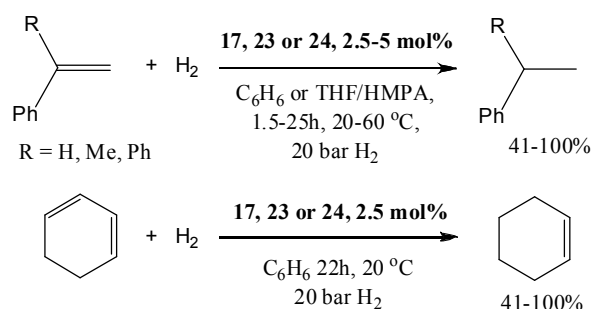
Side reactions producing dimers or oligomers resulting from single or multiple insertion of the alkene substrate into the calcium alkyl intermediate remained limited. Again, reactivity could be tuned by the choice of solvent: in polar THF or HMPA the reaction with styrene resulted exclusively in polymerisation, whereas in apolar benzene the hydrogenation product was obtained in 81-85% yield. In line with the organolanthanide-catalysed hydrogenation of alkenes the authors proposed the catalytic cycle outlined in Figure 11.

Figure 11. Catalytic cycle for the calcium-mediated hydrogenation of activated alkenes.
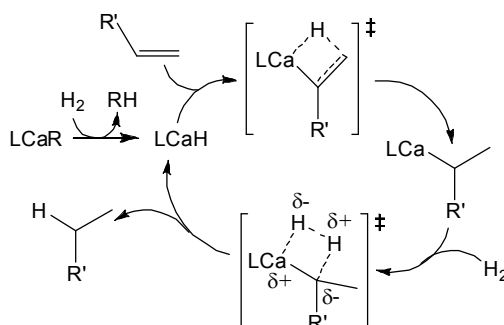
Stoichiometric reactions between **24** and 1,1-diphenylethene or 1,3-cyclohexadiene resulted in clean insertion of the least substituted end of the alkene into the calcium-hydride bond to form the intermediate calcium diphenylethyl and cyclohexenyl species **27** and **28** respectively (Scheme 33).[78, 79] Hydrogenation of the latter under 20 bar of H_2 regenerated the calcium hydride catalyst with liberation of the mono-hydrogenated alkene. Further evidence of the σ-bond metathesis process was obtained by saturation of a solution of the deuterated version of **24** with H_2, leading to fast H/D exchange.

Scheme 33. Stoichiometric insertion of activated alkenes into the Ca-H bond of X.
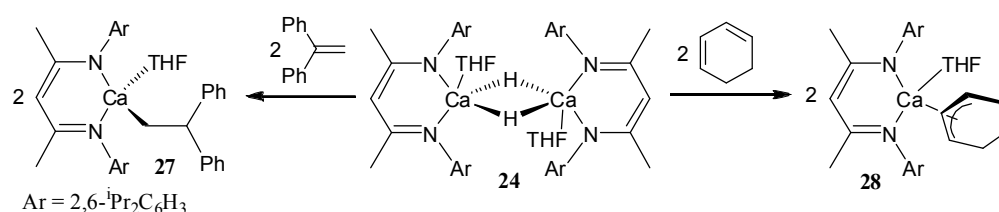
1.2.4 *Lewis acid-catalysed carbon-carbon bond formation*

In recent years the use of alkaline earth complexes as Lewis acid catalysts in synthetic Org. Chem. has increased dramatically. Usually prepared *in situ* over molecular sieves from readily available homoleptic metal alkoxides or amides and a variety of asymmetric ligands, these catalytic systems have attracted much interest owing to their reduced cost compared with more traditional transition metal catalysts, their biocompatibility, and their efficiency at catalysing a large array of asymmetric nucleophilic addition reactions with excellent yields and high enantio- or diastereoselectivity.

Hydroarylation of alkenes

It is particularly interesting to mention here the recent work by Niggemann and co-workers on the calcium-catalysed hydroarylation of alkenes.[80] The Lewis acidic [$Ca(NTf_2)_2$ + Bu_4NPF_6] system was found to catalyse the addition of electron-rich aromatic substrates across a variety of activated and even aliphatic alkene bonds at room temperature, under very mild conditions and in excellent yields (2.5-5 mol%

catalyst loading, 0.5-12h, 65-95% yield) (Scheme 34). A variety of functional groups, among which halides, hydroxides, ethers, furans and thiophenes, both present on the alkene and on the arene substrates, were tolerated under the mild reaction conditions employed. In contrast to the vast majority of alkaline earth-catalysed heterofunctionalisation reactions mentioned in this introduction, hydroarylation exclusively yielded the Markovnikov products, thus hinting at significant mechanistic differences. Although no mechanism was proposed by the authors, the presence of Bu_4NPF_6 proved critical for catalytic turnover to occur, suggesting the formation of a more reactive charge-separated $[Ca(NTf_2)]^+PF_6^-$ species. Moreover, reactions proceeded in dichloromethane without the exclusion of moisture or air, and were even inhibited under strictly anhydrous conditions, which led the authors to propose that a carbinol intermediate might be involved, although the latter could not be detected.

Scheme 34. Calcium Lewis acid-catalysed hydroarylation of alkenes.
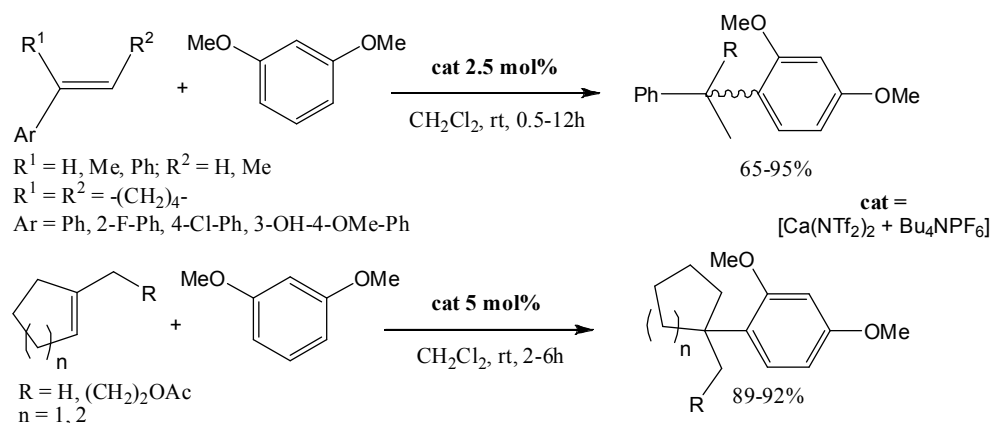
Enantioselective aldol reactions

The first example of enantioselective alkaline earth-mediated catalysis dates back to 1998, when Yamada and Shibasaki reported the asymmetric aldol reaction of a variety of aldehydes with excess acetophenone using a chiral barium catalyst prepared *in situ* from $[Ba(O^iPr)_2]$ and an excess of an (*R*)-2-hydroxy-2'-methoxy-l,l'-binaphthyl ligand precursor. Enantiomeric excesses remained moderate, ranging from 50 to 70%.[81] In 2001 Noyori and co-workers reported a more enantioselective system for the same reaction, prepared *in situ* from $[Ca\{N(SiMe_3)_2\}_2(THF)_2]$, KSCN and an excess of (*S,S*)-hydrobenzoin (Scheme 35).[82] The calcium catalyst was found to be several times more active than previously described systems, with moderate to good enantioselectivities

(66-91%). CSI-MS provided insight into the oligomeric nature of the catalyst, which was otherwise not characterised. The reaction of 3-(benzyloxy)-2,2-dimethylpropanal with acetophenone allowed the synthesis of the aldol (*R*) product, which is an intermediate in the synthesis of epothilone A, a chemotherapeutic drug, in 79% yield and 91% enantiomeric excess, thus paving the way for the application of these chiral alkaline earth catalyst systems in the synthesis of pharmaceutical and natural organic products. More recently, Yamaguchi *et al.* also described an (*S*)-BINOL/[Ba(O^{i}Pr)$_2$] system for the asymmetric aldol/retro-aldol reaction of *β-γ*-unsaturated esters with aldehydes leading to high selectivity for the (*E*)-*α*-adduct and enantiomeric excesses of up to 99% (Scheme 35).[83] The analogous lanthanide-based systems did not catalyse the reaction, showing once more that alkaline earth catalysts can not simply be considered as lanthanide-mimetic.

Scheme 35. Asymmetric calcium- and barium-mediated aldol reactions.
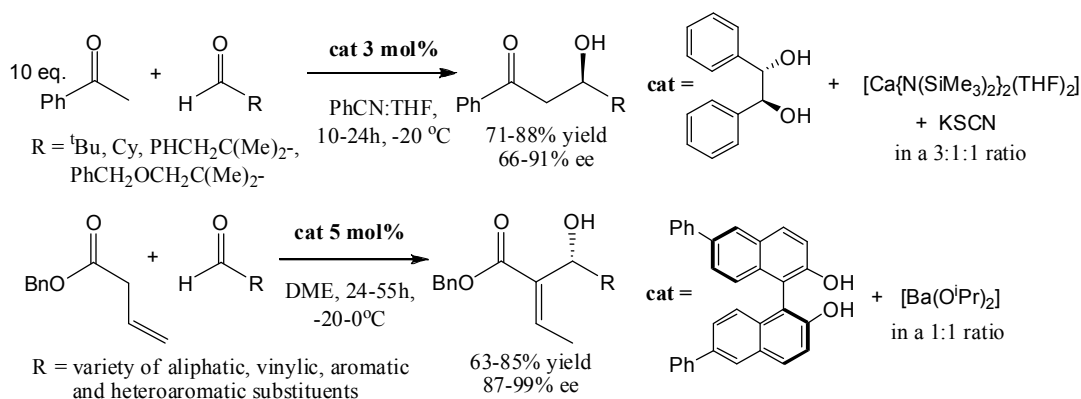
Asymmetric 1,4-addition and [2+3] cycloaddition reactions

Asymmetric Michael reactions and other 1,4-addition reactions have also been successfully catalysed by various homogeneous alkaline earth systems. In 2001 Kumaraswamy *et al.* described the use of a chiral CaCl$_2$/[KO^{t}Bu]/(*R*)-BINOL system as an inexpensive substitute for [La(O^{i}Pr)$_3$] for the asymmetric Michael addition of dimethylmalonate to linear and cyclic enones, albeit with relatively poor enantiomeric excess of the product.[84] Later, the same authors managed to greatly improve enantioselectivities by using the octahydro-BINOL version of the ligand precursor to generate Michael addition products containing quaternary stereocentres.[85] Kobayashi

and co-workers extended this work by using a chiral bis(sulfonamide) ligand precursor with $[Sr\{N(SiMe_3)_2\}_2]_2$ for the enantioselective Michael addition of di-*iso*-propylmalonate to a series of cyclic and acyclic chalcones.[86] After optimisation of the reaction conditions, high yields (>81%) and excellent selectivity (ee>90%) were achieved at room temperature within a few hours (Scheme 36). The analogous asymmetric 1,4-addition of malonates and *β*-ketoesters to nitroalkenes was successfully catalysed by a $[Ca\{O(4\text{-OMe-}C_6H_4)\}_2]/[$*anti*-5,4-diphenyl-PyBox] system (1:2.2 ratio) with good yields (>73%) and moderate to excellent enantioselectivities (65-96%), both for the formation of tertiary and quaternary carbon stereocentres.[87]

Scheme 36. Asymmetric strontium-catalysed Michael addition.

R^1 = Ph, 4-FPh, -CH=CHPh
R^2 = variety of aryl substituents

81-95% yield
90-98% ee
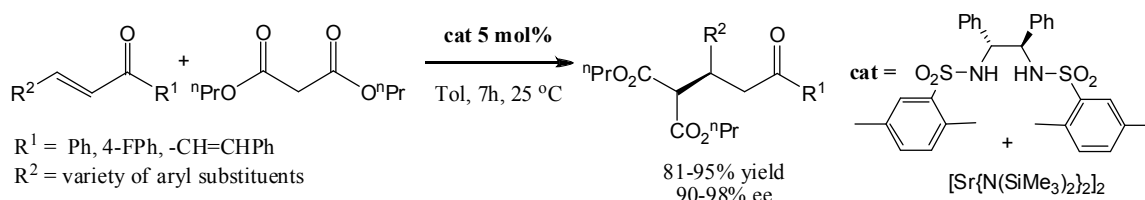
Other alkaline earth-catalysed 1,4-addition reactions include the addition of *α*-amino acid esters to *α,β*-unsaturated carbonyl substrates developed by Kobayashi and co-workers using a calcium catalyst prepared *in situ* from a chiral Ph-Box ligand and $[Ca(O^iPr)_2]$. Chiral glutamic acid derivatives were obtained in high yields under mild reaction conditions with enantiomeric excesses above 78% (Scheme 37).[88] The analogous magnesium system was catalytically inactive, while strontium and barium afforded much poorer enantioselectivities, likely due to their larger coordination sphere and looser transition states. NMR studies suggested that the catalyst was a monomeric calcium alkoxide complex supported by the chiral anionic ligand.

Scheme 37. Highly selective calcium-catalysed synthesis of chiral glutamic acid derivatives.

R^1 =H, Et, ^nBu, ^iBu, R^2 = H, R^4 = ^tBu
R^1 = H, R^2 = H, Me, Et, ^iPr, ^iBu, Cl, Ph, R^4 = Ph
R^3 = Me, Et, ^tBu, NMeOMe

46-100% yield
78-99% ee
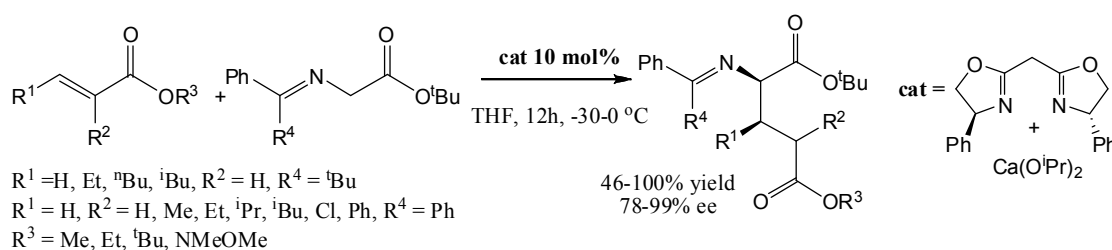
During the course of these studies the authors discovered that crotonate derivatives, instead of yielding the expected 1,4-addition product, underwent a [2+3] cycloaddition

process with the α-amino acid to yield highly enantiomerically and diastereomerically pure substituted pyrrolidines containing four stereocentres (Scheme 38). A whole range of α-amino acids including glycine, alanine, methionine, leucine and serine derivatives were successfully used. The reaction between crotonate derivatives and α-substituted α-amino acid esters yielded pyrrolidines containing contiguous, chiral, tertiary and quaternary carbon centres in good yields (41-98%) with excellent selectivity (ee>85%) despite longer reaction times. Such high stereoselectivity in the direct formation of highly sterically hindered chiral carbon centres is an achievement which places this calcium catalyst system among the very best in asymmetric [2+3] cycloaddition. Kobayashi and co-workers successfully applied this reactivity to the synthesis of chiral pyrrolidine cores for hepatitis-C virus RNA-dependent polymerase inhibitors in 83% yield and 85-88% enantiomeric excess.

Scheme 38. Highly diastereo- and enantioselective calcium-mediated [2+3] cycloaddition reactions.

$R^1 = R^5 = H$; $R^2 = $ amide; $R^3 = R^4 = $ Ph; $R^6 = $ ^{t}Bu
$R^1 = $ H, Me, $R^2 = $ alkoxide; $R^3 = $ aromatic substituent;
$R^4 = $ H; $R^5 = $ H, alkyl, Bn, $(CH_2)_2$SMe, CH_2O^tBu; $R^6 = $ alkyl

41-100% yield
70-99% ee

Mechanistic investigation of both the 1,4-addition and [2+3] cycloaddition processes led the authors to propose the catalytic cycle outlined in Figure 12. Catalyst initiation occurs *via* reversible σ-bond metathesis of the calcium alkoxide precatalyst with the α-amino acid ester, followed by 1,4-addition to the α,β-unsaturated carbonyl substrate. The reaction then either proceeds towards protonolysis and liberation of the 1,4-addition product or intramolecular cyclisation and protonolysis to liberate the chiral pyrrolidine.

Figure 12. Proposed catalytic cycles for the 1,4-addition and [2+3] cycloaddition of α,β-unsaturated carbonyl substrates to α-amino acid esters.
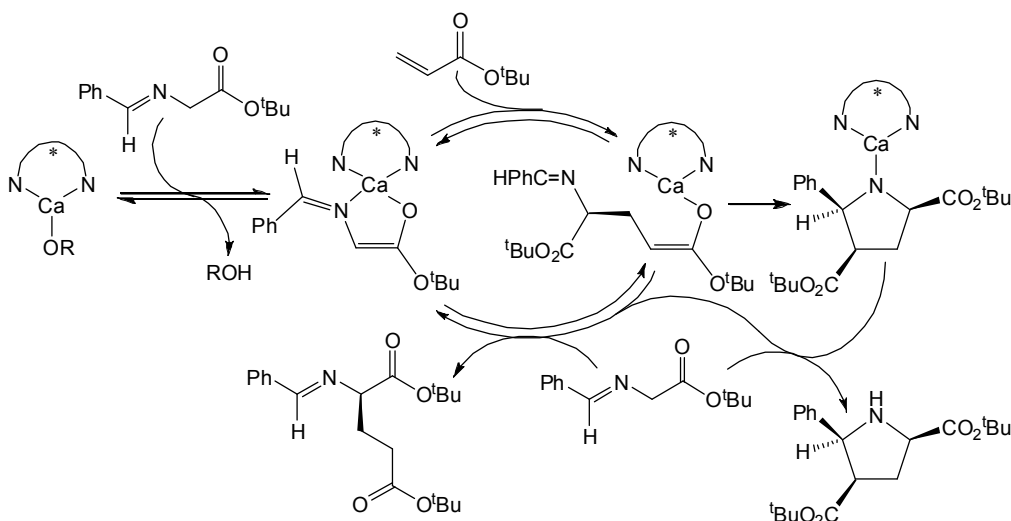
Asymmetric addition of esters and imidates to imines (Mannich-type reactions)

In 2010, Kobayashi and co-workers also reported that the enantioselective Mannich reaction of dibenzylmalonate with aromatic *N*-Boc imines using a [Ca(O^{i}Pr)$_2$]/[PyBox] system (1:1.5 ratio) afforded the resulting amines in excellent yields, with moderate to good selectivity (54-77% ee) within 2 hours at -20 °C.[89] Other Mannich reactions reported by the same group include the highly diastereoselective addition of *N*-Boc amides to *N*-diphenylphosphinoyl imines accompanied by Boc migration in the presence of a [Ba(O^{t}Bu)$_2$]/[2'-methoxybiphenyl-2-ol] system.[90] The related reaction of sulfonylimidates with aromatic and aliphatic *N*-Boc imines yielded interesting results: in the presence of a simple [Mg(O^{t}Bu)$_2$] catalyst in DMF without addition of ligand, excellent yields (>80%) and *anti*-diastereoselectivity (>80%) were achieved, whereas with a [Sr{N(SiMe$_3$)$_2$}$_2$(THF)$_2$]/[PyBox] system and a less polar solvent like THF, similarly excellent yields and *syn*-selectivity (>84%) were obtained (Scheme 39).[91] In 2007 Yamaguchi *et al.* described a similar Mannich-type reaction between β,γ-unsaturated esters and *N*-diphenylphosphinoyl imines, catalysed by a [Ba{O(4-MeO-C$_6$H$_4$)}$_2$]/[(*S*)-biaryldiol] system with high selectivity for the α,β-unsaturated α-adduct and good enantioselectivity (77-80%).[92] In all cases, catalyst initiation was thought to proceed through σ-bond metathesis between the metal alkoxide functionality and the

carbonyl substrate, followed by insertion of the imine and formation of the carbon-carbon bond.

Scheme 39. Diastereoselective reaction of sulfonylimidates with *N*-Boc imines.
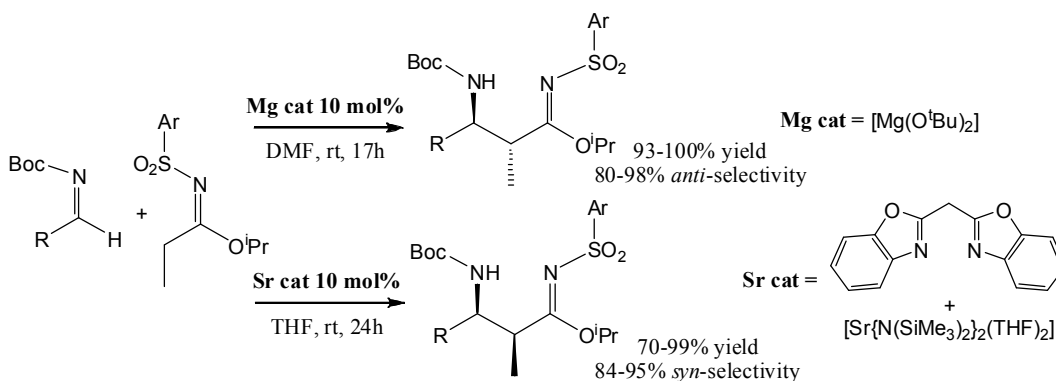
1.2.5 Catalytic dehydrocoupling of σ-bonds

The catalytic dehydrogenative coupling of σ-bonds remains a challenging type of reaction and to date, only a very limited number of examples have been reported in alkaline earth chemistry. In 2007 Buch and Harder described the dehydrocoupling of terminal alkynes and amines with silanes by the azametallacyclopropane complex [(Ph₂C-NPh)Ca(hmpa)₃], **29**, at room temperature (Scheme 40). Within the limited substrate scope examined, calcium precatalyst **29** displayed catalytic activity and selectivity similar to its Yb(II) analogue.[93]

Scheme 40. Calcium-mediated dehydrogenative silylation of amines and acetylenes.
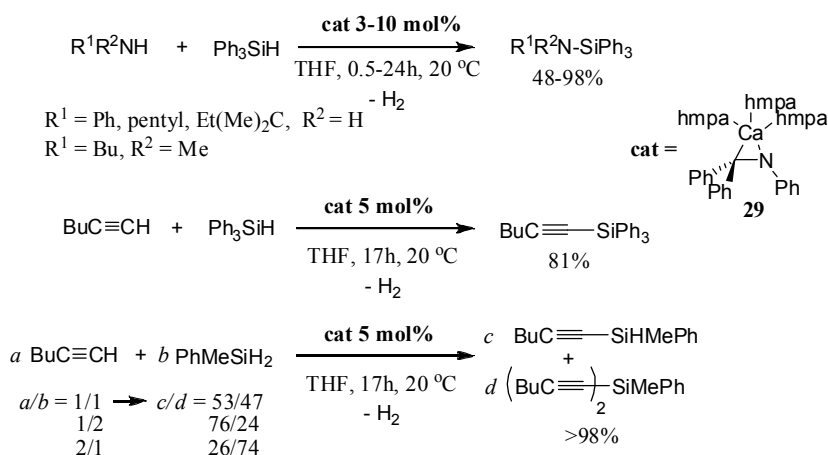
Contrary to the above-mentioned polymerisation and heterofunctionalisation reactions, the catalytic cycle does not involve any insertion step of an unsaturated bond.

Initiation occurs *via* σ-bond metathesis between the alkyl moiety of the ligand and the substrate to form either the calcium amide or acetylide catalyst, which in turn reacts with the silane to form an ill-defined calcium hydride intermediate and liberate the coupled silylated product. Further σ-bond metathesis with another equivalent of amine or acetylene regenerates the active species with quantitative release of H_2 (Figure 13).

Figure 13. Proposed catalytic cycles for the dehydrogenative silylation of amines and acetylenes.
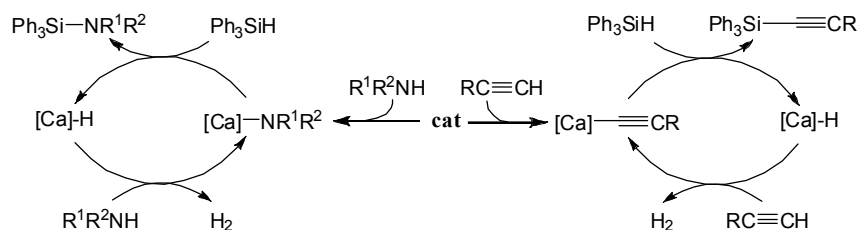
In 2009, Harder and co-workers also described the formation of the bis(anilino)borane $[HB\{NH(2,6\text{-}^iPr_2C_6H_3)\}_2]$ catalysed by magnesium β-diketiminate complex **30** in the presence of the aniline borane $[H_3B.H_2N(2,6\text{-}^iPr_2C_6H_3)]$ (Figure 14).[94] A heteroleptic magnesium borohydride complex was identified as a catalytically active intermediate, and the BH_3 by-product was observed in the ^1H NMR spectrum in the form of B_2H_6. The active catalyst, a β-diketiminate-supported magnesium amidoborane was readily isolated from the σ-bond metathesis of the related magnesium hydride complex with the aniline borane. In view of these observations, the authors proposed the two potential catalytic cycles outlined in Figure 14, both based on an intermediate $[LMg(NHAr\text{-}BH_2\text{-}NHAr\text{-}BH_3)]$ species, which either decomposes through β-hydride elimination to form the bis(anilino)borane and a magnesium hydride, or through a 1,3-hydride shift to release the product and form a magnesium borohydride intermediate.

Figure 14. Possible catalytic cycles for the catalytic dehydrocoupling of $[H_3B.H_2N(2,6-^iPr_2C_6H_3)]$.
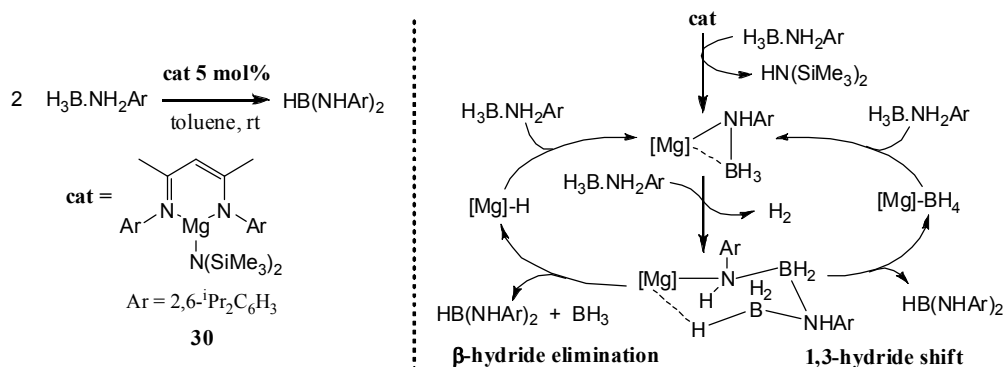
Stoichiometric σ-bond metathesis reactions between β-diketiminate-supported calcium and magnesium amides or hydrides with $H_3B.NH_2R$ (R = H, Me, ^iPr, 2,6-$^iPr_2C_6H_3$) by the same authors led to the isolation of a number of heteroleptic amidoborane complexes. These thermally decompose either into borylamide complexes (R = 2,6-$^iPr_2C_6H_3$) or into dimers, such as **31a-c**, bearing the dianionic ligand $[RN-BH-NR-BH_2]^{2-}$ (R = H, Me, ^iPr), in both cases with loss of H_2 (Scheme 41).[94, 95] Homoleptic and heteroleptic magnesium complexes bearing the monoanionic $[NMe_2-BH_2-NMe_2-BH_3]^-$ ligand were also recently isolated by Liptrot *et al.* from the reaction of $[Mg\{CH(SiMe_3)_2\}_2(THF)_2]$ and magnesium complex **1** with four and two equivalents of $Me_2NH.BH_3$ respectively.[96]

Scheme 41. Stoichiometric σ-bond metathesis reactions of group 2 complexes with amine boranes, demonstrating dehydrogenative B-N coupling.
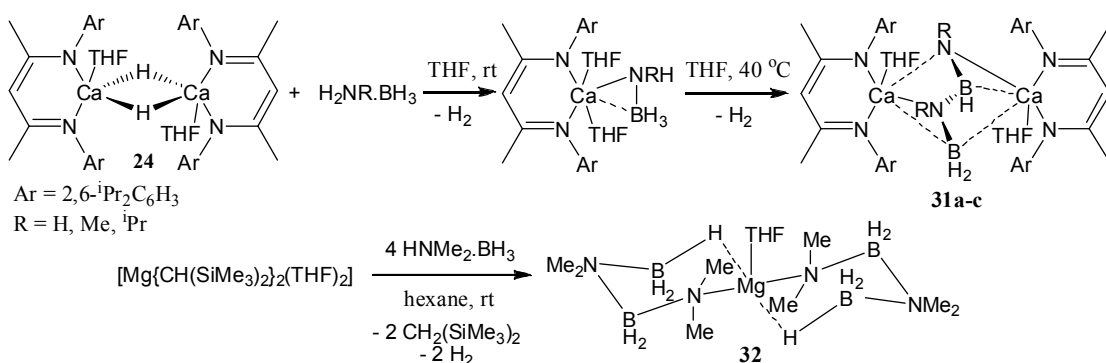
In the same work the authors also reported the selective catalytic dehydrocoupling of $Me_2NH.BH_3$ to the cyclic $[(H_2BNMe_2)_2]$ dimer with homoleptic alkyl precatalysts of the form $[M\{CH(SiMe_3)_2\}_2(THF)_2]$ (M = Mg, Ca), as well as magnesium and calcium β-diketiminate compounds **1** and **2**.[96] Monitoring of the reaction with the homoleptic magnesium precatalyst by ^{11}B NMR over 72 hours at 60 °C provided evidence of two

amidoborane intermediates which were identified as [Mg{N(Me$_2$)BH$_3$}$_2$] and **32** (Scheme 41), as well as of the formation of the minor *β*-hydride elimination by-product HB(NMe$_2$)$_2$. The much slower reaction with calcium precatalyst **2** also allowed the observation as small amounts of Me$_2$N=BH$_2$ and heteroleptic calcium hydride complex **24** as potential intermediates, leading the authors to propose the catalytic cycle outlined in Figure 15. The difference in catalytic activity between the magnesium and calcium precatalysts was explained by the higher polarising capacity of the smaller magnesium centre to effect the insertion and the hydride elimination steps.

Figure 15. Proposed catalytic cycle for the catalytic dehydrocoupling of H$_3$B.NHMe$_2$ into cyclic [(H$_2$BNMe$_2$)$_2$].
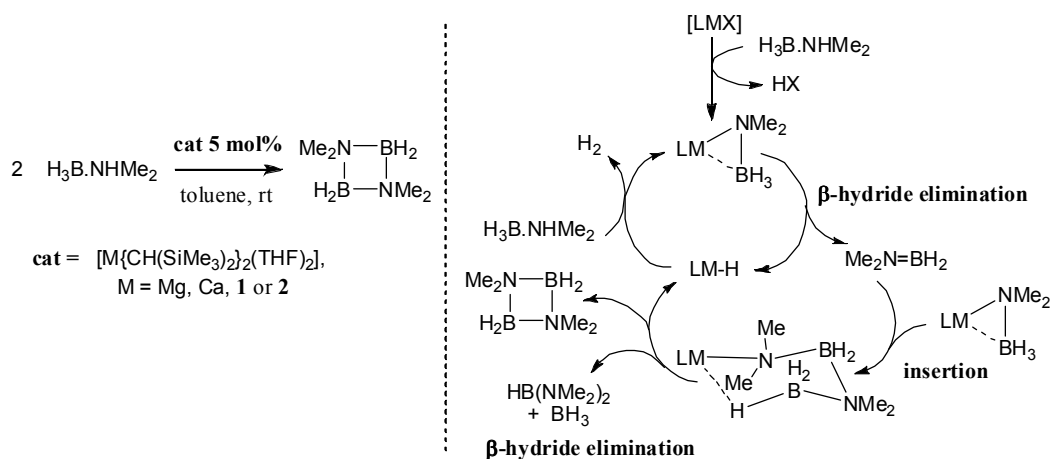
Despite these results only being preliminary, they will hopefully provide an important stepping stone for extending the catalytic reactivity of group 2 complexes towards more challenging dehydrocoupling reactions in the future.

1.3   Scope of this thesis

Chapter 2 of this thesis seeks to deepen our current mechanistic understanding of the alkaline earth-catalysed intramolecular hydroamination of aminoalkenes, with a particular focus on the predominant influence of group 2 cation charge density and polarisation, as well as on intrinsic differences with analogous lanthanide reactivity. As a result of these kinetic and mechanistic studies, it became apparent that ligand design was required to overcome two of the major problems commonly presented by alkaline

earth organometallics: the Schlenk equilibrium and the stabilisation of highly reactive group 2 alkyl species. The use of bis- and tris(carbene)borate ligands (Chapter 3) evidenced the stereoelectronic influence of the monoanionic spectator ligand on complex stability and catalytic activity, while also stressing the need for more robust C,H,N,O-based ligands. Finally, Chapter 4 describes how the unique dearomatisation properties of alkaline earth dialkyls may be harnessed to design new and stable heteroleptic group 2 alkyl complexes presenting unprecedented catalytic activity.

2 Hydroamination of aminoalkenes with group 2 precatalysts: influence of cation charge density and choice of ligands

2.1 Introduction

Amines and their derivatives play an important role in many industrial products, such as drugs, cosmetics, pesticides, polymers, dyes, antioxidants, stabilisers, and many more.[97] Current industrial processes for the synthesis of amines are mainly based on the metal-catalysed condensation of ammonia with alkyl halides or alcohols, which in turn are obtained from olefins.[98] The direct hydroamination of olefins thus represents an attractive, more cost-effective and atom-efficient alternative. Although the direct addition of amines to unsaturated bonds is thermodynamically achievable in terms of free energy ($\Delta G^{\mathrm{o}} \approx$ -17 kJ.mol^{-1}), the reaction presents a very high activation barrier due to the repulsion between the electron-rich π-system of the unsaturated substrate and the lone pair of the nucleophilic amine.[99] Additionally, the highly negative entropy of the process favours the reactants at high temperature. The use of catalysts to overcome these barriers is, therefore, indispensable.

Over the last thirty years a wide variety of homogeneous catalysts has been developed for the intramolecular hydroamination/cyclisation of aminoolefins into N-heterocyclic products, based on metals spanning the whole of the periodic table: alkali metal bases,[100-104] early transition metals,[105] such as scandium,[106, 107] yttrium,[107-109] titanium and zirconium,[109-117] late transition metals such as rhenium,[118] iron,[119] ruthenium,[120] rhodium and iridium,[121, 122] palladium,[123, 124] platinum,[124, 125] copper,[126] silver and gold,[127] zinc,[128, 129] as well as lanthanide[51, 53, 60, 130-135] and actinide derivatives.[136, 137]

Since alkaline earth Ae^{2+} species are d^0 and redox-inactive, only d^0 metal-catalysed intramolecular hydroamination reactions based on a single catalyst oxidation state will be presented herein. In all these cases, the 5-, 6- or 7-membered N-heterocyclic products arise from exocyclic addition of the olefin (Figure 16).

2.1.1 Lithium-catalysed intramolecular hydroamination

Figure 16. Scope and regioselectivity of d^0 metal-catalysed intramolecular hydroamination/cyclisation
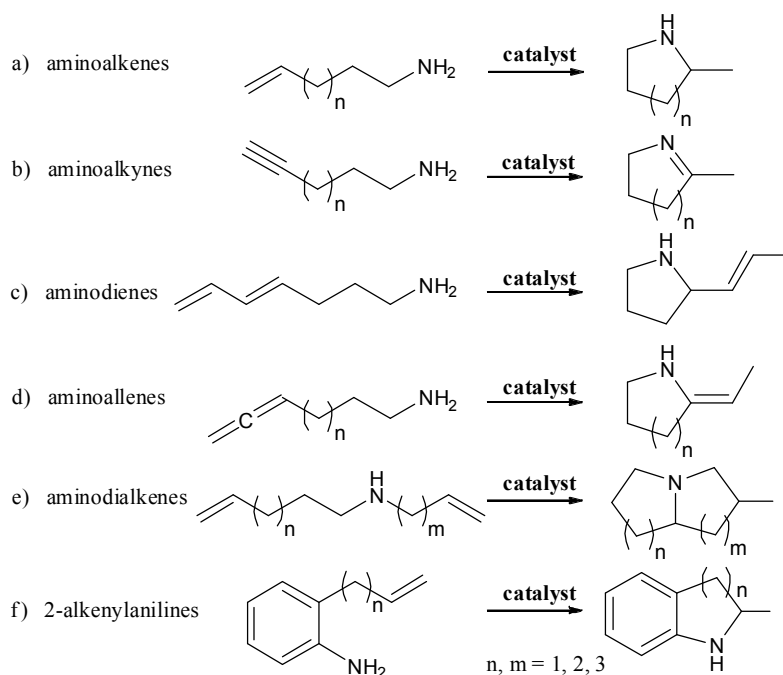
The first example of intramolecular hydroamination of aminoalkenes in the presence of catalytic amounts of *n*-BuLi was reported in 1992 by Fujita *et al.*[100] Since then lithium bases of the form [L$_n$LiX] (L = neutral ligand, X = monoanionic, reactive ligand) have been successfully used for the intramolecular hydroamination of unactivated alkenes, conjugated enynes and cyclohexa-2,5-dienes into five- and six-membered heterocycles, as well as bicyclic products.[101-104] Chiral diamidobinaphthyl and bisoxazoline ligands have been developed to achieve enantioselectivities of up to 91% ee.[103] In most cases, alkene isomerisation by-products were observed, but at higher temperatures these disappeared in favour of the N-heterocyclic products. Although no in-depth mechanistic studies have been carried out, reactions are thought to proceed *via* deprotonation of the amine moiety to form the catalytically active lithium amide species, followed by alkene insertion into the Li-N bond, formation of a transient lithium alkyl complex, and finally protonolysis with a second equivalent of substrate to regenerate the active species and liberate the cyclised product. It is noteworthy, however, that the stoichiometric reaction between *n*-BuLi and 1-amino-4-pentene yielded quantitative formation of the lithiated amidoalkene which, even after prolonged heating at reflux, did not undergo intramolecular hydroamination.[104] Rather, the addition of small amounts (10-20 mol%) of di-*iso*-propylamine was necessary to

achieve full cyclisation. It is therefore likely that coordinated amines play an important role in the charge stabilisation of the polarised alkene moiety during the transition state, thus suggesting a concerted insertion-protonation pathway (*vide infra*).

2.1.2 *Lanthanide-catalysed intramolecular hydroamination*

The highly efficient organolanthanide-mediated intramolecular hydroamination of aminoalkenes, -alkynes, -allenes, and -dienes pioneered by Marks and co-workers in the 1990s is probably one of the most-studied catalytic transformations.[130] In-depth kinetic and mechanistic experimental studies have established the catalytic cycle outlined in Figure 17.[53, 132] Catalyst activation occurs *via* σ-bond metathesis between the alkyl or amide co-ligand of the [L$_2$LnX] lanthanide precatalyst (L = monoanionic spectator ligand; X = reactive monoanionic ligand) and the amine moiety of the substrate, followed by polarisation of the unsaturated carbon-carbon bond, insertion of the latter into the Ln-N bond to form a transient alkyl species, and finally protonolysis by another equivalent of the substrate, leading to regeneration of the active catalyst and liberation of the N-heterocyclic product.

Figure 17. Catalytic cycle for the hydroamination/cyclisation of aminoalkenes by organolanthanide precatalysts.
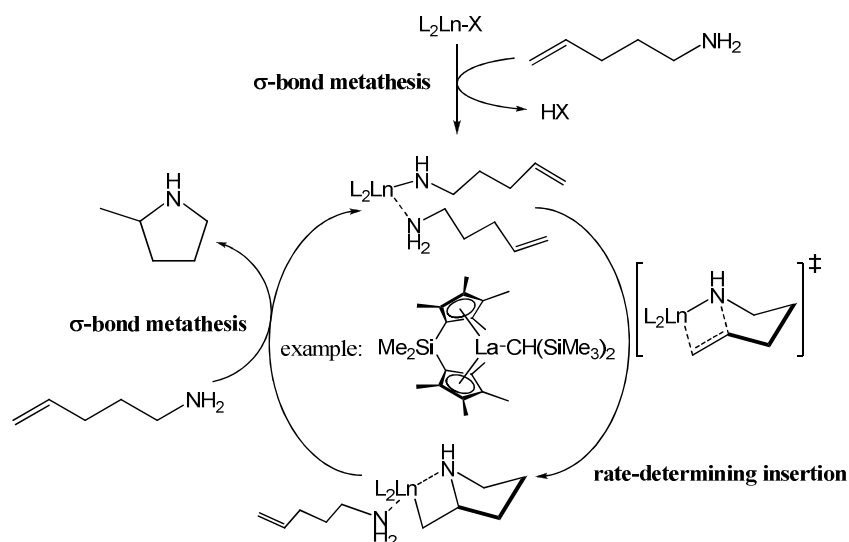
Kinetic studies showed that the reaction follows the rate law *rate* = k[substrate]^0[catalyst]^1 and is subject to substrate inhibition. The reaction rate can be tuned by the judicious choice of both the electronic and steric properties of the spectator ligands and the size of the lanthanide metal centre, as rates markedly decrease down the

series (La > Sm > Lu)[53] in correlation with the general trend of lanthanide-based olefin insertion reactions.[10] Furthermore, deuterium-labelling experiments and kinetic studies, yielding mild activation enthalpies ($\Delta H^{\ddagger} \sim 50$ kJ.mol^{-1}) and highly negative activation entropies ($\Delta S^{\ddagger} \sim -100$ J.mol^{-1}.K^{-1}), are all in agreement with the existence of a highly organised transition state leading to rate-determining olefin insertion.[53] High kinetic isotope effects have also suggested that neutral adducted aminoolefins play a role in the stabilisation of negative charge build-up on the polarised olefin moiety during the transition state.[53] First centred on cyclopentadienyl-based organolanthanide precatalysts, this field has rapidly expanded towards the use of chiral non-cyclopentadienyl dianionic ligands for the enantioselective hydroamination of aminoolefins with some examples shown in Figure 18.[131, 135] In recent years, a number of computational studies on the hydroamination/cyclisation of aminoalkenes, -alkynes, -allenes and -dienes with trivalent lanthanide catalysts have been carried out, confirming the experimental findings.[138] Similar studies for the actinide-catalysed hydroamination of aminoolefins suggest an analogous mechanism, based on σ-bond metathesis and insertion into the actinide-amide bond.[139]

Figure 18. Examples of chiral cyclopentadienyl and non-cyclopentadienyl precatalysts for the lanthanide-mediated hydroamination/cyclisation of aminoalkenes.
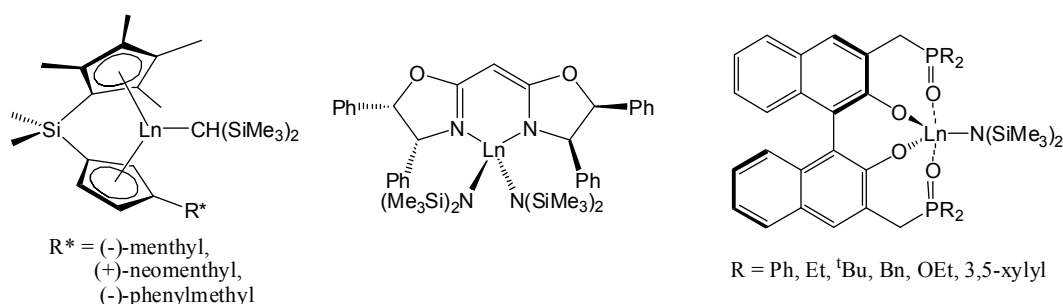
2.1.3 Group 4-catalysed intramolecular hydroamination

While at first limited to the cyclisation of aminoalkynes and -allenes,[110, 111] group 4-mediated intramolecular hydroamination has been expanding in recent years to the enantioselective cyclisation of unactivated aminoalkenes.[112, 115] Cationic group 4 complexes of the form [L$_2$MX]$^+$[A]$^-$ and neutral complexes of the form [L$_3$MX] bearing a single monoanionic substituent capable of undergoing protonolysis (L = monoanionic spectator ligand; X = reactive monoanionic ligand; A$^-$ = counteranion) have been shown

to catalyse hydroamination/cyclisation reactions in a manner similar to lanthanide complexes, albeit at much slower rates than their rare earth counterparts.[112, 113, 137] In contrast, neutral titanium(IV) and zirconium(IV) complexes of the form [L$_2$MX$_2$] have also demonstrated the capacity to form M=N imido bonds with the amine moiety of the substrate, and undergo subsequent [2+2] cycloaddition of the olefin residue with the M=N bond to complete ring closure.[110] In this particular mechanism, displayed in Figure 19, [L$_2$MX$_2$] first reacts with two molecules of substrate to yield an inactive [L$_2$M(NHR)$_2$] bis(amide) species which, in a reversible rate-determining process, is activated by N-H proton abstraction, elimination of RNH$_2$ and formation of the metal imido species. The latter can then undergo an M=N/C=C [2+2] cycloaddition followed by protonolysis of the resultant azametallacycle with another two equivalents of substrate, liberation of the N-heterocyclic product and regeneration of the active catalyst. The [2+2] cycloaddition process has been argued to be thermodynamically unfavourable, and in many cases a σ-bond metathesis/insertion process can not be discounted, as was demonstrated by Tobisch in a computational study on the cyclisation of aminoallenes.[140] In some cases, however, in which the steric crowding about the catalytic centre should in theory prevent alkene polarisation and insertion due to a lack of vacant coordination sites, catalysis rates have been seen to increase dramatically with steric crowding, an observation only compatible with the imido mechanism.[116]

Figure 19. Catalytic imido cycle for the hydroamination/cyclisation of aminoalkenes by neutral group 4 precatalysts.
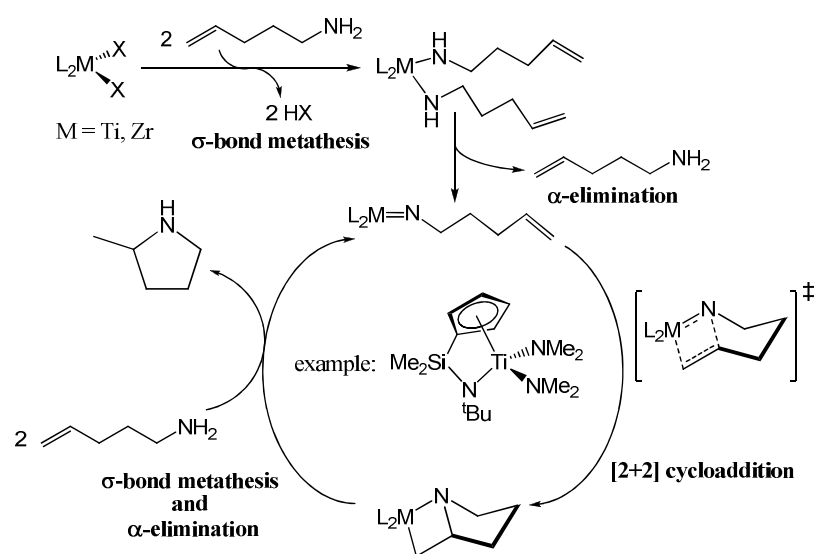
In general it seems that the preference for the amido/alkene insertion or the imido/alkene [2+2] cycloaddition route heavily depends not only on the availability of two protonolysable sites for M=N bond formation, but also the nature of the spectator ligand, the presence of free coordination sites and the substrate used, as secondary amines also prevent M=N bond formation.[117]

2.1.4 Group 2-mediated intramolecular hydroamination

As already outlined in the introduction to this thesis, mechanistic studies on the hydroamination/cyclisation of substituted aminoalkenes into pyrrolidines, piperidines and hexahydroazepines with β-diketiminate magnesium and calcium precatalysts **1** and **2** have confirmed a lanthanide-type catalytic cycle based upon σ-bond metathesis and rate-limiting insertion steps, with either reversible (**2**) or irreversible catalyst initiation (**1**), depending on the acidity of the reactive monoanionic substituent (Figure 6). While the larger calcium metal centre of complex **2** was found, in all cases, to provide the fastest turnover rates, magnesium precatalyst **1** proved more selective for the hydroamination/cyclisation of 6- and 7-membered rings.[54] In other comparative intramolecular hydroamination studies using calcium and strontium triazenide and aminotroponiminate precatalysts (Figure 4), the strontium derivatives proved to be more sluggish that their calcium counterparts.[60, 61] Later studies upon the intermolecular hydroamination of activated alkenes with homoleptic group 2 bis(amide) precatalysts [M{N(SiMe$_3$)$_2$}$_2$] (M = Mg, Ca, Sr, Ba), however, found strontium to be significantly superior to calcium, while magnesium and barium, although catalytically active, provided extremely slow turnover frequencies.[65] A computational study suggested that the interplay between the ability of the group 2 metal-amide bond to polarise the C=C alkene bond and the polarisability of the alkaline earth dication dictates the height of the activation barrier towards the alkene insertion step. Kinetic analyses also revealed that the strontium precatalyst benefits from a considerable entropic advantage arising from a less constrained insertion transition state, which results in superior catalytic activity despite a higher activation barrier towards the insertion. It thus became apparent that the catalytic reactivity of group 2 metal centres is not only dependent on cation size but also on more subtle charge density variations. The following study, therefore, seeks to base previous qualitative observations on the alkaline earth-catalysed intramolecular hydroamination of aminoalkenes on a more quantitative level, in an unprecedented

comparison of complexes spanning the whole group 2 series from magnesium to barium, assessing the influence of the nature of the metal centre as well as of the various ligands and co-ligands employed.

2.2 Selection of homoleptic and heteroleptic precatalysts

It had been previously shown that catalytic turnover is inhibited by Lewis bases such as THF, substrate or product binding to the metal centre, thus creating coordinative saturation.[54] It was therefore of interest to compare hydroamination with calcium precatalyst **2** and its recently reported unsolvated analogue [{ArNC(Me)CHC(Me)NAr}Ca{N(SiMe$_3$)$_2$}], **33**, (Ar = 2,6-di-*iso*-propylphenyl) which, although only three-coordinate, proved stable towards ligand redistribution equilibria in solution.[21, 36, 141] Due to contamination with the homoleptic and catalytically inactive complex [{ArNC(Me)CHC(Me)NAr}$_2$Sr(THF)] during synthesis and in solution, the analogous heteroleptic strontium species **34** was at first deemed unsuitable for catalysis. However, if the two-step route designed by Sarish *et al.* was used in place of the usual one-pot synthesis,[39] the heteroleptic strontium compound **34** could be isolated in satisfactory purity and yield (Scheme 42). A preliminary test with 1-amino-2,2-diphenyl-4-pentene at 5 mol% catalyst loading showed that **34** was efficient at catalysing the hydroamination/cyclisation process at temperatures up to 60 °C and over periods up to several days without any apparent redistribution towards the homoleptic complex detectable in the ^{1}H NMR spectra.

Scheme 42. Synthesis of heteroleptic *β*-diketiminate supported magnesium, calcium and strontium precatalysts.
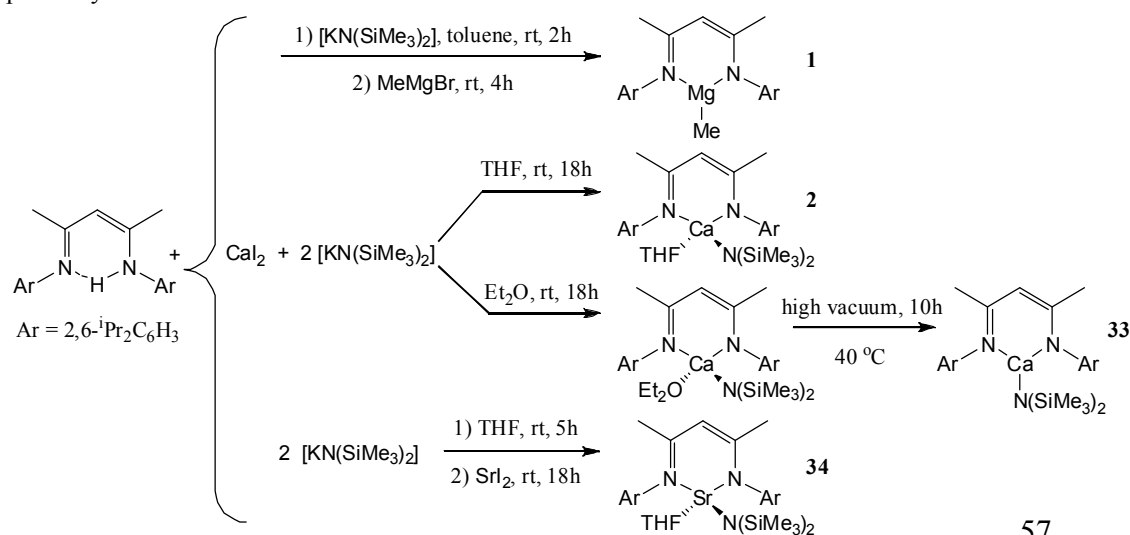
Initial attempts to effect the hydroamination/cyclisation of the linear and unsubstituted aminoalkene 1-amino-4-pentene with the homoleptic calcium amide [Ca{N(SiMe₃)₂}₂]₂ had resulted in failure, even at high catalyst loading and temperature.[52] Subsequent assessment of the ability of [Ca{N(SiMe₃)₂}₂]₂ to cyclise 1-amino-2,2-diphenyl-4-pentene, however, proved highly successful. For this reason the complete series of readily available homoleptic amides [M{N(SiMe₃)₂}₂]₂ (M = Mg **35a**, Ca **35b**, Sr **35c**, Ba **35d**),[142] along with their THF-solvated counterparts [M{N(SiMe₃)₂}₂(THF)₂] (M = Mg **36a**, Ca **36b**, Sr **36c**, Ba **36d**),[143] were included in this comparative and mechanistic study on the hydroamination/cyclisation reaction (Scheme 43). In addition the recently reported group 2 dialkyls [M{CH(SiMe₃)₂}₂(THF)₂] (M = Mg **37a**, Ca **37b**, Sr **37c**, Ba **37d**), whose reactivity has yet to be fully investigated, were also included in this study.[144]

Scheme 43. Synthesis of homoleptic alkaline earth amide and alkyl precatalysts.

MgBu₂ + 2 HN(SiMe₃)₂   THF, rt, 18h → [M{N(SiMe₃)₂}₂(THF)₂] **35a-d**

MI₂ + 2 [KN(SiMe₃)₂]   1) Et₂O, rt, 18h → [M{N(SiMe₃)₂}₂]₂ **36a-d**

M = Ca, Sr, Ba   2) high vacuum, 40 °C, 8h

MI₂ + 2 [KCH(SiMe₃)₂]   THF, rt, 18h → [M{CH(SiMe₃)₂}₂(THF)₂] **37a-d**

M = Mg, Ca, Sr, Ba   **glass-coated stirrer bar**
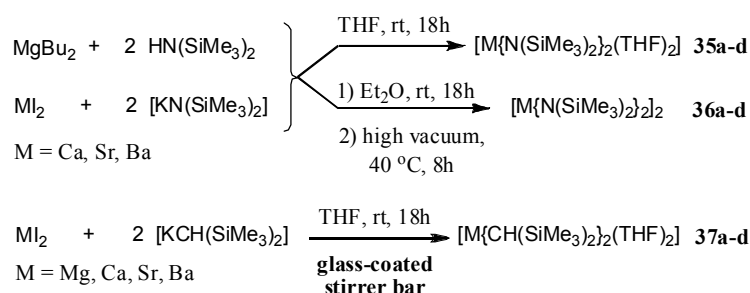
The magnesium dialkyl [Mg{CH(SiMe₃)₂}₂(THF)₂] **37d** was synthesised in an manner analogous to that of the previously reported calcium, strontium and barium dialkyls (Scheme 43). Regarding the synthesis of compounds **37a-d** it was found that the use of glass-coated stirrer bars instead of the usual PTFE stirrer bars greatly improved purity and yields as both the potassium and heavier alkaline earth alkyls (Ca, Sr, Ba) may react with PTFE, yielding impure compounds. Storage of a hexane solution of **37a** at -30 °C yielded a crop of colourless crystals suitable for X-ray diffraction. The result of this experiment is presented in Figure 20. The compound crystallises as a *pseudo*-tetrahedral bis(THF) adduct with C_2 symmetry around the magnesium centre. The Mg-C distance of 2.1882(15) Å is significantly longer than the ones in the related solvent-free, polymeric [Mg{CH(SiMe₃)₂}₂]ₙ [2.117(4) and 2.105(4) Å],[145] the diethyl ether-solvated monomer [Mg{CH(SiMe₃)₂}₂(OEt)] [2.141(2) Å][146] or the solvent-free two-coordinate tris(trimethylsilyl)methyl derivative [Mg{C(SiMe₃)₃}₂] [2.116(2) Å].[147]

58

Attempts to prepare the analogous series of unsolvated group 2 dialkyl compounds [M{CH(SiMe$_3$)$_2$}$_2$] (M = Mg, Ca, Sr, Ba) following a similar procedure in diethyl ether instead of THF repeatedly failed due to ether cleavage side reactions.

Figure 20. ORTEP representation of compound **37a**. Thermal ellipsoids drawn at 30% probability. H atoms removed for clarity. Selected bond lengths (Å): Mg-C(1) 2.1882(15), Mg-O 2.1043(12). Selected angles ($^{\circ}$): C(1)-Mg-C(1)' 137.32(9), C(1)-Mg-O 106.51(5), C(1)-Mg-O' 104.34(5), O-Mg-O' 86.07(7).
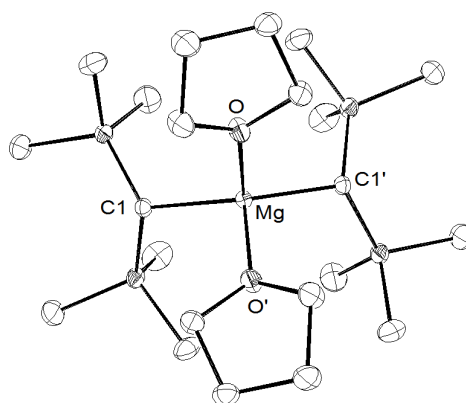
2.3   Reaction scope

Hydroamination/cyclisation with magnesium, calcium and strontium precatalyst loadings of 2-20 mol% afforded a series of substituted pyrrolidines and piperidines in near quantitative yields under relatively mild conditions (25-100 $^{\circ}$C). Formation of hexahydroazepines was only observed in low to moderate yield at high temperature and over extended periods of time with magnesium precatalysts **35a** and **36a** (Table 1, entry 20). The structures of the cyclised products were assigned by comparison with literature ^{1}H NMR data. Comparative results for the reactions performed with the bis(amides) **35a-c** and **36a-c** and the dialkyls **37a-c** are listed in Table 1. Data related to the β-diketiminate-stabilised complexes **1**, **2**, **34** and **35** are provided in Table 2.

Attempts to catalyse the hydroamination/cyclisation of 1-amino-2,2-diphenyl-4-pentene with barium precatalysts **35-37d** resulted in a maximum of two turnovers and was accompanied by the precipitation of insoluble, unidentifiable products. This implies that reactivity is limited to a stoichiometric reaction of the substrate with both amide or alkyl moieties of the precatalyst. This behaviour is likely the consequence of the very large size of the cationic barium centre in which the diffuse charge is not efficient at polarising the alkene bond in order to effect the insertion of the C=C bond.

59

A limitation of strontium system **34** became apparent at temperatures above 60 ^{o}C, in which case catalysis was accompanied by irreversible Schlenk-like ligand redistribution towards the homoleptic species, as observed by ^{1}H NMR spectroscopy. The dialkyl systems **37a-c** also showed serious limitations at temperatures above 40 ^{o}C or over periods of time exceeding 30 hours at room temperature. Under such conditions these precatalysts underwent irreversible degradation into insoluble, and as yet unidentified, catalytically inactive species. As a result, compounds **37a-c** could only be used for the cyclisation of a very limited number of substrates. Monitoring of C_6D_6 solutions of **37a-c** in the absence of substrate over a week showed that these alkyl species tend to decompose over time, even at room temperature, into $CH_2(SiMe_3)_2$ and unidentified insoluble species, the degradation rate increasing dramatically down the group.

In all cases, calcium precatalysts **35-37b** displayed higher catalytic activities than their strontium analogues **35-37c**, which in turn proved far more reactive than the magnesium species **35-37a**. Previous comparison between calcium complex **2** and the related magnesium compound **1** had already shown **2** to be the more active species.[54] It was proposed that the increase in ionic radius from 0.72 Å for Mg^{2+} to 1.00 Å for Ca^{2+} (in six-coordinate complexes) provides higher coordinative unsaturation at the calcium centre, and thus improved access towards substrate binding and alkene pre-coordination. A similar trend can be found in the lanthanide series where turnover frequency markedly decreases with the ionic radius of the metal centre.[53] An extrapolation of this rationale to strontium, with a six-coordinate Sr^{2+} radius of 1.16 Å, would therefore provide the expectation of even higher turnover frequencies than calcium. Previous qualitative comparison of calcium and strontium systems for the hydroamination/cyclisation of aminoalkenes, however, had shown than strontium triazenide and aminotroponiminate precatalysts are less active than their calcium counterparts.[60, 61] Similarly, among the precatalysts studied here, the strontium systems were less active than their calcium counterparts, both in qualitative and quantitative analyses.

As expected, the coordinative unsaturation of the calcium centre in complex **33** afforded a substantial increase in catalytic activity when compared to the THF-solvated complex **2**. The unsolvated bis(amide) complexes **35a-c**, however, displayed lower turnover frequencies than their THF-solvated analogues **36a-c**, except in the case of substrates bearing secondary amine functionalities in which catalytic activity was reversed (Table 1, entries 22-28).

Table 1. Scope of intramolecular hydroamination of aminoalkenes with precatalysts **35-37**.

Entry	Substrate	Product	Catalyst (mol %)	Time / h			T / °C	NMR yield / %[a]		
				35	**36**	**37**		**35**	**36**	**37**
1	(structure)	(structure)	**a-c** (10 mol%)		48		100		0	
2	(structure)	(structure)	**a** (10 mol %)	5 d	4 d	16	80	60	75	2[b]
3			**b** (2 mol %)	6	5	16	60		>99	
4			**c** (2 mol %)	10	8	16	60		97-99	
5	(structure)	(structure)	**a** (10 mol %)	48	42	16	25	95	97	2[b]
6			**b** (2 mol %)	1	0.75	0.25	25		93-99	
7			**c** (2 mol %)	24	8	0.25	25		96-98	
8	(structure)	(structure)	**a** (2 mol %)	6	5	0.25	25		98-99	
9			**b** (2 mol %)	0.25	0.25	0.1	25		98-99	
10			**c** (2 mol %)	24	8	0.25	25		96-98	
11	(structure)	(structure)	**a** (10 mol %)	62	36	4d	25	99	99	2[b]
12			**b** (10 mol %)	24	16	15 d	25	96	99	58[c]
13			**c** (10 mol %)	66	66	10 d	60	27[c]	48[c]	47[c]
14	(structure)	(structure)	**b** (20 mol%)	6 d	6 d	6 d	100	0	63	0
15			**c** (20 mol%)	6 d	6 d	6 d	100	0	0	0
16	(structure)	(structure)	**a-c** (20 mol %)	24	24	24	100	0	0	0

	The following experiments were carried out with **35** and **36** only			**35**	**36**			**35**	**36**	
17	(structure)	(structure)	**a** (10 mol %)	16	16		60		>99:0[d]	
18			**b** (10 mol %)	23	23		60	51:33[d]	40:54[d]	
19			**c** (10 mol%)	5d	5d		60	6:33[d]	9:37[d]	
20	(structure)	(structure)	**a** (10 mol %)	9 d	9 d		100	19:0[d]	55:0[d]	
21			**b** (20 mol %)	3 d	3 d		80	0:7[d]	0:21[d]	
22			**c** (20 mol%)	2 d	2 d		100	0:4[d]	0:5[d]	
23	(structure)	(structure)	**b** (10 mol%)	45	21		25	94	7	
24				-	8		80	-	>99	
25			**c** (10 mol%)	21	45		25	7	92	
26				-	18		80	-	98	
27	(structure)	(structure)	**a** (10 mol%)	2 d	2 d		60	43	95	
28			**b** (10 mol%)	2 d	2 d		25	8[e]	12[e]	
29			**c** (10 mol%)	2 d	2 d		25	<5[e]	6[e]	
30	(structure)	(structure)	**b** (2 mol%)	-	0.5		25	-	>99	
31			**c** (2 mol%)	-	1.5		25	-	>99	

a) NMR scale reactions carried out in C_6D_6 or d_8-toluene, yields calculated from an internal TMSS standard. b) Solid instantly precipitated out of solution. Only one turnover observed. c) Solid slowly precipitated out of solution until catalysis stopped. d) Cyclisation: isomerisation. e) Substrate conversion >99%: the remaining products derive from isomerisation and recombination reactions.

Table 2. Scope of intramolecular hydroamination with precatalysts **1**, **2**, **33** and **34**.

Entry	Substrate	Product	Catalyst (mol %)	Time / h	T / °C	NMR yield / %[a]
1			**2** (10 mol%)[54]	21	25	90
2			**33** (10 mol%)	24	60	0
3			**34** (10 mol%)	24	60	0
4			**2** (2 mol %)[54]	2	25	>95
5			**33** (2 mol%)[54]	1.5	25	>99
6			**34** (2 mol %)	30	25	97
7			**1** (5 mol %)[54]	2	25	96
8			**2** (2 mol %)[54]	0.5	25	98
9			**33** (2 mol %)	0.2	25	97
10			**34** (2 mol %)	7	25	98
11			**1** (2 mol %)[54]	2	25	99
12			**2** (2 mol %)[54]	0.15	25	>99
13			**33** (2 mol %)	0.1	25	>99
14			**34** (2 mol %)	0.15	25	>99
15			**1** (5 mol %)[54]	0.5	25	86
16			**2** (5 mol %)[54]	0.5	25	92
17			**33** (5 mol %)	0.3	25	>99
18			**34** (5 mol %)	5	25	98
19			**1**[54], **2**[54], **33**, **34** (20 mol %)	3 d	80	0
20			**1** (10 mol %)	4	25	97:0[d]
21			**2** (10 mol %)	4	25	83:16[d]
22			**33** (10 mol %)	4	25	66:15[d]
23			**34** (10 mol %)	48	25	28:62[d]
24			**1** (20 mol %)	3 d	100	97:0[d]
25			**2** (20 mol %)	1 d	80	0:20[d]
26			**33** (20 mol %)	2 d	80	5:25[d]
27			**34** (20 mol %)	4 d	60	5:15[d]
28			**1** (20 mol %)[54]	2 d	25	81
29			**2** (20 mol%)[54]	2 d	25	>99
30			**33** (10 mol %)	18	25	95
31			**34** (20 mol %)	2 d	25	90
32			**1** (10 mol %)	2 d	80	95
33			**2** (10 mol %)	8	60	98
34			**33** (10 mol %)	3	25	>99
35			**34** (10 mol %)	18	25	78
36			**1** (10 mol %)	2 d	60	96
37			**2** (10 mol %)	2 d	25	60[e]
38			**33** (10 mol %)	18	25	47[e]
39			**34** (10 mol %)	18	25	<5[e]
40			**2** (2 mol %)	0.15	25	>99

As previously reported for the hydroamination/cyclisation of a range of substrates with precatalysts **1** and **2**,[54] the rate of catalysis was found to be heavily dependent on the substitution pattern of the aminoalkene (Figure 21). Substrates presenting sterically demanding geminal substituents in the *β*-position of the amine moiety gave the highest reaction rates at minimal catalyst loading and room temperature (Table 1, entries 5-10; Table 2, entries 7-14). These substrates benefit from a favourable Thorpe-Ingold effect: the bulkier the geminal substituents (Ph > Cy > Me >>> H), the more constrained the conformational freedom of the aminoalkene, which in turn provides a favourable conformation for the alkene insertion step. In contrast to the formation of 2-methylpyrrolidine observed in the presence of calcium precatalyst **2** (Table 2, entry 1)[54] cyclisation of the unsubstituted 1-amino-4-pentene substrate was observed with neither of the homoleptic precatalysts **35-37** (Table 1, entry 1), nor with the *β*-diketiminato strontium species **34** or the THF-free heteroleptic calcium compound **33**, even after prolonged heating at 60 °C (Table 2, entries 2-3). These observations suggest that substrates which do not intrinsically benefit from a favourable Thorpe-Ingold effect require the presence of the sterically constraining *β*-diketiminate ligand, combined with the relatively small calcium metal centre and the added steric demands of the THF co-ligand in order to induce a propitious conformation for the alkene to approach the metal centre and induce the insertion step.

Figure 21. Influence of the substitution pattern of the aminoalkene on catalysis rates.
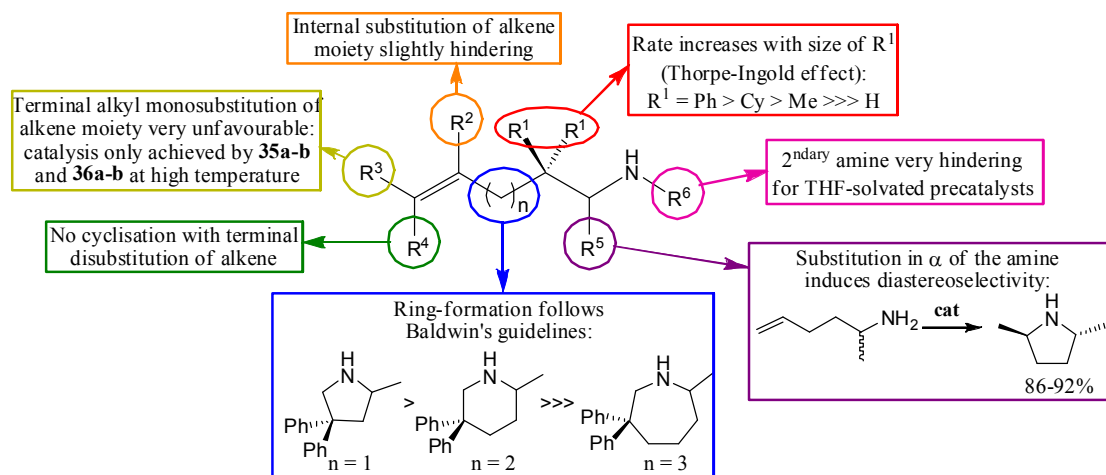
Alkyl substitution of the alkene moiety induced a significant decrease in the reaction rate. Both terminal mono- and disubstitution entirely prevented cyclisation for the *β*-diketiminate derivatives **33** and **34** (Table 2, entry 19). Transformation of a terminally

alkyl-monosubstituted aminoalkene, 1-amino-2,2-diphenyl-4-hexene, into 2-ethyl-4,4-diphenylpyrrolidine could, however, be achieved with calcium precatalyst **36b** (Table 1, entry 14) under forcing conditions (100 $^{\circ}$C), although the high catalyst loading (20 mol%) combined with a low yield (63%) militate against a truly catalytic process. Although generally more active than the homoleptic bis(amide) compounds, the calcium and strontium β-diketiminato species **2**, **33** and **34** were observed to undergo competitive and irreversible ligand redistribution towards the homoleptic species at such high temperatures and, therefore, may be judged as unsuitable for the cyclisation of substrates with unactivated internal olefins. This is most likely the consequence of electronic factors as the presence of electron-donating alkyl substituents on the alkene moiety could destabilise the insertion transition state which involves negative charge build-up and partial 2° and 3° alkyl character on the alkene residue. This was confirmed by the facile cyclisation of phenyl-substituted 1-amino-2,2-dimethyl-5-phenyl-4-pentene (Table 1, entries 30-31 and Table 2, entry 40), in which the negative charge on the incipient benzylic carbon is stabilised by the phenyl group. Whereas lanthanide catalysts have been designed to specifically allow the facile hydroamination of aminoalkenes bearing unactivated internal olefins,[134, 135] this is a rare example of successful cyclisation of such as substrate by a group 2 complex.[62]

As has been reported previously,[54] ring formation followed Baldwin's guidelines, with formation of five-membered rings being significantly easier than that of six- or seven-membered heterocycles.[148] In all cases higher catalyst loadings, temperatures and time periods were necessary to obtain piperidines compared to pyrrolidines. Although formation of a seven-membered ring could be observed with the magnesium compounds **35a** and **36a** (Table 1, entry 20), and to a much lesser extent with calcium and strontium species **33** and **34** (Table 2, entries 26-27), reaction conditions and the formation of alkene-isomerised by-products diminish the viability of this reaction with these latter precatalysts. Only β-diketiminate-stabilised magnesium precatalyst **1** provided a near quantitative route towards formation of hexahydroazepines (88%) after prolonged periods of time at 80 $^{\circ}$C.[54]

As previously reported for similar catalysis performed with **2**,[54] the cyclisation of 1-amino-2,2-diphenyl-5-hexene with all calcium and strontium precatalysts in this study afforded, next to the cyclised piperidine, the alkene isomerisation by-product *trans*-1-amino-2,2-diphenyl-4-hexene, identified by ^{1}H NMR, as the major product (Table 1, entries 18-19; Table 2, entries 21-23). The *trans* geometry was unambiguously assigned

by comparison with the independently synthesised *trans*-1-amino-2,2-diphenyl-4-hexene. In the case of calcium precatalysts **35b** and **36b**, a small amount of cyclisation of the isomerisation product *trans*-1-amino-2,2-diphenyl-4-hexene into 2-ethyl-4,4-diphenylpyrrolidine was observed at temperatures above 60 $^{\circ}$C. As was the case with magnesium precatalyst **1**,[54] no such isomerisation was observed with the bis(amide) species **35a** and **36a**, which contain the smaller and, therefore, more sterically congested Mg^{2+} cation (Table 1, entry 17).

While alkene isomerisation by-products have not been reported in lanthanide-catalysed intramolecular hydroamination, they have been observed during the cyclisation of *N*-benzyl-1-amino-4-pentenes and *N*-benzyl-1-amino-5-hexenes with [Ir(COD)Cl]$_2$,[122] as well as for the hydroamination of a variety of 1-amino-4-pentenes catalysed by *n*-BuLi.[101, 104] It was apparent that the proportion of isomerised by-product increases with the size of the metal cation, as well as with conformational freedom around the metal centre and reaction temperature. These observations can be rationalised by taking into consideration the isomerisation mechanism – dependent on the conformational freedom of the alkene chain – of the amide resting state laid out in Scheme 44. In the first case, insertion of the alkene into the metal-amide bond followed by protonolysis leads to liberation of the piperidine. In the second, isomerisation to a boat-type conformation may lead to intramolecular proton-transfer to yield an η^3-allyl complex which, upon protonolysis, liberates either the internally isomerised aminoalkene or the substrate.

Scheme 44. Isomerisation versus cyclisation for 1-amino-2,2-diphenyl-5-hexene.

65
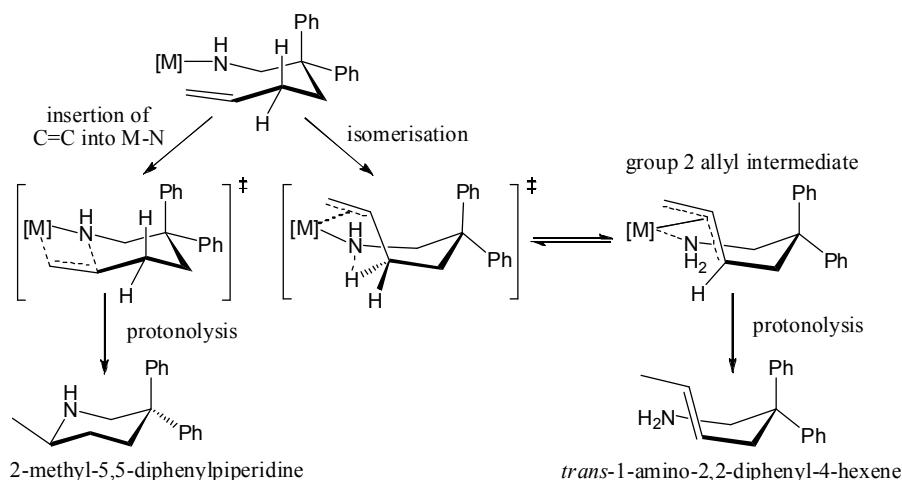
Attempts to cyclise 1-amino-2,2-diphenyl-6-heptene with the homoleptic and heteroleptic calcium and strontium species **35-36b**, **35-36c**, **33** and **34** resulted in the formation of a small amount of *trans*-1-amino-2,2-diphenyl-5-heptene as the only identifiable product (Table 1, entries 21-22; Table 2, entries 26-27). Further isomerisation to 1-amino-2,2-diphenyl-4-heptene or cyclisation of the isomerised chain could not be observed under the reaction conditions. Again, no isomerisation occurred with the magnesium precatalysts **35a** and **36a** (Table 1, entry 21).

Alkene isomerisation by-products were also observed during the reaction of N-allyl-1-amino-4-pentene with all calcium and strontium precatalysts (Table 1, entries 28-29; Table 2, entries 37-39). ^{1}H NMR spectra showed a complex mixture of at least half a dozen different products, depending on the nature and concentration of the precatalyst and the reaction temperature. The mono-cyclised product *N*-allyl-2-methylpyrrolidine recently reported with **2** could, in all cases, be easily identified,[54] as well as its *N*-(*trans/cis*-1-propenyl)-2-methylpyrrolidine isomers and various isomers of the substrate. A scale-up of the reaction to 300 mg of substrate with 10 mol% of **36c** at 80 °C over three days, and subsequent fractional distillation of the volatile products, allowed isolation of further components, among which small amounts of the bi-cyclised product already reported for lanthanide-mediated tandem hydroamination/cyclisation, 1-amino-4-pentene and *(E)-N-((E)-2-methylpent-2-enylidene)pent-4-en-1-amine* **38** which were unambiguously identified by NMR spectroscopy as well as by ESI-MS (Scheme 45).

Scheme 45. Range of products obtained from the attempted hydroamination/cyclisation of *N*-allyl-1-amino-4-pentene with calcium and strontium precatalysts **35-36b**, **35-36c**, **2**, **33** and **34**.
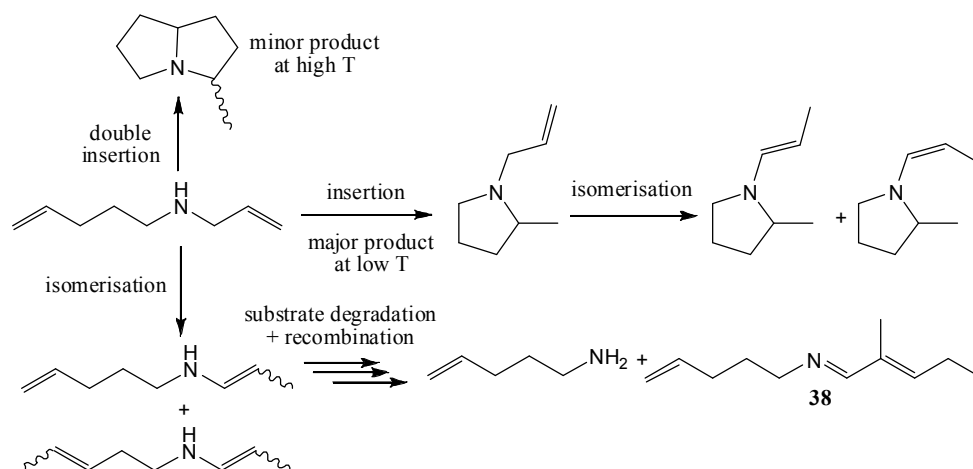
The proportion of **38**, easily identifiable in the ^{1}H NMR spectra by a low-field singlet at 8.32 ppm for the imine N=C*H* and a corresponding ^{13}C NMR signal at 165.8 ppm,

increased with temperature and size of the precatalyst metal centre. It is as yet unclear what mechanism might be at work in the formation of this product. Magnesium compounds **35-36a** and **1** were the only precatalysts to cleanly afford mono-cyclised *N*-allyl-2-methylpyrrolidine as the single product (Table 1, entry 27; Table 2, entry 36).

Another secondary amine substrate, *N*-benzyl-(1-allylcyclohexyl)methylamine, was cleanly converted by all precatalysts into the expected *N*-heterocyclic product (Table 1, 23-26; Table 2, entries 32-35). A marked increase in reactivity was observed for the THF-free *β*-diketiminate complex **33** compared to the solvated analogue **2**. The reaction using 10 mol% of **33** proceeded to completion within 3 hours at room temperature, whereas the reaction with 10 mol% of **2** required heating to 60 $^{\circ}$C for 8 hours, showing that access to the metal centre is essential for the pre-coordination/protonolysis of encumbered secondary amines (Table 2, entries 30-31). Contrary to observations for all primary amine substrates, the unsolvated bis(amide) species **35a-c** presented significantly faster catalysis than THF-solvated compounds **36a-c** for this substrate (Table 1, entries 22-25) . An attempt to explain this inversion of reactivity will be provided through the kinetic studies described later (*vide infra*).

In the presence of **33** and **34**, 2-amino-5-hexene, a substrate possessing two prochiral centres, underwent diastereoselective hydroamination/cyclisation, yielding the *trans*-pyrrolidine in diastereomeric excess of 72% and 76% for **33** and **34** respectively (Table 2, entries 27-28). For comparison the calcium and magnesium analogues **1** and **2** provided a diastereomeric excess of 78% and 84% respectively.[54] Similarly, Roesky and co-workers had reported a 60% diastereomeric excess for the same reaction with calcium aminotroponiminate precatalyst **5**.[59] The relative stoichiometry of the products was assigned by integrating two distinct ^{1}H NMR multiplets of the *trans* (3.15 ppm) versus the *cis* product (2.92 ppm). This confirms the trend that diastereoselectivity increases inverse to the size of the group 2 metal centre when using a given ligand set. The *trans*-selectivity can be rationalised by comparing the four isomers of the 7-membered chair transition state shown in Figure 22. For both the (*S*) and the (*R*) enantiomers of the substrate, the transition state leading to the *cis* product is disfavoured by a 1,3-diaxial methyl-proton interaction, which may be exacerbated by the additional steric crowding and shorter M-N and M-C bond lengths around a smaller metal cation, or in the presence of coordinated THF. This leads to the observed trend of decreasing diastereomeric excess for **1** > **2** > **34** > **33**. Marks and co-workers have reported a similar trend in related chemistry utilising the lanthanide series.[53]

Figure 22. Qualitative comparison of the transition state energies for the cyclisation of racemic 2-amino-5-hexene.
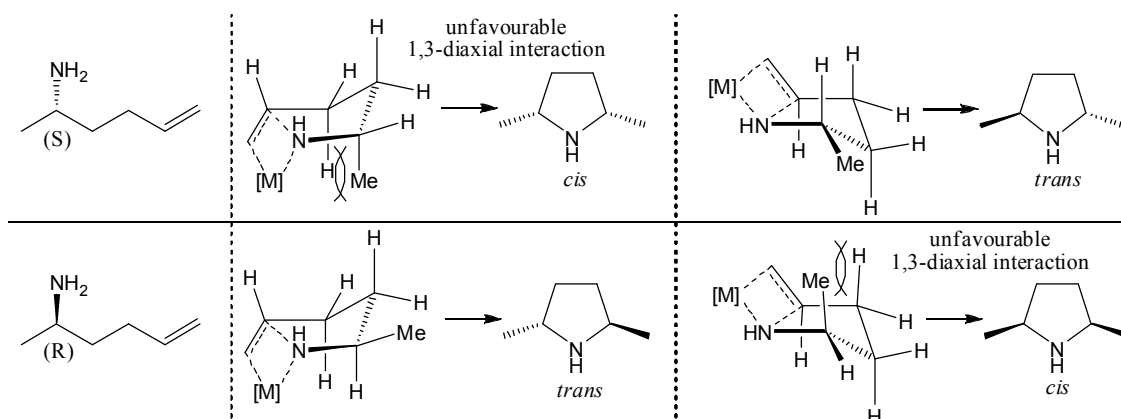
These qualitative observations all lead to the conclusion that the group 2-mediated hydroamination/cyclisation of aminoalkenes is largely dominated by steric (influence of the sterically demanding β-diketiminate ligand and THF co-ligand, Thorpe-Ingold effect, ease of ring-formation, substitution of the amine, diastereoselectivity, alkene isomerisation side reactions) and electronic effects (substitution of the alkene moiety, non-linear effect of the metal centre: Ca > Sr >Mg >>> Ba), the key step seeming to be the creation of a favourable conformation for the alkene pre-coordination and insertion to take place.

2.4   Mechanistic analyses

2.4.1   Catalyst initiation

As was highlighted previously, reactions involving silylamide precatalysts may provide reversible entry into the catalytic cycle due to the comparable acidity of the aminoalkene substrate and the protonolysis product, hexamethyldisilazane.[54] The stoichiometric reaction of **2** with benzylamine, for example, provided a quantifiable dynamic equilibrium between a dimeric heteroleptic calcium benzylamide complex and the starting materials, which lay in favour of the benzylamide species at room temperature (ΔG^{o} (298 K) = -11.4 kJ.mol^{-1}).[56] In contrast, the reaction of **2** with the potentially bidentate 2-methoxyethylamine resulted in quantitative formation of the heteroleptic calcium primary amide and demonstrated that, under certain conditions, the position of the amine/amide equilibrium may be perturbed significantly to one side.[54, 55]

In order to further quantify the potentially reversible protonolytic entry into the catalytic cycle, similar analyses were performed upon stoichiometric reactions between the calcium and strontium complexes **35-36b** and **35-36c** (0.19 M) and two equivalents of the non-cyclisable substrate 1-amino-2,2-diphenyl-5,5-dimethyl-4-pentene. In each case variable temperature ^{1}H NMR experiments indicated the establishment of similar transamination equilibria for these homoleptic precatalysts. These were followed by integrating the bis(trimethylsilyl)amide singlet of the precatalyst against that of the protonated hexamethyldisilazane. Examination of the resultant ^{1}H NMR spectra seemed to suggest that, despite the presence of two silylamide substituents per alkaline earth centre and, thus, two potential catalytic sites, never more than one of these underwent amine/amide exchange at a time. Although it is probable that the complexes resulting from this amine/amide exchange are dimeric in solution, by analogy with previously characterised heteroleptic calcium and magnesium primary amides obtained by protonolysis with a primary amine,[54] the exact nuclearity of each of the reactions remains uncertain. A variety of equilibria may indeed be envisaged, as depicted in Scheme 46.

Scheme 46. Possible transamination equilibria between **35b-c** or **36b-c** and 1-amino-2,2-diphenyl-5,5-dimethyl-4-pentene.
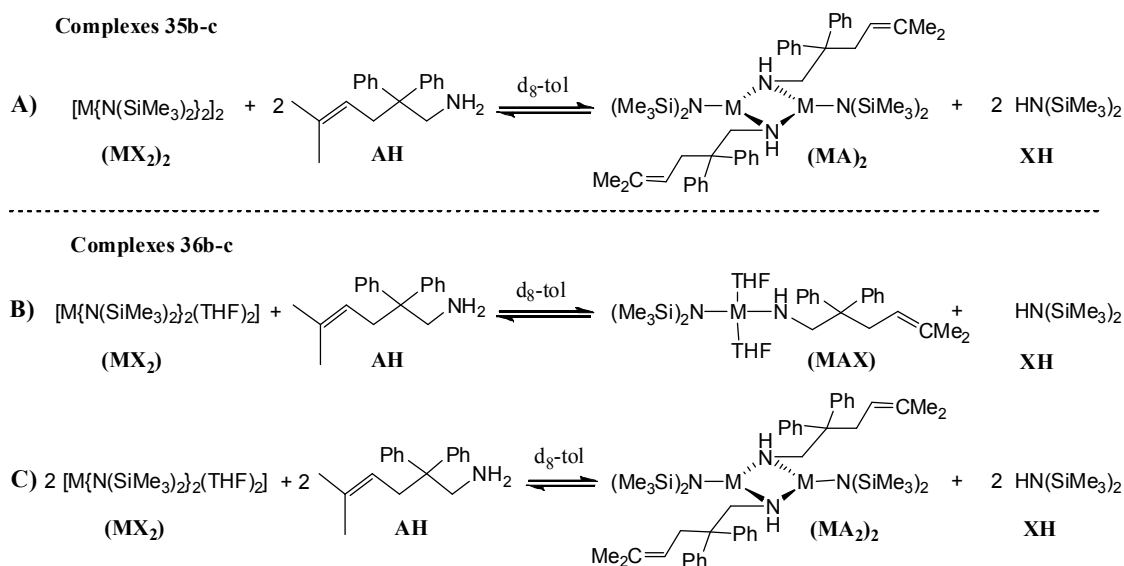
The complexity of these equilibria, which might coexist in solution, and the consequent uncertainty over the nuclearity of the various alkaline earth-containing components would make a quantitative discussion of these data imprudent. Inspection of the temperature-dependent data, however, revealed each reaction to be mildly

endothermic (ΔG^o (298 K) ~ 6 kJ.mol^{-1}) irrespective of the reaction stoichiometry employed to deduce the equilibrium constants (Figure 23).

Figure 23. van't Hoff analyses of equilibria A-C for complexes **35b-c** and **36b-c** (Scheme 46).
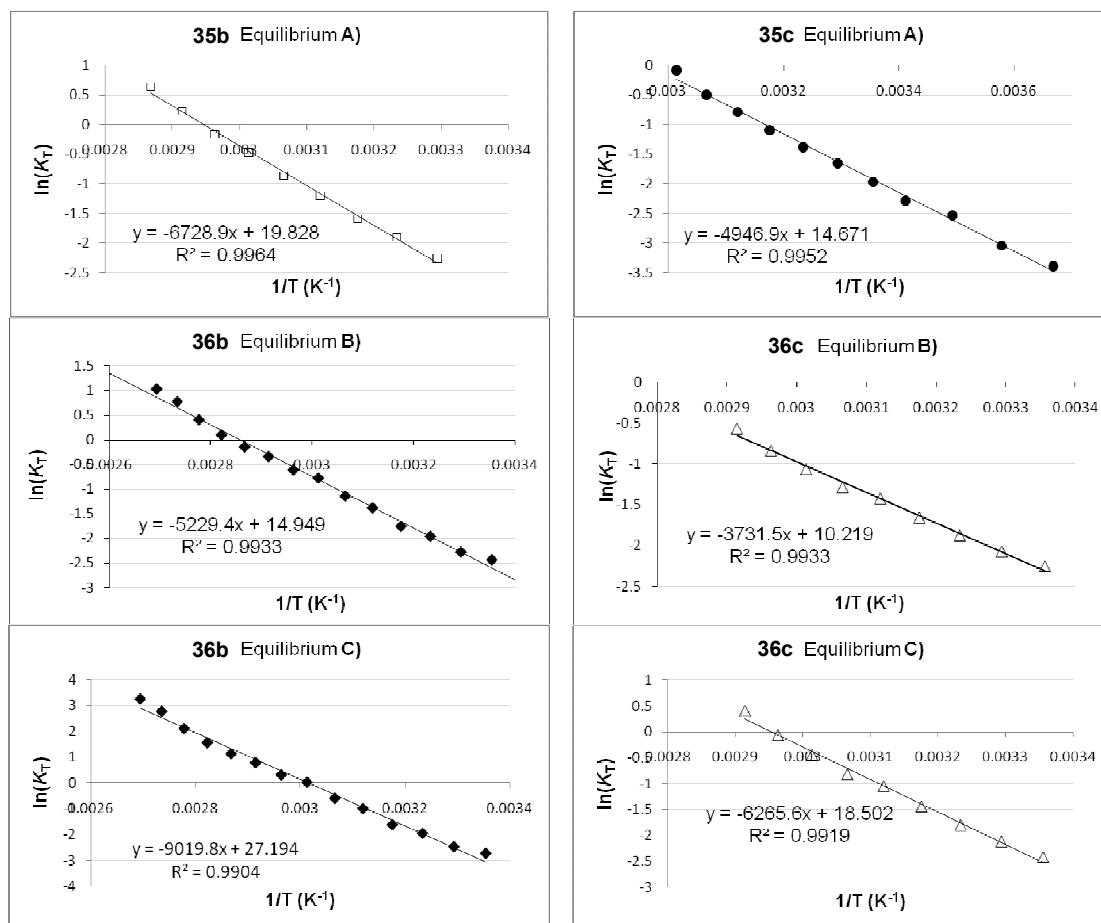
Thermodynamic data for each of the equilibria A-C presented in Figure 23 are displayed in Table 3. Similarly, for each of the catalytic reactions involving silylamide precatalysts presented in Tables 1 and 2, examination of the ^{1}H NMR data suggested that the equilibrium lies in favour of the starting materials during catalysis, which makes the use of alkyl-based catalysts with irreversible initiation all the more desirable.

Table 3. Thermodynamic data for equilibria A-C (Scheme 46)

	calcium			strontium		
	ΔH^o (kJ.mol^{-1})	ΔS^o (J.mol^{-1}.K^{-1})	ΔG^o(298 K) (kJ.mol^{-1})	ΔH^o (kJ.mol^{-1})	ΔS^o (J.mol^{-1}.K^{-1})	ΔG^o(298 K) (kJ.mol^{-1})
A)	55.9	165	6.8	41.1	122	4.8
B)	43.5	124	6.4	31.0	85	5.7
C)	75.0	226	7.6	52.1	154	6.3

70

Addition of a stoichiometric quantity of *tert*-butylamine or di-*iso*-propylamine to a C_6D_6 solution of **34** did not lead to any observable reaction, even after prolonged heating at 60 °C. Addition of one equivalent of 2,6-di-*iso*-propylaniline or diphenylamine, however, resulted in complete and instantaneous protonolysis of the hexamethyldisilazido group, followed by rapid, irreversible and quantitative redistribution towards the known homoleptic species [{ArNC(Me)CHC(Me)NAr}$_2$Sr(THF)] (Ar = 2,6-di-*iso*-propylaniline) and ill-defined strontium anilido or diphenylamido complexes. The stoichiometric addition of benzylamine to **34** at room temperature in C_6D_6, however, resulted in nearly complete conversion (95%) to the heteroleptic strontium benzylamide complex **40**. Two further species could be characterised in solution as strontium complex **34** (4%) and its benzylamine adduct **39** (1%), which persisted as components of a dynamic equilibrium with complex **40**, as shown in Scheme 47. It has previously been reported that the analogous reaction between calcium complex **34** and one equivalent of benzylamine results in a similar equilibrium between **34** and a heteroleptic calcium benzylamide complex which was isolated and characterised by X-ray crystallography as a dimeric species in the solid state.[56] Although no crystals of the strontium benzylamide complex suitable for X-ray diffraction analysis could be obtained, variable temperature ^{1}H NMR studies upon a d$_8$-toluene solution of the reaction mixture confirmed the existence of a dynamic equilibrium between **34**, **39** and **40**. As was the case in our previous study, elevated temperatures favoured both the starting materials and benzylamine adduct **39**, observed by the distinctive signals of the ligand backbone methine protons. Formation of homoleptic [{ArNC(Me)CHC(Me)NAr}$_2$Sr(THF)] was not observed within the temperature range (238-368 K) of the experiment. At temperatures below 288 K further fluxional processes prevented analysis of the data, but a ^{1}H NMR spectrum recorded at 238 K revealed two broad and highly shielded signals at -0.07 ppm and -1.19 ppm, tentatively attributed to the N*H$_2$* resonance of the benzylamine adduct **39** and the N*H* signal of the benzylamide complex **40** respectively. Due to the complexity of these equilibria involving three distinct strontium species and the uncertainty about the nuclearity of each of them, a quantitative assessment of the variable temperature ^{1}H NMR data was not carried out.

Scheme 47. Stoichiometric reactions between **34** and various amines.

Ar = 2,6-^{i}Pr$_2$C$_6$H$_3$
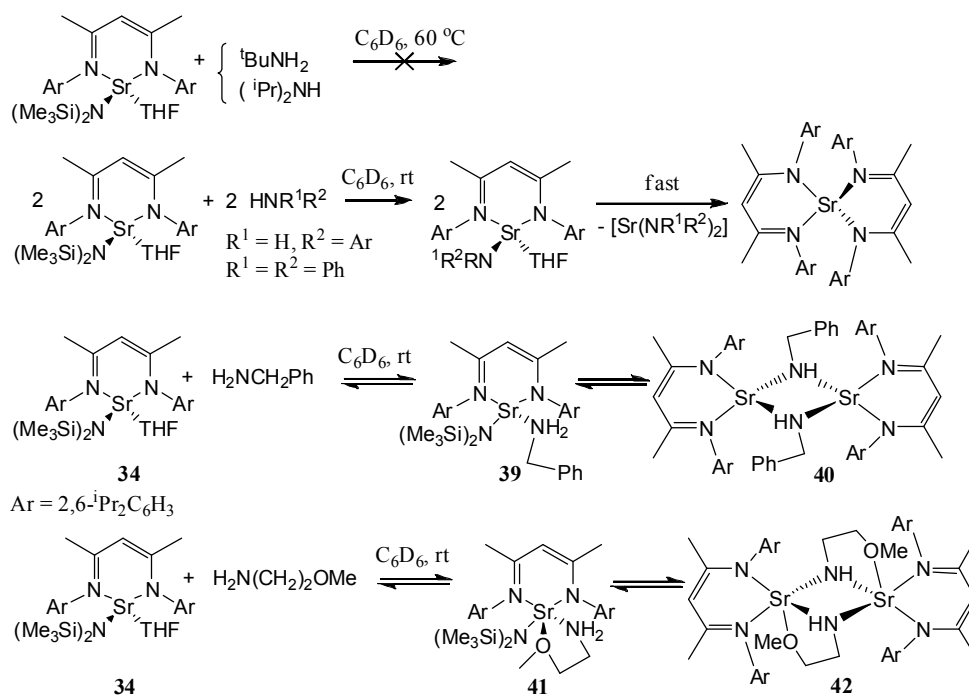
Reaction at room temperature between **34** and the potentially bidentate methoxyethylamine resulted in a 75:25 mixture of the amine adduct **41**, displaying a broad NH_2 triplet at -0.09 ppm in the ^{1}H NMR spectrum, and the amine/amide exchange product **42**, recognisable by a highly shielded NH resonance at -1.75 ppm. This observation contrasts markedly with the previously reported outcome of the analogous reaction with calcium compound **2**, which resulted in the stoichiometric formation of the heteroleptic calcium primary amide species.[55] The formation of a methoxyethylamine adduct species as the major component of the strontium-centred equilibrium was confirmed through the ambient temperature crystallisation of colourless crystals of compound **41** suitable for X-ray diffraction analysis. The result of this experiment is illustrated in Figure 24. Selected bond length and angle data are displayed in Table 4. The five-coordinate strontium centre adopts a slightly distorted square pyramidal geometry ($\tau = 0.22$)[149] with the bis(trimethylsilyl)amide ligand in the axial position. The β-diketiminate ligand backbone is planar and, similarly to the parent complex, **34**, forms a six-membered C$_3$N$_2$Sr ring envelope conformation with the metal centre. As a result of the near square pyramidal geometry the distance between the plane formed by the ligand framework and the strontium atom increases from 0.724 Å in **34** to 1.313 Å in **41**.[39] A significant increase in the Sr-N bond lengths to both the β-diketiminate and the silylamide ligands was also observed [Sr-N(1) 2.5742(14); Sr-N(2)

2.5424(14); Sr-N(3) 2.4909(14); Sr-O 2.6022(13) Å in **41** compared to Sr-N(1) 2.554(2); Sr-N(2) 2.514(2); Sr-N(3) 2.446(2); Sr-O 2.536(2) Å in **34**].[39] The strontium-amine bond distance of 2.7113(17) Å, is relatively short in comparison with the range of 2.743(4) to 2.853(4) Å described by Ruhlandt-Senge and co-workers for strontium-ethylenediamine interactions,[150] as well as the 2.702(13) to 2.830(2) Å range reported by Park *et al.* for a series of strontium diketonate complexes with polyamine donor ligands.[151] A space-filling model of the X-ray crystal structure demonstrates how efficiently the three ligands encapsulate the strontium metal centre from all sides (Figure 24).

Figure 24. Left: ORTEP representation of compound **41**. Thermal ellipsoids drawn at 30% probability. H atoms removed for clarity except those bound to N(4). Right: Space-filling model of **41** illustrating the total encapsulation of the metal centre.
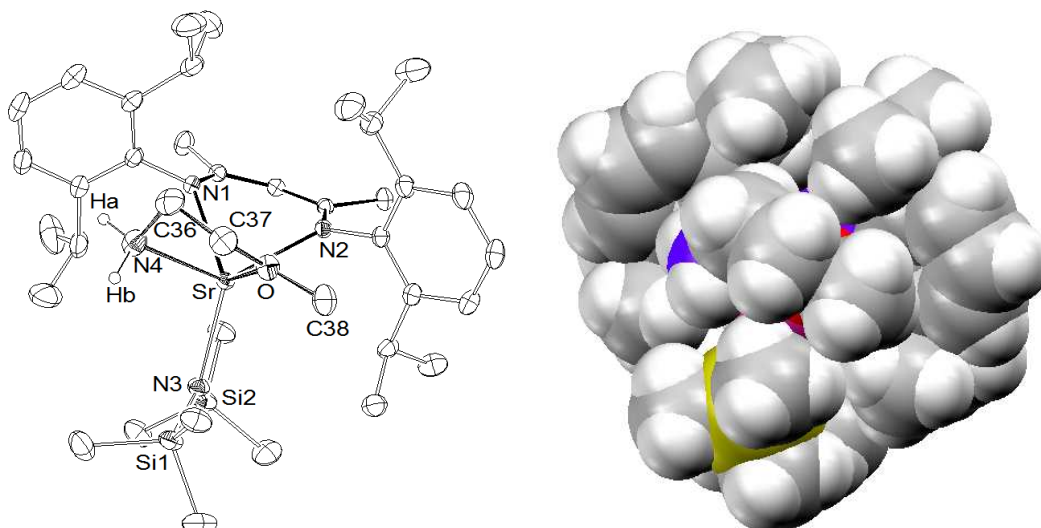
Table 4. Selected bond lengths (Å) and angles (°) for compound **41**.

Bond lengths (Å)	**41**	Angles (°)	**41**
Sr-N(1)	2.5742(14)	N(1)-Sr-N(2)	73.77(4)
Sr-N(2)	2.5424(14)	N(1)-Sr-N(3)	123.62(5)
Sr-N(3)	2.4909(14)	N(2)-Sr-(N3)	121.24(5)
Sr-N(4)	2.7113(17)	N(1)-Sr-O	117.55(4)
Sr-O	2.6022(13)	N(2)-Sr-O	87.96(4)
N(4)-C(36)	1.465(3)	N(3)-Sr-O	117.00(5)
		N(4)-Sr-O	64.75(5)
		Sr-N(4)-C(36)	103.97(12)
		Sr-O-C(37)	118.36(12)

Although a general interpretation of these individual transamination equilibria should be treated with caution, it is apparent that the mild endo- or exothermicity of catalyst initiation is dependent not only upon the identity of the alkaline earth catalytic centre but also upon the characteristics of the resultant acid/base pair. Although not rate-determining, these potentially reversible catalyst initiation equilibria certainly play an influential role in any specific catalytic reaction employing an alkaline earth precatalyst derived from the conveniently employed hexamethyldisilazide anion.

2.4.2 Kinetic studies

With these considerations in mind, a kinetic study of the cyclisation of (1-allylcyclohexyl)methylamine with the calcium and strontium precatalysts **2**, **33**, **34**, **35-36b** and **35-36c** in C_6D_6 (determination of order in catalyst, 0.56 M substrate solutions) or d_8-toluene (Eyring and Arrhenius plots, 0.80 M substrate solutions, 2 mol% catalyst loading) was conducted by ^{1}H NMR spectroscopy (Figure 25).

Figure 25. Example of ^{1}H NMR stack plot of the cyclisation of (1-allylcyclohexyl)methylamine with calcium and strontium group 2 amide precatalysts.

74
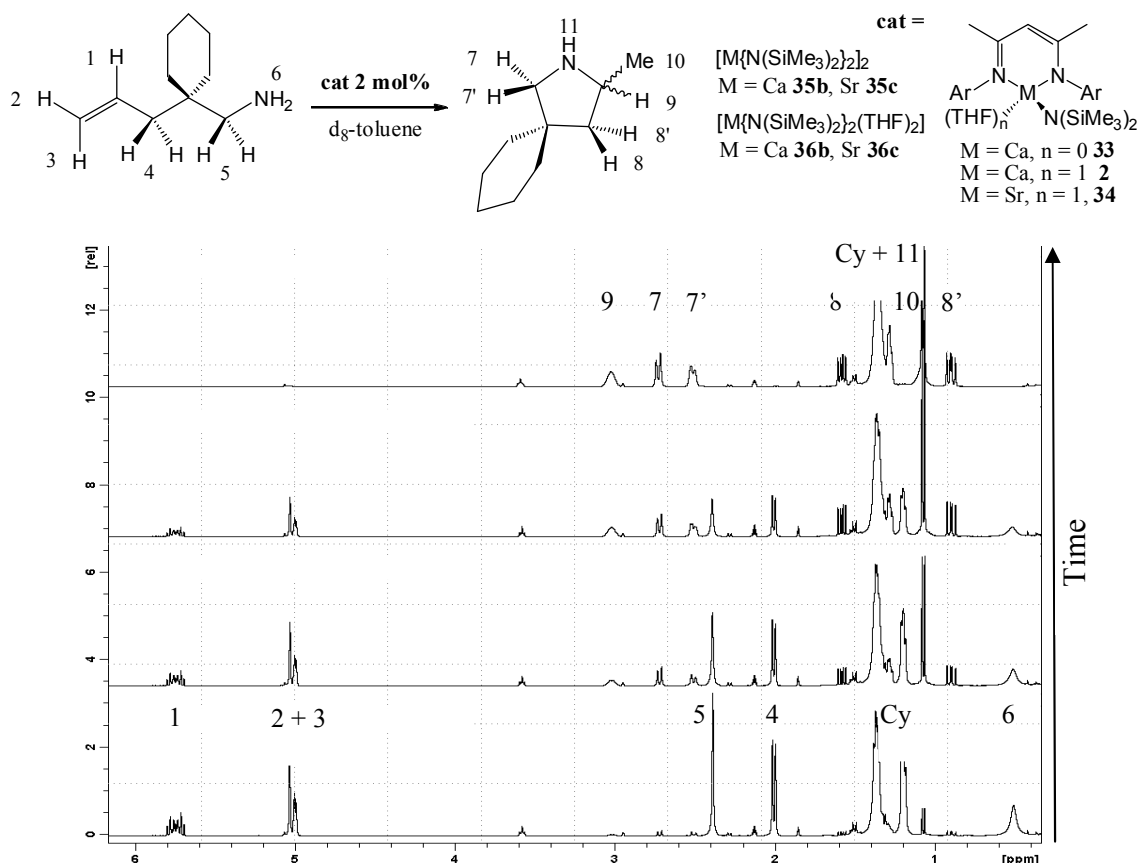
The dialkyl species **37b-c** could not be reliably assessed due to the extremely rapid conversion of the chosen substrate, which generally resulted in more than 70% conversion even before start of the NMR monitoring. Magnesium precatalysts **1** and **35-36a** were not included in this kinetic study either due to their exceedingly low turnover frequency at such low catalyst loading. NMR solutions were prepared in the glovebox, immediately frozen to 193 K and then thawed directly before transferring them to the NMR spectrometer. Conversion to the heterocyclic product was followed by integrating substrate and product peaks relative to an internal tetrakis(trimethylsilyl)silane (TMSS) standard. Substrate consumption was monitored over three half-lives. Reaction rates were derived from plots of $\ln([substrate]_t/[substrate]_{t=0})$ versus time. As previously determined with **1** and **2**,[54] reactions evidenced an apparent first-order decline in [substrate] as shown by the example in Figure 26.

Figure 26. Example of variable temperature kinetic analysis: plot of $\ln([substrate]_t/[substrate]_{t=0})$ versus time (min) at 4 different temperatures for 0.8 M (1-allylcyclohexyl)methylamine and 2 mol% of **34** in d_8-toluene. The slope of each linear set of data points corresponds to the reaction rate constant k (min^{-1}).
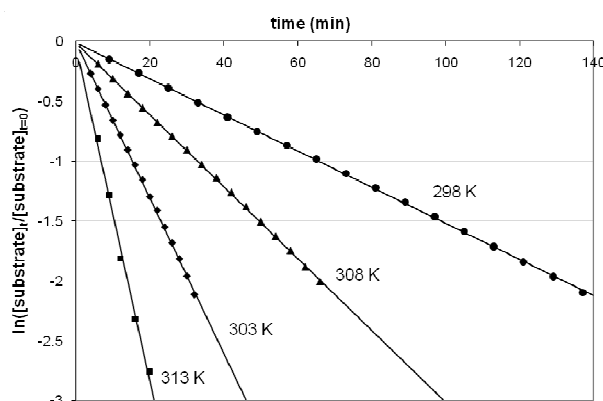
For each precatalyst, substrate cyclisation was monitored at four to five different temperatures. The temperature range of these experiments remained limited to 20 $^{\circ}$C, outside which the reaction was either to fast or to slow to monitor over three half lives. This resulted in relatively high standard errors, especially in the case of activation entropies, although comparison with literature data shows that errors of this magnitude are by no means uncommon in the determination of $\Delta S^{\ddagger}$ (see Table 5).

Arrhenius analyses of the data sets thus obtained afforded activation energies (E_a) of 81.2 (1.4) (**36b**), 84.7 (5.5) (**35b**), 86.2 (3.2) (**36c**) and 93.6 (0.7) kJ.mol^{-1} (**35c**) in accordance with the qualitative decrease of reaction rate already observed for this series of bis(amide) precatalysts, and of 65.5 (1.9) (**2**), 81.9 (3.5) (**33**) and 87.9 (2.8) kJ.mol^{-1} (**34**) for the β-diketiminate-stabilised complexes (Figure 27). Surprisingly the activation

energy for **33** was significantly higher than for **2** despite the fact that **33** was found, in all cases, to provide the fastest turnover.

Figure 27. Top: Arrhenius plot of ln(k) (k = reaction rate, s^{-1}) versus 1/T (T = temperature, K) for calcium complexes **35-36b** and strontium complexes **35-36c**. Bottom: *idem* for calcium and strontium β-diketiminate complexes **2**, **33** and **34**. Activation energies (E_a) were calculated from the slope (E_a/R; R = 8.314472 J.mol^{-1}.K^{-1}) of each linear set of data points. Data were collected at [(1-allylcyclohexyl)methylamine] = 0.8 M and 2 mol% catalyst loading in d$_8$-toluene.
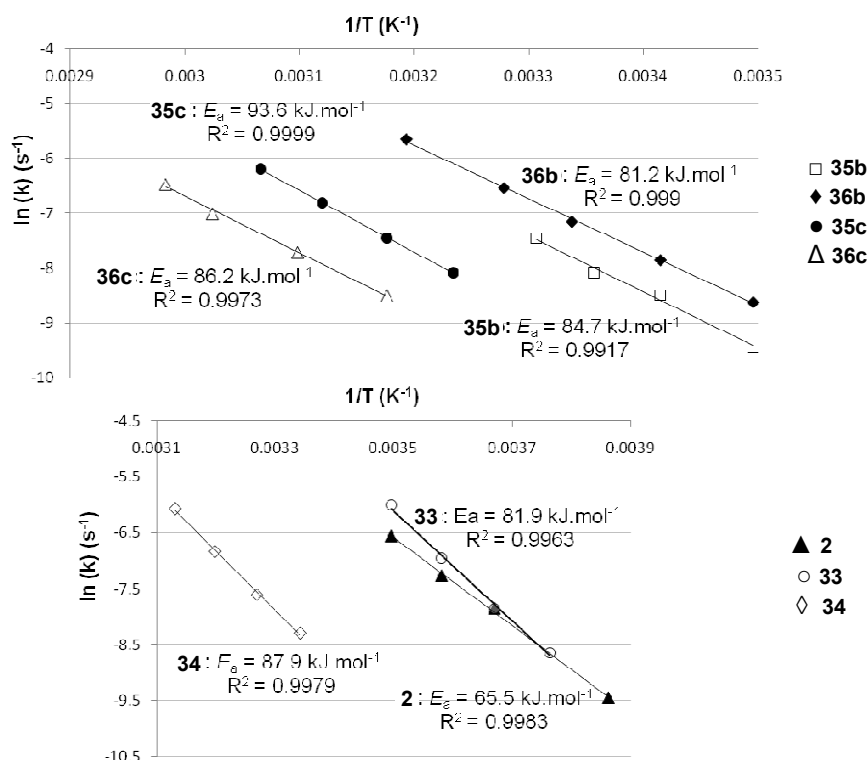
Eyring analyses (Figure 28) provided activation enthalpies ($\Delta H^{\ddagger}$) of a similar magnitude ($\Delta H^{\ddagger}$ = 78.7 (1.4) (**36b**), 82.5 (5.5) (**35b**), 83.5 (3.2) (**36c**) and 91.0 (0.6) kJ.mol^{-1} (**35c**) for the bis(amides); $\Delta H^{\ddagger}$ = 63.2 (1.9) (**2**), 79.6 (3.5) (**33**) and 85.4 (2.8) kJ.mol^{-1} (**34**) for the β-diketiminato compounds). While activation entropies ($\Delta S^{\ddagger}$) displayed only marginal variations across the series of homoleptic precatalysts ($\Delta S^{\ddagger}$ = -41.3 (4.8) (**36b**), -34.1 (18.8) (**35b**), -32.8 (9.7) (**36c**) and -18.2 (2.0) J.mol^{-1}.K^{-1} (**35c**)) the β-diketiminate-stabilised complexes showed more significant differences, with the THF-solvated calcium species **2** providing the most negative value of $\Delta S^{\ddagger}$ ($\Delta S^{\ddagger}$ = -78.0 (7.0) (**2**), -16.7 (12.8) (**33**) and -28.9 (9.1) J.mol^{-1}.K^{-1} (**34**)). It is proposed that these values are a quantitative reflection of the relative organisation of the four-membered alkene insertion transition states when assembled about the group 2 metal centres, with the smaller calcium cations and the THF-containing species providing a more

76

constrained configuration of the substrate and the catalytic centre. In the case of calcium complex **2**, the smaller metal centre, the steric demands of the (2,6-di-*iso*-propylphenyl)-substituted *β*-diketiminate ligand and the presence of the, at least initially, adducted molecule of THF appear to have a summative effect in enforcing the most constrained transition state inferred from the most negative $\Delta S^{\ddagger}$ value.

Figure 28. Top: Eyring plot of $\ln(kh/k_BT)$ (k = reaction rate constant, s^{-1}; T = temperature, K; h = $6.626068*10^{-34}$ m^2.kg.s^{-1}; $k_B = 1.3806503*10^{-23}$ m^2.kg.s^{-1}.K^{-1}) versus 1/T (K^{-1}) for calcium complexes **35-35b** and strontium complexes **35-36c**. Bottom: *idem* for *β*-diketiminate-stabilised complexes **2**, **33** and **34**. Activation enthalpies $\Delta H^{\ddagger}$ were calculated from the slope ($\Delta H^{\ddagger}$/R) of each linear set of data points, and $\Delta S^{\ddagger}$ from the intercept ($\Delta S^{\ddagger}$/R). Data were collected at [(1-allylcyclohexyl)methylamine] = 0.8 M and 2 mol% catalyst loading in d$_8$-toluene.
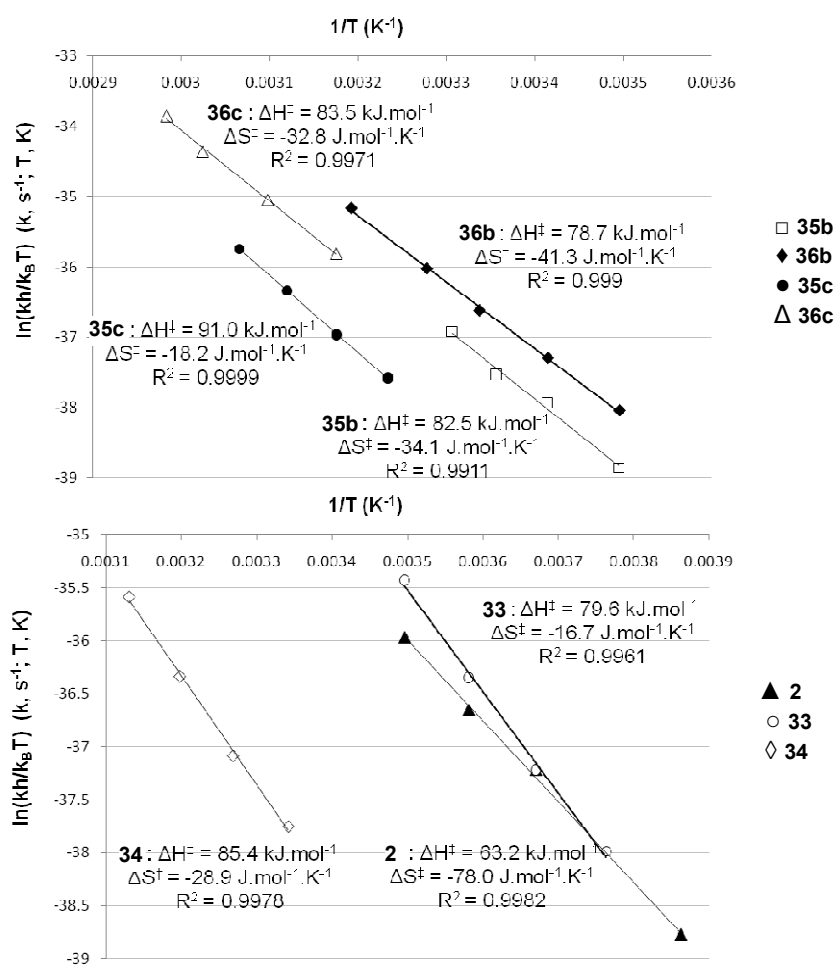
At 298 K, the calculated $\Delta G^{\ddagger}$ values reflect the relative reactivity series deduced from the qualitative experimental findings (homoleptic amides: $\Delta G^{\ddagger}$ (298 K) = 91.0 (**36b**), 92.6 (**35b**), 93.2 (**36c**) and 96.4 kJ.mol^{-1} (**35c**); *β*-diketiminato species: $\Delta G^{\ddagger}$ (298 K) = 86.5 (**2**), 84.6 (**33**) and 94.0 kJ.mol^{-1} (**34**)). A previous kinetic analysis of the hydroamination/cyclisation of 1-amino-4-pentene with the lanthanum precatalyst [Cp*$_2$La{CH(SiMe$_3$)$_2$}] by Marks and co-workers provided $\Delta H^{\ddagger}$ and $\Delta S^{\ddagger}$ values of 53.2

kJ.mol^{-1} and -113.0 J.mol^{-1}.K^{-1} respectively.[53] Thus, despite a significantly lower activation enthalpy than those reported herein, the highly negative activation entropy deduced for the lanthanide-centred species results in a free energy of activation of 86.7 kJ.mol^{-1}, which is comparable to those values obtained for **2** and **33** (Table 5).

Table 5. Comparison of activation parameters for the hydroamination/cyclisation of (1-allylcyclohexyl)methylamine with 2 mol% of the homoleptic and heteroleptic calcium and strontium precatalysts. Standard errors are indicated in parentheses.

Precatalyst	$\Delta H^{\ddagger}$ (kJ.mol^{-1})	$\Delta S^{\ddagger}$ (kJ.mol^{-1})	$\Delta G^{\ddagger}$ (298 K) (kJ.mol^{-1})
35b	82.5 (5.5)	-34.1 (18.8)	92.6
35c	91.0 (0.6)	-18.2 (2.0)	96.4
36b	78.7 (1.4)	-41.3 (4.8)	91.0
36c	83.5 (3.2)	-32.8 (9.7)	93.2
2	63.2 (1.9)	-78.0 (7.0)	86.5
33	79.6 (3.5)	-16.7 (12.8)	84.6
34	85.4 (2.8)	-28.9 (9.1)	94.0
[Cp*$_2$LaCH(SiMe$_3$)$_2$]^a	53.2 (5.9)	-113.0 (20.9)	86.7
[Me$_2$SiCp''$_2$Sm{CH(SiMe$_3$)$_2$}]^b	74.1 (8.8)	-103.4 (20.9)	104.9

a- Substrate = 1-amino-4-pentene, 2.8 mol% catalyst.[53]
b- Substrate = 1-amino-2,2-dimethyl-4-hexene, 5 mol% catalyst.[134]

The case of the THF-free β-diketiminate-stabilised calcium precatalyst **33** is of particular note since the kinetic studies yielded a considerably higher activation enthalpy for **33** than for **2**. This apparent disadvantage is compensated, however, by a significantly less negative $\Delta S^{\ddagger}$ value and a consequential lower $\Delta G^{\ddagger}$ (298 K) value, which agrees with the reactivity series deduced from the qualitative findings outlined above. This mirrors the results of our recent kinetic study on the intermolecular hydroamination of styrene with piperidine catalysed **35b** and **35c**, in which the higher activation enthalpy for strontium was counterbalanced by a tangible entropic advantage, leading to an overall lower $\Delta G^{\ddagger}$ (298 K) value for the more active strontium precatalyst, in agreement with the qualitative observations.[65]

It is also apparent that the THF-free homoleptic precatalysts **35a-c** are considerably less active than their THF-solvated analogues **36a-c**, whereas the solvent-free β-diketiminato calcium complex **33** provided higher turnover frequencies than its THF-solvated analogue **2**. To further inform our understanding of this phenomenon, kinetic studies were carried out at constant substrate concentration (0.56 M) and temperature

for varying catalyst loadings to determine the order in [catalyst] of each reaction. For the β-diketiminate derivatives and the THF-solvated homoleptic species **36b-c**, the reaction was first-order in [catalyst]. In contrast, a second-order dependence upon [catalyst] was deduced for the homoleptic complexes **35b-c** (Figure 29). This result is consistent with the reduction in activity observed for the THF-free precatalysts at equal catalyst loading and most likely indicates a rate-determining process involving two catalyst molecules. This latter observation is supported by the fact that these species commonly exist as dimers in non-coordinating solvents.[142] At high catalyst concentrations (typically > 0.05 M) a deviation from the linear plots was observed in most cases, followed by a significant drop in activity for concentrations above 0.1 M. This phenomenon may be due to increasing catalyst aggregation in solution at high concentrations. In the case of substrates bearing a secondary amine moiety, the steric hindrance provided by the second substituent may prevent dimerisation and thus restore the otherwise expected order of reactivity, leading to higher turnover rates for the THF-free homoleptic species. Hydroamination with β-diketiminato precatalysts **33** and **34** showed a first-order dependence in [catalyst], as had previously been determined for **1** and **2**.[54]

Figure 29. Top left: linear plot of k (min^{-1}), *pseudo* first-order rate constant, versus [**35b**]^2 (mol^2.L^{-2}) obtained by varying [**35b**] at constant concentration of (1-allylcyclohexyl)methylamine (0.56 M). Data were collected at 298 K in C$_6$D$_6$. Bottom left: *idem* with [**35c**]^2 (mol^2.L^{-2}) at 313 K. Top right: *idem* with [**36b**] (mol.L^{-1}) at 293 K. Bottom right: *idem* with [**36c**] (mol.L^{-1}) at 308 K. Data points diverging from the linear plot at high catalyst loading may be due to catalyst aggregation in solution.
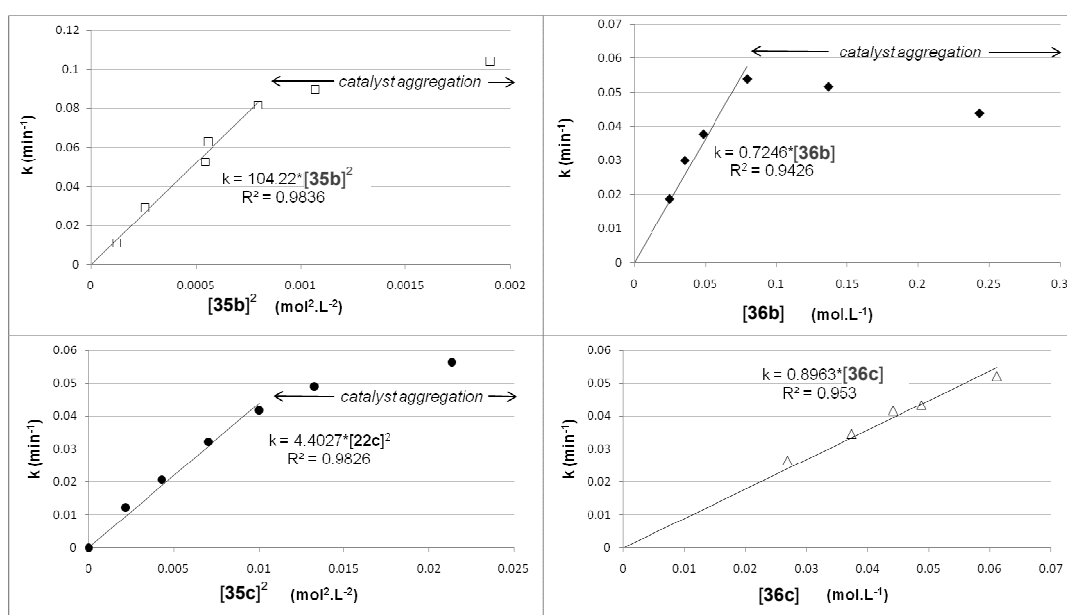
In line with previous findings,[54] the rate of cyclisation of (1-allylcyclohexyl)methylamine in the presence of homoleptic calcium precatalyst **36b** at constant concentration (0.02 M in C_6D_6) was dependent on the initial aminoalkene concentration, with turnover frequency decreasing with increasing substrate concentration (Figure 30). As had previously been demonstrated in the case of lanthanide-mediated hydroamination/cyclisation[53] and by the isolation of the strontium amide amine adduct **41** reported earlier in this study, a number of substrate and/or product molecules may bind to the metal centre as neutral donor ligands and thus block free coordination sites required for the alkene insertion step. A near-linear dependence between the *pseudo* first-order rate constant *k* and the inverse of the initial substrate concentration could be derived from these data sets.

Figure 30. Above: Inhibition kinetics: plot of $\ln([substrate]_t/[substrate]_{t=0})$ versus time (min) at 4 different initial substrate concentrations at 0.02 M of **36b** in C_6D_6 at 298 K. Below: plot of *k* (min^{-1}) versus the inverse of the initial substrate concentration ($L.mol^{-1}$).
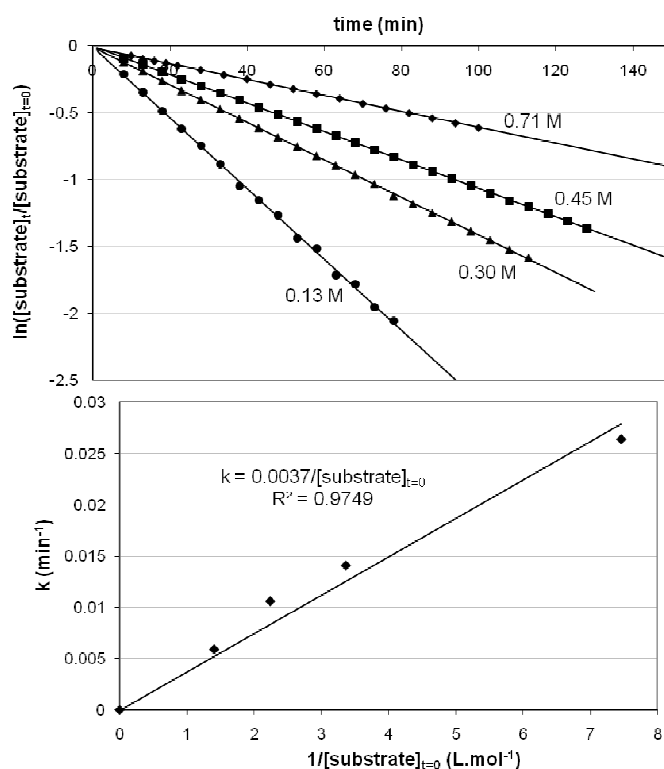
2.4.3 Substrate deuteration

Previous deuterium-labelling experiments with (1-allylcyclohexyl)methylamine-*d₂* (> 95% deuteration) showed that deuteration of the cyclised product was limited to the exocyclic methyl substituent, and was interpreted as providing evidence for a short-

lived alkyl intermediate in the catalytic cycle (Figure 31).[54] In order to quantify the dependence of the kinetic isotope effect on the nature of the metal centre, diprotio (RNH$_2$) and dideuterio (RND$_2$) substrate cyclisation with 2 mol% of the calcium and strontium bis(amide) precatalysts **36b** and **36c** (0.56 M of (1-allylcyclohexyl)methylamine in C$_6$D$_6$) were monitored by ^{1}H NMR at 298 K and 318 K respectively (Figure 31). The reactions exhibited *pseudo* first-order kinetics in [substrate] and rates of 2.56 h^{-1} (**36b**, RNH$_2$), 0.564 h^{-1} (**36b**, RND$_2$), 2.46 h^{-1} (**36c**, RNH$_2$) and 0.72 h^{-1} (**36b**, RND$_2$), yielding high kinetic isotope effects (KIEs) of k_H/k_D = 4.5 (298 K) and 3.4 (318 K) for **36b** and **36c** respectively.

Figure 31. Left: plot of ln([substrate]$_t$/[substrate]$_{t=0}$) versus time (min) for the cyclisation of (1-allylcyclohexyl)methylamine (RNH$_2$) and (1-allylcyclohexyl)methylamine-d$_2$ (RND$_2$) with calcium precatalyst **36b**. Data were collected at 298 K, [substrate]$_{t=0}$ = 0.8 M and 2 mol% catalyst loading in C$_6$D$_6$. Right: *idem* for strontium precatalyst **36c**. The slope of each linear set of data points corresponds to the *pseudo* first-order reaction rate k (h^{-1}).
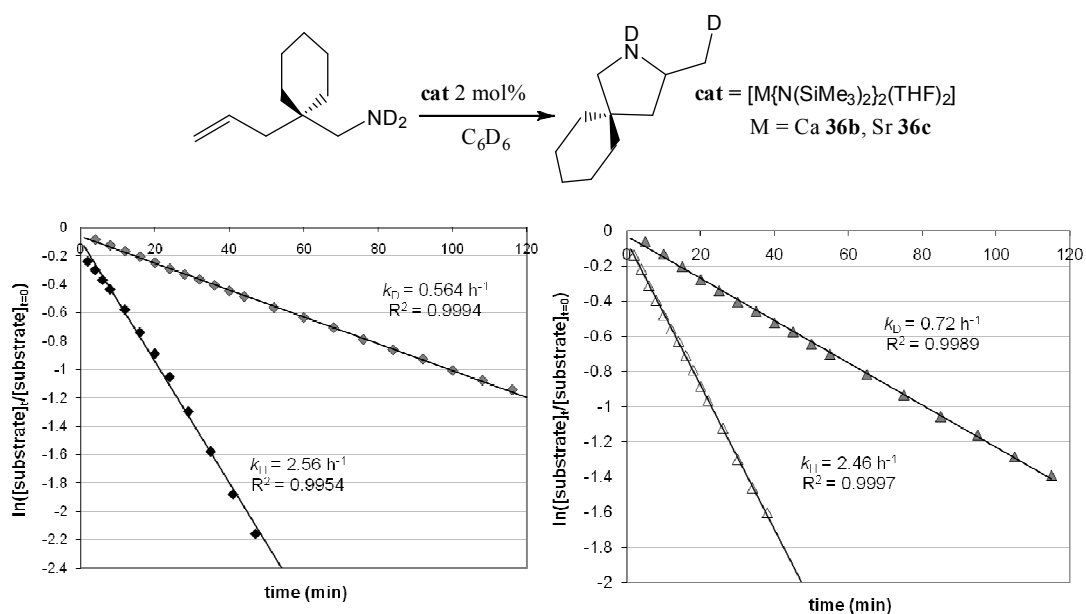
Although such large KIEs might be naively interpreted to militate against a rate-determining alkene insertion step involving no N-H or N-D bond breaking during the course of the catalytic turnover, these observations are precedented by kinetic analyses of lanthanide-based cyclisations.[53] In these latter cases KIEs of a similar magnitude were interpreted as a reflection of the direct involvement of additional amine in the coordination sphere of the lanthanide centre during the rate-determining insertion step. It therefore appears reasonable to suggest that a similar rationale may be applied to the group 2-mediated hydroamination of aminoalkenes reported in this study. Such a model is attractive as it views the augmented polarisation of the alkene moiety as a

consequence of both the polarising effect of the Ae-N bond and the simultaneous formation of an initial intramolecular N-H(δ+)···C(δ-)=C interaction, prior to onset of a concerted insertion/protonolysis step (Scheme 48), a hypothesis supported by a recent publication by Sadow and co-workers showing that an isolated tris(oxazolinyl)borate magnesium amidoalkene complex would not undergo alkene insertion unless one equivalent of a "dummy" amine was added to the solution, resulting in rapid cyclisation of the aminoalkene.[63] In this scenario, both substrate access to the metal centre and substrate polarisation, affected by the intrinsic properties (*i.e.* electropositivity and ionic radius) of the individual alkaline earth Ae^{2+} cation under observation, are key elements of the rate-determining insertion step. Computational studies may be of advantage to assess the polarising effect of adducted amines and their viability as "proton shuttles" in a concerted insertion/protonolysis pathway.

Scheme 48. Possible concerted insertion/protonolysis mechanism accounting for the high observed kinetic isotope effects.
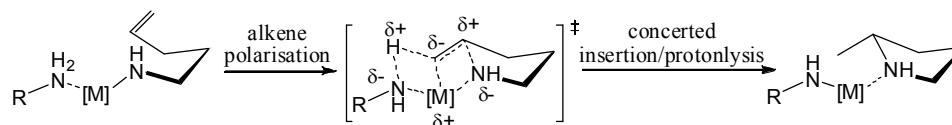
2.4.4 Derivation of a rate law

Previous observations and kinetic analyses led by Hill and co-workers on this subject had proposed a mechanism involving both product and substrate inhibition and suggested that for the rate-determining insertion to occur, the catalyst must go *via* an amidoalkene intermediate bare of amine adducts.[54] The resulting rate law (Equation 1), derived using steady state theory reminiscent of enzyme kinetics, reflected the observed first-order dependence of the reaction in [catalyst] as well as substrate and product inhibition, but failed to reproduce the observed *pseudo* first-order decline in [substrate] during the course of the reaction or to take into account the effect of non-protic Lewis bases such as THF.

$$rate = \frac{k_d k_3 [cat]_0}{k_a [sub]_0 + k_3} \qquad \textbf{(1)}$$

Where: $[cat]_0$ = total catalyst concentration,
           $[sub]_0$ = initial substrate concentration,
           k_a, k_d = respectively rate of association and dissociation of neutral substrate or product,
           k_3 = rate of insertion.

Taking into account the observed high kinetic isotope effects suggestive of a concerted insertion/protonolysis mechanism involving an adducted molecule of amine, and the presence of THF/amine adduct exchange, a modified mechanism may now be envisaged, as shown in Scheme 49. For simplification this model is based upon irreversible catalyst initiation.

Scheme 49. Proposed reaction steps for group 2-mediated intramolecular hydroamination catalysis. Model based upon fast, irreversible catalyst initiation. I = non protic inhibitor e.g. THF, SH = substrate, PH = product.
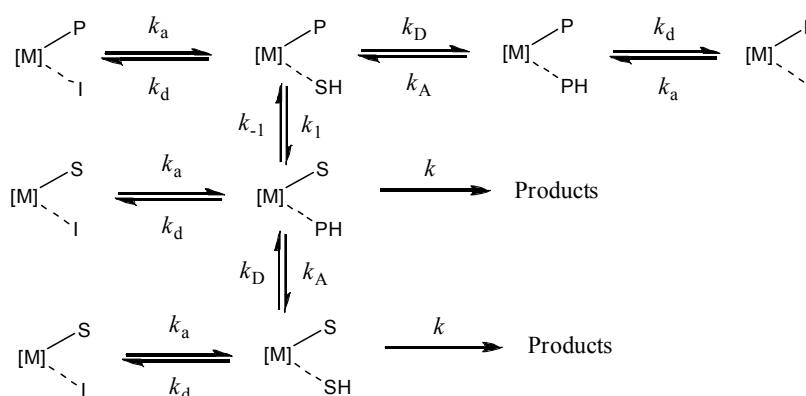
In a manner reminiscent of the rules of enzyme kinetics, which are subject to similar inhibition equilibria, using the assumptions that the neutral substrate and product have equal binding constants to the catalyst ($k_A \approx k_D$) and that the rate of the amine/amide exchange is equal in both directions ($k_{-1} \approx k_1$), it is possible to derive a relatively simple rate law (Equation 2) which reflects all the aspects of the reaction previously described in this study and is very similar to the Michaelis-Menten equation commonly used in enzyme inhibition kinetics.

$$rate = \frac{k[cat]_0 [sub]_t}{[sub]_0 + K_I [I]} \quad \text{where} \quad K_I = \frac{k_d}{k_a} \quad \textbf{(2)}$$

Under this regime the reaction rate increases with increasing catalyst concentration and decreases with increasing initial substrate and THF concentration. From this

equation it is also possible to take into account reversible catalyst initiation through the addition of a third term in the denominator of the equation, related to the initial catalyst concentration and the amine/amide exchange constant between the silylamide co-ligand and the substrate or product. While equation 2 is appropriate for systems based upon the alkaline earth β-diketiminate and the THF-solvated bis(amide) precatalysts used in this study, it accounts neither for the observed second-order dependence in [catalyst] observed for the THF-free bis(amide) species **36b** and **36c**, nor for recent observations made by Hultzsch and co-workers on the catalytic intramolecular hydroamination activity of a series of magnesium phenoxyamine complexes, in which the cyclisation rate of 1-amino-2,2-diphenyl-4-pentene was found to display either a zero-order or second-order decline in [substrate].[152] Although no explanation was given for these observations, these results highlight the complexity of group 2-catalysed intramolecular hydroamination reactions and the limitations of the above-given mechanism, which may only apply in specific cases.

2.5   Conclusion and future work

2.5.1 *Mechanistic conclusions*

It has become apparent from this study that, in contrast to previous lanthanide-catalysed intramolecular hydroamination reactions displaying smooth trends across the series, the alkaline earth metals exhibit a rather more complex behaviour, marked by notable discontinuities arising from the intricate interplay between kinetic and thermodynamic factors. Calcium remains the metal of choice for the highest catalysis rates while magnesium provides greater selectivity, albeit at the cost of efficiency. After focusing primarily on the hydroamination/cyclisation of aminoalkenes further studies will be needed to systematically investigate the group 2-mediated intramolecular hydroamination of other types of aminoolefins, such as aminoalkynes, aminoallenes and aminodienes, and to explore whether similar or different reactivity patterns also apply in these closely related systems. Detailed computational studies of each of these reactions would provide valuable mechanistic information and help understand the fundamental

differences between lanthanides and alkaline earth metals, and among the different alkaline earth metals themselves.

2.5.2   Limitations of the β-diketiminate ligand framework

This study has also demonstrated that reactivity is greatly influenced by the choice of both the ancillary spectator ligand and the reactive amide or alkyl ligand. Although the β-diketiminate ligand precursor [ArNC(Me)CHC(Me)NHAr] (Ar = 2,6-di-*iso*-propylphenyl) has the advantage of being readily synthesised in a one-step procedure,[153] and has provided a useful platform for the first mechanistic studies of the magnesium-, calcium- and strontium-mediated intramolecular hydroamination of aminoalkenes, allowing the isolation of key intermediates and the acquisition of valuable kinetic data, it has also reached its limits in certain ways.

The problem of ligand lability, in particular, common to these large, electropositive elements, is a key issue which needs to be addressed, especially if reactions are to be made enantioselective. Indeed, while magnesium complex **1** and its derivatives are immune to Schlenk-like ligand redistribution processes in solution, analogues of calcium complex **2** bearing less sterically demanding co-ligands often tend to redistribute, either over time at room temperature or at high temperature, to the homoleptic species.[19] The problem becomes even more acute with strontium complex **34** whose synthesis is always accompanied by the formation of a non-negligible amount (25-40%) of the homoleptic species [{ArNC(Me)CHC(Me)NAr}$_2$Sr(THF)][19] which may only be separated with difficulty by fractional crystallisation. Even then, isolated samples of **34** remained usually contaminated with traces of the homoleptic compound.

Furthermore, while reactive alkyl ligands provide attractive, irreversible entry into the catalytic cycle, independent attempts by Harder and Hill to obtain the benzyl or alkyl derivatives of β-diketiminato alkaline earth complexes using the [ArNC(Me)CHC(Me)NAr]$^-$ ligand systematically resulted in C-H activation of one of the methyl groups on the ligand backbone and precipitation of insoluble and catalytically inactive material (Scheme 50).[154, 155] The high basicity of alkaline earth organometallics needs, therefore, to be taken into account when designing new ligand systems for the kinetic stabilisation of heteroleptic group 2 alkyl precatalysts.

Scheme 50. C-H activation of β-diketiminate backbone methyl groups by alkaline earth dialkyls **37b-d**.
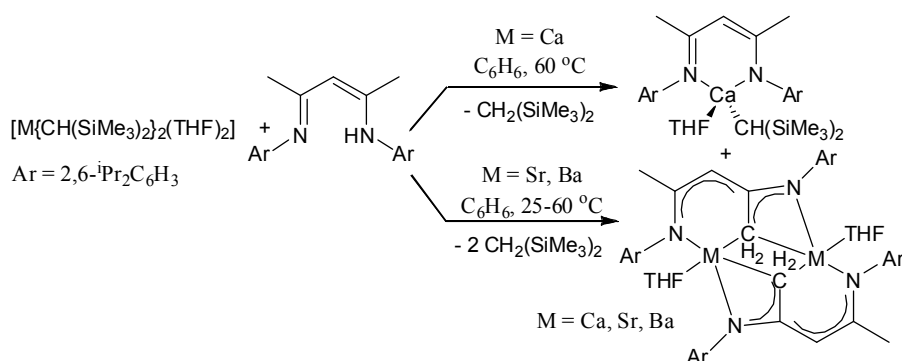
The issue of the Schlenk equilibrium

One way of preventing deleterious Schlenk-like ligand redistribution processes in solution for alkaline earth β-diketiminate complexes may simply be to increase the steric demands of the nitrogen-bound substituents. The limits of this approach became apparent, however, when trying to substitute the 2,6-di-*iso*-propylphenyl groups by 2,6-diphenylmethyl-4-methylphenyl substituents (Scheme 51), using a method reported by Berthon-Gelloz *et al.* for the synthesis of the aniline precursor.[156]

Scheme 51. Synthesis of a (2,6-diphenylmethyl-4-methylphenyl)-substituted β-diketiminate ligand precursor.[156]
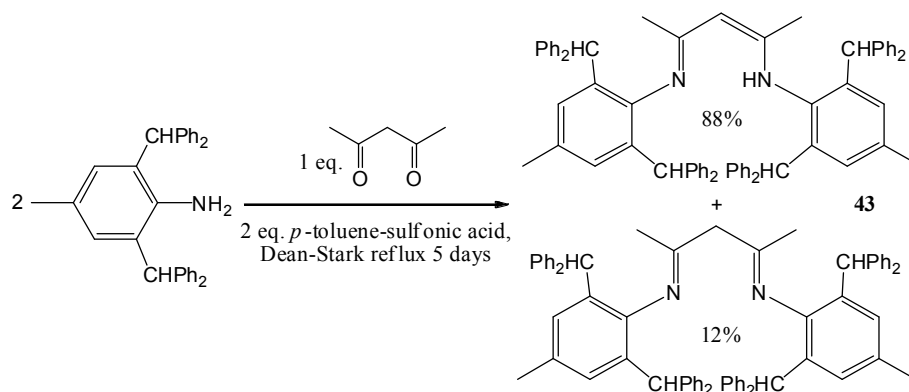
After purification by column chromatography ligand precursor **43** was isolated as colourless solid in an 88:12 mixture of the amino-imine and the diimine respectively, as indicated by ^{1}H NMR spectroscopy. Recrystallisation from hot chloroform yielded crystals of the amino-imine isomer suitable for X-ray diffraction analysis. The result of this experiment is illustrated in Figure 32. Selected bond length and angle data are given in Table 6.

Figure 32. Ortep representation of one of the two molecules in the asymmetric unit of compound **43**. Thermal ellipsoids drawn at 30% probability. Hydrogens omitted for clarity, except N-*H* proton.
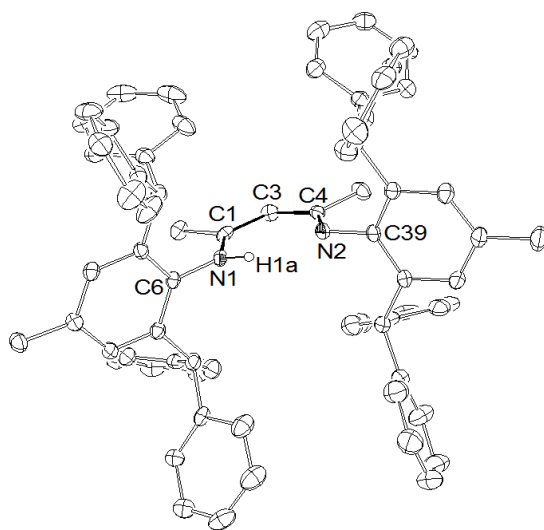
Table 6. Selected bond lengths (Å) and angles (°) for compounds **43** and **44**.

	43	44		43	44
N(1)-C(1)	1.345(5)	1.326(5)	C(6)-N(1)-C(1)	124.5(3)	119.4(3)
C(1)-C(3)	1.383(6)	1.404(6)	N(1)-C(1)-C(3)	122.1(3)	122.8(3)
C(3)-C(4)	1.423(6)	1.403(6)	C(1)-C(3)-C(4)	125.8(3)	130.0(4)
C(4)-N(2)	1.314(5)	1.335(5)	C(3)-C(4)-N(2)	121.7(3)	123.5(4)
N(1)-C(6)	1.423(5)	1.440(5)	C(4)-N(2)-C(39)	120.4(3)	118.8(3)
N(2)-C(39)	1.421(5)	1.448(5)	N(1)-Mg-N(2)		90.97(13)
Mg-N(1)		2.082(3)	C(6)-N(1)-Mg		118.6(3)
Mg-N(2)		2.084(4)	C(39)-N(2)-Mg		119.4(3)
Mg-C(37)		2.131(5)			
Mg-O		2.105(3)			

While reaction of ligand **43** with one equivalent of dibutylmagnesium in THF at 60 °C for two hours provided the desired heteroleptic complex, **44**, in quantitative yield (Scheme 52), attempts to obtain the potassium complex by heating a THF suspension of the ligand precursor and potassium hydride at 60 °C for two days failed. Further attempts to deprotonate the ligand precursor with [KN(SiMe₃)₂] equally met with failure.

Scheme 52. Synthesis of magnesium *β*-diketiminate complex **44**.
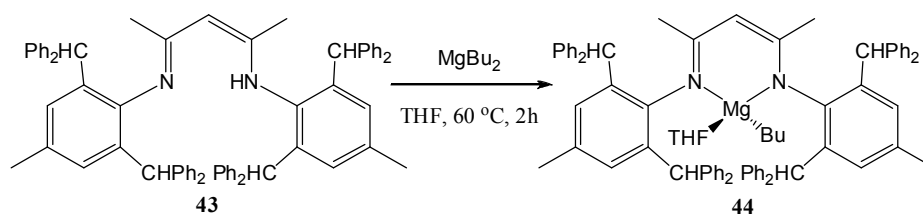
The reason for this became apparent upon inspecting the results of an X-ray diffraction experiment on single crystals of complex **44** obtained from a 10:1 toluene/THF solution at room temperature over a period a three days. As shown by the space-filling model of the structure in Figure 33 the magnesium centre is tightly encapsulated by four of the phenyl groups of the bulky side arms so that there is virtually no access to the metal centre. The small size of the ligand cavity may indeed not be capable of accommodating the increase in ionic radius of the four-coordinate metallic cation from Mg^{2+} (0.57 Å) to K^+ (1.37 Å). The complexity of the $^{13}C\{^1H\}$ NMR spectrum, in which all the carbon nuclei of the 2,6-diphenylmethyl-4-methylphenyl groups appear as inequivalent, clearly demonstrated that the ligand conserves its constrained geometry in solution. NMR spectroscopic analysis also indicated that the adducted THF molecule was removed upon prolonged drying *in vacuo* of complex **44**. Preliminary hydroamination/cyclisation experiments with 1-amino-2,2-diphenyl-4-pentene indicated that **44** is catalytically active despite reduced substrate access to the metal centre.

Figure 33. Left: Ortep representation of compound **44**. Thermal ellipsoids drawn at 30% probability. Hydrogens omitted for clarity. Right: space-filling model of complex **44**.
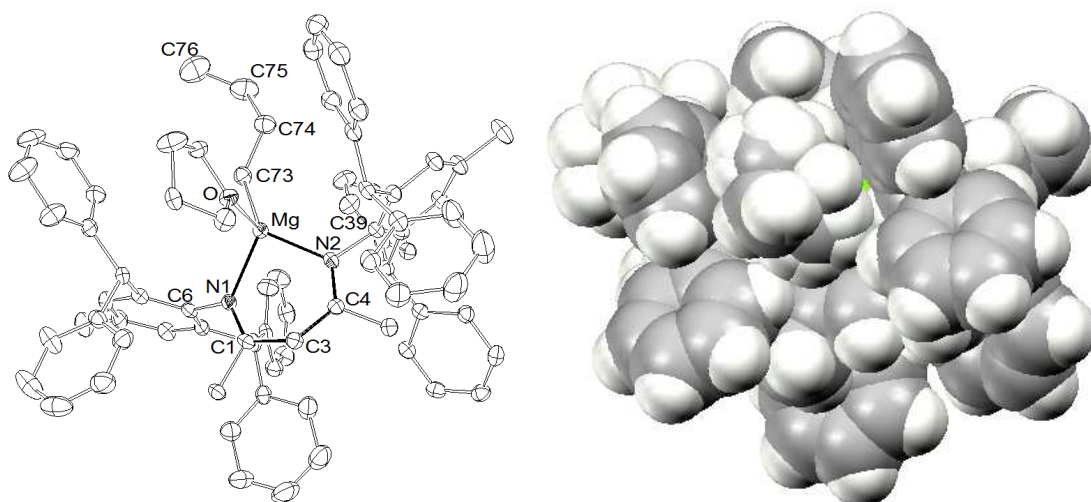
Preliminary efforts to obtain a calcium analogue of **44** by reacting the ligand precursor **43** with [Ca{X(SiMe₃)₂}₂(THF)₂] (X = N **36b**, CH **37b**) were also thwarted by either the lack of reactivity of **36b** towards the ligand precursor, or the tendency of **37b** to deprotonate the benzylic carbon atoms of the nitrogen-bound ligand substituents instead of the amine functionality, resulting in the formation of insoluble dark red products. Although different synthetic approaches may allow the isolation of a calcium analogue of compound **44**, substrate access to the calcium metal centre may still be too hindered for catalytic activity to occur. It seems essential, therefore, to find the right balance between increasing the steric demands of the ligand to prevent Schlenk-type redistribution processes from occurring, and sufficient space inside the ligand cavity to accommodate and ultimately access the group 2 dication for catalysis to proceed.

Increasing the denticity of the *β*-diketiminate ligand may be another solution to improve the stabilisation of heteroleptic alkaline earth complexes. Similarly to the tris[3-(2-methoxy-1,1-dimethyl)pyrazolyl]hydroborate ligand designed by Chisholm and co-workers,[157] additional coordination may be provided by replacing one or both of the nitrogen substituents on the *β*-diketiminate framework with flexible N- or O-donor arms. Only few examples of magnesium and calcium complexes of this type have been reported in recent years (Figure 34) and the field remains open to extend this chemistry to the heavier alkaline earth metals and their application to homogeneous catalysis.[158]

Figure 34. Examples of heteroleptic alkaline earth complexes of tridentate and tetradentate monoanionic *β*-diketiminate ligands.

X = ⁱPr, N(ⁱPr)₂

M = Mg, X = Bu, N(SiMe₃)₂, R = Me, -(CH₂)₅
M = Ca, X = N(SiMe₃)₂, R = Me

The issue of ligand C-H activation

Rather than increasing the size of the *β*-diketiminate nitrogen-bound substituents, another option may be to augment the steric demands of the 2,4-dimethyl substituents

on the β-diketiminate backbone, which in turn would cause the nitrogen-bound substituents to move closer to the metal centre through the effects of steric repulsion. El-Kaderi *et al.* have shown that replacing the methyl groups with *tert*-butyl groups in the ligand precursor [ArNC(^{t}Bu)CH$_2$C(^{t}Bu)NAr] (Ar = 2,6-di-*iso*-propylphenyl) not only allows the isolation of heteroleptic β-diketiminate calcium and strontium iodide complexes but also of the analogous barium iodide complex, which could not be stabilised with the conventional methyl-substituted β-diketiminate ligand.[159] Replacing the methyl functionalities with *tert*-butyl or phenyl groups may also address a second complication, that of C-H activation of the β-diketiminate backbone methyl substituents (Scheme 50).[154, 155] A potential synthetic route towards stable β-diketiminate calcium and strontium alkyl complexes is outlined in Scheme 53.

Scheme 53. Proposed synthetic route towards stable β-diketiminate calcium and strontium alkyl complexes.

$Ar = 2,6\text{-}^i Pr_2 C_6 H_3$

$M = Ca, Sr$

Chiral β-diketiminates and related ligands

Ultimately, further work may involve designing new chiral β-diketiminate-type ligand precursors in order to obtain enantiopure heteroleptic alkaline earth complexes for the enantioselective hydroamination/cyclisation of aminoalkenes. To date, the only examples in this area remains the attempt by Harder and co-workers to use a chiral (*S*)-(Ph-Box)-stabilised calcium amide precatalyst,[18] and by Hultzsch and co-workers using an amidobinaphthyl magnesium precatalyst,[129] which both resulted in rather poor enantioselectivity (ee < 14%) due to deleterious Schlenk-type ligand redistribution processes during the course of catalysis. More recently Sadow and co-workers obtained enantioselectivities up to 36% with a chiral tris(oxazolinyl)borate magnesium precatalyst while the calcium analogue only provided 18% ee.[63] It is possible that other, more sterically demanding oxazoline-containing ligands may prove capable of preventing ligand redistribution (Figure 35C). Although enantiopure β-diketiminate ligands bearing 2-phenylethyl substituents (Figure 35A) have been successfully

employed to stabilise copper, zinc and zirconium complexes,[160] they did not provide sufficient steric protection against ligand redistribution for the larger calcium metal centre.[18] Furthermore, due to the attested reactivity of group 2 alkyls towards benzylic protons, any ligand bearing benzyl substituents would certainly be unsuitable for the stabilisation of alkaline earth alkyl functionalities. A potential *β*-diketiminate ligand candidate capable of providing sufficient protection against Schlenk equilibria and CH-activation is presented in Figure 35B but remains to be synthesised. IAN-amines, derived from isoquinolines and aminonaphthalenes, may provide another class of related ligands which could be tuned for these purposes (Figure 35D).

Figure 35. Examples of chiral *β*-diketiminate ligands and related chiral bis(oxazoline) and IAN-amine ligands.

R¹ = H, alkyl or aryl group
R² = sterically demanding alkyl or aryl group

R¹, R² = sterically demanding alkyl or aryl groups
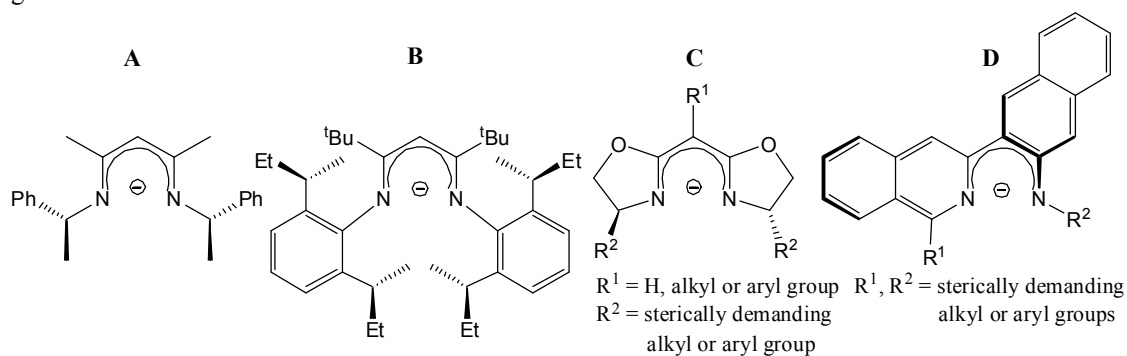
Although there still remains some scope for the development of new *β*-diketiminate-derived ligands for alkaline earth precatalysts, it also remains important to design new, more adaptable monoanionic ligands to solve both the problem of the Schlenk equilibrium and the issue of the stabilisation of highly reactive group 2 alkyl moieties.

3 Bis- and tris(carbene)borate ligands for the kinetic stabilisation of alkaline earth complexes

3.1 Introduction

3.1.1 Importance of N-heterocyclic carbene complexes

Since the report of the first transition metal carbene complexes by Öfele[161] and Wanzlick in the 1960s,[162] and Lappert's studies on late transition metal carbene complexes during the following decade,[163] the area of N-heterocyclic carbene (NHC) organometallic chemistry has expanded dramatically following the isolation by Arduengo *et al.* of the first stable free carbene in 1991.[164] First used in catalysis by Herrmann and co-workers in 1995,[165] NHC complexes have found numerous catalytic applications and the area has been regularly reviewed in recent years.[166, 167] The major significance of these ligands was recognised by the award of the 2005 Nobel Prize for the development of Grubbs' second generation catalysts for olefin metathesis.[168, 169] Recent developments in organocatalysis have also demonstrated the use of NHCs as metal-free catalysts in their own right.[170] Although at first considered to be simple phosphine-mimics due to their mainly σ-donating character,[171] NHC complexes are generally more thermally stable than their phosphine-based counterparts, due to stronger metal-ligand interactions.[166, 172, 173] Numerous comparative catalytic studies have proven the superiority of NHC-stabilised catalysts over their phosphine analogues,[174] especially in ruthenium-catalysed olefin metathesis reactions,[168] and palladium-catalysed coupling reactions.[175] Studies showed that the least basic NHCs are still 10 pK_b units more basic than the most basic phosphine, P^{t}Bu$_3$.[176] The ease of preparation of saturated or unsaturated NHCs of different ring sizes bearing a wide variety of nitrogen-bound substituents allows for fine-tuning of the stereoelectronic properties of these ligands (Figure 36).[173, 177] It is thought that NHC stabilisation mainly occurs through donation from the adjacent nitrogen lone pairs into the vacant π-orbital of the carbene centre, and a certain degree of aromaticity.[178] Structural and computational analyses have also shown evidence for a non-negligible amount of π-back-bonding from the metal centre to the carbene ligand, particularly in group 11 and uranium

complexes,[179] while DFT studies upon unusually stable 14-electron rhodium and iridium complexes supported by *tert*-butyl-substituted NHC ligands even suggested the possibility of π-donation from the carbene fragment into the vacant d orbitals of the metal centre.[180] Other studies upon the variation of metal-carbene bond strengths also suggest that bonding is essentially controlled by electrostatic factors.[181]

**Figure 36.** Examples of N-heterocyclic carbene ligands.
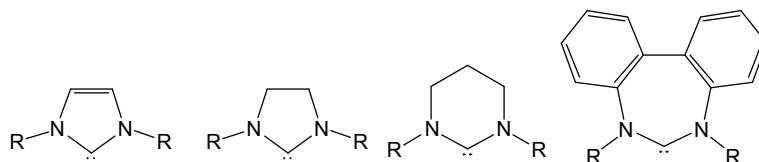
3.1.2 NHC complexes of rare earth and alkaline earth metals

Whereas late transition metal NHC complexes have been studied extensively, examples of s-block and f-block carbene complexes remain relatively rare. A recent review by Arnold and Casely details the whole extent of group 3, lanthanide and actinide complexes bearing NHC ligands, as well as their reactivity.[182] The first lanthanide NHC complexes, [{C$_5$Me$_4$Et}$_2$Sm{C(NRCMe)$_2$}] (R = Me, ^{i}Pr) were reported in 1994 by Schumann *et al.* and obtained by reacting [{C$_5$Me$_4$Et}$_2$Sm(THF)] with the free carbene.[183] In the same year, Arduengo et al. used a similar method to synthesise [(Cp*)$_2$Yb(NHC)$_n$] (n = 1, 2) and tris(diketonate) europium and yttrium NHC complexes.[184] Computational studies have shown that the strength of the NHC-lanthanide bond owes mainly to the σ-donating power of the carbene fragment, although in some cases π-back-bonding from amide co-ligands within the metal coordination sphere has been observed.[185, 186] The problem of ligand lability commonly encountered in these complexes was overcome by developing NHC ligands tethered to anionic amido or alkoxo functionalities which strongly bind to hard, electropositive metal centres.[187] Among the few catalytic applications of rare earth metal carbene complexes, the amido-functionalised NHC yttrium bis(amide) complex **45** was reported for the ring-opening polymerisation of rac-lactide, yielding highly heterotactic polymers with low polydispersity,[188] while the indenyl-tethered NHC yttrium complex **46** was found to be active for the catalytic 3,4-selective living polymerisation of isoprene (Figure 37).[189, 190] More recently, Lv et al. reported the cis-1,4-selective version of the same

reaction using the CCC-pincer bis(NHC) rare earth dibromide complexes **47a-e** (Figure 37).[191] Whether the carbene ligand remains bound to the metal centre during these catalytic reactions remains unclear.
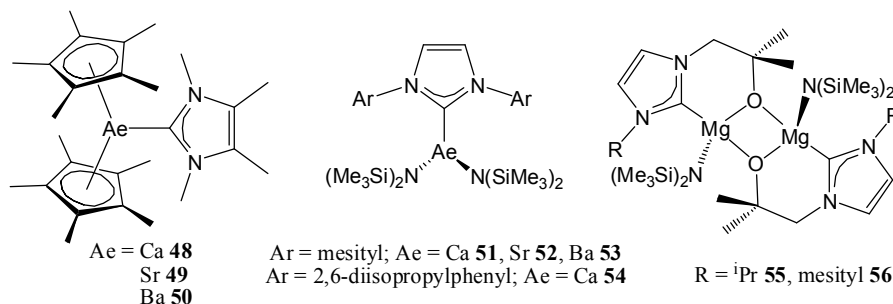
Figure 37. Rare earth NHC polymerisation precatalysts.

45   **46**   **47a-e** Ln = Y, Nd, Gd, Dy, Ho
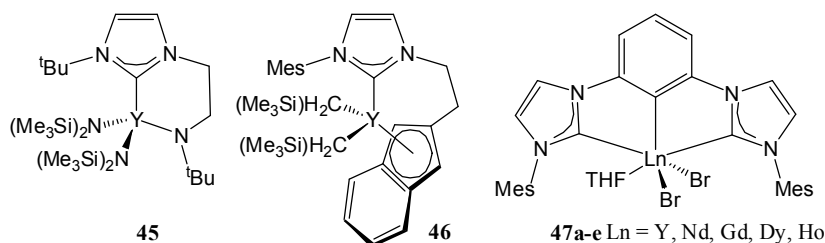
While a number of NHC complexes of the alkali metals have been synthesised and characterised,[189, 192] only a handful of examples of alkaline earth NHC complexes has been reported to date. In 1993, Arduengo *et al.* reported the first dialkyl magnesium carbene adducts obtained from the direct reaction of diethylmagnesium with [**:**C(NRCH)$_2$] (R = mesityl, adamantyl).[193] Two years later a beryllium dichloride complex was reported to form a stable adduct with 1,3-dimethylimidazolin-2-ylidene.[194] The alkaline earth metallocene compounds [(Cp*)$_2$M{C(NMeCMe)$_2$}] (M = Ca **48**, Sr **49**, Ba **50**) synthesised by Arduengo and co-workers in 1998,[195] and the related NHC complexes of group 2 metallocenes (M = Mg, Ca, Sr, Ba) described by Schuman *et al.* in 2001,[196] remained for nearly a decade the only examples of NHC adducts of the heavier alkaline earth elements (Figure 38). Only recently has the synthesis of simple NHC adducts of heavier alkaline earth bis(amides) been described by Hill and co-workers.[197] The compounds [{(HCNAr)$_2$C}M{N(SiMe$_3$)$_2$}$_2$] were obtained either by reacting the imidazolium chloride (Ar = mesityl; M = Ca **51**, Sr **52**, Ba **53**) or the free carbene (Ar = 2,6-di-*iso*-propylphenyl; M = Ca **54**) with the corresponding homoleptic group 2 amides [M{N(SiMe$_3$)$_2$}$_2$]$_2$. Although characteristic low-field ^{13}C{^{1}H} NMR carbene resonances between 193 and 199 ppm, and multinuclear NMR experiments suggested that, in solution, the NHC ligand stays bound to the metal centre on the NMR time scale, these complexes underwent ligand dissociation in the presence of protic substrates or harder Lewis bases, making them unstable under catalytically relevant conditions. Arnold and co-workers have also reported a variety of magnesium complexes bearing amide- or alkoxide-functionalised NHC ligands, of which **55** and **56** were successfully used as precatalysts for the ring-

opening polymerisation of *rac*-lactide with activities superior to the analogous zinc catalysts, yielding polymers of modest heterotacticity.[181, 198, 199] Furthermore, carbene ligands have been used to stabilise a hydride-rich Mg_4H_6 cluster, **25**, which displays the highest hydride to magnesium ratio described to date (Scheme 29).[76]

Figure 38. Examples of group 2 NHC complexes.

Ae = Ca **48**
Sr **49**
Ba **50**

Ar = mesityl; Ae = Ca **51**, Sr **52**, Ba **53**
Ar = 2,6-diisopropylphenyl; Ae = Ca **54**

R = ^{i}Pr **55**, mesityl **56**

### 3.1.3 Monoanionic poly(carbene)borate "scorpionate" ligands

Since the description of the first tris(pyrazolyl)borate ligand by Trofimenko in 1966,[200] an ever-growing variety of scorpionate ligands has been reported and the area has been reviewed several times.[201] Variation of the substituents borne by the pyrazolyl residues and the boron bridgehead atom allows for steric and, to a lesser degree, electronic tuning of the original tris(pyrazolyl)borate ligand. The term "scorpionate", introduced by Trofimenko in 1999,[202] now applies to a class of ligands bearing three donor fragments tethered by a monoanionic bridge, in which two of the donor groups act as "claws" while the third one arches over to "sting" the metal centre. Recent years have focused on replacing the pyrazolyl fragments by stronger donors, such as thioimidazolyl, selenoimidazolyl, phosphine or NHC donors, thus offering a wider range of steric and electronic tuning.[203]

Bearing in mind the tendency of heteroleptic *β*-diketiminate calcium complexes with small monoanionic co-ligands to undergo Schlenk-type ligand redistribution to the homoleptic species [{ArNC(Me)CHC(Me)NAr}₂Ca] (Ar = 2,6-di-*iso*-propylphenyl) Chisholm and co-workers developed a series of kinetically stable calcium tris(pyrazolyl)borate complexes for the catalytic polymerisation of *rac*-lactide, of which two examples, complexes **3** and **4** are displayed in Figure 39.[21, 36] Despite the high kinetic stability of these species, even when coordinated to small aryloxide

functionalities, a certain degree of lability of the pyrazolyl fragments and rapid ligand exchange in solution were observed in some cases.[204] It was hoped that the more strongly donating poly(carbene)borate ligands might provide enhanced kinetic stability for the heavier group 2 elements and avoid detrimental ligand lability.

First reported by Fehlhammer in 1996,[205] the use of tris(carbene)borate ligands in both transition metal and main group chemistry has remained relatively limited.[206-209] Studies on the $\nu_{N=O}$ IR frequencies of various tris(carbene)borate nickel nitrosyl complexes have shown that this class of ligand is by far the most strongly σ-donating of the scorpionates.[209] Furthermore it seems that, in contrast to monodentate NHC ligands, the electronic properties of tris(carbene)borates may be tuned by varying the nitrogen-bound substituents on the carbene fragments. Modification of the substitution on the boron bridgehead atom, however, had little influence on the $\nu_{N=O}$ IR shifts.[209] The only example of an alkaline earth metal complex bearing a tris(carbene)borate ligand is the magnesium complex **57** [{HB(Im^{t}Bu)$_3$}MgBr] which was obtained from the reaction of the boronium salt precursor [HB(Im^{t}Bu)$_3$]Br$_2$ with three equivalents of [MeMgBr] and used by Smith and co-workers as an intermediate in the synthesis of the analogous iron (II) complex.[207] More recently lithium and nickel complexes of the bidentate [H$_2$B(Im^{t}Bu)$_2$]$^-$ ligand have been reported by Nieto *et al.*[210]

Figure 39. Examples of alkaline earth scorpionate complexes.

X = N(SiMe$_3$)$_2$ **3**, O-(2,6-^{i}Pr$_2$C$_6$H$_3$) **4**   **57**
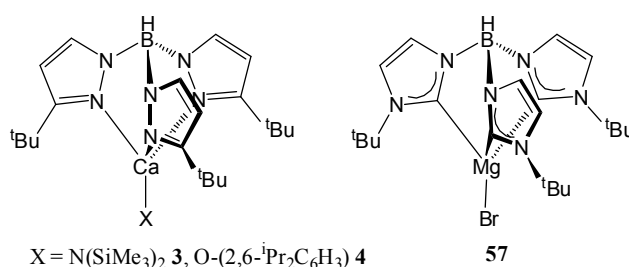
3.2   Synthetic, structural and catalytic studies of calcium and strontium bis(imidazolin-2-ylidene-1-yl)borate complexes.[211]

3.2.1 *Synthesis of ligand precursors*

The ligand precursor boronium salt [H$_2$B(Im^{t}Bu)$_2$]I, compound **58**, was synthesised by adapting the procedure recently described by Nieto *et al.* by refluxing two

equivalents of *tert*-butylimidazole with Me$_3$N.BH$_2$I in chlorobenzene (b.p. 131 °C),[210] which had already been used by the same authors for the synthesis of the related tridentate ligand precursor [HB(Im^{t}Bu)$_3$]Br$_2$,[207] rather than the lower boiling solvent toluene (b.p. 110.6 °C) (Scheme 54). The analogous bromide salt, compound **59**, and the respective [H$_2$B(ImMes)$_2$]X analogues (X = I, **60**; Br, **61**) were obtained following the same method and isolated as colourless crystalline solids after recrystallisation from water (**58**), dichloromethane (**59**), or chloroform (**60** and **61**). In general, the use of the iodoborane instead of the bromoborane precursor afforded much shorter reaction times (3-5h instead of 10-15h) and better yields.

Scheme 54. Synthesis of dihydro-bis(imidazole)boronium bromide and iodide ligand precursors **58-61**.

58 R = ^{t}Bu, X = I,
59 R = ^{t}Bu, X = Br,
60 R = 2,4,6-Me$_3$C$_6$H$_2$, X = I,
61 R = 2,4,6-Me$_3$C$_6$H$_2$, X = Br
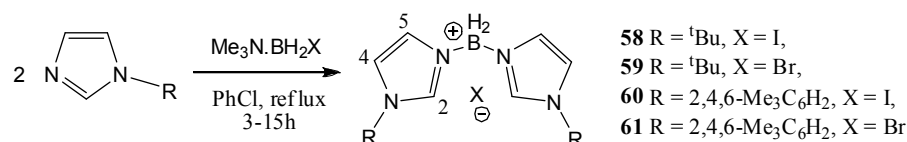
Compound **58** provided ^{1}H and ^{13}C{^{1}H} NMR chemical shift data in concordance with those quoted recently by Smith and co-workers.[210] All four ligand precursors displayed characteristic ^{1}H NMR low field resonances around 9.5 ppm corresponding to the imidazole *H-2* proton as well as a distinctive triplet between -6.10 and -9.90 ppm in the proton-coupled ^{11}B NMR spectra. The B-H bonds were indentified in the IR spectrum as a broad band around 2440 cm^{-1} correlating with the findings of Smith and co-workers for the related tridentate ligand.[207] The structures of compounds **58** and **60** are illustrated in Figure 40. Selected bond length and angle data are provided in Table 7. Although showing some internal variation, the B-N distances within the cationic units of **58** [1.545(8), 1.568(8) Å] and **60** [1.567(2) Å] are within the range of distances observed in the previously reported boronium cations, [(^{t}BuNH$_2$)(1-methylimidazole)BH$_2$]$^+$ [1.557(4) Å] and [(Me$_3$N)(1-methylimidazole)BH$_2$]$^+$ [1.555(3), 1.604(3) Å].[212] Mesityl compound **60** displays C_s symmetry and a slightly smaller N-B-N bite angle than its *tert*-butyl analogue [N(1)-B-N(1)' 107.38(18)° **60**; N(1)-B-N(3) 109.0(5)° **58**]. The imidazolium rings in both compounds remain planar, forming a ca. 106° angle with the mesityl substituents in ligand precursor **60**.

Figure 40. Ortep representations of compounds **58** (left) and **60** (right). Thermal ellipsoids drawn at 30% probability. C(2) and C(3) inverted in **60** for the sake of comparison.
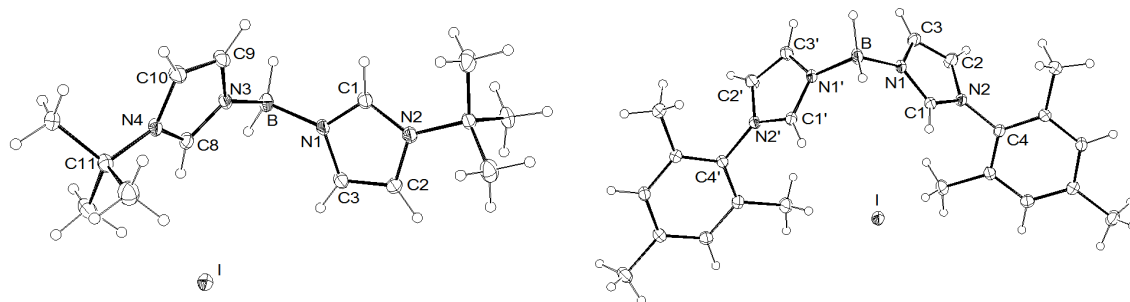

Table 7. Selected bond lengths (Å) and angles (°) for ligand precursors **58** and **60**.

Bond lengths (Å)	**58**	**60**[a]	Angles (°)	**58**	**60**[a]
B-N(1)	1.545(8)	1.567(2)	N(1)-B-N(3)	109.0(5)	107.38(18)[d]
B-N(3)	1.568(8)	-	B-N(1)-C(1)	126.5(5)	125.51(16)
N(1)-C(1)	1.343(7)	1.3267(19)	B-N(3)-C(8)	125.5(5)	-
N(3)-C(8)	1.332(7)	-	C(1)-N(1)-C(3)	106.3(5)	107.58(13)
N(1)-C(3)	1.383(7)	1.379(2)	C(8)-N(3)-C(9)	107.3(5)	-
N(3)-C(9)	1.382(7)	-	C(1)-N(2)-C(2)	107.7(5)	107.67(13)
C(1)-N(2)	1.336(7)	1.3376(19)	C(8)-N(4)-C(10)	107.2(5)	-
C(8)-N(4)	1.344(7)	-	N(1)-C(1)-N(2)	110.4(5)	109.68(13)
N(2)-C(2)	1.382(7)	1.378(2)	N(3)-C(8)-N(4)	110.1(5)	-
N(4)-C(10)	1.382(7)	-	B-N(1)-C(3)[e]	127.2(5)	126.91(16)
C(2)-C(3)	1.354(8)	1.348(2)	B-N(3)-C(9)	127.1(5)	-
C(9)-C(10)	1.356(8)	-	-	-	-
B-H(1A)	1.10(6)	1.14(3)[b]	-	-	-
B-H(1B)	1.07(7)	1.11(3)[c]	-	-	-

a- Symmetry transformations used to generate equivalent atoms: x, -y+½ , z
b- B(1)-H(1)   c- B(1)-H(2)   d- N(1)-B(1)-N(1)'

3.2.2 Synthesis of calcium and strontium bis(carbene)borate complexes

Following a "one pot" procedure similar to the one used in the synthesis of calcium β-diketiminate complex **2**,[21, 36] addition of THF at low temperature to a solid mixture of three equivalents of [KN(SiMe$_3$)$_2$], one equivalent of the ligand precursor (**58** or **59**) and either CaI$_2$ or SrI$_2$ provided after extraction into hexane the desired heteroleptic complexes **62** and **63** (Scheme 55). The analogous reactions employing BaI$_2$ as the alkaline earth starting material did not yield any tractable products: NMR analysis of the crude solids obtained after extraction and drying *in vacuo* showed a complex mixture of

products, among which the presence of free *tert*-butylimidazole was indicative of the fragmentation of the ligand precursors during the reactions (*vide infra*). Storage of concentrated solutions of **62** and **63** at -20 $^{\circ}$C for extended periods allowed the isolation of both compounds as colourless crystalline solids in moderate to good yields (50-70%). Both yield and purity of the products were improved by using the iodide ligand precursor **58** rather than the bromide **59**, which may be due to the lesser solubility of the reaction-driving KI salt metathesis by-product in hydrocarbon solvents compared with KBr.

Scheme 55. "One-pot" synthesis of heavier alkaline earth bis(carbene)borate amides **62** and **63**.
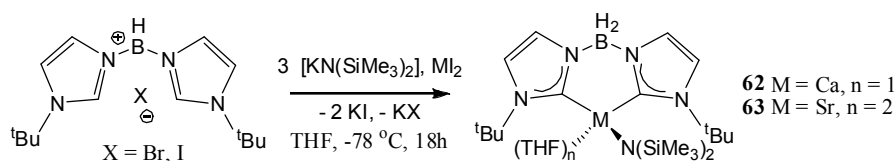
The ^{1}H and ^{13}C{^{1}H} NMR data were consistent with the expected structures. The BH_2 ^{1}H NMR resonances appeared as broad signals at ca. 4.3 ppm. Integration of the THF multiplets indicated one coordinated THF molecule for calcium complex **62** and two for strontium complex **63**. The ^{11}B{^{1}H} NMR resonance was broadened and shifted slightly downfield compared with that of the free ligand precursors. Particularly diagnostic were the signals ascribed to the metal-coordinated *C-2* carbenoid centres of the borate ligands which appeared at 195.0 ppm (**62**) and 201.5 ppm (**63**) in the respective ^{13}C{^{1}H} NMR spectra. This correlates well with previous observations of a series of alkaline earth bis(amides) with neutral NHC ligands, compounds **51-54** (Figure 38), in which it was noted that the smaller and more Lewis acidic metal centres induced a higher upfield shift ($\Delta\delta_{13C}$) in the resonance of the *C-2* centre from that of the free carbene.[213] Examination of these, related alkaline earth tris(imidazolin-2-ylidene-1-yl)borate complexes described in this work (*vide infra*) and other relevant literature data listed in Table 8 reveal that the nature of the Lewis basic carbene σ-donors is apparently not perturbed by incorporation into the bidentate monoanionic borate ligand.

Table 8. Comparison of M-C$_{carbene}$ bond lengths and δ_{13C} NMR data for calcium, strontium and barium NHC complexes.

Compound	M-C$_{carbene}$ (Å)	δ_{13C} C-2 carbene centre (ppm)	Reference
62	-	195.0	This work
64	2.583(3), 2.646(4)	195.0	This work
66	-	196.0	This work
67	2.562(13), 2.562(14)	-	This work
73	-	198.5	This work
76	-	195.5	This work
76′	2.582(5), 2.510(5), 2.526(4)	-	This work
77	2.544(2), 2.564(2), 2.559(2)	199.5	This work
[{L^1}Ca{N(SiMe$_3$)$_2$}$_2$] **51**	2.598(2)	193.3	[213]
[{L^2}Ca{N(SiMe$_3$)$_2$}$_2$] **53**	2.6259(2)	195.4	[213]
[(Cp*)$_2$Ca{L^3}] **48**	2.562(2)	196.2	[195]
63	2.739(3), 2.757(4)	201.5	This work
65	-	198.9	This work
74	2.749(3), 2.776(3), 2.811(3)	201.6	This work
74′	-	201.5	This work
78	2.810(3), 2.802(3), 2.805(3)	198.9	This work
[{L^1}Sr{N(SiMe$_3$)$_2$}$_2$] **52**	2.731(3)	199.0	[213]
[(Cp*)$_2$Sr{L^3}] **49**	-	198.2	[195]
[(Cp*)$_2$Sr{L^3}$_2$]	2.868(5), 2.854(5)	203.7	[195]
75	2.977(3), 2.947(3), 2.978(3)	205.9	This work
[{L^1}Ba{N(SiMe$_3$)$_2$}$_2$] **53**	2.915(4)	-	[213]
[(Cp*)$_2$Ba{L^3}] **50**	2.951(3)	203.5	[195]

L^1 = 1,3-bis(2,4,6-trimethylphenyl)imidazol-2-ylidene; L^2 = 1,3-bis(2,6-di-*iso*-propylphenyl)imidazol-2-ylidene; L^3 = 1,3,4,5-tetramethylimidazol-2-ylidene.

Variable temperature ^{1}H and ^{13}C{^{1}H} NMR studies performed on calcium compound **62** showed some evidence of fluxional behaviour in solution (Figure 41). Cooling of a sample of **62** in d$_8$-toluene revealed a decoalescence of the bis(imidazolin-2-ylidene-1-yl)borate and bis(trimethylsilyl)amide ligand resonances into a series of singlets of equal intensity as the temperature was lowered. Although a splitting of the broad B-*H* resonance around δ_{1H} 4.3 ppm was also observed down to the low temperature limit (208 K) of the ^{1}H{^{11}B} NMR spectrum, consistent with the formation of a labile agostic-type interaction with the calcium metal centre, this process was ill-defined due

to the diastereotopic nature of the BH_2 protons and coupling to the 20% quadrupolar ^{10}B nucleus. The fluxional behaviour was therefore best characterised by examination of the aromatic protons of the imidazolin-2-ylidene fragments which provided a value of $\Delta G^{\ddagger}$ = 48.7 kJ.mol^{-1} for a coalescence temperature of 238 K (Scheme 56). It is noteworthy that the *C-2* carbene resonance in the ^{13}C{^{1}H} NMR spectrum also split into two (199.8 and 198.8 ppm) at the low temperature limit (218 K) of the experiment.

**Scheme 56.** Proposed isomerisation mechanism of compound **62** in solution.
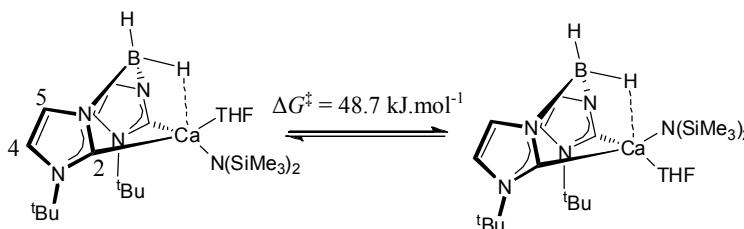
Figure 41. Top: variable temperature ^{1}H NMR stack-plot of a d$_8$-toluene solution of **62** taken every 10 K from 298 to 198 K. Bottom: ^{13}C{^{1}H} NMR spectrum of **62** at 218 K.

101
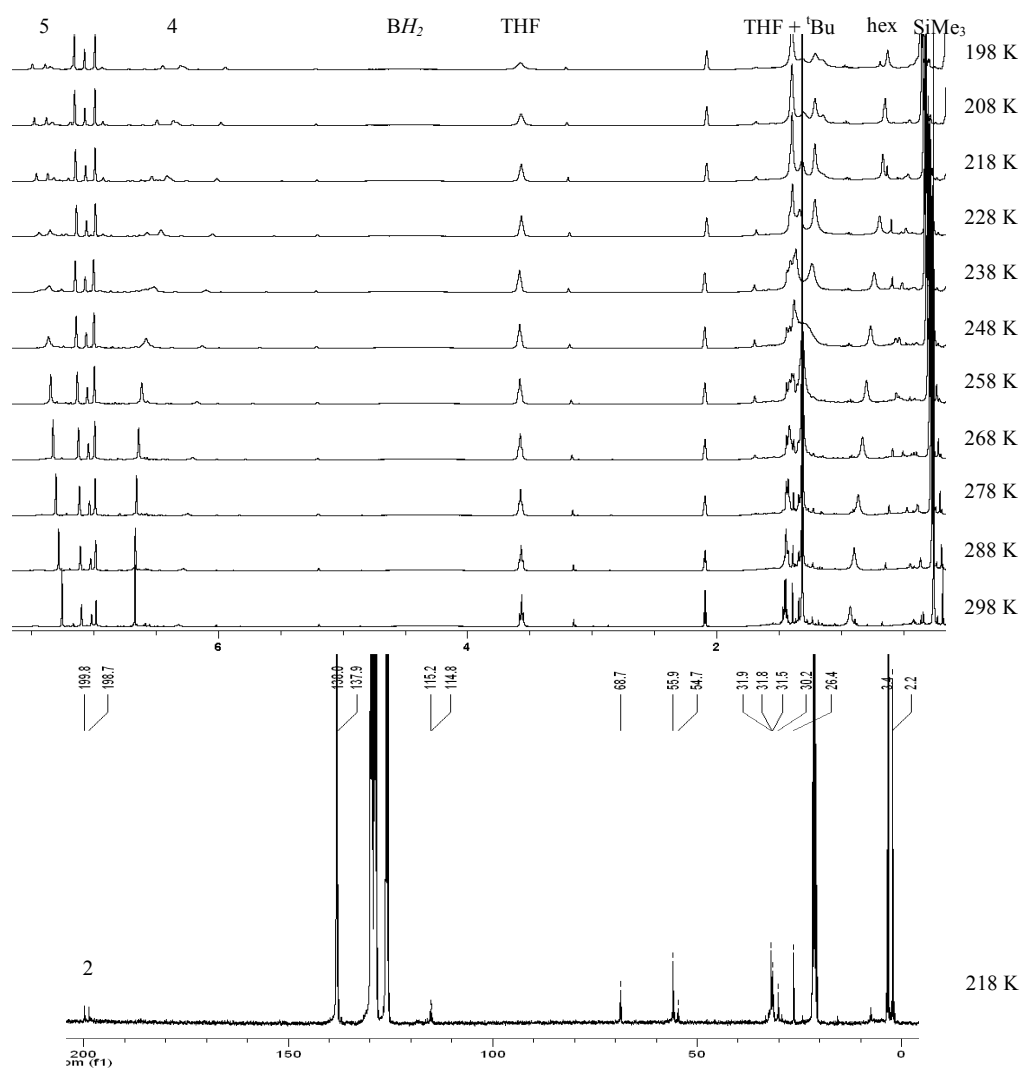
In the structure of the homoleptic nickel complex [{H$_2$B(Im^{t}Bu)$_2$}$_2$Ni] recently reported by Smith and co-workers the nickel centre displayed a square planar coordination geometry while the six-membered BN$_2$C$_2$Ni between the metal and the borate ligands adopted a boat conformation, a geometry that was retained in solution at room temperature.[210] This bonding situation contrasts with that of the related octahedral bis(pyrazolyl)borate complex, [{H$_2$B(^{t}BuPz)$_2$}$_2$Ni], in which two agostic-type Ni···H-B bonds completed the coordination sphere of the metal centre (Figure 42).[214] Similar M···H-B (M = Ca, Sr) interactions were observed in the solid state analyses of the group 2 complexes reported herein (*vide infra*) and are reminiscent of the general coordination behaviour of scorpionate bis(pyrazolyl)borate coordination complexes.[202] Although alternative processes can not be discounted unequivocally, we propose, therefore, that the fluxional solution behaviour observed for compound **62** is a consequence of the lability of the metal to ligand interactions typically observed in heavier group 2 complexes, and indicative of equilibration of the geometric isomers illustrated in Scheme 56. Variable temperature studies performed upon the strontium analogue of **62**, compound **63**, revealed similar, but less well defined, fluxional behaviour, most likely as a consequence of the reduced charge density of the larger Sr^{2+} cation.

Figure 42. Left: geometry of the square planar [{H$_2$B(Im^{t}Bu)$_2$}$_2$Ni] complex. Right: geometry of the octahedral [{H$_2$B(^{t}BuPz)$_2$}$_2$Ni] complex displaying Ni···H-B agostic-type interactions.
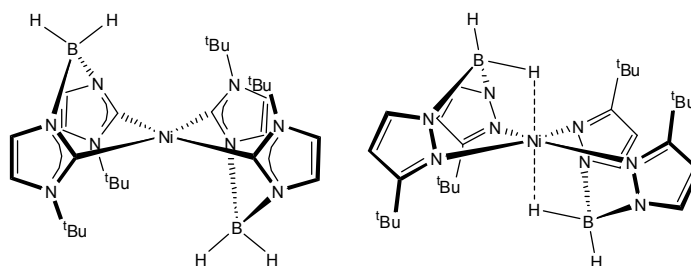
Crystals of compound **63** suitable for X-ray diffraction analysis were isolated from a hexane solution at -20 °C. The results of this experiment are illustrated in Figure 43 and selected bond length and angle data are provided in Table 9. Compound **63** adopts a distorted *pseudo*-octahedral coordination geometry in the solid state with a facial O$_2$N donor set provided by two molecules of THF, one of which is disordered, and the silylamide co-ligand. The other face is occupied by the bis(imidazolin-2-ylidene-1-yl)borate ligand which adopts a boat conformation and an effective tridentate

coordination mode. In this latter case, donation to the strontium cation is provided by the two imidazolin-2-ylidene carbene centres and an apparent agostic-type interaction with a boron B-H bond. The Sr-C$_{carbene}$ distances [2.757(4) - 2.739(3) Å] are comparable to that observed within the recently reported three-coordinate neutral carbene adduct **52** [(NHC)Sr{N(SiMe$_3$)$_2$}$_2$] [2.731(3) Å][213] despite the increased coordination number at strontium (Table 8). The interaction between the strontium cation and a hydridic hydrogen of the BH$_2$ unit [Sr···H(1a), 2.87(3) Å], although long, is within the range established [2.59(3)-2.89(3) Å] within several borohydride and phosphinoborane-substituted carbanionic strontium derivatives.[215, 216] Several attempts to obtain a crystal structure of the calcium analogue **62** failed due to the extremely temperature-sensitive nature of the crystals.

Figure 43. Ortep representation of compound **63**. Thermal ellipsoids drawn at 30% probability. *Tert*-butyl methyl groups and hydrogens omitted for clarity, except those attached to the boron atom. Sr-H(1A) agostic interaction represented as a dashed bond.
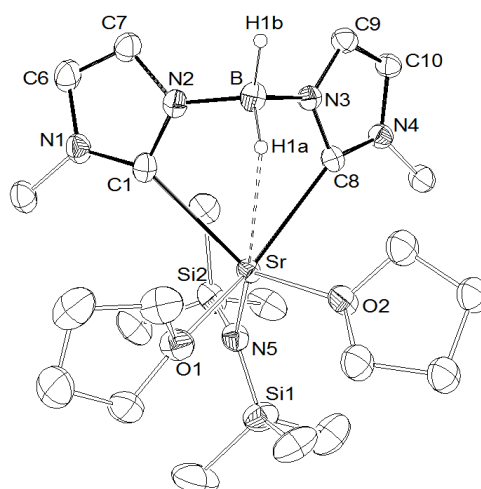
**Table 9.** Selected bond lengths (Å) and angles ($^{\circ}$) for complexes **63** and **64**.

Bond lengths (Å)	**63**[a]	**64**[b]	Angles ($^{\circ}$)	**63**[a]	**64**[b]
M-C(1)	2.757(4)	2.583(3)	C(1)-M-C(8/4)[c]	83.29(11)	83.74(11)
Ca-C(7)	-	2.640(4)	C(7)-Ca-C(10)	-	85.77(11)
M-C(8/4)[c]	2.739(3)	2.646(4)	N(2/1)-B(1)-N(3)[c]	112.0(3)	111.0(3)
Ca-C(10)	-	2.607(3)	N(5)-B(2)-N(7)[d]	-	111.2(3)
M-O(1)	2.592(3)	2.467(3)	C(1)-N(2/1)-B(1)[c]	123.3(3)	122.7(3)
Sr-O(2)	2.606(4)	-	C(7)-N(5)-B(2)[d]	-	122.9(3)
B(1)-N(2/1)[c]	1.555(5)	1.549(5)	C(8/4)-N(3)-B(1)[c]	123.0(3)	124.4(3)
B(2)-N(5)[d]	-	1.552(5)	C(10)-N(7)-B(2)[d]	-	123.3(3)
B-N(3)	1.544(5)	1.552(6)	N(2/1)-C(1)-M[c]	109.0(2)	113.3(2)
B-N(7)[d]	-	1.546(5)	N(5)-C(7)-Ca	-	106.9(2)
N(2/1)-C(1)[c]	1.367(5)	1.365(4)	N(3)-C(8/4)-M[c]	109.6(2)	111.5(2)
N(5)-C(7)[d]	-	1.361(5)	N(7)-C(10)-Ca	-	109.7(2)
N(3)-C(8/4)[c]	1.371(5)	1.362(5)	N(1)-C(1)-N(2)	103.6(3)	104.4(3)
N(7)-C(10)	-	1.363(4)	N(5)-C(7)-N(6)[d]	-	104.0(3)
Sr-N(5)	2.510(3)	-	N(3)-C(8/4)-N(4)[c]	104.3(3)	104.0(3)
M···H(1a)	2.87(3)	-	N(7)-C(10)-N(8)[d]	-	104.5(3)
B-H(1a)	1.12(3)	-			
B-H(1b)	1.14(4)	-			

a- M = Sr   b- M = Ca   c- (Complex **63/64**)   d- Complex **64** only

In an attempt to synthesise heteroleptic alkaline earth iodide derivatives, two molar equivalents of [KN(SiMe$_3$)$_2$] were used instead of three, in reactions similar to the one presented in Scheme 55 with the more efficient iodide ligand precursor **58** (Scheme 57). Both reactions employing calcium and strontium iodides provided similar results and yielded homoleptic species, compounds **64** [{H$_2$B(Im^{t}Bu)$_2$}$_2$Ca(THF)] and **65** [{H$_2$B(Im^{t}Bu)$_2$}$_2$Sr(THF)$_2$], which are evidently formed due to the reduced steric demands of the intended iodide compared with the hexamethyldisilazide co-ligand employed in the syntheses of compounds **62** and **63**. Although both compounds proved to be extremely air-, moisture- and temperature-sensitive, preventing the acquisition of accurate microanalytical data, promptly prepared samples analysed by ^{1}H and ^{13}C{^{1}H} NMR spectroscopy displayed similar spectral features suggestive of a single borate ligand environment. The chemical shifts attributed to the donor-carbon carbene resonances [**64**, δ_{13C} 195.0; **65**, 198.9 ppm] also bore close comparison to those

observed for the heteroleptic species **62** and **63**, indicative of comparable binding modes and charge donation (Table 8).

Scheme 57. Synthesis of homoleptic calcium and strontium bis(carbene)borate complexes **64** and **65**.
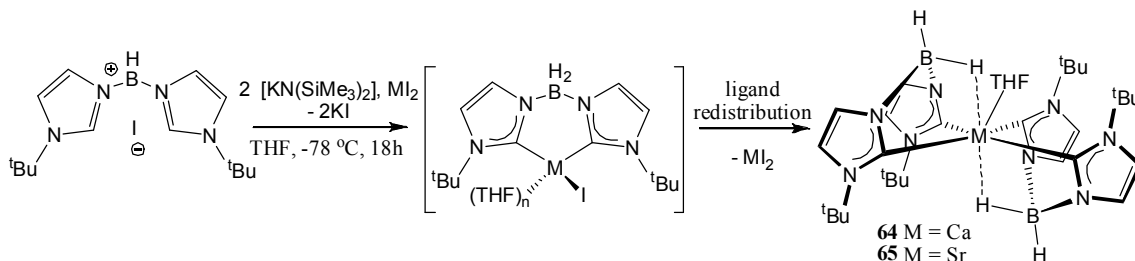
This deduction was confirmed by a further X-ray structural analysis obtained for the calcium compound **64**. Although crystals of **64** required handling under a cryogenic N_2 stream to prevent decomposition and were weakly diffracting, the structure was unambiguous and revealed a similar κ^3-*CC'H*-binding of the borate ligands to that observed for **63**. The structure of compound **64** is illustrated in Figure 44 and selected bond length and angle data are provided in Table 9. The range of calcium-carbon distances [2.583(3) - 2.646(4) Å] is similar to that observed within the neutral NHC adducts [(NHC)Ca{N(SiMe$_3$)$_2$}$_2$] [**51**, 2.598(2); **54**, 2.6259(2) Å][213] and **48** [(Cp*)$_2$Ca(NHC)] [2.562(2) Å][195] listed in Table 8, as well as the range of distances reported by Harder and co-workers for several calcium bis(iminophosphoranyl)methandiyl derivatives [2.528(2) - 2.805(1) Å].[45, 217] Although substantially longer than those observed within the previously reported dialkyldihydridoborate [HC{C(Me)CN(2,6-^{i}Pr$_2$C$_6$H$_3$)$_2$}Ca(H$_2$BR$_2$)] (R = the anion formed from 9-borabicyclo[3.3.1]nonane) [2.17(4) - 2.31(4) Å][218] and the calcium tetrahydroborate [(DME)$_2$Ca(BH$_4$)$_2$] [2.35(3) - 2.58(3) Å],[215] the Ca$\cdots$H(1b/2a) distances within **64** [2.97 - 2.83 Å] again describe a structurally significant interaction such that the calcium centre may be depicted as effectively seven-coordinate. As for the heteroleptic strontium complex **63**, the carbene-calcium vectors are not coplanar with the imidazole rings. It is also notable that the chelating framework of the borate ligand evidently possesses little flexibility as the N-B-N bond angles display little variation across the precursor **58** [109.0(5)^o] and the calcium and strontium complexes **64** [111.0(3), 111.2(3)^o] and **63** [112.0(3)^o] respectively. The same observation can also be made about the other angles and distances within the ligand framework as shown by a more comprehensive list of measurements displayed in Table 9.

Figure 44. Ortep representation of compound **64**. Thermal ellipsoids drawn at 30% probability. *Tert*-butyl methyl groups and hydrogens omitted for clarity, except those attached to the boron atom. Ca-H(1a/2a) agostic interactions represented as dashed bonds.
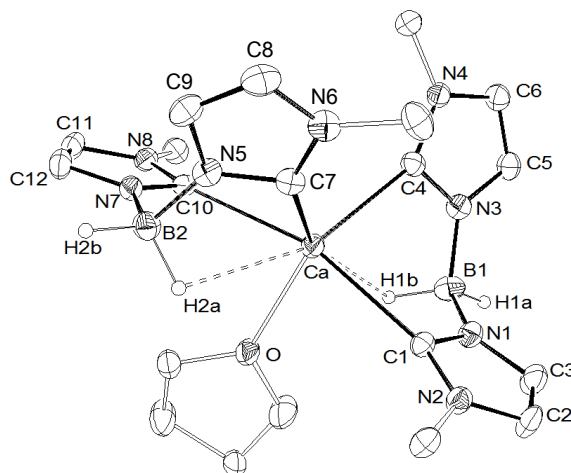
Attempts to elaborate a rational synthesis of these homoleptic species were unsuccessful. Although an analogous "one pot" procedure employing four equivalents of the silylamide base produced materials with ^{1}H and ^{13}C{^{1}H} NMR spectra reminiscent of those of **64** and **65**, these materials contained no coordinated THF. Rather, additional singlet resonances at δ_{1H} 0.84 (9H), 6.36 (1H) and 7.13 (1H) ppm were attributed to coordinated 1-*tert*-butylimidazole which was evidently produced by rupture of the B-N bonds of the ligand precursor during borate anion formation. Although no evidence of ligand degradation subsequent to anion formation was observed, it appears that such B-N cleavage is a common feature of this ligand class at some stage in the deprotonation of, and the necessary charge distribution within, the ligand precursors. Similar difficulties also blighted attempts to synthesise analogues of compounds **62-65** utilising the *N*-mesityl substituted precursors, **60** and **61** *via* the "one pot" procedures illustrated in Scheme 55 and Scheme 57. In these cases the reactions turned deep crimson in colour, and were shown by NMR analysis of the crude solids to contain a complex and intractable mixture of products. This problem was partially circumvented through the adoption of an alternative synthetic route, which utilised the homoleptic calcium amide [Ca{N(SiMe$_3$)$_2$}$_2$(THF)$_2$], **36b**, as both base and source of the group 2 metal. Reaction of 1.5 equivalents of **36b** with the boronium iodide salt precursor compound **60** (Scheme 58) provided the colourless complex **66**, which provided NMR spectra indicative of the intended heteroleptic formulation. Although the ^{13}C{^{1}H} NMR carbene resonance of **66** (196.0 ppm) was again similar to that observed

in compounds **62** and **64**, variable temperature ^{1}H NMR studies revealed none of the fluxional behaviour attributed to the heteroleptic species described above.

Scheme 58. Synthesis of compound **66**.
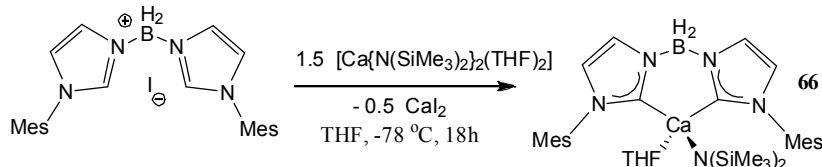
Whilst compound **66** provided well-formed single crystals at low temperature, multiple attempts to acquire X-ray diffraction data were frustrated by the extremely rapid decomposition of the material once removed from the chilled mother liquor. A data set collected on a more durable crystal from one of these reactions yielded the structure of an unanticipated heteroleptic iodide species, compound **67** (Figure 45). Although the data set for **67** was very weak and yielded residuals for the structure which were unacceptably high ($R1 = 0.1107$, $wR2 = 0.2617$), precluding any detailed discussion, the connectivity was unambiguous. The borate ligands again adopts a tridentate coordination mode, while the presence of the iodide ligands highlights the propensity towards redistributative processes of heavier group 2 centres.

Figure 45. Ortep representation of the dimeric compound **67**. Thermal ellipsoids drawn at 30% probability. Hydrogens omitted for clarity, except those attached to the boron atom. Ca⋯H(1a) agostic interaction represented as a dashed bond.
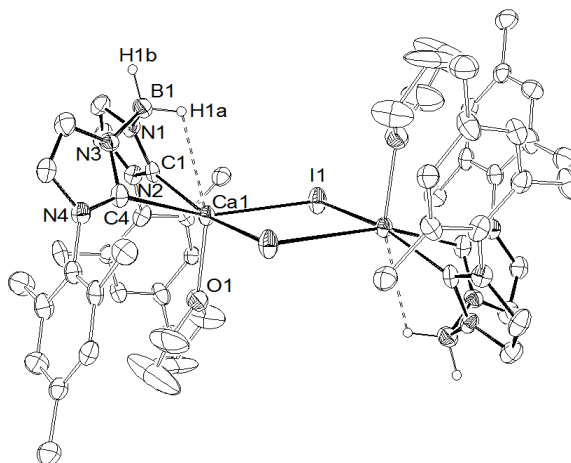
Several attempts to obtain analogues of compounds **62-67** less prone to ligand redistribution and/or B-N bond cleavage failed. Indeed, refluxing in chlorobenzene of Me$_3$N.BH$_2$I with two equivalents of the more sterically demanding 1-(2,6-di-*iso*-propylphenyl)imidazole or the potentially bidentate 1-(2-methoxyphenyl)imidazole precursors, both prepared according to literature procedures,[219] yielded complex

107

mixtures of boron-containing products out of which the desired boronium salts could not be isolated in satisfying purity. Although a chiral version of the ligand precursor using 1-((*S*)-*α*-phenylethyl)imidazole was prepared, albeit in modest yield, neither the "one-pot" salt metathesis-based synthesis used to obtain **62** and **63** nor the reaction with 1.5 equivalents of [Ca{N(SiMe$_3$)$_2$}$_2$(THF)$_2$] in cold THF yielded any tractable products. ^{1}H NMR data of the crude hexane extraction mixtures once again provided evidence for considerable B-N bond cleavage and presence of the free imidazole precursor.

3.2.3 DFT calculations

The nature of the metal to ligand coordination in complexes **62** and **63** was assessed by DFT calculations on the model heteroleptic complexes [{H$_2$B(NHC)$_2$}M{N(SiH$_3$)$_2$}(OMe$_2$)$_2$] **68** (M = Ca) and **69** (M =Sr) (NHC = 3-methylimidazol-2-ylidene) using the B3LYP density functional theory and LAN2DZ *pseudo*potentials (and basis set) implemented in Gaussian03.[220] The geometry optimisations were performed by selecting an initial geometry based upon that deduced for the structure of the heteroleptic strontium complex **63** and, in both cases, were confirmed as true minima by independent frequency calculations which did not yield any imaginary frequencies. To reduce computational expense the *tert*-butyl groups of the borate ligands were replaced by methyl groups, the methyl groups of the silylamide ligands by hydrogen atoms, and the coordinated THF molecules were simplified to two molecules of dimethyl ether. The second molecule of coordinated solvent was retained within the coordination sphere of the calcium centre of **68** despite the lower coordination number determined for the "real case" of compound **62**. It was felt that this was necessary to take into account the reduced steric demands of the truncated ligands and to allow for internal consistency when comparing the two calculated structures. Figure 46 illustrates the results of this study. In both cases the calcium and strontium contacts to the carbon donors of the κ^3-coordinated ligands replicate the distances observed within the structures of compounds **63** and **64** respectively, to within ca. 0.02 Å (see Figure 46 caption). Especially notable was the agreement between the calculated M···H-B distances [**68**, 2.93 Å; **69**, 2.87 Å] and the values determined in the X-ray studies. The calculated ν_{B-H} stretching vibrations for both model compounds (**68** 2503,

2412 cm^{-1}; **69** 2499, 2401 cm^{-1}), corresponding to the symmetric and asymmetric stretching of both B-H bonds, are somewhat higher than those observed for the heteroleptic species **62** (2385, 2252 cm^{-1}) and **63** (2363, 2252 cm^{-1}). However this may be ascribed to the decreased reduced mass of the oscillators within the simplified models and it is notable that Δv, the difference between the stretching vibrations in both the real and model compounds, is of a similar magnitude (ca. 100 cm^{-1}) across all four sets of data. For both **68** and **69** natural bond orbital (NBO) calculations were undertaken and the calculated charges on the Ca^{2+} (**68**, +1.83) and Sr^{2+} (**69**, +1.86) centres were suggestive of essentially ionic bonding. In both cases the donor carbon centres bear only a modest negative charge (< -0.03) indicating that they retain the essentially pure σ-donor character implicated in the formation of neutral alkaline earth carbene adducts such as [(NHC)M{N(SiMe$_3$)$_2$}$_2$], **51-54**.[213] Although the majority of the anionic charge of the ligands is borne by the boron-bound imidazolin-2-ylidenyl nitrogen centres (ca. -0.63), the electrostatic nature of the M···H-B interactions is indicated by the hydridic nature (ca. -0.11 for the "coordinated" hydrogen) of the borohydride subunits.

Figure 46. Representations of the optimised (DFT, B3LYP/LAN2DZ) structures of compounds **68** (left) and **69** (right). Calculated NBO charges for selected atoms shown in parenthesis. Selected bond lengths (Å); **68**: Ca-C(avg.) 2.63; Ca-N 2.47; Ca···H-B 2.93; Ca-O(avg.) 2.48. **69**: Sr-C(avg.) 2.79; Sr-N 2.55; Sr···H-B 2.87; Sr-O(avg.) 2.62.
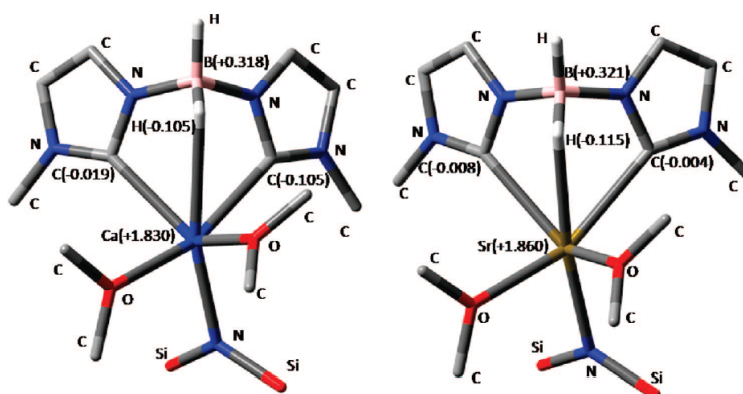

3.2.4 Stoichiometric and catalytic reactivity

We have reported previously that neutral NHC ligands readily dissociate from alkaline earth cations in solution in the presence of harder (e.g., N- and O-centred) donors.[213] This observation is especially relevant to the potential application of group 2

complexes in hydroamination catalysis where the reaction conditions are innately disposed towards carbene displacement. In order to assess the stability of the bis(carbene)borate alkaline earth systems, compounds **62** and **63** were subjected to stoichiometric NMR scale reactions with various Brønsted acids. While reaction of calcium complex **62** with terminal acetylenes resulted in instantaneous protonation and displacement of the ligand, reaction with benzylamine yielded complete consumption of the amine and conversion to the heteroleptic calcium benzylamide complex **70** (Scheme 56), displaying a characteristic broad Ca-N*H* ^{1}H NMR resonance at -1.25 ppm within the first point of analysis. Monitoring of a sample of **70** in solution over a week, however, showed gradual protonation and degradation of the bis(carbene)borate ligand into free *tert*-butylimidazole, a process significantly accelerated at higher temperatures, which prevented the assessment of a potential amine-amide equilibrium through van't Hoff analysis for comparison with the analogous reaction involving *β*-diketiminate complex **2**.[56] Reaction of **62** with 2-methoxyethylamine similarly yielded rapid and quantitative conversion to the heteroleptic amine-amide exchange product **71**, displaying a very broad high-field resonance at δ_{1H} -0.89 ppm (Scheme 59). Again, isolation of this compound was prevented by slow protonation of the ligand carbene residues in solution over a period of several days. The analogous stoichiometric reaction with diphenylamine instantly resulted in partial ligand protonation as well as rapid redistribution towards the homoleptic species. Analogous stoichiometric reactions with strontium complex **63** led to similar results, albeit with faster ligand redistribution and protonation.

Scheme 59. Stoichiometric reactions of calcium complex **62** with primary and secondary amines.

R = CH$_2$Ph **70**, (CH$_2$)$_2$OMe **71**
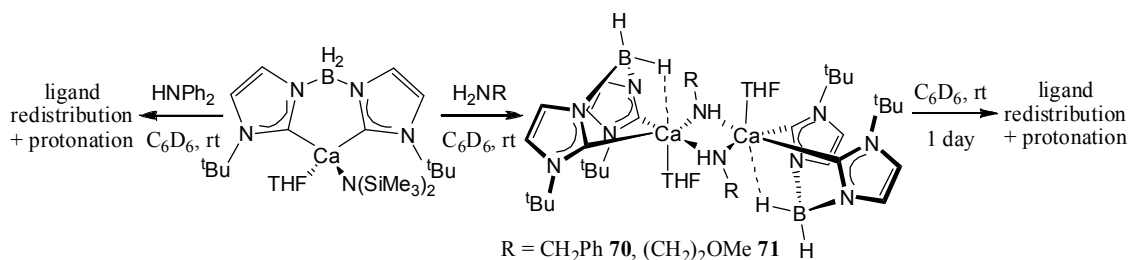
Stoichiometric addition of non-cyclisable 1-amino-2,2-diphenyl-5-methyl-4-hexene to a C$_6$D$_6$ solution of calcium and strontium compounds **62** and **63**, however, resulted in an amine-amide equilibrium significantly in favour of the starting materials. After one week at room temperature ligand protonation and redistribution remained limited to less

than 5%. Encouraged by this last result, therefore, compounds **62** and **63** were assessed for the intramolecular hydroamination of a range of substituted aminoalkenes on an NMR scale in C_6D_6. In all cases, careful inspection of the NMR spectra revealed no significant protonation or dissociation of the borate ligand throughout reaction times up to a period of one week and temperatures up to 70 ^{o}C. The imidazole ^{1}H NMR signals and the ^{13}C{^{1}H} carbene resonances remained effectively unaltered and no conclusive evidence for Schlenk-type ligand redistribution was observed, except at temperatures above 70 ^{o}C.

Examination of the results listed in Table 10 indicated that the amidocalcium complex **62** displayed similar activity to that reported for the *β*-diketiminato calcium precatalyst, **2**.[54] In common with these previous studies, bulky geminal substituents in the *β*-position of the amine favoured cyclisation due to a Thorpe-Ingold effect (entries 3-7), while alkyl monosubstitution of the alkene moiety considerably hindered the reaction and terminal disubstitution prevented it entirely (entries 8-11). Catalytic activity also rapidly diminished with increasing ring-size (5 > 6 > 7; entries 12-16).

Generally, cyclisation occurred faster, with better conversion, and at lower temperature and catalyst loading with the strontium complex **63** than with its calcium counterpart. This conflicts with the observations made for heteroleptic calcium and strontium *β*-diketiminate and homoleptic bis(amide) complexes (Tables 1 and 2) as well as with previous reports by Datta *et al.* and Hill and co-workers in which strontium aminotroponiminate and triazenide precatalysts were found to be significantly less active than their calcium counterparts for the intramolecular hydroamination of aminoalkenes.[60, 61] Although detailed kinetic studies would provide a more quantitative insight into the inversion of reactivity observed in these preliminary results, qualitative comparison of the catalytic activity of tris(imidazolin-2-ylidene-1-yl)borate calcium and strontium complexes, in which the strontium complex also displayed significantly higher activity, seems to suggest that this phenomenon might be linked to the stereoelectronic properties of this specific class of ligand in combination with the catalytic strontium centre, rather than being an intrinsic feature of the group 2 element selected (*vide infra*). Despite an apparently positive influence on the catalytic activity of calcium and strontium complexes, the anionic [$H_2B(Im^tBu)_2$]$^-$ ligand generally provided neither advantageous kinetic protection against ligand redistribution compared to the more readily accessible *β*-diketiminate ligand, nor better selectivity or improved scope for the intramolecular hydroamination reaction. The following study aims to address the

issue of kinetic protection by employing the more sterically demanding, monoanionic [HB(Im^{t}Bu)$_3$]$^-$ ligand.

Table 10. Scope of intramolecular hydroamination with calcium and strontium bis(carbene)borate precatalysts **62** and **63**.

Entry	Substrate	Product	Catalyst (mol %)	Time / h	T /°C	NMR yield / %[a]
1			**62** (10 mol %)	2	25	>95
2			**63** (5 mol %)	1	25	>95
3			**62** (5 mol %)	0.5	25	30
4			**62** (5 mol %)	0.15	70	>95
5			**63** (5 mol %)	0.15	25	95
6			**62** (5 mol %)	0.3	25	95
7			**63** (5 mol %)	0.15	25	>99
8			**62** (5 mol %)	1 d	25	50
9			**63** (5 mol %)	1	70	>99
10			**62** (5 mol %)	2 d	70	0
11			**63** (20 mol %)	3 d	70	0
12			**62** (5 mol %)	1 d	25	55:5[b]
13			**62** (10 mol %)	6	25	80:6[b]
14			**63** (5 mol %)	4	25	68:20[b]
15			**62** (10 mol %)	3 d	75	10:65[b]
16			**63** (10 mol %)	2 d	75	12:68[b]

a- NMR scale reactions carried out in C$_6$D$_6$ or d$_8$-toluene, yields calculated from an internal TMSS standard.
b- Cyclisation: isomerisation.

3.3 Synthetic, structural and catalytic studies of heavier alkaline earth tris(imidazolin-2-ylidene-1-yl)borate complexes.[221]

### 3.3.1 Synthesis of calcium, strontium and barium tris(carbene)borate complexes

The ligand precursor salt **72** [HB(Im^{t}Bu)$_3$]Br$_2$ was synthesised following the procedure described by Smith and co-workers (Scheme 60)[207] and crystallised from dichloromethane. ^{1}H and ^{13}C{^{1}H} NMR chemical shift data were in accordance with those reported by Nieto *et al.*, with a characteristic low-field *H-2* imidazole proton resonance at δ_{1H} 9.85 ppm.[207] The analogous diiodide salt could not be obtained due to complications in attempts to isolate the Me$_3$N.BHI$_2$ precursor.

Scheme 60. Synthesis of [HB(Im^{t}Bu)$_3$]Br$_2$ **72**.
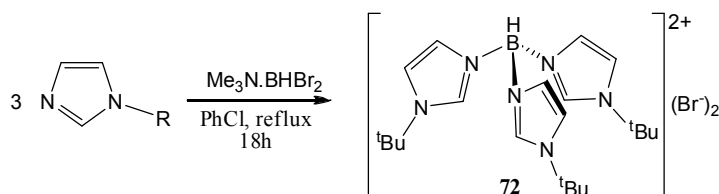
Using a "one-pot" procedure similar to that employed in the synthesis of bis(carbene)borate complexes **62** and **63**, addition of THF at -78 °C to a mixture of four equivalents of [KN(SiMe$_3$)$_2$], one equivalent of the ligand precursor **72** and either CaI$_2$, SrI$_2$ or BaI$_2$ provided, after extraction into toluene, the desired heteroleptic alkaline earth amides **73**, **74** and **75** (Scheme 61). Contrary to the previously described group 2 bis(imidazolin-2-ylidene-1-yl)borate amides, whose coordination sphere is completed by THF, NMR and X-ray data of compounds **74** and **75** showed the presence of 1-*tert*-butylimidazole adducts arising from fragmentation of the ligand precursor during the reaction. Such decomposition had already been observed in the NMR spectra of the crude reaction mixtures of the bis(imidazolin-2-ylidene-1-yl)borate compounds. After separation from KI and KBr by-products and storage of concentrated toluene solutions at -20 °C, complexes **73-75** could, however, be isolated as colourless crystalline, very low-melting solids in moderate to good yields (48-88%).

Scheme 61. Synthesis of heavier alkaline earth tris(carbene)borate complexes **73-75**.

73 M = Ca, n = 0
74 M = Sr, n = 1
75 M = Ba, n = 1.5
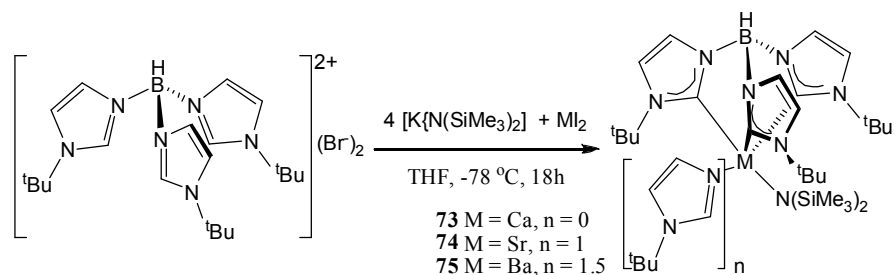
Repeating the synthesis of **74** without the use of the potentially acidic Celite during filtration, and washing of the Schlenk flasks with a basic isopropanol solution of potassium hydroxide before drying for one day at 150 °C, yielded a 60:40 mixture of the desired THF adduct **74′** and compound **74** respectively, which were separated by fractional crystallisation from toluene at -20 °C. Although suitable crystals of compound **74′** could not be prepared for X-ray crystallography, ^{1}H and ^{13}C{^{1}H} NMR data and elemental analyses of **74′** were in accordance with the expected structure. Analogous reaction and filtration conditions for the synthesis of the barium silylamide complex, however, did not yield the THF adduct and instead resulted in decomposition of the ligand. ^{1}H and ^{13}C{^{1}H} NMR data of **73**, **74**, **74′** and **75** were consistent with the expected structures. Particularly diagnostic were the low-field ^{13}C{^{1}H} signals attributed to the metal-coordinated *C-2* carbene centres of the borate ligand appearing at 196.2 (**73**), 201.5 (**74**), 198.7 (**74′**) and 205.9 ppm (**75**) respectively. This trend correlates well with that observed in the calcium and strontium bis(imidazolin-2-ylidene-1-yl)borate species **62-66** as well as in the neutral NHC adducts [(NHC)M{N(SiMe$_3$)$_2$}$_2$], **51-54**,[213] confirming that the magnitude of the upfield shift ($\Delta\delta_{13C}$) of the *C-2* centre from that of the free carbene decreases with the Lewis acidity of the group 2 metal (Table 8). As for its bidentate counterpart, it appears that the incorporation of the NHC fragments into the tridentate monoanionic borate ligand does not affect the behaviour of the *C-2* carbene centres as pure σ-donors. Crystals of compounds **74** and **75** suitable for X-ray diffraction analysis were obtained from toluene solutions at -20 °C. The results of these experiments are illustrated in Figure 47 and Figure 48 respectively. Selected bond length and angle data are provided in Table 11 and Table 12 respectively. Compound **74** adopts a highly distorted square pyramidal coordination geometry in the solid state (τ = 0.16)[149] in which the axial position is occupied by one of the arms of the ligand. The strontium centre is bound to all three carbene carbons of the anionic ligand which is only slightly distorted from C_{3v}

114

symmetry. The Sr-C distances [2.776(3), 2.811(3) and 2.749(3) Å] are very similar to those of the strontium bis(imidazolin-2-ylidene-1-yl)borate silylamide analogue, **63** [2.757(4) - 2.739(3) Å] and the neutral carbene adduct [(NHC)Sr{N(SiMe$_3$)$_2$}$_2$] [**52**, 2.731(3) Å][213] despite the increased coordination number at the strontium centre (Table 8).

Figure 47. Ortep representation of compound **74**. Thermal ellipsoids drawn at 30% probability. *Tert*-butyl methyl groups and hydrogens removed for clarity, except those attached to the boron atom.
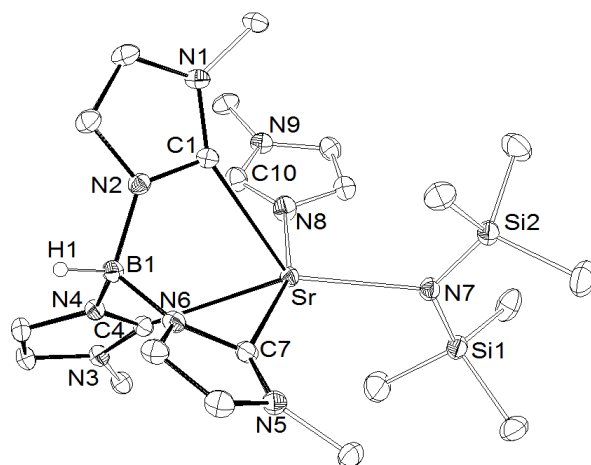
Although crystals of compound **75** were extremely temperature-sensitive and had to be selected under a cryogenic flow of N$_2$ to avoid melting, the structure was unambiguous. The asymmetric unit of compound **75** is composed of two distinct barium tris(imidazolin-2-ylidene-1-yl)borate silylamide units solvated by one and two imidazole heterocycles respectively (Figure 48). The five-coordinate barium complex adopts a distorted square pyramidal coordination geometry (τ = 0.33).[149] Two arms of the tris(imidazolin-2-ylidene-1-yl)borate ligand occupy equatorial positions together with the silylamide co-ligand and the imidazole adduct while the third arm of the scorpionate ligand occupy the axial position. The other six-coordinate barium monomer adopts a very distorted *pseudo*-octahedral geometry instead, with a *facial* C$_3$ donor set provided by the tridentate carbene ligand while the other face is occupied by the silylamide co-ligand and the two coordinated imidazole ligands. As observed for the strontium analogue **74**, the anionic ligand adopts a κ^3-coordination mode through all three carbene carbons. The Ba-C distances [2.977(3), 2.947(3), 2.978(3), 2.904(3), 2.934(3) and 2.953(3) Å] are comparable to that of the neutral carbene adducts reported by Arduengo [**50**, 2.951(3) Å][195] and by Hill and co-workers [**53**, 2.915(4) Å].[213] In

both compounds **74** and **75** the carbene-metal vectors do not lie in the plane of the imidazole rings so that the NHC fragments are slightly distorted from the ideal C_{3v} symmetry, most likely due to high crystal packing forces. Similar observations had already been made by Arduengo and co-workers for the neutral carbene adducts.[195]

Table 11. Selected bond lengths (Å) for compounds **74**, **75**, **76′**, **77** and **78**.

	74	75	76′	77	78
B(1)-N(2)	1.555(3)	1.546(4)	1.547(6)	1.552(3)	1.555(4)
B(1)-N(4)	1.554(4)	1.549(4)	1.559(6)	1.554(3)	1.552(4)
B(1)-N(6)	1.557(4)	1.554(4)	1.546(6)	1.554(3)	1.553(4)
B(2)-N(13)	-	1.555(4)	-	-	-
B(2)-N(15)	-	1.551(4)	-	-	-
B(2)-N(17)	-	1.563(4)	-	-	-
C(1)-N(1)	1.373(3)	1.373(4)	1.364(6)	1.367(3)	1.372(4)
C(1)-N(2)	1.372(3)	1.372(4)	1.369(6)	1.367(3)	1.378(4)
C(4)-N(3)	1.374(3)	1.372(4)	1.366(6)	1.368(3)	1.371(4)
C(4)-N(4)	1.370(3)	1.364(4)	1.364(6)	1.364(3)	1.379(4)
C(7)-N(5)	1.369(3)	1.370(4)	1.363(6)	1.367(3)	1.368(4)
C(7)-N(6)	1.375(3)	1.365(4)	1.368(6)	1.366(3)	1.367(4)
C(42)-N(12)	-	1.371(4)	-	-	-
C(42)-N(13)	-	1.369(4)	-	-	-
C(45)-N(14)	-	1.364(3)	-	-	-
C(45)-N(15)	-	1.374(3)	-	-	-
C(48)-N(16)	-	1.369(3)	-	-	-
C(48)-N(17)	-	1.366(3)	-	-	-
B(1)-H(1)	-	1.14(3)	-	1.13(2)	1.15(3)
B(2)-H(2)	-	1.14(2)	-	-	-
Ca-I	-	-	3.0490(9)	-	-
Ca-Br	-	-	-	2.8930(4)	-
Ca-Br'	-	-	-	2.9040(4)	-

116

Table 12. Selected angles (°) for compounds **74**, **75**, **76′**, **77** and **78**.

	74	75	76′	77	78
N(2)-B(1)-N(4)	110.9(2)	112.6(3)	109.5(4)	112.42(17)	111.6(2)
N(2)-B(1)-N(6)	113.2(2)	112.9(3)	110.6(4)	111.33(17)	112.4(2)
N(6)-B(1)-N(4)	112.1(2)	111.3(2)	112.3(4)	109.57(17)	112.9(2)
N(13)-B(2)-N(15)	-	113.1(2)	-	-	-
N(13)-B(2)-N(17)	-	112.3(2)	-	-	-
N(17)-B(2)-N(15)	-	110.5(2)	-	-	-
C(1)-N(2)-B(1)	128.7(2)	129.4(2)	127.2(4)	127.07(17)	128.8(2)
C(4)-N(4)-B(1)	128.5(2)	128.3(2)	125.4(4)	127.26(17)	128.7(2)
C(7)-N(6)-B(1)	128.4(2)	128.6(2)	126.0(4)	126.67(17)	127.9(2)
C(42)-N(13)-B(2)	-	128.6(2)	-	-	-
C(45)-N(15)-B(2)	-	127.9(2)	-	-	-
C(48)-N(17)-B(2)	-	127.3(2)	-	-	-
N(1)-C(1)-N(2)	103.5(2)	103.6(2)	104.4(4)	104.24(17)	103.8(2)
N(3)-C(4)-N(4)	103.9(2)	103.9(2)	104.0(4)	104.50(17)	103.5(2)
N(5)-C(7)-N(6)	103.7(2)	103.8(2)	104.4(4)	104.11(17)	103.9(2)
N(12)-C(42)-N(13)	-	103.9(2)	-	-	-
N(14)-C(45)-N(15)	-	103.8(2)	-	-	-
N(16)-C(48)-N(17)	-	103.9(2)	-	-	-

Figure 48. Ortep representation of the asymmetric unit of compound **75**. Thermal ellipsoids drawn at 30% probability. *Tert*-butyl methyl groups and hydrogens removed for clarity, except those attached to the boron atoms.
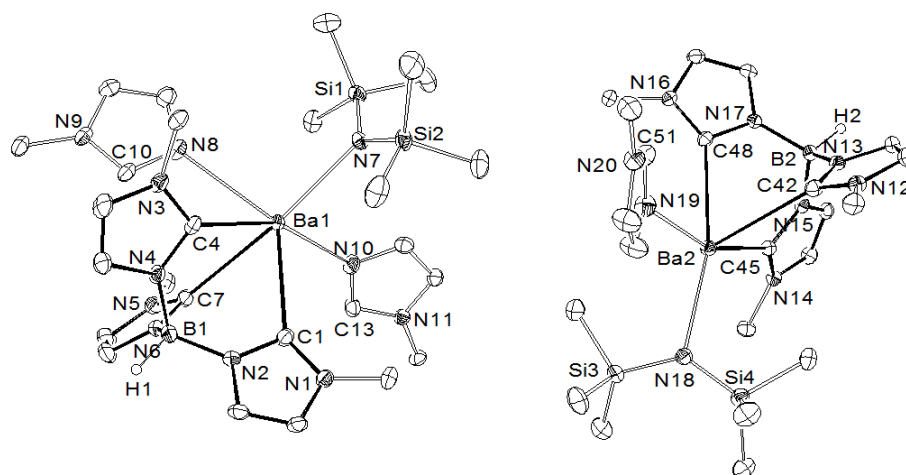
The synthesis of the heteroleptic calcium iodide derivative followed a similar reaction scheme employing three rather than four equivalents of [KN(SiMe$_3$)$_2$] and yielded monomeric compound **76** [{HB(Im^{t}Bu)$_3$}CaI(N-Im^{t}Bu)] and compound **76′** [{HB(Im^{t}Bu)$_3$}CaI(THF)] in a 9:1 mixture (Scheme 62). Fractional crystallisation from

117

toluene allowed the isolation of crystals of the THF adduct **76′** after two days at -20 °C and of the imidazole adduct **76** after another two days at -20 °C. Although suitable for an X-ray crystallographic analysis, quantities of **76′** did not allow the collection of NMR spectra or elemental analysis. Repeated attempts to isolate larger amounts of the complex for these purposes failed. Conversely, although complex **76** was repeatedly obtained in good yield (68%) and purity, no crystals suitable for X-ray diffraction analysis could be isolated. Elemental analysis as well as ^{1}H and ^{13}C{^{1}H} NMR spectra were, however, in accordance with the expected structure containing a single borate ligand environment and a coordinated *tert*-butylimidazole fragment.

Scheme 62. Synthesis of compounds **76** and **76′**.
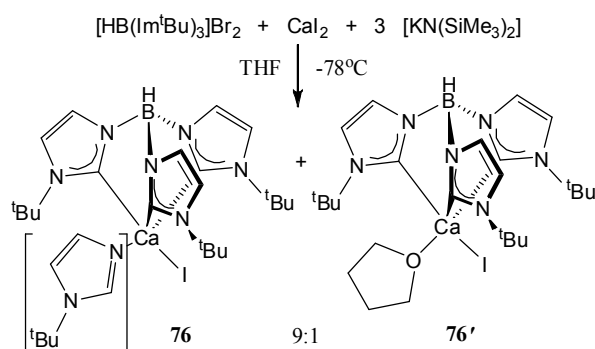
The ^{13}C{^{1}H} chemical shift of the carbene carbon in **76** at 195.5 ppm was slightly further downfield than that observed for the silylamide analogue **73** at 198.5 ppm, and compares well with the carbene shifts in calcium bis(imidazolin-2-ylidene-1-yl)borate compounds described earlier in this thesis (Table 8). X-ray structural studies of compound **76′** confirmed a similar κ^3-binding mode of the borate ligand to that observed in compounds **74** and **75**.[*] The results of this experiment are illustrated in Figure 49 and selected bond length and angle data are provided in Table 11 and Table 12 respectively. The complex presents a highly distorted square pyramidal geometry (τ = 0.39)[149] in which the third arm of the scorpionate ligand occupies the axial position. The Ca-I distance [3.0490(9) Å] is slightly shorter than the range of bond lengths reported by Westerhausen for a series of arylcalcium iodides [3.178(3) - 3.306(1) Å][4, 5] or for the aminotroponiminate complex [{(^{i}Pr)ATI}CaI(THF)$_3$] reported by Roesky and co-workers [3.1365(8) Å].[222] The Ca-C distances [2.582(5), 2.510(5) and 2.526(4) Å] are similar to those of the neutral calcium carbene adducts [(NHC)Ca{N(SiMe$_3$)$_2$}$_2$]

[*] *The structure of complex 76′ was determined by Dr Peter B. Hitchcock, University of Sussex.*

[**51**, 2.598(2) Å; **54**, 2.6285(16) Å)],[213] the homoleptic bis(carbene)borate species **65** [2.583(3), 2.646(4) Å] described earlier (Table 8), as well as the range of calcium-carbene carbon distances described in the bis(iminophosphoranyl)-methandiyl calcium complexes [2.528(2) - 2.805(1) Å][45, 217] reported by Harder and co-workers.

Figure 49. Ortep representation of compound **76′**. Thermal ellipsoids drawn at 30% probability. *Tert*-butyl methyl groups and hydrogens removed for clarity, except that attached to the boron atom.
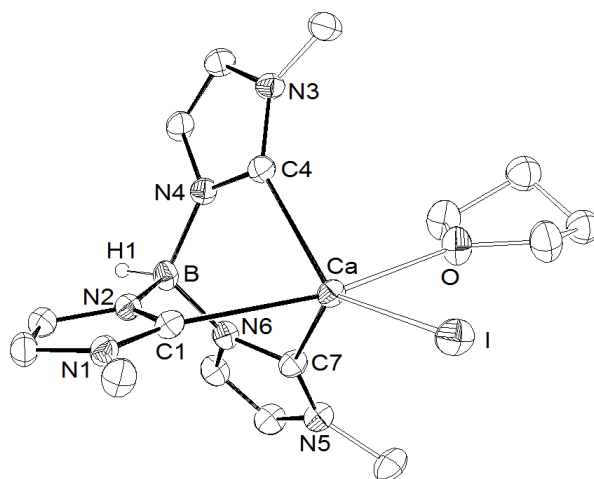
To obtain the calcium tris(imidazolin-2-ylidene-1-yl)borate bromide, 1.5 equivalents of the homoleptic silylamide species [Ca{N(SiMe$_3$)$_2$}$_2$(THF)$_2$] and one equivalent of ligand precursor **72** were combined in THF at low temperature (Scheme 63). Extraction into toluene followed by concentration of the solution and two days at -20 ºC afforded compound **77** as a colourless solid in good purity and yield (69%). ^{1}H and ^{13}C{^{1}H} NMR data were in agreement with the expected calcium bromide species. The characteristic ^{13}C{^{1}H} NMR shift for the carbene carbon at 199.4 ppm is the furthest downfield of all calcium NHC derivatives described so far (Table 8).

Scheme 63. Synthesis of compounds **77** and **78**.
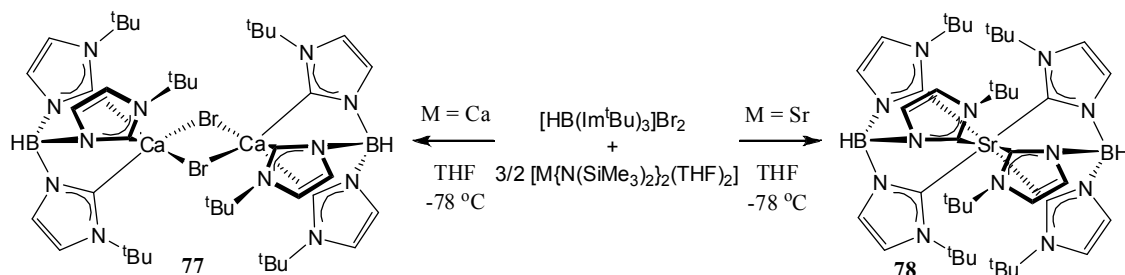
X-ray structural analysis of the crystals showed that the compound crystallises as a dimer with bridging bromides. The result of this experiment is shown in Figure 50 and selected bond length and angle data are provided in Table 11 and Table 12 respectively. As in compounds **74**, **75** and **76′**, the calcium centre adopts a highly distorted square pyramidal geometry (τ = 0.39).[149] Ca-Br distances [2.8930(4) - 2.9040(4) Å] are similar to those in the phenylcalcium bromide complex [2.8899(8) Å] reported by Westerhausen and co-workers and the simple complex [$CaBr_2(THF)_4$] [2.8425(3) Å].[4, 223] The calcium-carbene carbon bond lengths [2.544(2), 2.564(2) and 2.559(2) Å] are similar to those in the mononuclear calcium iodide complex **76′** described above.

Figure 50. Ortep representation of compound **77**. Thermal ellipsoids drawn at 30% probability. *Tert*-butyl methyl groups and hydrogens removed for clarity, except those attached to the boron atoms.
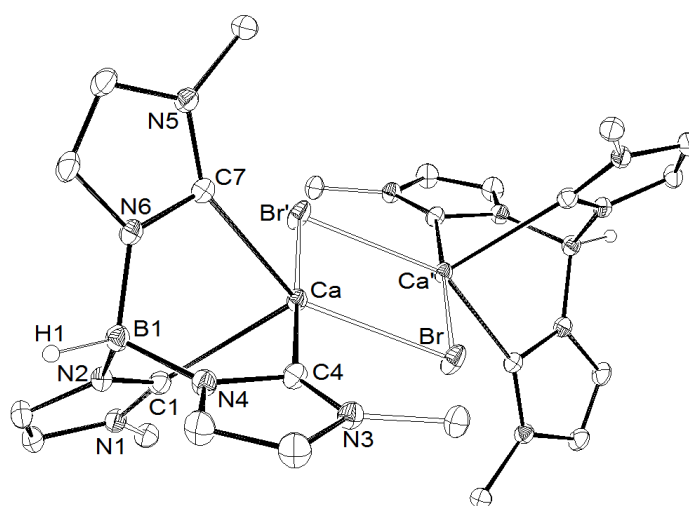

An analogous synthesis using the homoleptic strontium silylamide [$Sr\{N(SiMe_3)_2\}_2(THF)_2$] provided the homoleptic species **78** [$\{HB(Im^tBu)_3\}_2Sr$] in 54% yield based on the initial amount of the ligand precursor (Scheme 63). Among by-products, free imidazole and compound **74** could be identified in the ^{1}H NMR spectrum of the crude extraction solids. ^{1}H and ^{13}C{^{1}H} NMR data of **78** displayed similar features to those of related complexes mentioned above, suggesting a single borate ligand environment. The downfield [13]C{[1]H} chemical shift of the donor-carbon carbene resonances at 201.6 ppm was very similar to that of the heteroleptic strontium silylamide species **74**. Fine needle-like crystals suitable for X-ray diffraction analysis confirmed the homoleptic nature of this complex, which is evidently a result of the lesser steric demands of the bromide ligand compared to the bulky

bis(trimethylsilyl)amide co-ligand of compound **74**, combined with the larger ionic radius of strontium compared to the calcium centre of compound **77** (Figure 51).

Figure 51. Ortep representation of compound **78**. Thermal ellipsoids drawn at 30% probability. *Tert*-butyl methyl groups and hydrogens removed for clarity, except those attached to the boron atoms.
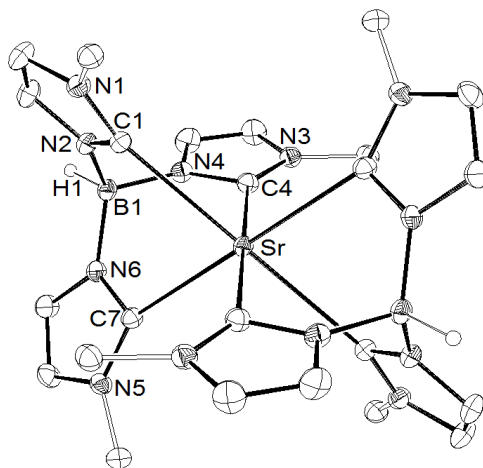
Repeated attempts to synthesise the strontium iodide analogue of compounds **76** and **76'** also failed and gave complex mixtures of free 1-*tert*-butylimidazole, compound **74**, and the homoleptic species **78.** After consideration of these results, no attempts were made to synthesise an analogous barium halide species. The structure of **78** is displayed in Figure 51 and selected bond length and angle data are provided in Table 11 and Table 12 respectively. The complex adopts an octahedral geometry with equatorial angles of 103.87(9)° and 76.13(9)° and crystallographically imposed C_{3v} symmetry around the (BSrB) axis. In this case, contrary to all previously described structures, the imidazole rings are perfectly co-planar with the Sr-C bonds. The two C_{3v}-symmetric ligands adopt a staggered conformation leading to an overall D_{3d} symmetry of the complex. The Sr-C distances [2.810(3), 2.802(3) and 2.805(3) Å] can be considered identical and are similar to those in compound **74**. Over the whole series of compounds described in this study, the geometry of the ligand varies only slightly, with N-B-N angles ranging from 109.5(4)° to 113.2(2)°, showing the relative rigidity of the tris(imidazolin-2-ylidene-1-yl)borate ligand even in the presence of large metal cations such as Sr^{2+} or Ba^{2+}. A similar observation had already been made for the calcium and strontium bis(imidazolin-2-ylidene-1-yl)borate compounds described earlier.

Attempts to synthesise mesityl-substituted analogues of compounds **73-78** either by the "one pot" salt metathesis procedure or with the homoleptic alkaline earth bis(trimethylsilyl)amides usually led to the reaction mixture turning crimson upon reaching room temperature, a potential sign of deprotonation of the mesityl methyl

substituents and formation of benzylic species. ^{1}H NMR spectra of the crude extraction mixtures proved too complex to decipher. In the case of the reaction between the ligand precursor [HB(ImMes)$_3$]Br$_2$, four equivalents of [KN(SiMe$_3$)$_2$] and one equivalent of SrI$_2$, however, colourless crystals of complex **79** suitable for X-ray diffraction studies could be isolated. The result of this experiment is illustrated in Figure 52. Although the structure could be refined to a satisfactory degree ($R1$ = 0.0600 and $wR2$ = 0.1244) and there can be no doubt as to the presence of the κ^3-coordinated mesityl-substituted tris(imidazolin-2-ylidene-1-yl)borate ligand, refinement of the diffraction data also suggested the potential presence of a superoxide O$_2$$^-$ bridging unit with the oxygen atoms disordered over three position in a 0.75:0.75:0.50 ratio. The positioning of the oxygen atoms and the O-O bond distances of 1.181(7) Å and 1.346(8) Å, however, do not fit the average structure of bridging superoxides. Since there was insufficient crystalline material to acquire elemental analysis data and repeated attempts to reproduce this result failed, the nature of this bridging unit remains unclear.

Figure 52. Ortep representation of compound **79**. Thermal ellipsoids drawn at 30% probability. Mesityl methyl groups and hydrogens removed for clarity, except those attached to the boron atoms.
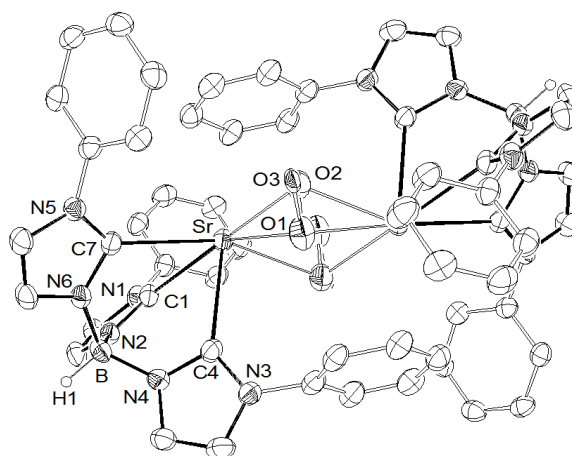
Further attempts to use the more sterically demanding 2,6-di-*iso*-propylphenyl-substituted and the chiral (S)-α-phenylethyl-substituted versions of ligand precursor **72** also met with serious problems of ligand degradation and redistribution during synthesis, preventing the isolation of any compounds of interest. Furthermore, replacing the hydrogen on the boron bridgehead with a phenyl substituent promoted a significant increase in ligand cleavage reactions during attempted syntheses.
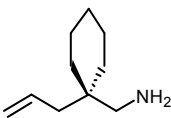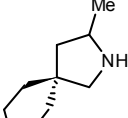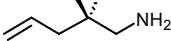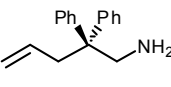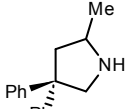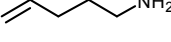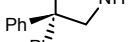
3.3.2 Hydroamination studies

Attempted intramolecular hydroamination with **73** and **74** was much less efficient than with their bidentate counterparts **62** and **63**. For aminoalkenes requiring high cyclisation temperatures yields did not exceed 20% due to complete protonation and decomposition of the tris(imidazolin-2-ylidene-1-yl)borate ligands into free *tert*-butylimidazole fragments, leading to solutions turning first yellow then brown within hours at temperature above 50 °C. This process was easily detected by the appearance of a *tert*-butyl ^{1}H NMR singlet at 0.98 ppm in d_8-toluene and disappearance of the equivalent ligand signal around 1.3-1.4 ppm. A slight amount of ligand decomposition (5-20%) was also observed at lower temperatures but did not prevent catalysis. Heating of d_8-toluene solutions of **73**, **74** and **75** at 80 °C over a period of six days, however, did neither result in any visible decomposition nor in ligand redistribution towards the homoleptic species. The presence of a protic substrate seems, therefore, required to degrade the ligand by protonation of the carbene fragments, a process which inevitably competes with the amine-amide exchange of the catalytic insertion step. Similar decomposition and the formation of intractable products were also observed in the presence of one equivalent of other protic substrates such as diphenylamine or phenylacetylene.

The low conversion rates for the intramolecular hydroamination reactions, especially for calcium catalyst **73**, could be due to the high kinetic activation barrier of the insertion step of the catalytic cycle, as the metal centre is tightly encapsulated by the ligand and access for substrate pre-coordination is blocked by the highly sterically demanding hexamethyldisilazide co-ligand. Although the larger ionic radius of strontium in **74** allows better access for pre-coordination of both the amine and the alkene moiety to the catalytic metal centre, the steric demands of the tridentate carbene ligand noticeably hinder the insertion step compared with the previously mentioned bidentate carbene analogue **63**. Despite these limitations strontium complex **74** was significantly more active than its calcium counterpart **73** as is apparent from the limited results displayed in Table 13. These observations are consistent with earlier findings for bis(imidazolin-2-ylidene-1-yl)borate complexes **62** and **63** but contrast with those for calcium and strontium *β*-diketiminate complexes **2** and **34**, homoleptic complexes **35b-c**, **36b-c** and **37b-c**, and previous reports for calcium and strontium aminotroponiminate

and triazenide complexes.[60, 61] As suggested earlier with regard to the catalytic activity of bis(carbene)borate complexes **62** and **63**, this inversion of reactivity might reflect the intrinsic stereoelectronic effects of the highly σ-donating ligand on the catalytic alkaline earth metal centre. Barium complex **75** showed little activity even with 1-amino-2,2-diphenyl-4-pentene and heating at 50 $^\circ$C for seven days. At 5 mol% catalyst loading the amount of cyclised product indicated a single turnover most likely achieved before the catalyst was entirely dismantled by protonation and B-N bond cleavage.

Table 13. Scope of intramolecular hydroamination with calcium and strontium tris(carbene)borate precatalysts **73** and **74**. Experiments were performed at 5 mol% catalyst loading in C_6D_6.

Entry	Substrate	Product	Catalyst	Time / h	T / $^\circ$C	NMR yield / %[a]
1			**73**	3 d	45	11
2			**74**	24	25	86
3			**73**	4 d	45	85
4			**74**	1.8	25	97

3.4   Limitations of the (carbene)borate systems and further work

As evidenced by this study the synthesis of alkaline earth bis- and tris(carbene)borate complexes seems to invariably involve a certain amount of ligand decomposition by B-N bond cleavage. As shown in the synthesis of compounds **74′** and **76′**, even precautions such as washing all glassware with a base solution and avoiding filtration through potentially acidic Celite only leads to various proportions of (THF) and imidazole adduct mixtures. In virtually all reactions crystallisation and selection of crystals were made particularly difficult due to the presence of oily non-coordinated 1-*tert*-butylimidazole in the toluene solution. Coordination-induced B-N bond cleavage of tris(pyrazolyl)borate ligands has been previously observed.[202] For example, Harding *et al.* isolated [Co(Tp^{Ph2})(O$_2$CMe)(Hpz^{Ph2})] containing a coordinated pyrazole ligand resulting from B-N bond cleavage induced by the Lewis acidic Cu(II) centre,[224] while Hamon and co-workers have described the formation of [*trans*-FeCl$_2$(^{t}Bu-pzH)$_4$] as the only isolable product from the attempted synthesis of an iron tris(pyrazolyl)borate

complex.[225] Similarly, partial decomposition has also been observed during the synthesis of lanthanum and neodymium tris(pyrazolyl)borate complexes by Domingos *et al.* who suggested this propensity towards decomposition was a result of B-N bond elongation and twisting of the pyrazole fragments caused by the polarisation of the large Lewis acidic metal cation.[226]

The synthesis of compound **73** yielded crystals of a by-product which was structurally characterised as the homoleptic compound **80** [Ca{N(SiMe$_3$)$_2$}$_2$(*N*-Im^{t}Bu)$_2$] (Figure 53, left). ^{1}H and ^{13}C{^{1}H} NMR shifts of complex **80** allowed its identification in the crude mixtures of **76** and **77**, as well as the analogous strontium and barium species in the crude mixtures of **74**, **75** and **78**. A possible indication as to the fate of the boron backbone in such ligand cleavage reactions was provided by the unexpected structure of the single isolable compound of the attempted synthesis of the diphenyl-substituted analogue of **62**, [{Ph$_2$B(Im^{t}Bu)$_2$}Ca{N(SiMe$_3$)$_2$}(THF)]. X-ray diffraction analysis of compound **81** revealed the dimeric boron NHC complex displayed in Figure 53 (right), containing a single imidazolin-2-ylidene-1-yl arm coordinated to a second boron centre. As suggested by the reaction conditions in the synthesis of compounds **74′** and **76′**, which did not completely avoid B-N bond cleavage, residual acid traces on the glassware are only partly responsible for the decomposition mechanism of the ligand. It is likely, therefore, that other factors, such as the necessary redistribution of charge within the ligand framework during deprotonation, are implicated in the degradative pathways.

It thus seems clear that the fragility of both bis- and tris(imidazolin-2-ylidene-1-yl)borate ligands towards B-N bond cleavage reactions makes them rather unsuitable for the stabilisation of heavier alkaline earth metal centres. The resulting isolable heteroleptic complexes, although presenting greater kinetic stability than previously reported *β*-diketiminate, triazenide or aminotroponiminate complexes, are much more prone to ligand protonation in the presence of protic substrates, limiting their catalytic applications. Moreover, all attempts to obtain heteroleptic alkaline earth alkyl complexes stabilised by these ligand systems were thwarted by total degradation of the ligand precursors in the presence of either [K{CH(SiMe$_3$)$_2$}$_2$] or [M{CH(SiMe$_3$)$_2$}$_2$(THF)$_2$] (M = Ca, Sr, Ba) used during the synthesis, even if reactions were carried out at low temperature. The challenge of a straightforward synthesis of kinetically stable heteroleptic heavier alkaline earth alkyl complexes thus remains and will certainly require the use of more robust ligands.

Figure 53. Ortep representations of ligand decomposition by-products **80** and **81**. Thermal ellipsoids drawn at 30% probability. Hydrogens omitted for clarity.
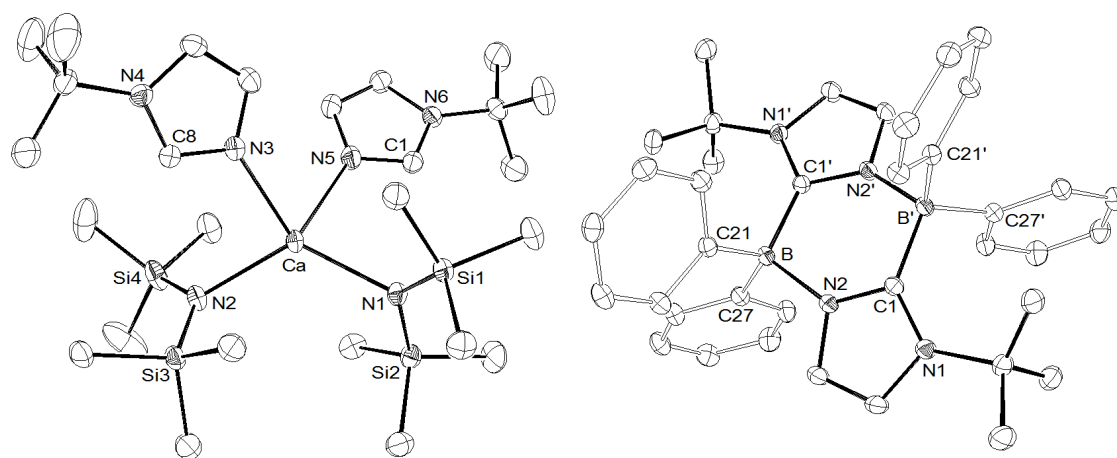
The problem of the fragility of the B-N bonds in the presence of alkaline earth bases may easily be overcome by using other types of monoanionic scorpionate carbene ligands in which the bridgehead element is, for example, a carbon atom, as well as other monoanionic pincer-type carbene ligands based on C, H, N and O such as those presented in Figure 54.[187, 191, 198, 227] These ligand systems, other than being more stable towards ligand decomposition and providing a larger scope for the tuning of stereoelectronic properties, could also provide access to the more desirable heteroleptic alkaline earth alkyl complexes.

Figure 54. Examples of monoanionic scorpionate and CCC or CNC pincer-type bis(carbene) ligands.
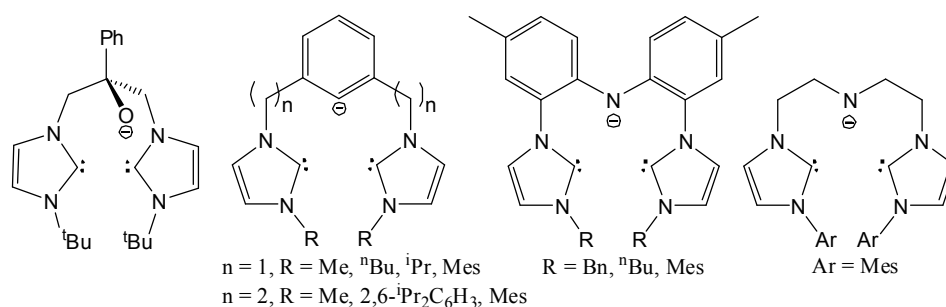
4 Towards stable heteroleptic group 2 alkyl precatalysts

## 4.1 Deprotonation and dearomatisation of a bis(imino)pyridine ligand with group 2 dialkyls[228]

4.1.1 Introduction

In the search for post-metallocene catalysts,[229] transition metal complexes stabilised by the versatile 2,6-bis(imino)pyridine ligands have received much attention during the past decade since the independent discovery in 1998 by Brookhart and Gibson of the exceptional ethylene polymerisation activity of bis(arylimino)pyridine iron and cobalt (II) complexes activated with MAO.[230] Much of the research has focused on the use of these complexes and their derivatives for both homogeneous[231] and heterogeneous oligomerisation, polymerisation and copolymerisation reactions.[232] A number of theoretical studies have been carried out on this subject to investigate the oxidation state of the redox active metal centre during these transformations.[233] Further catalytic applications include the epoxidation of cyclohexene,[234] the cyclopropanation of styrene,[235] hydrogenation and hydrosilylation reactions,[236] the $[2\pi + 2\pi]$ cycloaddition of 1,6-dienes and the reductive cyclisation of 1,6-enynes and -diynes.[237] Modification of the original bis(arylimino)pyridine ligand has given rise to a wealth of related coordination compounds which can be easily tuned for their stereoelectronic properties.[238]

In many reactions the bis(imino)pyridine ligand was found to be non-innocent. The methyl-substituted ligand $[2,6-\{ArN=C(CH_3)\}_2C_5H_3N]$ (Ar = 2,6-di-*iso*-propylphenyl), **82**, in particular, has been observed to possess a remarkable capacity to function either as a passive ancillary ligand or to undergo anionisation *via* either hydrogen abstraction at one or both of the methyl groups attached to the imine carbon atoms[239, 240] or through direct alkylation.[241-245] In this latter case alkylation may occur not only at the carbon of the imine function but also at the C^2 and, less commonly, the N^1 and C^4 positions of a dearomatised pyridine ring, as shown by the examples of the reactivity of magnesium dialkyls[242] and aluminium trialkyls[243] towards **82** in Scheme 64. The only example of alkylation in the C^3 position is that of a vanadium (I) dialkyl complex

reported by Gambarotta and co-workers.[244] Dearomatisation reactions are usually accompanied by a radical colour change of the reaction mixtures from colourless to intense red, green, blue or purple.

Scheme 64. Alkylation pattern of bis(imino)pyridine ligand **82** with aluminium and magnesium alkyls.
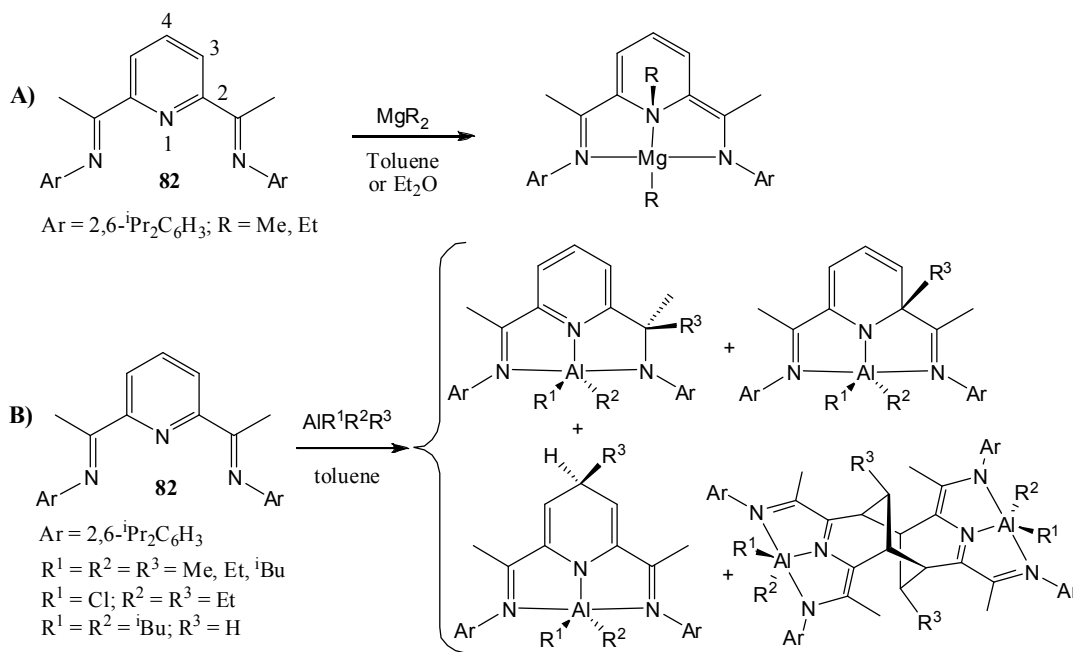

4.1.2 NMR spectroscopic study of the reactions between 37a-d and 82

Encouraged by the results of the reaction of MgR_2 (R = Me, Et, ^{i}Pr) with **82** and related ligand precursors (Scheme 64A),[242] NMR scale reactions were carried out between **82** and the series of group 2 dialkyls $[M\{CH(SiMe_3)_2\}_2(THF)_2]$ (M = Mg **37a**; Ca **37b**; Sr **37c**; Ba **37d**) in the hope of obtaining analogous heteroleptic group 2 alkyl species. Addition of magnesium dialkyl **37a** to a C_6D_6 solution of **82** caused the instantaneous formation of an orange solution, which, from the simplicity of its ^{1}H NMR spectrum, was inferred to contain a C_2-symmetric bis(imino)pyridine adduct of the dialkyl species as the only magnesium-containing compound. Monitoring of this solution heated at 60 °C by ^{1}H NMR spectroscopy for 24 hours indicated conversion of this species to a single product, compound **86a**, the result of deprotonation of both of the methyl groups attached to the imine functionalities of the bis(imino)pyridine unit. In contrast to the analogous reactivity observed with calcium, strontium and barium dialkyls **37b-d** (*vide infra*), the only identifiable intermediate species during the course

of this reaction was the monodeprotonated species, compound **85a**, and the reaction mixture remained red-brown in colour throughout the reaction (Scheme 65).

Scheme 65. Double deprotonation of **82** with group 2 dialkyls **37a-d**, and intermediate monodeprotonated and dearomatised species.
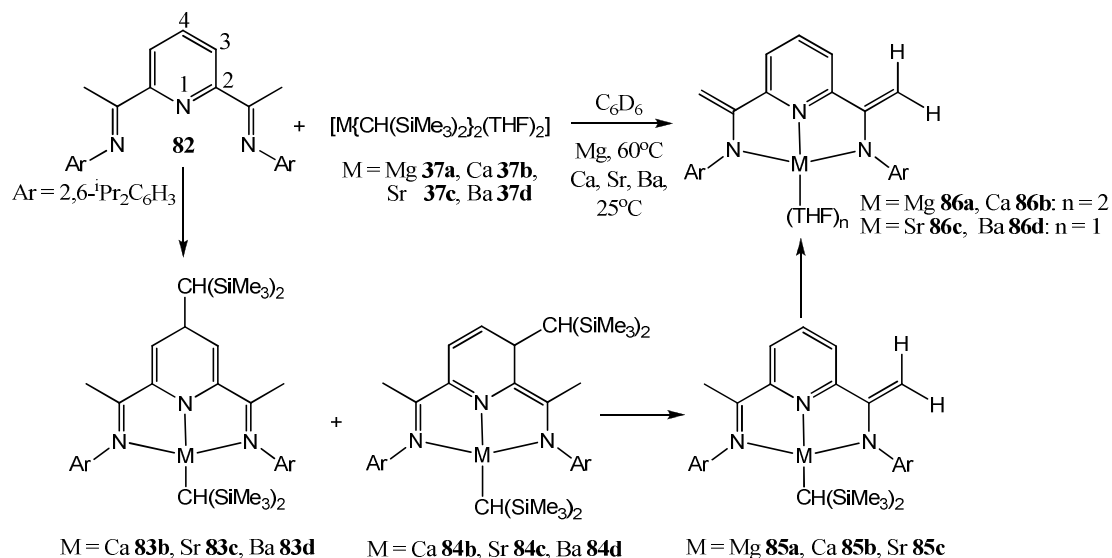

This latter observation contrasts markedly with analogous reactions performed with the heavier alkaline earth compounds **37b-d**. Combination of the relevant metal dialkyl with **82** in C_6D_6 provided, in each case, the instantaneous formation of a deep blue solution. Analysis of the calcium- and strontium-based reactions by ^{1}H NMR spectroscopy revealed the presence of singly deprotonated species analogous to **85a**, compounds **85b** and **85c**, which appeared as 20-40% of the total bis(imino)pyridine-derived species in solution at the first point of analysis (Scheme 65). Further monitoring of both these reactions at 298 K indicated that **85b** and **85c** were consumed during the course of the continued reactions over periods of 12 hours and 1.5 hours respectively. The signals in the ^{1}H NMR spectra attributed to compounds **85b** and **85c** appeared in both reactions alongside two further isomeric species which were identified as the dearomatised metal alkyl compounds **83b** and **84b** (calcium), and **83c** and **84c** (strontium) formed by migration of a single alkyl residue to either the C^3 or C^4 positions of the pyridine ring (Scheme 65). In contrast to these observations, the reaction with the barium dialkyl **37d** provided no evidence for any singly deprotonated species. Rather, the respective C^3- and C^4-dearomatised species, **83d** and **84d**, were observed as the only intermediate products throughout the course of reaction (Scheme 65). Although the C^3-dearomatised compounds **84b**, **84c** and **84d** were present in excess (ca. 2:1 - 3:1 ratios)

129

during the course of the respective reactions, continued NMR monitoring indicated progressive consumption of all intermediate species accompanied by a gradual fading of the blue colour of the solutions into green-brown over several hours (Ca, 36 hours; Sr, 2 hours; Ba, 8 hours). At this point the NMR spectra for all three reactions were reminiscent of that obtained for the synthesis of compound **86a** and indicated a stoichiometric formation of calcium, strontium and barium complexes **86b**, **86c** and **86d**, containing an identical pyridine-based ene-diamido ligand. An annotated ^{1}H NMR spectrum obtained from the reaction performed with the strontium dialkyl at a lower (ca. 0.04 M) concentration is provided in Figure 55 and illustrates the clean formation of each of the intermediate species, **83c**, **84c** and **85c**, identified by combining ^{1}H, ^{13}C, COSY, HMQC and HMBC NMR techniques.

For all intermediates the ^{1}H NMR upfield singlet of the M-CH(SiMe$_3$)$_2$ alkyl ligand was identified by integration against the other characteristic signals of the compounds. The symmetric C^4-alkylated intermediates **83b-d** presented a characteristic doublet integrating for two protons at ca. 5 ppm, coupled to a less distinctive (1H) multiplet at ca. 4.7 ppm. COSY experiments revealed coupling of the latter to an upfield proton signal at ca. 0.3 ppm assigned to the -CH(SiMe$_3$)$_2$ alkyl substituent. Although the shifts of the proton doublet in the *meta*-position of the dearomatised pyridine ring are similar to those (4.87-5.10 ppm) of C^4-alkylated and -hydrogenated products observed in the reaction of **82** with various aluminium alkyls (Scheme 64),[243] the *para*-proton shifts of the latter are significantly higher upfield (3.52-3.81 ppm), possibly a reflection of the more covalent nature of the aluminium to ligand bonding.

The asymmetric C^3-alkylated intermediates **84b-d** were characterised by three distinct pyridine proton resonances in a 1:1:1 ratio: a doublet at ca. 6.3 ppm, coupled to a doublet of doublets at ca. 5.3 ppm, itself coupled to a broad multiplet at ca 4.4 ppm. Again, COSY experiments allowed the identification of the -CH(SiMe$_3$)$_2$ C^3-substituent at ca. 0.3 ppm. Contrary to the symmetric dearomatised intermediates, **83b-d**, the methyl resonances were inequivalent and appeared as two distinct singlets at ca. 1.7 and 1.8 ppm respectively. Given that the only other reported compound bearing a C^3-dearomatised bis(imino)pyridine ligand is a paramagnetic vanadium (I) complex,[244] no NMR comparison can be provided. Although imine, N^1-, and C^2-alkylation are more commonly observed, it seems that, in this case, the steric bulk of the -CH(SiMe$_3$)$_2$ alkyl substituent combined with that of the 2,6-di-*iso*-propylphenyl ligand appendages gives preference to the less sterically hindered C^3 and C^4 positions.

Figure 55. Annotated (30 min, rt) ^{1}H NMR spectrum ((a) –2 to 2.5 ppm region; (b) 3.5 to 8.5 ppm region) obtained from the reaction of **37c** and **82** (0.04 M) illustrating the formation of **86c** and each of the intermediate species. The numbers in the coloured boxes refer to the assignments indicated for **82** (yellow), **83c** (blue), **84c** (green), **85c** (orange) and **86c** (red).
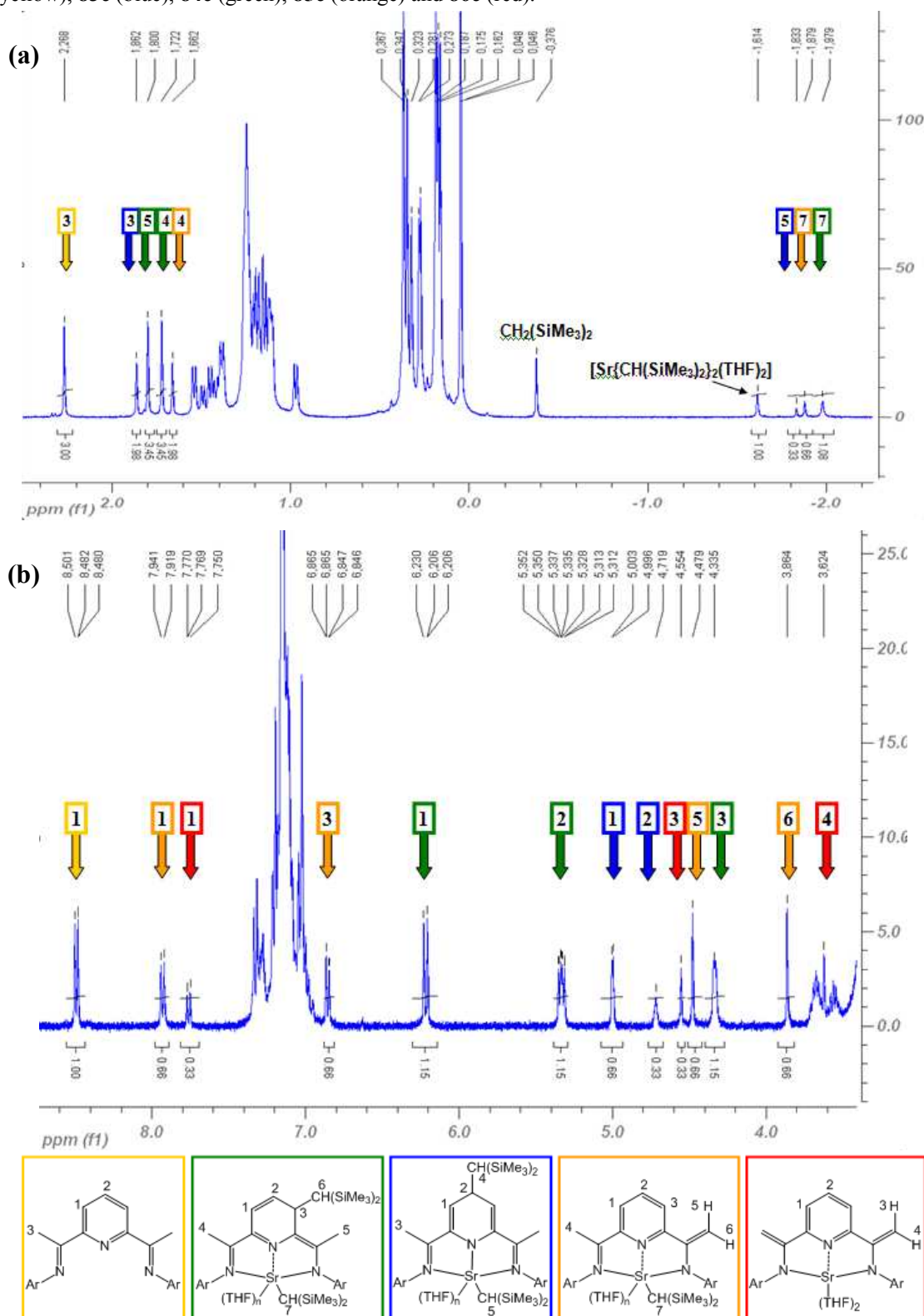
The monodeprotonated (imino-amido)pyridine intermediates **85a-c** displayed three distinct (1H) pyridine resonances in a 1:1:1 ratio reflecting the asymmetric nature of the complexes. HMBC NMR experiments identified the doublet at ca. 7.8 ppm as the proton in the *meta* position of the pyridine backbone on the side bearing the methyl substituent and the other doublet at ca. 6.9 ppm as the proton in the *meta* position on the deprotonated side. Compared with the ligand and the final doubly deprotonated products **86a-c**, the shift of the proton in the *para* position of the pyridine backbone was barely affected. Two (1H) singlets in a 1:1 ratio at ca. 3.9 and 4.5 ppm respectively were attributed to the methylene resonances, while a singlet at ca. 1.7 ppm integrating for three protons corresponded to the intact methyl substituent. These shifts were essentially comparable to those observed for an analogous lithium complex.[245]

The symmetric ene-diamido complexes **86a-d** were characterised by two sharp methylene singlets at ca. 3.6 and 4.5 ppm, as well as a downfield doublet at ca. 7.6 ppm corresponding to the protons in the *meta* position of the pyridine ring. As the protons in the *para* position were overlapping with the multiplet of the aromatic substituents their chemical shifts (ca. 7.1 ppm) were identified by COSY NMR experiments. Again, these shifts are closely comparable to those observed in related lanthanide complexes bearing the same doubly deprotonated ligand.[240]

Comparison of these chemical shifts for the different alkaline earth intermediates and products did not yield any smooth trends in descending the group from magnesium to barium, as shown by the summary of ^{1}H NMR shifts in Figure 56. Most shifts are fairly similar across the series of calcium, strontium and barium analogues, with the exception of the highly upfield M-CH(SiMe$_3$)$_2$ singlets which are strongly influenced by the proximity of the metal centre, although again without obvious trend. It is, however, noteworthy that the Mg-CH(SiMe$_3$)$_2$ singlet at -1.57 ppm in intermediate **85a** is 0.25 ppm further downfield than in its calcium counterpart **85b**, reflecting the reduced ionic character of the metal to ligand binding in the magnesium complexes.

Figure 56. ^{1}H NMR shifts (ppm, C_6D_6, 298 K, 300 MHz) of intermediates and products **83-86** of the reaction outlined in Scheme 65. The symbols in front of the shifts represent: M = ○ Mg, ● Ca, □ Sr, ■ Ba.
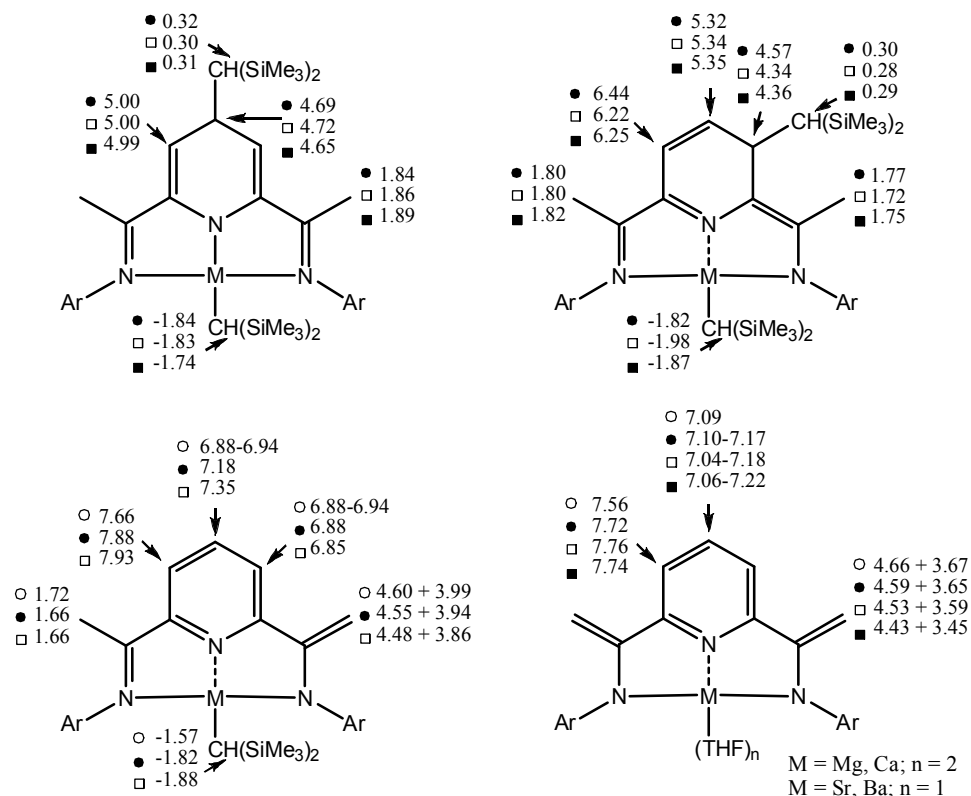

4.1.3 Structural studies of doubly deprotonated products

Compounds **86a-d** were isolated as yellow, orange, bright red and dark red crystals respectively, which were suitable for X-ray diffraction analyses. The magnesium and calcium derivatives **86a** and **86b** were found to be mononuclear and isostructural, and to contain a five-coordinate metal centre comprising the tridentate N_3-ene-diamido ligand and two molecules of THF. The structures of compounds **86a** and **86b** are illustrated in Figure 57. Selected bond length and angle data are listed in Table 14. In contrast, and although compounds **86c** and **86d** were found to crystallise with only a single molecule of coordinated THF, the coordination number of the strontium and barium centres was maintained through an additional intermolecular methylene to metal centre interaction such that the compounds assembled into isostructural six-fold symmetric cyclic arrays. The intermolecular $M \cdots CH_2$ contacts between the alkaline earth centres and the methylene unit of the adjacent molecule within compounds **86c** and **86d** [Sr$\cdots$C(14') 2.942(3); Ba$\cdots$C(14') 3.142(8) Å] are significantly longer than either of the $M \cdots CH_2$ contacts within the recently reported products resulting from β-diketiminate methyl

133

deprotonation [Sr⋯CH$_2$ 2.759(3), 2.815(3); Ba⋯CH$_2$ 2.966(2), 3.001(2) Å].[155] The structure of a single molecule of **86c** and the hexameric unit of compound **86d** are illustrated in Figure 58. Selected bond length and angle data for compounds **86c** and **86d** are provided in Table 14.

Figure 57. Ortep representations of compounds **86a** (left) and **86b** (right). Thermal ellipsoids drawn at 30% probability. Hydrogens omitted for clarity, except for methylene protons.
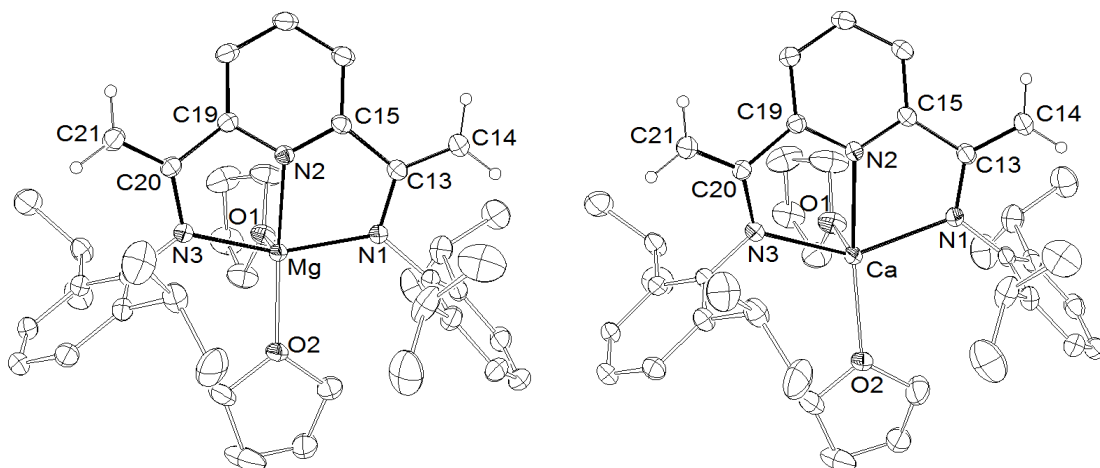
All four complexes adopt a distorted square pyramidal coordination geometry (**86a**, τ = 0.37; **86b**, τ = 0.55; **86c**, τ = 0.15; **86d**, τ = 0.08).[149] Unlike other compounds bearing the same ene-diamido ligand in which the pyridine ring, the two ene-amido functions and the metal centre are more or less coplanar, the ligand in all four alkaline earth complexes is distorted from its usual planarity, displaying an angle ranging from 9.3° (**86d**) to 22.5° (**86b**) between the plane of the pyridine backbone and those of the ene-amido functionalities. Furthermore, the metal centre is situated at a distance of 0.645-1.220 Å above the pyridine plane, the distance increasing with the size of the alkaline earth cation. The deprotonation of the two former methyl groups within **82** is apparent from the values of the C-C distances [1.354(10) Å to 1.381(5) Å] as expected for a conjugated double bond, while the short C-N single bond distances [1.341(4) Å to 1.376(3) Å] indicate some degree of delocalisation over the ene-amido system.

Figure 58. Ortep representations of a single molecule of strontium complex **86c** (left) and the hexameric unit of barium compound **86d** (right). Thermal ellipsoids drawn at 30% probability. Hydrogens omitted for clarity, except for methylene protons. Ba···CH$_2$ interactions in **86d** represented as dashed bonds.
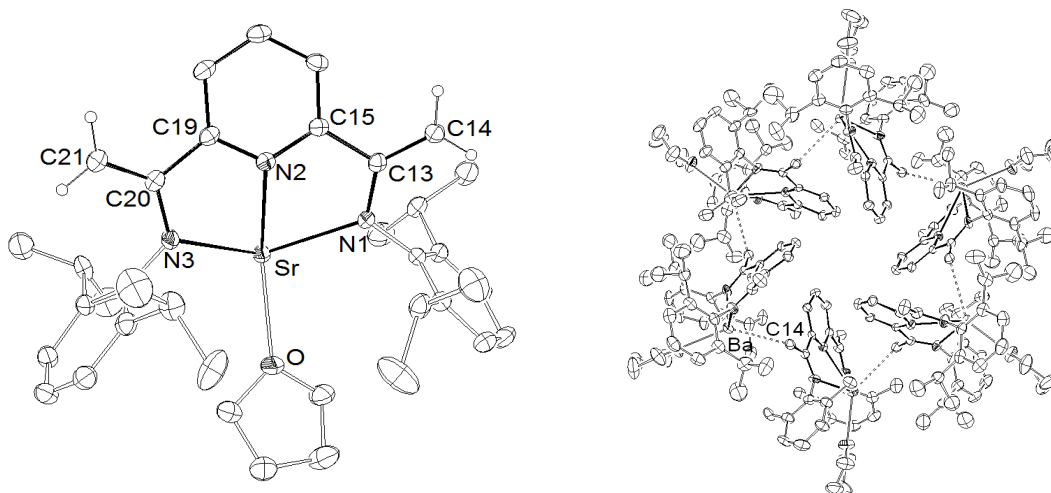

Table 14. Selected bond lengths and angles in complexes **86a-d**.

	86a[a]	86b[b]	86c[c]	86d[d]
M-N(1)	2.1096(18)	2.321(2)	2.524(3)	2.642(6)
M-N(2)	2.0739(17)	2.3718(18)	2.538(3)	2.725(6)
M-N(3)	2.1190(18)	2.334(2)	2.456(3)	2.573(7)
M-O(1)	2.0977(17)	2.3612(18)	2.495(2)	2.684(6)
M-O(2)	2.0804(16)	2.3432(17)	-	-
N(1)-C(13)	1.376(3)	1.368(3)	1.341(4)	1.343(9)
N(3)-C(20)	1.344(3)	1.376(3)	1.365(4)	1.362(10)
C(13)-C(14)	1.357(3)	1.358(3)	1.381(5)	1.354(10)
C(20)-C(21)	1.363(3)	1.357(3)	1.360(5)	1.371(12)
C(13)-C(15)	1.491(3)	1.493(3)	1.514(4)	1.516(10)
C(20)-C(19)	1.487(3)	1.499(3)	1.493(5)	1.481(11)
C(15)-N(2)	1.339(3)	1.344(3)	1.353(4)	1.346(9)
C(19)-N(2)	1.344(3)	1.346(3)	1.348(4)	1.346(9)
M-C(14)'	-	-	2.942(3)	3.142(8)
N(1)-M-N(3)	146.34(7)	133.94(7)	120.21(9)	113.4(2)
C(13)-N(1)-M	116.77(13)	121.23(15)	122.0(2)	124.4(5)
C(20)-N(3)-M	117.89(13)	119.98(14)	120.4(2)	123.5(5)
N(1)-C(13)-C(15)	112.65(17)	112.98(19)	113.7(3)	113.2(6)
N(3)-C(20)-C(19)	113.94(17)	113.68(19)	113.9(3)	113.7(7)
C(15)-N(2)-C(19)	122.80(17)	122.11(18)	121.3(3)	121.5(6)

a- M = Mg   b- M = Ca   c- M = Sr   d- M = Ba

4.1.4 Kinetic analysis

Kinetic data relating to the relative abilities of heavier group 2 organometallic compounds to participate in even apparently simple deprotonation chemistries are, to date, non-existent. We undertook, therefore, to place our understanding of the course of the reactions to produce compounds **86a-d** on a more quantitative foundation. The appearance and decay of each intermediate identified in Scheme 65 as well as the consumption of the ligand precursor **82** and the production of the final doubly deprotonated products **86a-d** were readily monitored by ^{1}H NMR spectroscopy and evidenced some rather complex metal-dependent behaviour. From experiments undertaken at 298 K and with 0.10 M concentrations of the reagents in C_6D_6, it was apparent that although the barium dialkyl provided the most rapid, effectively instantaneous, consumption of the ligand precursor (Figure 59a) this did not translate to the most facile formation of the final doubly deprotonated product. In addition, the failure to observe a barium-centred analogue of the singly deprotonated complexes, **85a-c**, indicated that the dearomatised intermediate species **83d** and **84d** possess enhanced stability for this heaviest and most electropositive member of the group 2 series. This observation was further borne out by direct monitoring of the total concentration of the two dearomatised species for each metal (Figure 59b). Although the appearance and decline of each of these species could not be fitted to any simple rate dependence, it may be deduced that the subsequent proposed intermediate, a singly deprotonated barium complex analogous to **85b** and **85c**, is consumed immediately to form the ultimate reaction product, compound **86d**. It thus seems that the ability of alkaline earth metal alkyls to effect the second deprotonation of the monodeprotonated intermediates increases with the size and electropositivity of the metal cation (Figure 59c).

Monitoring of the consumption of the ligand precursor in reactions with the calcium and strontium dialkyls **37b** and **37c** provided an apparent first-order dependence upon both [ligand] and [**37b** or **37c**] such that -d[**82**]/dt = k[**82**][**37b** or **37c**] and gave $k =$ 0.0713 $mol^{-1}.min^{-1}$ for the calcium dialkyl **37b** and $k = 0.468$ $mol^{-1}.min^{-1}$ for the strontium dialkyl **37c** (Figure 60). From this data it is further apparent that the reactivity series of the metal dialkyl towards an initial reaction with the ligand precursor varies in the order Ba > Sr > Ca, which may be a simple reflection of the increasing Ae^{2+} radii

and access to the metal centre on descending the group. Conversely, the rate of formation of the final reaction products, **86b-d** (Figure 61), is then a more complex interplay of the stability of the various dearomatised and monodeprotonated intermediate species that varies in the order Sr > Ba > Ca.

Figure 59. (a) Disappearance of **82** in reaction with **37b** (green), **37c** (red) and **37d** (blue) (Ba >> Sr > Ca). **(b)** Total concentration of dearomatised intermediates **83b** + **84b** (green), **83c** + **84c** (red), **83d** + **84d** (blue). **(c)** Formation and consumption of the singly deprotonated intermediate species, **85b** (green) and **85c** (red) during the reaction of **37b** and **37c** with **82** (apparent stability Ca > Sr >>>> Ba).
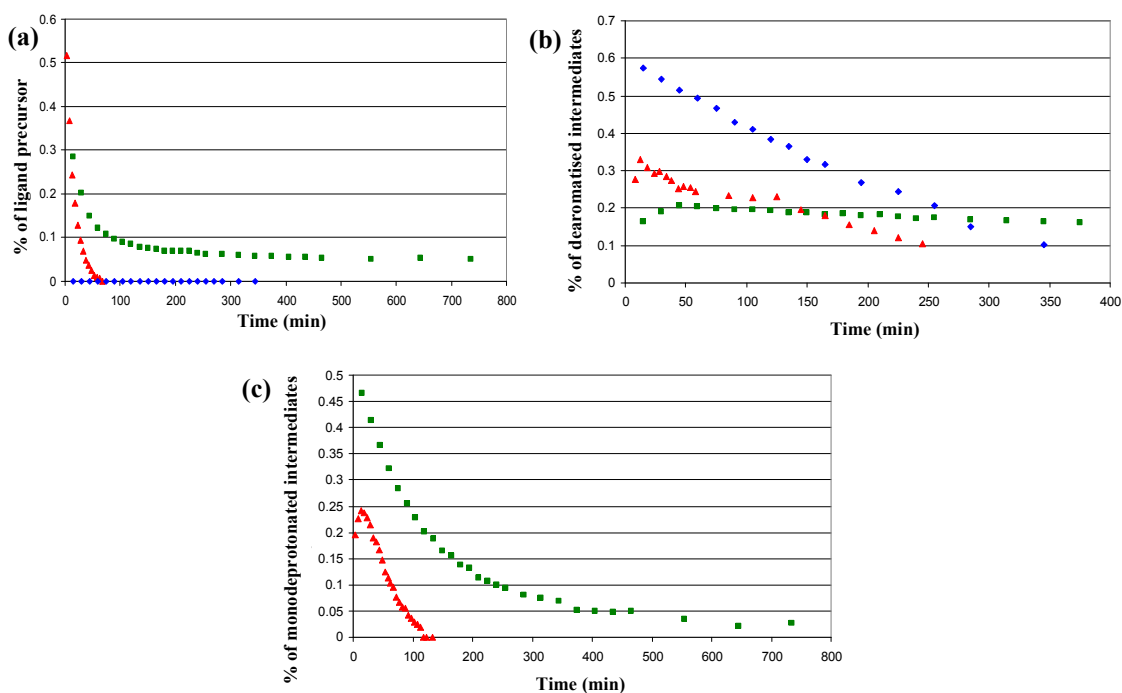
Figure 60. Overall apparent second-order reaction of **82** with **37b** (green) and **37c** (red).

$$-\frac{d[\,\mathbf{82}\,]}{dt} = k[\,\mathbf{82}\,][\,\mathbf{37b}\text{ or }\mathbf{37c}\,] = k[\,\mathbf{82}\,]^2$$

137
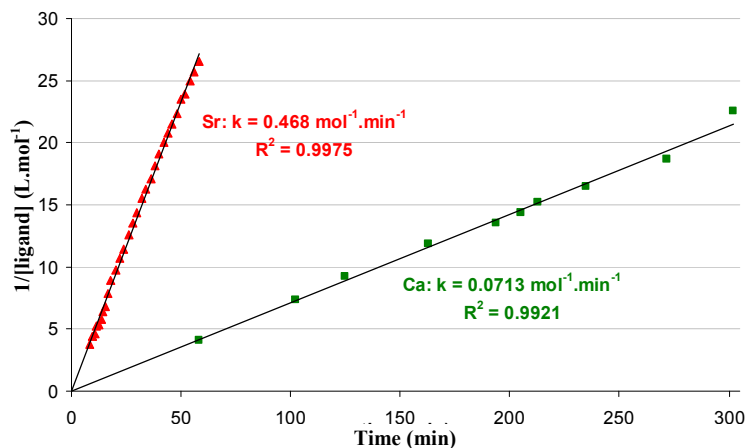
This study shows once again that the reactivity of group 2 metals is more complex than simply size-dependent. Consequently, the activation barriers towards the individual molecular steps encountered in the construction of a typical catalytic cycle will also show a more nuanced dependence upon the identity of the alkaline earth cation.

Figure 61. Formation of the final (ene-diamido)pyridine complexes **86b** (green), **86c** (red) and **86d** (blue).
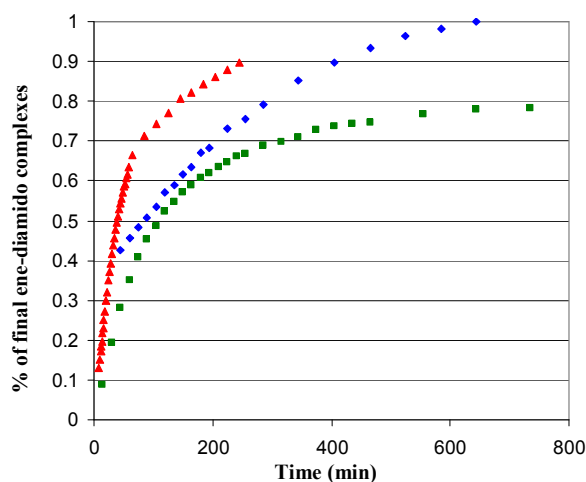
4.1.5 Attempt at "trapping" the dearomatised group 2 alkyl intermediates

Treatment of the calcium complex **86b** with two equivalents of methyl iodide and subsequent heating at 60 ^{o}C quantitatively afforded the ethyl-substituted bis(imino)pyridine ligand **87** (Scheme 66) which was isolated by extraction with dichloromethane and recrystallisation from hot methanol.

Scheme 66. Synthesis of the ethyl-substituted bis(imino)pyridine **87**.
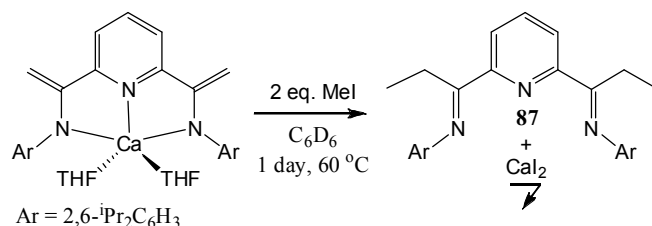
It was expected that the reaction between ligand precursor **87** and group 2 dialkyls **37b-d** might enable the 'trapping' of the alkylated dearomatised analogues of **83c-d** and **84c-d** since the protons of the ethyl substituents are considerably less acidic and prone to deprotonation than those of the methyl-substituted ligand precursor **82**. The reaction between calcium dialkyl **37b** and **87** in C$_6$D$_6$, however, did not lead to the formation of

138

a deep blue solution as had been observed with **37b** and **82**, rather the solution turned orange, and the simplicity of the ^{1}H NMR data suggested the formation of a bis(imino)pyridine adduct of the calcium dialkyl similar to the one observed upon addition of the magnesium dialkyl **37a** to ligand precursor **82** (Scheme 67). Only small amounts (<5%) of the expected dearomatised species were observed. Prolonged heating of this solution at 60 $^{\circ}$C did not result in increased alkylation/dearomatisation of the ligand. Instead the solution turned dark red over a period of one week. Monitoring of the reaction by ^{1}H NMR spectroscopy showed slow consumption of the bis(imino)pyridine adduct and protonation of the alkyl co-ligands into $CH_2(SiMe_3)_2$. Although this suggested deprotonation of the ligand, increased broadening of the signals prevented the unambiguous identification of the calcium complex formed.

Scheme 67. Reaction of calcium and strontium dialkyls **37b** and **37c** with ligand precursor **87**.
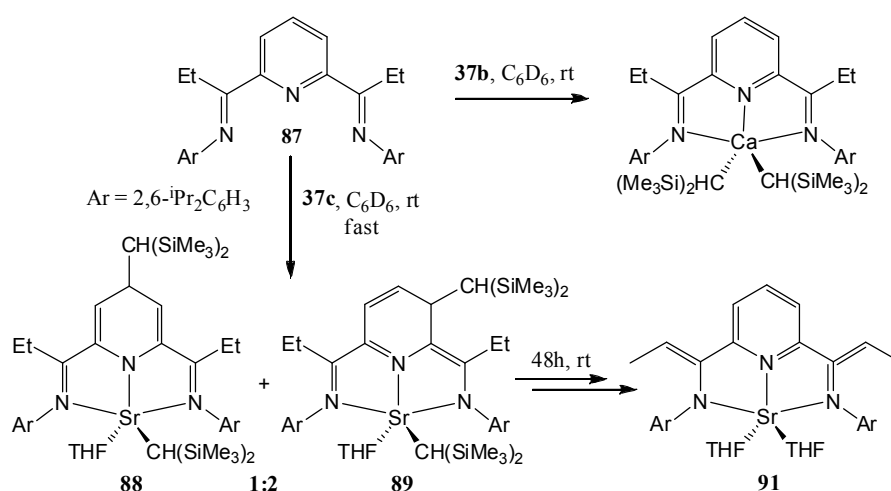
In contrast, the reaction between the strontium dialkyl **37c** and **87** in C_6D_6 instantly resulted in complete solubilisation of the ligand precursor and the formation of a deep blue solution reminiscent of those obtained in previous reactions with **82**. ^{1}H NMR data at the first point of analysis showed complete conversion of the starting materials into the desired C^4- and C^3-alkylated products **88** and **89** in a 1:2 ratio (Scheme 67). Attempts to isolate these compounds, however, were marred by the slow deprotonation of both ethyl methylene fragments over a period of two days at room temperature to yield the ene-diamido strontium complex **91**. Cooling of a d$_8$-toluene solution of the reaction mixture to -30 $^{\circ}$C did not prevent deprotonation, which reached completion after a period of eight days. Monitoring of the slow disappearance of both dearomatised intermediates, however, demonstrated that the deprotonation process proceeds in the

order proposed in Scheme 65, first *via* the dearomatised intermediates, which are then converted into the monodeprotonated and finally the doubly deprotonated species (Figure 62). Indeed, the decay of **88** and **89** in the ^{1}H NMR is accompanied at first by a slow increase in concentration of the monodeprotonated intermediate **90**, analogous to **85c**, suggesting conversion of **88** and **89** into **90** (Figure 63). Furthermore, while the C^3-alkylated intermediate **89** is consumed from the start of the reaction, the concentration of the C^4-alkylated intermediate **88** only starts to decrease after an induction period of about 10 hours. Although no definite reaction mechanism can be inferred from these observations it seems reasonable to suggest that deprotonation probably occurs *via* an intramolecular pathway in which the alkyl substituent of the dearomatised pyridine backbone attacks one of the methylene protons of the ethyl substituent, the process being likely driven by the re-aromatisation of the pyridine ring. The closer proximity of the alkyl fragment to the ethyl substituent in the C^3-alkylated complex **89** would then explain the faster deprotonation rate obtained with this intermediate. It remains as yet unclear whether intermediate **88** must first be converted into **89** to achieve deprotonation.

Figure 62. ^{1}H NMR stack plot monitoring the reaction of **37c** with **87** in C_6D_6 at 25 ^{o}C (▲ **88**, ♦ **89**, ■ **90**, ● **91**).
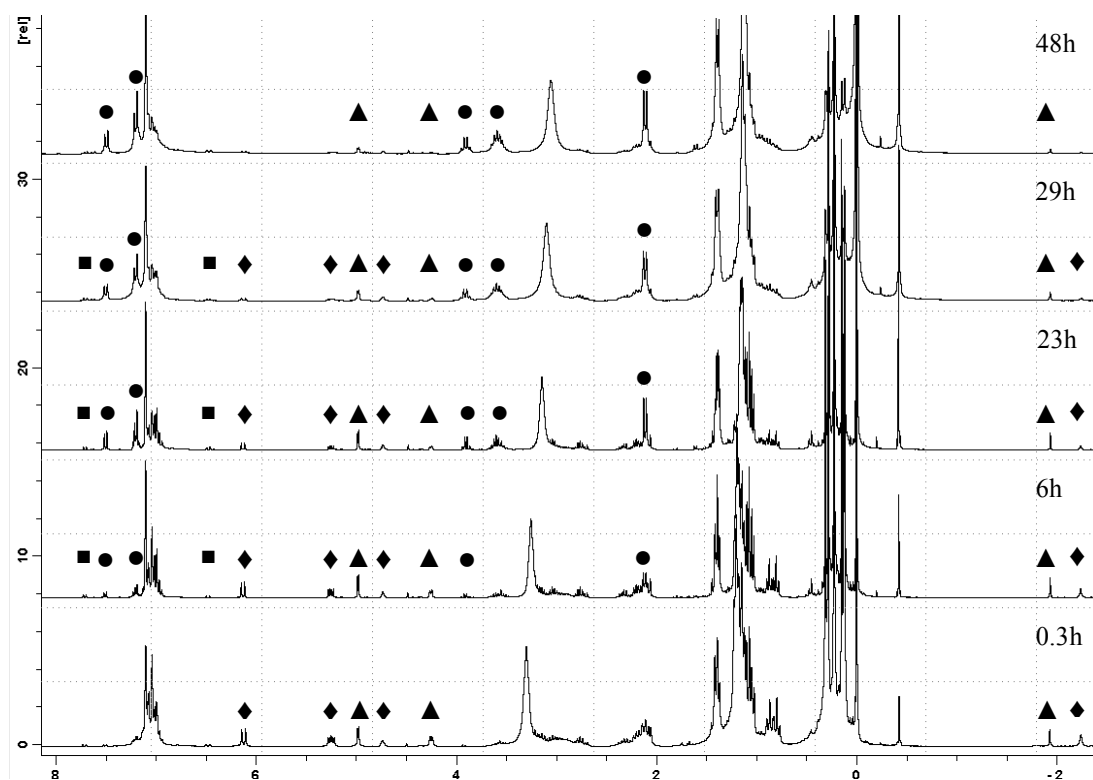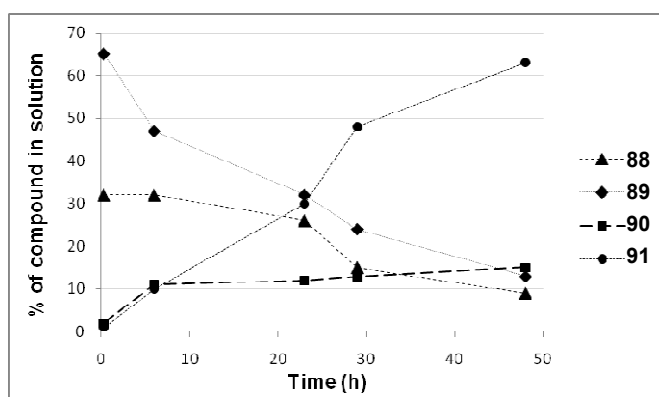

140

Figure 63. Variation of the concentration of compounds **88-91** in solution over a period of 48 hours.


4.1.6 Conclusion and further work

Although the reaction of group 2 dialkyls **37a-d** with methyl- and ethyl-substituted bis(imino)pyridine ligand precursors did not yield the desired heteroleptic alkaline earth alkyl complexes, this study has demonstrated the unprecedented capacity of these dialkyl species to dearomatise a pyridine ligand backbone and, for the first time, allowed the identification by NMR spectroscopy of C^3-alkylated versions of this class of ligand. While ^1H NMR kinetic studies have allowed some insight into a potential mechanism of these complex reactions, these results are only preliminary. Computational studies upon the stability of the various dearomatised and monodeprotonated intermediates, as well as of possible reaction pathways, would be of great interest and would provide a deeper understanding of the significant variations observed in the reactivity of the different alkaline earth metal cations involved in these reactions. Additionally, the use of a phenyl-substituted bis(imino)pyridine ligand precursor,[246] entirely immune to deprotonation, may enable the isolation of the desired heteroleptic alkaline earth alkyl species bearing either C^3- or C^4-alkylated ligands (Scheme 68A). CNC pyridine-bridged bis(carbene) ligands[186, 247] may also allow this dearomatisation chemistry to be combined with the σ-donating properties of N-heterocyclic carbenes studied earlier in this work and could provide regioselective alkylation of the *para* position of the pyridine backbone (Scheme 68B).

141

Scheme 68. Suggested reactions with other pyridine-centred ligand precursors which may provide access to heteroleptic alkaline earth alkyl species bearing dearomatised ligands.

A)

$Ar = 2,6\text{-}^iPr_2C_6H_3$

$[M\{CH(SiMe_3)_2\}_2(THF)_2]$

?

M = Mg, Ca, Sr, Ba

B)

$[M\{CH(SiMe_3)_2\}_2(THF)_2]$

?
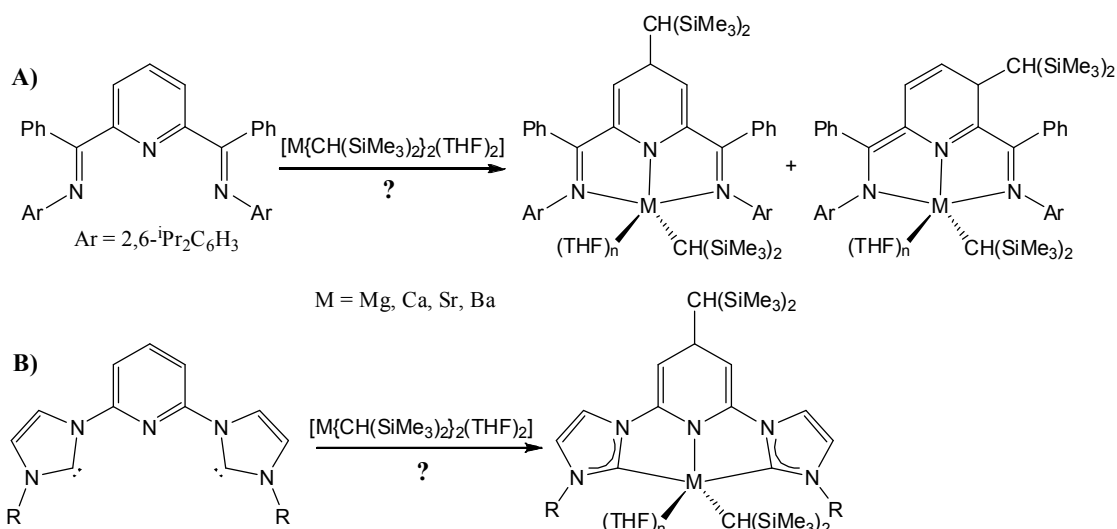
In view of making alkaline earth-catalysed reactions enantioselective, the use of the readily accessible chiral pyridine-2,6-bis(oxazoline) (PyBox) ligands, which have already proven their use in enantioselective transition metal catalysis,[248] may also be envisaged in combination with these group 2 dialkyls precursors, as proposed in Scheme 69. It is indeed noteworthy that the dearomatised calcium, strontium and barium alkyl intermediates **83b-d**, **84b-d**, **88** and **89** described in this section did not seem to show any sign of the Schlenk-type ligand redistribution processes which commonly prevent efficient enantioselective group 2-mediated catalysis.

Scheme 69. Suggested route towards chiral PyBox derivatives of heteroleptic alkaline earth alkyl species.

$[M\{CH(SiMe_3)_2\}_2(THF)_2]$

?

R = sterically demanding
alkyl or aryl substituent

M = Mg, Ca, Sr, Ba
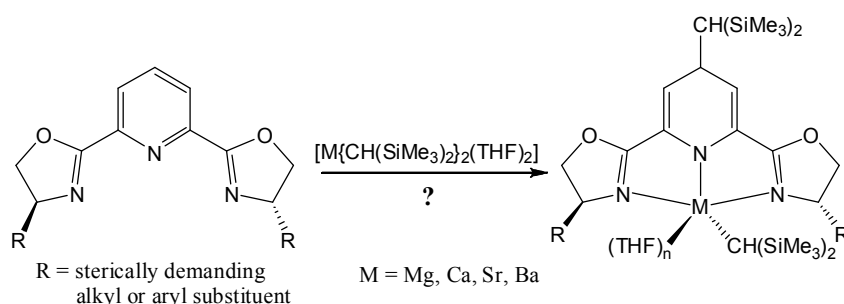
Beyond bis(imino)pyridine ligands, this novel alkylation/dearomatisation reactivity may also apply to other types of bis(imine) ligands bearing aromatic backbones, thus enlarging the scope of available monoanionic ligands for the stabilisation of highly reactive, heteroleptic heavier alkaline earth alkyl complexes.

4.2 Selective dearomatisation of a BIAN ligand with group 2 dialkyls

4.2.1 Introduction

In the catalogue of readily available diimine ligands, bis(imino)acenaphthene (BIAN) ligands (Figure 64) have gained some prominence over the last 2 decades. Although first reported in the 1960s,[249] the use of this class of ligand only became popular in the late 1990s.

**Figure 64.** BIAN ligand precursors.

R = aryl or alkyl
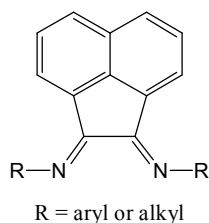
The ability of neutral BIAN ligands to act as strong and rigid chelators for metals in a variety of oxidation states has given rise to a rich transition metal coordination and catalytic chemistry.[250, 251] In particular, Elsevier and co-workers have reported the use of palladium and platinum aryl-BIAN complexes for catalytic C-C bond formation, hydrogenation and hydrosilylation reactions,[252] while Brookhart[253] and Coates[254] have demonstrated the efficiency of cationic nickel(II), palladium(II) and platinum(II) aryl-BIAN precatalysts in the polymerisation of olefins. Due to the presence of the naphthalene backbone, BIAN ligands may also act as electron acceptors in the presence of strongly reducing metals. For example the addition of one, two, three or four equivalents of elemental sodium to dipp-BIAN (dipp = 2,6-di-*iso*-propylphenyl) respectively yielded the mono-, di-, tri- and tetra-anion salts [{dipp-BIAN}$^{n-}$ {Na$_n$(S)$_m$}$^{n+}$] (n = 1, m = 0; n = 2, (S)$_m$ = (Et$_2$O)$_3$; n = 3, (S)$_m$ = (Et$_2$O)$_2$; n = 4, (S)$_m$ = (THF)$_4$).[255] This chemistry, extended to group 1,[256-258] group 2,[258-263] several p-block metals[263, 264] and, more recently, f-block elements,[261, 265] has been extensively explored, especially by the group of Fedushkin.

The reaction between magnesium, calcium, strontium or barium metal and dipp-BIAN in THF or DME invariably led to the isolation of alkaline earth complexes of the di-anion [dipp-BIAN]$^{2-}$. The magnesium species [{dipp-BIAN}Mg(THF)$_3$], **92**, has been shown to act as a reducing agent for non-enolisable ketones *via* single electron

transfer to form the corresponding alcoholate magnesium radical-anion complex.[266] Complex **92** was also oxidised by halogenated tin, copper, mercury or silicon reagents to the radical-anion magnesium halide [{dipp-BIAN}MgX(S)$_n$] (X = Cl, Br, (S)$_n$ = (THF)$_2$; X = I, (S)$_n$ = DME) (Scheme 70).[267] Furthermore, compound **92** and its strontium and barium analogues may deprotonate acidic substrates such as enolisable ketones,[268] phenylacetylene[269] or α-acidic nitriles[270] to give the corresponding enolate, acetylide or keteniminate group 2 complexes of the protonated monoanionic amine-amido ligand [dipp-BIAN(H)]$^-$. Alkylation of the imine carbon of the BIAN ligand has also been observed in several cases. For example the reaction between **92** and ethyl halides resulted in the formation of a racemic imine-amido magnesium halide species through ethylation of the carbon adjacent to the amide functionality (Scheme 70).[271] The mechanism proposed by the authors for the formation of these compounds involves a single electron transfer from **92** to the ethyl halide, yielding the intermediate radical-anion magnesium halide and Et$^{\bullet}$, followed by radical attack of Et$^{\bullet}$ to form the ethylated magnesium halide complex. A similar alkyl transfer has also been observed in the reaction between n-BuLi or MR$_3$ (M = Al, R = ^{i}Bu; M = Ga, R = Et; M = In, R = Me) and dipp-BIAN in non-coordinating solvents, leading to the formation of a imine-amido complex bearing an alkyl substituent on the carbon adjacent to the amide functionality.[272, 273]

Scheme 70. Versatile reactivity of the BIAN magnesium complex **92**.
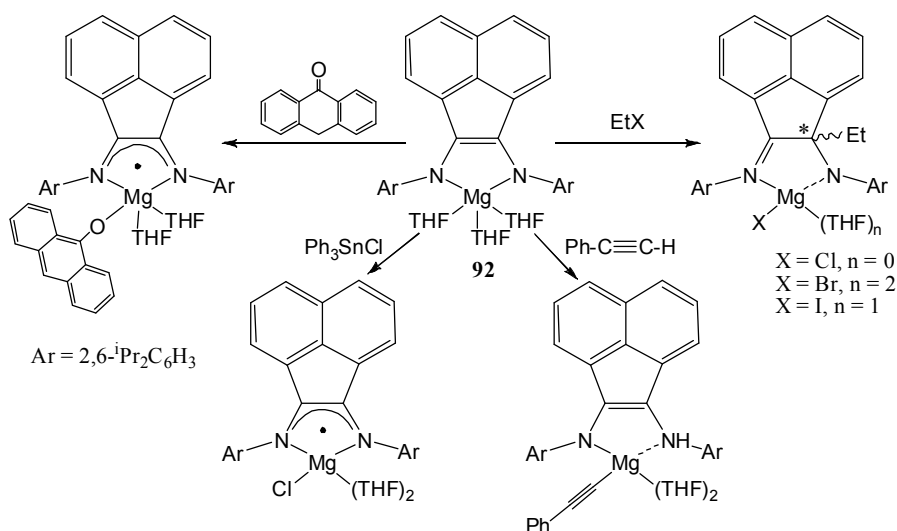

The following study describes the facile synthesis of a series of NMR-active alkaline earth BIAN complexes *via* a novel, selective alkylation/dearomatisation process of the

ligand naphthalene backbone and their application to the intramolecular hydroamination of aminoalkenes.

4.2.2 Synthetic and structural study of group 1 and group 2 C^5-alkylated dearomatised BIAN compounds

Addition of [KCH(SiMe$_3$)$_2$] to a suspension of dipp-BIAN in C$_6$D$_6$ caused instant solubilisation of the ligand precursor, accompanied by a rapid colour change from bright orange to dark green (Scheme 71). ^{1}H NMR data indicated complete consumption of both starting materials and the formation of a single alkylated dearomatised potassium species, **93**, characterised by six distinct multiplets in the region from 4.4 to 6.5 ppm. A COSY NMR experiment identified the alkylation of the acenaphthene backbone as having occurred in the C^5 position (Scheme 71), which was confirmed by a subsequent X-ray diffraction analysis. As a consequence of the chiral centre thus formed, the two magnetically inequivalent (Si(CH_3)$_3$) groups appear as two separate (9H) singlets at 0.18 and 0.04 ppm respectively. The asymmetry of the monoalkylated ligand is reflected by a splitting of the *iso*-propyl methine and methyl resonances, both in the ^{1}H and ^{13}C{^{1}H} NMR spectra.

Scheme 71. Synthesis of potassium dimer **93**.
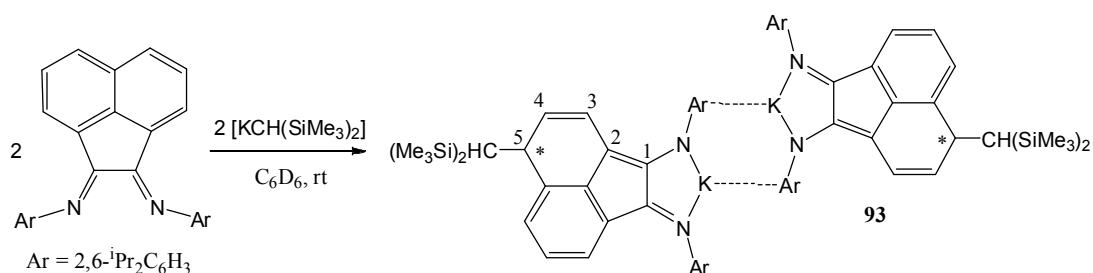
Recrystallisation at room temperature in toluene afforded dark green crystals of compound **93** suitable for X-ray diffraction. The result of this experiment is displayed in Figure 65, and selected bond length and angle data are listed in Table 15 and Table 16 respectively. This is, to our knowledge, the first example of alkylation/dearomatisation of the naphthalene backbone in a BIAN ligand.

Figure 65. Ortep representation of compound **93**. Thermal ellipsoids drawn at 30% probability. Hydrogens omitted except for those attached to chiral centre C(31).
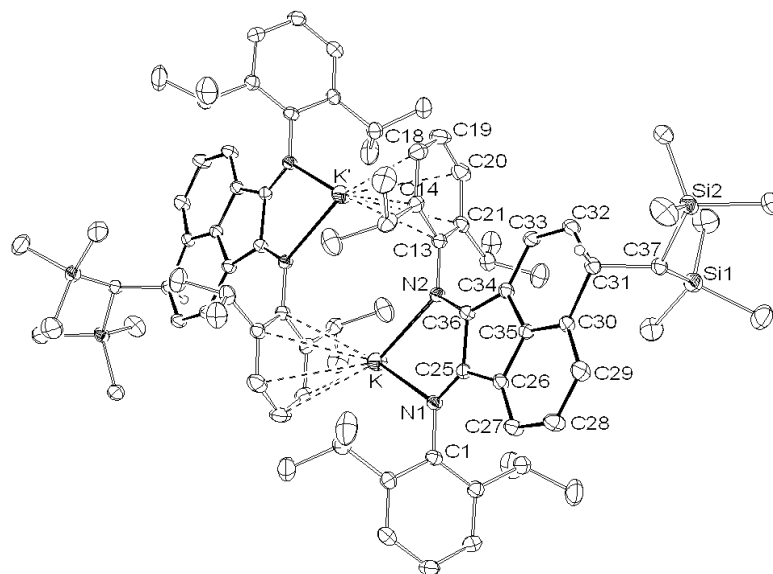

Table 15. Selected bond lengths (Å) for compounds **93**, **99**, **100** and **101**.

	93[a]	99	100[b]	101[a]
M-N(1)	2.694(3)		2.571(4)	2.702(4)
M-N(2)	2.703(3)		2.372(5)	2.762(4)
N(1)-C(25)	1.281(4)	1.263(4)	1.287(7)	1.267(5)
N(2)-C(36)	1.335(4)	1.283(5)	1.355(7)	1.318(5)
C(25)-C(36)	1.518(4)	1.513(5)	1.489(8)	1.521(6)
C(25)-C(26)	1.496(4)	1.489(5)	1.494(8)	1.489(6)
C(34)-C(36)	1.393(4)	1.487(5)	1.418(8)	1.415(6)
C(30)-C(31)	1.533(5)	1.523(5)	1.519(9)	1.524(6)
C(31)-C(32)	1.517(5)	1.563(5)	1.510(9)	1.514(7)
C(32)-C(33)	1.351(5)	1.501(5)	1.344(8)	1.390(6)
C(32)-C(32')		1.557(6)		
M-C(13)	3.243(3)			3.150(4)[c]
M-C(14)	3.133(3)			3.321(5)[d]
M-C(18)	3.096(4)			3.169(4)[e]
M-C(19)	3.142(4)			2.974(4)[f]
M-C(20)	3.223(4)			
M-C(21)	3.289(3)			
M-centroid	2.866(4)			2.884(5)

a- M = K   b- M = Ca   c- K'-C(30)   d- K'-C(33)
e- K'-C(34)   f- K'-C(35)

146

Similarly to the related potassium complex containing the radical-anion [dipp-BIAN]$^{\bullet}$ ligand, compound **93** crystallises as a dimer in which the coordination environment about both potassium centres is provided by one of the η^6-aryl substituents of the second molecule of **93**, and the bidentate imine-amido dearomatised BIAN ligand.[257] The K-centroid and K-K' distances of 2.866(4) and 4.5657(17) Å respectively are shorter than those in [{dipp-BIAN}K] [K-centroid 2.904; K-K' 4.619 Å].[257] Despite the asymmetry of the ligand framework the potassium-imine and potassium-amide K-N distances of 2.694(3) and 2.703(3) Å can be considered identical and within the range of those observed in [{dipp-BIAN}K].[257] Whereas the N(1)=C(25) bond length of 1.281(4) Å falls within the range of N=C bonds lengths of the ligand precursor [1.250(6) and 1.295(6) Å][257] the N(2)-C(36) bond of the amido fragment shows substantial elongation to 1.335(4) Å, although the distance is still short for a formal N-C single bond. While the ethanediylidyne C(25)-C(36) bridge remain unaffected by the charge redistribution [**93**, 1.518(4); dipp-BIAN 1.526(3) Å] the C(36)-C(34) distance is considerably shortened compared to that in the ligand precursor [**93** 1.518(4); dipp-BIAN 1.505(5) Å].[257] The dearomatised naphthalene ligand backbone is only slightly distorted from its original planar geometry. The C-C bond lengths and angles of the aromatic C_6H_3 ring [1.374(5) – 1.410(5) Å; 116.6(3) – 122.3(3)$^{\circ}$] remain within the range of those of the ligand precursor, whereas the dearomatised C_6H_3 ring is distorted due to the presence of the sp^3 C(31) carbon centre [C(30)-C(31) 1.533(5); C(31)-C(32) 1.517(5) Å; C(30)-C(31)-C(32) 111.6(3)$^{\circ}$]. The four-coordinate C(31) stereocentre is *pseudo*-tetrahedral [C(32)-C(31)-C(37) 111.3(3)$^{\circ}$; C(32)-C(31)-C(30) 111.6(3)$^{\circ}$; C(30)-C(31)-C(37) 113.4(3)$^{\circ}$].

Table 16. Selected angles (^{o}) for compounds **93**, **99**, **100** and **101**.

	93[a]	**99**	**100**[b]	**101**[a]
N(1)-M-N(2)	63.52(8)		70.08(15)	61.95(11)
M-N(1)-C(1)	121.28(19)		132.0(3)	118.7(3)
M-N(2)-C(13)	126.18(18)		130.7(3)	123.0(3)
M-N(1)-C(25)	118.2(2)		109.7(3)	119.7(3)
M-N(2)-C(36)	117.4(2)		114.8(3)	118.2(3)
N(1)-C(25)-C(36)	121.7(3)	122.0(3)	121.5(5)	119.0(4)
N(2)-C(36)-C(25)	119.0(3)	121.3(3)	120.1(5)	121.0(4)
C(30)-C(31)-C(32)	111.6(3)	114.4(3)	111.8(5)	109.6(4)
C(30)-C(31)-C(37)	113.4(3)	114.7(3)	113.6(5)	110.5(4)
C(32)-C(31)-C(37)	111.3(3)	110.1(3)	111.8(5)	109.7(4)
C(31)-C(32)-C(33)		117.9(3)		
C(33)-C(32)-C(32')		109.9(2)		
C(31)-C(32)-C(32')		110.7(4)		
N(1)-M-N(3)			169.65(14)	
N(1)-M-N(4)			115.92(15)	
N(2)-M-N(3)			115.99(15)	
N(2)-M-N(4)			117.49(16)	
N(1)-M-O(1)			84.08(14)	
N(2)-M-O(1)			123.06(16)	
N(3)-M-O(1)			85.57(14)	
N(4)-M-O(1)			119.42(16)	

a- M = K   b- M = Ca

Similarly, addition of [M{CH(SiMe$_3$)$_2$}$_2$(THF)$_2$] (M = Ca **37b**, Sr **37c**) to a suspension of dipp-BIAN in C$_6$D$_6$ resulted in instant solubilisation of the starting materials and a rapid colour change to dark green. The analogous reaction with [Mg{CH(SiMe$_3$)$_2$}$_2$(THF)$_2$] required 24 hours heating at 60 ^{o}C to yield the same result (Scheme 72). In all three cases ^{1}H NMR spectra were reminiscent of that of **93**, showing clean formation of the heteroleptic alkaline earth organometallic species **94**, **95** and **96**, with the additional (18H) and (1H) singlets of the metal-bound monoanionic [CH(SiMe$_3$)$_2$]$^-$ co-ligand at ca. 0.3 ppm and -1.7 ppm respectively. Figure 66 shows the annotated ^{1}H NMR spectrum of the calcium complex **95** synthesised in toluene.

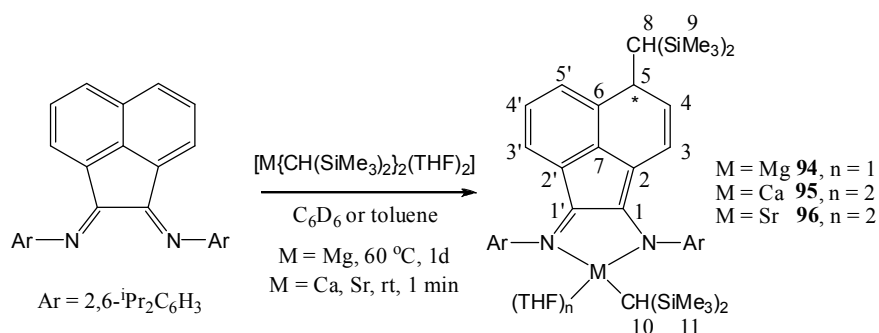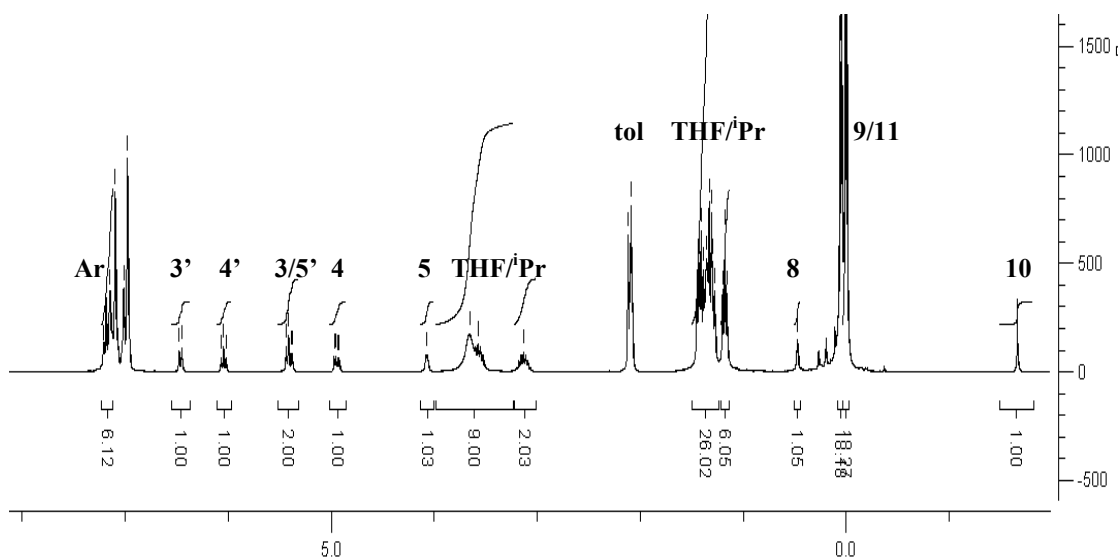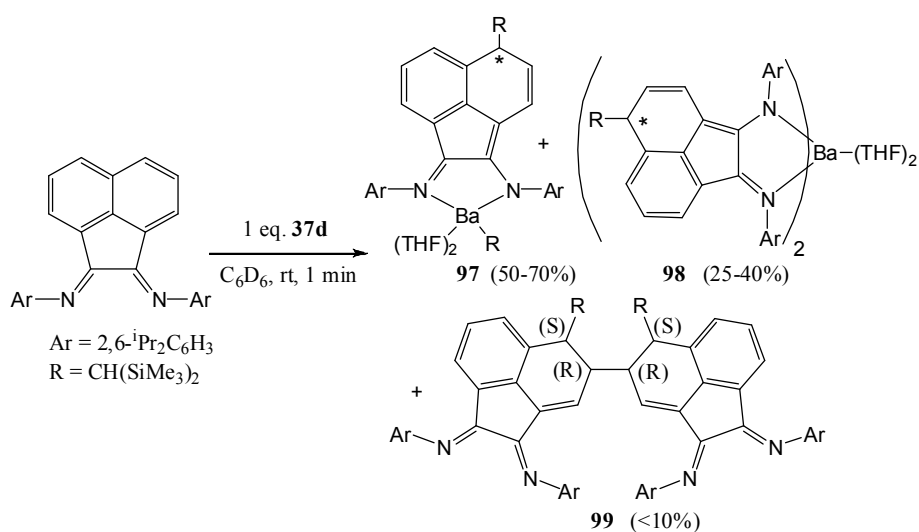**Scheme 72.** Synthesis of magnesium, calcium and strontium compounds **94**, **95** and **96**.

**Figure 66.** Annotated ^{1}H NMR spectrum of the dearomatised calcium complex **95**.

Although the analogous reaction with the barium dialkyl **37d** also led to an instant colour change to dark green, ^{1}H NMR data at the first point of analysis showed the formation of three distinct dearomatised species, among which the heteroleptic barium alkyl complex **97** (50-70% yield) was identified by the characteristic upfield Ba-C*H*(SiMe$_3$)$_2$ proton shift at -1.73 ppm (Scheme 73). A subsequent independent synthesis of the homoleptic barium complex **98** from the reaction between two equivalents of the potassium complex **93** and barium iodide (*vide infra*) enabled the identification of the second component of the reaction mixture as complex **98**, present in 25-40% yield.

Scheme 73. Reaction of the barium dialkyl **37d** with dipp-BIAN.

Ar = 2,6-^{i}Pr$_2$C$_6$H$_3$
R = CH(SiMe$_3$)$_2$

1 eq. **37d**
C$_6$D$_6$, rt, 1 min

97 (50-70%)   **98** (25-40%)

99 (<10%)

Crystallisation of this reaction mixture from a 1:2 toluene/hexane solution at -30 ^{o}C over several days also provided orange crystals suitable for X-ray diffraction, which yielded the surprising structure of compound **99**, composed of two C^5-alkylated dearomatised BIAN ligands coupled at the C^4 position. The result of this experiment is displayed in Figure 67. Selected bond length and angle data are provided in Table 15 and Table 16 respectively. Compound **99** crystallises as a single (4*R*, 4'*R*, 5*S*, 5'*S*) enantiomer (absolute structure parameter = 0.03(15)) in the chiral space group P 3$_1$ 2 1. As in the ligand precursor, both N-C bond lengths [1.263(4), 1.283(5) Å] are indicative of imine bonds. The presence of the two *pseudo*-tetrahedral sp^3 carbon centres, C(31) [C(30)-C(31)-C(32) 114.4(3)^o; C(30)-C(31)-C(37) 114.7(3)^o; C(32)-C(31)-C(37) 110.1(3)^o] and C(32) [C(31)-C(32)-C(33) 117.9(3)^o; C(33)-C(32)-C(32') 109.9(2)^o; C(31)-C(32)-C(32') 110.7(4)^o], induces a significant distortion of the alkylated C$_6$H$_3$ ring of the ligand backbone, accompanied by an increase in the C-C bond lengths [C(30)-C(31) 1.523(5); C(31)-C(32) 1.563(5); C(31)-C(32) 1.501(5) Å]. Although the mechanism of formation of **99** remains unclear, it may be explained by taking into account the well-known ability of the BIAN ligand to act as electron acceptor. Two-electron oxidation of the alkylated ligand to form the coupled product **99** may thus be accompanied by two-electron reduction of one equivalent of either the dipp-BIAN ligand precursor or the alkylated/dearomatised ligand. Efforts are currently under way to rationalise the synthesis of compound **99**.

Figure 67. Ortep representation of compound **99**. Thermal ellipsoids drawn at 30% probability. *Iso*-propyl methyl groups and hydrogens omitted except for those attached to the chiral centres C(31) and C(32).
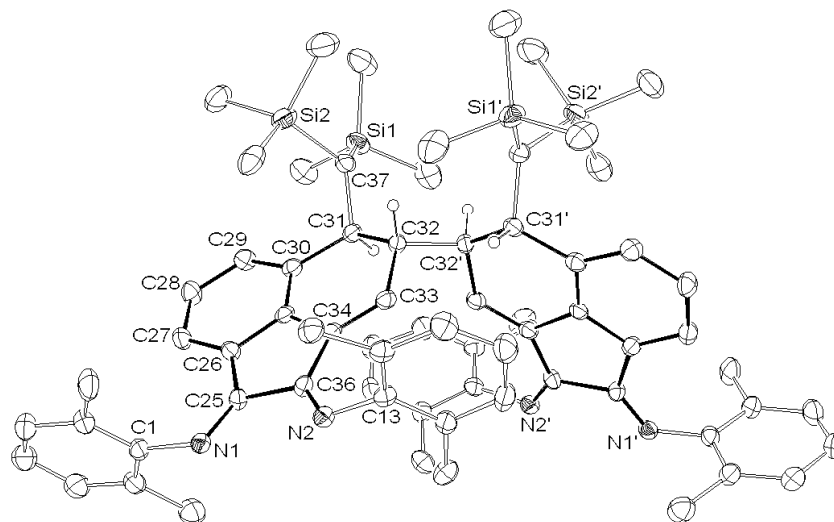

Multiple attempts to obtain crystals of the alkaline earth organometallic complexes **94-97** suitable for X-ray analyses were thwarted by the extreme solubility of these compounds even after months of storage at -30 $^{\circ}$C in minimal amounts of hydrocarbon solvents such as hexane or pentane. NMR data and elemental analyses of the crude magnesium, calcium and strontium products, however, left no doubt as to their formulation. Attempts to recover the alkylated amino-imine ligand by controlled hydrolysis of the organometallic complexes initially led to a colour change from green to purple, followed by a gradual change towards dark red over a period of several hours. ^{1}H NMR data and later recrystallisation of the crude product from toluene showed quantitative conversion to the re-aromatised dipp-BIAN ligand precursor with formation of the alkane $CH_2(SiMe_3)_2$. Although the mechanism of this reaction remains to be elucidated it is possible that the extreme stability of the aromatic BIAN ligand may be the driving force of this de-alkylation process.

The kinetic stability of the heteroleptic complexes **94**, **95** and **96** was assessed by heating a d_8-toluene solution of these compounds at 80 $^{\circ}$C for a week. Apart from a slight amount of protonolysis of the alkyl ligand into the alkane $CH_2(SiMe_3)_2$ in the cases of **95** and **96** (< 5%), possibly due to reaction with the solvent, the ^{1}H NMR spectra remained virtually unchanged, suggesting an absence of Schlenk-type ligand redistribution processes. Addition of two equivalents of the ligand precursor to one equivalent of the magnesium, calcium or strontium dialkyl species in d_8-toluene did not yield the expected homoleptic complexes at room temperature. Rather, the heteroleptic

complexes **94**, **95** and **96** were formed while the excess ligand remained unreacted. Heating of these mixtures at 90 °C over a period of several days did not result in reaction with the second equivalent of ligand. Instead, partial protonation of the alkyl co-ligand and a substantial decrease in the methyl signal of the toluene solvent peak were observed, suggesting deprotonation of the solvent had occurred. In contrast, the analogous reaction with the barium dialkyl, **37d**, in d_8-toluene led to the complete solubilisation of both equivalents of ligand within ten minutes at room temperature (Scheme 74). ^{1}H NMR data showed complete consumption of the ligand precursor and **37d**, concomitant with the clean formation of a single dearomatised species identified as the homoleptic barium compound **98** by comparison with the NMR data obtained from the independent synthesis of **98** from the potassium complex **93** and barium iodide. Although the ^{1}H NMR spectrum of **98** remained relatively simple, the complexity of the ^{13}C{^{1}H} spectrum indicated that the 2,6-di-*iso*-propylphenyl groups are no longer equivalent due to the conformational restriction induced by the steric crowding about the barium metal centre.

Scheme 74. Independent syntheses of the homoleptic barium complex **98**.
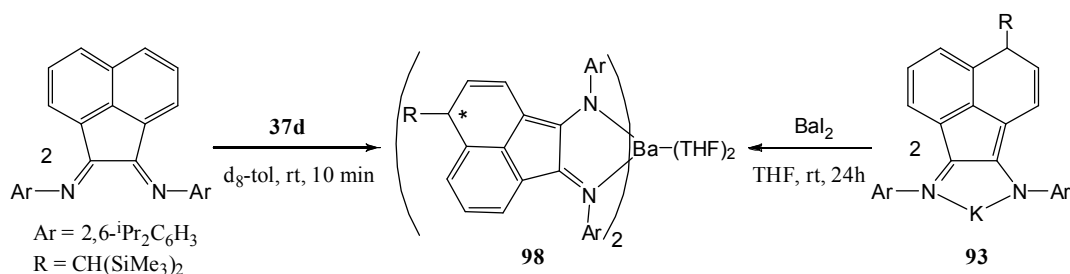
Stoichiometric NMR scale reactions of calcium complex **95** with protic substrates such as hexamethyldisilazane, diphenylamine or diphenylphosphine in C_6D_6 resulted in immediate protonolysis of the alkyl co-ligand, as observed in the ^{1}H NMR spectra by the disappearance of the up-field Ca-CH(SiMe$_3$)$_2$ singlet at -1.72 ppm and the appearance of the characteristic alkane resonance at -0.2 ppm (Scheme 75). Given the comparable steric demands of the bis(trimethylsilyl)amide and bis(trimethylsilyl)methanide co-ligands, the resulting heteroleptic calcium bis(trimethylsilyl)amide complex evidenced solution stability similar to complex **95**. In contrast, monitoring by ^{1}H NMR spectroscopy of the heteroleptic calcium complexes bearing the less sterically demanding diphenylamide and diphenylphosphide co-ligands under the same conditions suggested slow Schlenk-type ligand redistribution towards

the homoleptic calcium species **100** characterised by the broadening and shifting of the dearomatised ligand backbone and *iso*-propyl resonances, accompanied by precipitation of insoluble colourless products tentatively attributed to homoleptic calcium amide and phosphide species (Scheme 75) which are known to be insoluble in non-coordinating hydrocarbon solvents.[274] An independent synthesis of complex **100** by the reaction between two equivalents of potassium complex **93** and calcium iodide in THF confirmed the nature of the complex formed.

Scheme 75. Stoichiometric reactivity of calcium complex **95** with protic substrates.
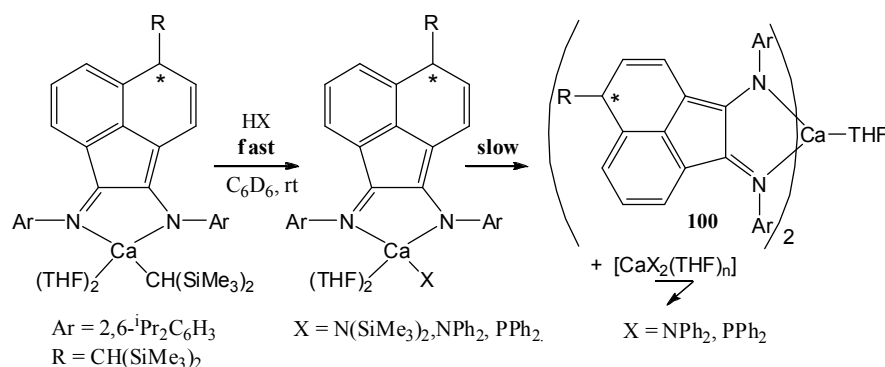
Crystals of compound **100** suitable for X-ray diffraction analysis were isolated from the reaction of **95** with diphenylphosphine after storage in a 4:1 toluene-THF mixture at -30 °C for several weeks. The result of this experiment is displayed in Figure 68. Selected bond length and angle data are listed in Table 15 and Table 16 respectively. Contrary to the homoleptic calcium β-diketiminate complex [{HC(CMeNAr}$_2$}$_2$Ca] (Ar = 2,6-di-*iso*-propylphenyl),[275] but similarly to the homoleptic complex of the radical-anion [{dipp-BIAN}$_2$Ca(THF)],[260] compound **100** crystallises as a mono-THF adduct. The five-coordinate calcium centre presents a highly distorted trigonal bipyramidal geometry (τ = 0.78)[149] with both imine nitrogen atoms in axial positions. The mean planes formed by the two almost planar ligand backbones form an angle of 82.8°. While in the case of complex **93** the KN_2C_2 ring remains planar, the presence of the large calcium centre in **100** causes a slight distortion in the CaN_2C_2 rings. The N(1)-Ca-N(2) and N(3)-Ca-N(4) bite angles of the two alkylated BIAN ligands [70.08(15) and 69.66(15)° respectively] are notably smaller than the N-Ca-N angles observed in calcium complexes supported by a doubly reduced BIAN ligand [75.76(7) − 78.5(2)°][259] or the homoleptic complex of the radical-anion [{dipp-BIAN}$_2$Ca(THF)] [73.58(9) °].[260] The Ca-N$_{imine}$ distances of 2.571(4) and 2.573(5) Å are substantially

153

longer than the Ca-N$_{amide}$ bonds of 2.372(5) and 2.353(5) Å, reflecting the stronger bonding between the metal centre and the anionic amide moiety of the ligand. As for the potassium complex **93** the N(2)-C(36) and N(4)-C(79) bond lengths of the amide residues [1.355(7) and 1.347(7) Å] are significantly longer than the N(1)=C(25) and N(3)=C(68) bond lengths of the imine moieties [1.287(7) and 1.279(7)Å], while the ethanediylidyne bridges are slightly shorter in **100** than in **93** [**100** 1.489(8) and 1.509(8) Å; **93** 1.518(4) Å]. As previously observed for compound **93**, the dearomatisation of the alkylated C$_6$H$_3$ rings only induces a slight distortion from planarity despite the presence of the sp^3 C(31) and C(74) carbon centres indicated by the elongated C-C bond lengths [C(30)-C(31) 1.519(9); C(31)-C(32) 1.510(9); C(73)-C(74) 1.521(8); C(74)-C(75) 1.499(8) Å] and the *pseudo*-tetrahedral angles [C(32)-C(31)-C(30) 111.8(5); C(32)-C(31)-C(37) 111.8(5); C(30)-C(31)-C(37) 113.6(5); C(75)-C(74)-C(73) 111.4(5); C(75)-C(74)-C(80) 111.9(5); C(73)-C(74)-C(80) 114.8(5)°].

Figure 68. Ortep representation of compound **100**. Thermal ellipsoids drawn at 30% probability. *Iso*-propyl methyl groups and hydrogens omitted except for those attached to the chiral centres C(31) and C(74).
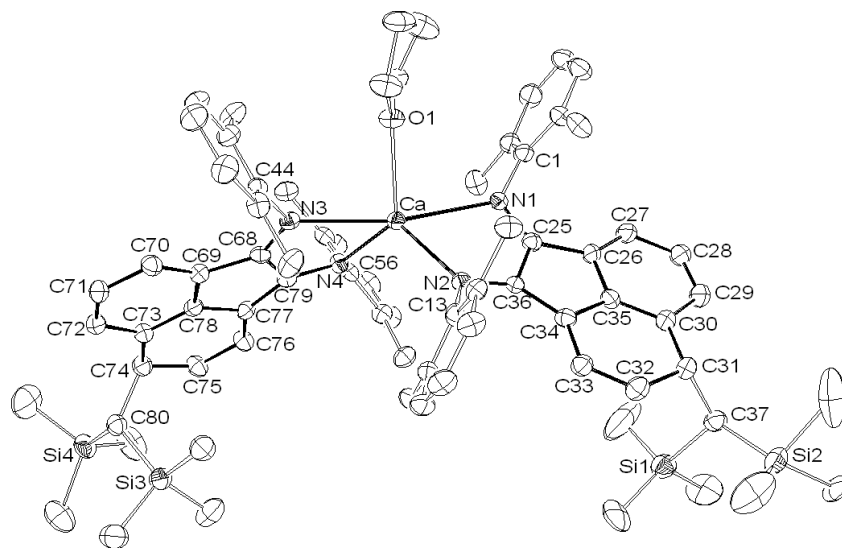
An interesting insight into the possible mechanism of formation of these alkylated/dearomatised BIAN complexes came from the result of the reaction between the potassium benzyl complex [K{CH(SiMe$_3$)(2-NMe$_2$-C$_6$H$_4$)}] and dipp-BIAN in toluene (Scheme 76). As for the analogous reaction with [KCH(SiMe$_3$)$_2$] the reaction mixture instantly turned dark green. ^{1}H NMR data indicated the formation of complex

154

101 as a mixture of two diastereomeric dearomatised potassium complexes alkylated in the C^5 position of the acenaphthene backbone in an 88:12 mixture.

Scheme 76. Synthesis of the potassium hexamer **101**.
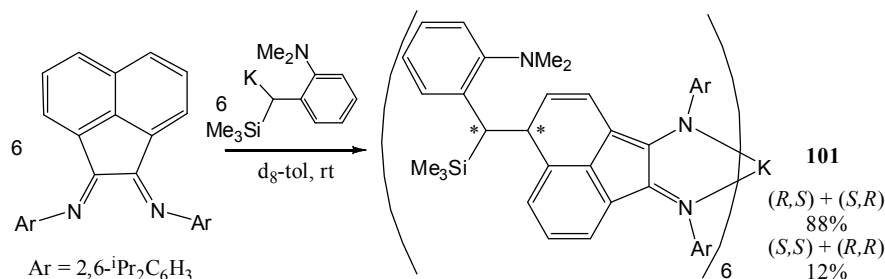
Crystallisation from this solution after one day at room temperature yielded green crystals of compound **101** suitable for X-ray diffraction analysis. The result of this experiment is illustrated in Figure 69. Selected bond length and angle data are listed in Table 15 and Table 16 respectively. Compound **101** crystallises as a single (*R,S*) + (*S,R*) diastereomer which, according to crystalline yield (~80%), was identified as the major diastereomer observed in the ^{1}H NMR spectrum. Each potassium centre is coordinated to the imine and amide functionalities of the dearomatised BIAN ligand and completes its coordination sphere by an η^4 interaction with the conjugated system of the alkylated C_6H_3 ring of the ligand backbone, with a K-centroid distance of 2.884(5) Å. Contrary to potassium complex **93** the K-N bond lengths in **101** reflect the asymmetry of the alkylated amido-imine ligand [K-N_{imine} 2.762(4); K-N_{amide} 2.702(4) Å]. The π-interaction between the potassium centres and the ligand backbone causes a strong distortion of the latter from planarity in both the aromatic and the alkylated C_6H_3 rings of the naphthalene fragment. Although calculations would be required to support this hypothesis, it seems possible that alkylation of the ligand occurs *via* pre-coordination of the relevant metal alkyl complex to the aromatic naphthalene backbone in these cyclic arrays, followed by alkyl transfer by insertion.

Figure 69. Ortep representation of compound **101**. Ellipsoids drawn at 30% probability. Left: two-molecule view of the complex. *Iso*-propyl methyl groups and hydrogens omitted except for those attached to the chiral centres C(31) and C(37). Right: hexameric unit of complex **101**. Hydrogens omitted for clarity except for those attached to the chiral centres C(31) and C(37).
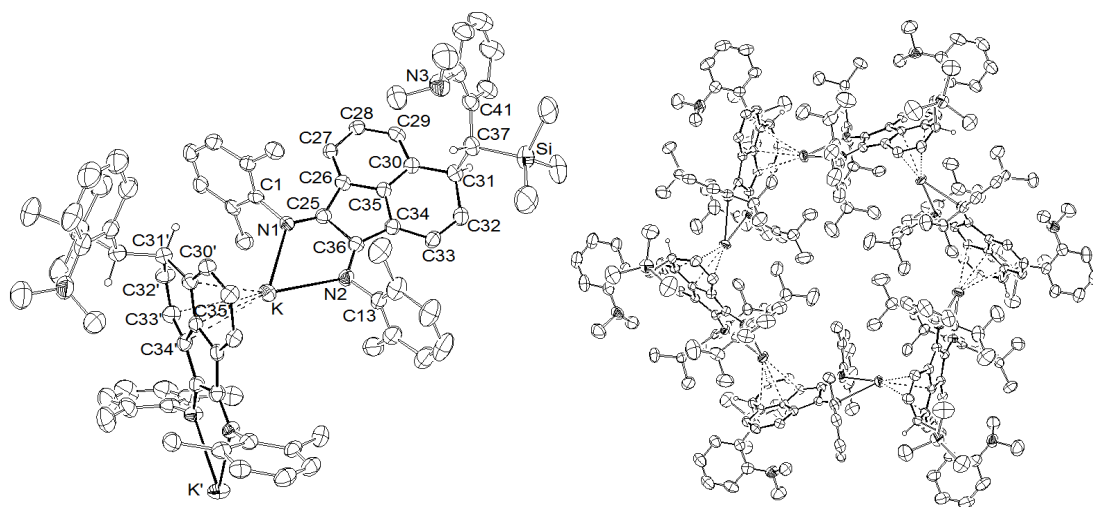
4.2.3 Computational study of alkylation regioselectivity

Preliminary DFT calculations were undertaken to investigate the regioselectivity of this BIAN alkylation process on the model complexes [{C^n-^{i}Pr-(^{t}Bu-BIAN)}Ca(^{i}Pr)] (n = 3, **102**; 4, **103**; 5, **104**) using B3LYP density functional theory and a 6-31G basis set implemented in Gaussian03.[220] Independent frequency calculations confirmed the optimised geometries as true minima. To reduce computational expense, the bulky 2,6-di-*iso*-propylphenyl groups were replaced by less demanding *tert*-butyl groups thought to best reflect the steric demands of these substituents, while the silicon atoms and methyl groups of the CH(SiMe$_3$)$_2$ fragments were replaced by carbon and hydrogen atoms respectively. Although NMR and elemental analysis data confirmed the presence of two adducted THF molecules on the parent complex **95**, their presence was deemed unnecessary in an assessment of alkylation regioselectivity. Figure 70 illustrates the results of this study in the form of an energy diagram.

Figure 70. Energy diagram of the optimised (DFT, B3LYP/6-31G) structures of compounds (a) **102**, (b) **103** and (c) **104**.

(b)

(a)

(c)

121.8 kJ.mol⁻¹
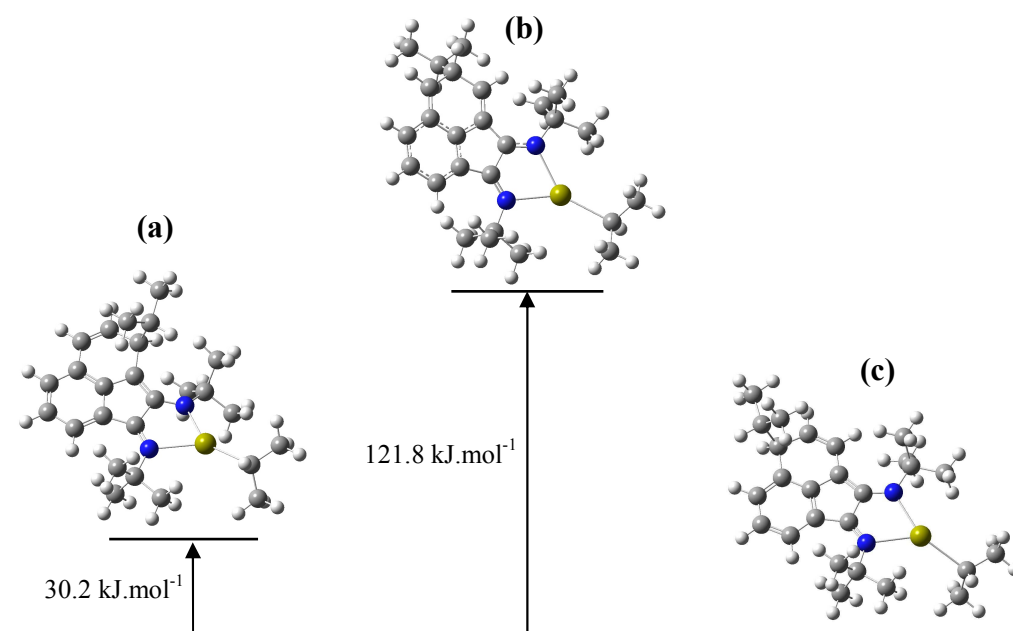
30.2 kJ.mol⁻¹

The C^5-alkylated isomer **104** was calculated to be the most stable product with the C^3- and C^4-alkylated isomers 30.2 kJ.mol⁻¹ and 121.8 kJ.mol⁻¹ higher in energy respectively. The observed regioselectivity may arise from both electronic stabilisation and minimisation of the steric repulsion between the alkyl substituent on the naphthalene backbone and the nitrogen-bound substituents. The bond lengths and angles calculated in **104** show good agreement with those obtained experimentally from the crystal structure of the homoleptic calcium complex **100** (compare Tables 15 and 16 and Figure 71, caption), except for the Ca-N bond lengths which are considerably longer in compound **100** (avg. 2.73 Å) compared to the model complex **104** (avg. 2.53 Å). This is most likely due to the lower coordination number employed for complex **104**. The shorter Ca-N(2) bond length [2.48 Å] compared to Ca-N(1) [2.57 Å] in **104**, however, confirms the asymmetric nature of the bonding between the alkaline earth dication and the alkylated amido-imine ligand. The calculated Ca-C(50) bond length of 2.57 Å between the calcium centre and the alkyl co-ligand is slightly longer than that in the calcium dialkyl precursor [2.4930(18) Å],[144] which can be explained by the difference in polarity arising from the replacement of the silicon atoms with carbon atoms. Molecular orbital (MO) analysis showed that the LUMO (Figure 71b) is delocalised over the conjugated π-system of the ligand, while the HOMO remains localised on the side of the ligand which underwent dearomatisation and on the amido functionality (Figure 71c). The HOMO-1 (Figure 71d) encompasses the σ-antibonding

157

between the metal centre and the ligands. Natural Bond Orbital (NBO) calculations were undertaken and the calculated charges (Ca +1.12, N(1) -0.68, N(2) -0.79, C(50) -0.44) were indicative of essentially ionic bonding.

Figure 71. (a) Optimised (DFT, B3LYP/6-31G) structure of compound **104**. Selected bond lengths (Å): Ca-C(50) 2.57, Ca-N(1) 2.48, Ca-N(2), 2.38, N(1)-C(25) 1.31, N(2)-C(36) 1.35, C(25)-C(36) 1.56, C(25)-C(26) 1.50, C(34)-C(36) 1.41, C(30)-C(31) 1.52, C(31)-C(32) 1.51, C(32)-C(33) 1.36. Selected angles (°): N(1)-Ca-N(2) 70.58, Ca-N(1)-C(25) 114.50, Ca-N(2)-C(36) 117.86, N(1)-C(25)-C(36) 119.65, N(2)-C(36)-C(25) 116.55, C(30)-C(31)-C(32) 111.13, C(30)-C(31)-C(37) 112.44, C(32)-C(31)-C(37) 111.75. (b) LUMO of **104**. (c) HOMO of **104**. (d) HOMO-1 of **104**.
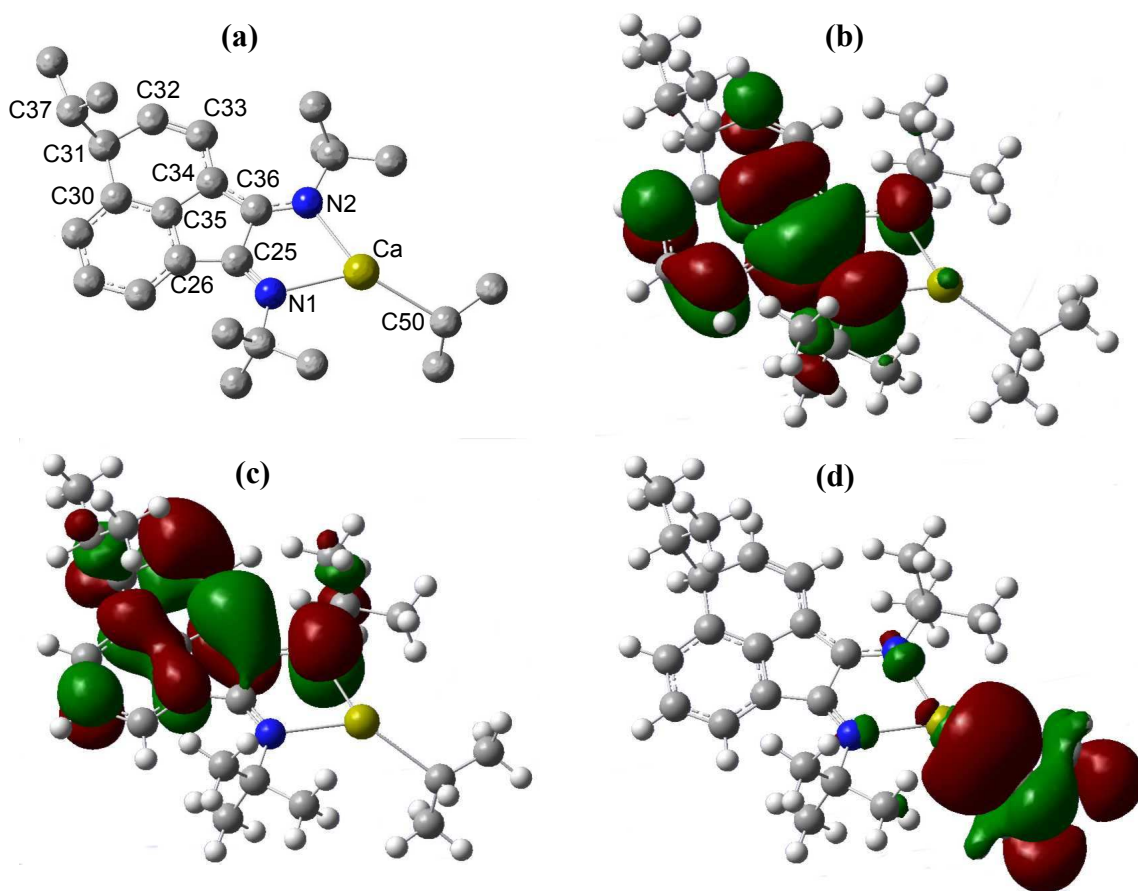
4.2.4   Preliminary scope of intramolecular hydroamination

Calcium complex **95** was assessed for the intramolecular hydroamination of a wide range of substituted aminoalkenes on an NMR scale in C_6D_6 or d_8-toluene. In all cases careful inspection of the ^{1}H NMR data showed no change suggestive of ligand redistribution in the characteristic shifts of the dearomatised ligand backbone throughout the reaction times.

158

Table 17. Scope of hydroamination/cyclisation with magnesium and calcium precatalysts **94** and **95**.

Entry	Substrate	Product	Catalyst (mol %)	Time / h	T / °C	NMR yield / %[a]
1			**95**, 2 mol %	1	25	95
2			**95**, 1 mol %	0.3	25	99
3			**95**, 0.5 mol %	0.25	25	>99
4			**95**, 2 mol %	1	25	98
5			**95**, 5 mol %	5	25	95
6			**95**, 5 mol %	24	110	0
7			**95**, 2 mol %	1	25	85:11[b]
8			**94**, 20 mol %	24	80	95:0[b, c]
9			**95**, 20 mol%	48	90	0:21[b]
10			**95**, 5 mol %	3.5d	60	92
11			**95**, 5 mol %	3.5d	60	22[d]
12			**95**, 5 mol %	18	60	24

a- NMR yields were measured against TMSS as an internal standard in C_6D_6 or d_8-toluene.
b- Cyclisation: isomerisation.
c- Yield after hydrolysis.
d- Substrate conversion >99%: the remaining products derive from recombination and isomerisation reactions.

Complete disappearance of the distinctive up-field alkyl singlet at ca. -1.7 ppm within the first point of analysis was indicative of rapid and irreversible catalyst initiation. Comparison of the results listed in Table 17 with previous intramolecular hydroamination experiments carried out with the THF-free calcium β-diketiminate complex **33** (Table 2) indicated that cyclisation with **95** generally occurred faster, and at lower temperature and catalyst loading, with the exception of more hindered α-substituted or secondary aminoalkenes (Table 17, entries 10-12). Especially remarkable was the fast cyclisation of 1-amino-2,2-diphenyl-4-hexene at room temperature (entry 5) as shown by the ^{1}H NMR stack plot displayed in Figure 72. The only other calcium precatalyst to have achieved this reaction, [Ca{N(SiMe$_3$)$_2$}$_2$(THF)$_2$] (Table 2, entry 14), required forcing conditions and gave much lower yields (20 mol%, 100 ^{o}C, 6 days, 63% yield).

Figure 72. ^{1}H NMR stack plot from the room temperature intramolecular hydroamination of 1-amino-2,2-diphenyl-4-hexene ($\blacklozenge$ characteristic signals of the dearomatised ligand backbone).
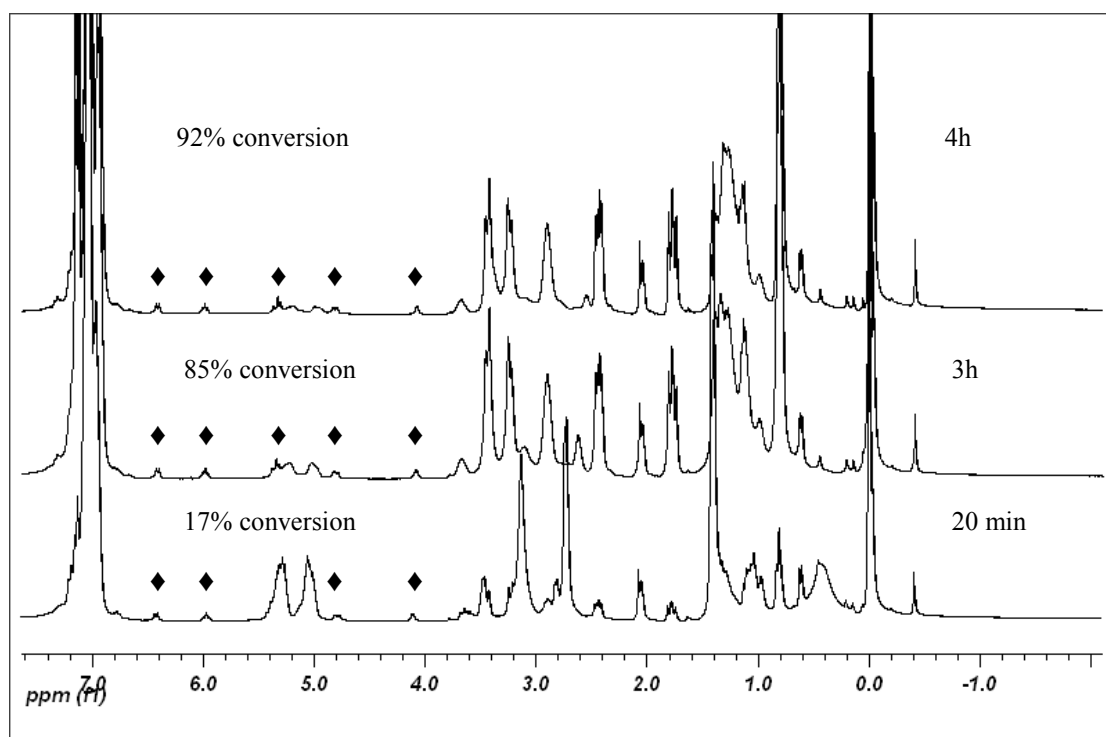
The terminally disubstituted aminoalkene 1-amino-2,2-diphenyl-5-methyl-4-hexene, however, did not undergo cyclisation under the forcing reaction conditions employed (Table 17, entry 6). Similarly to all other calcium precatalysts studied thus far **95** did not allow the cyclisation of 1-amino-2,2-diphenyl-6-heptene (entry 9). The same reaction

performed with the magnesium analogue **94**, however, yielded surprisingly swift conversion of this substrate to the hexahydroazepine product (**94**: 20 mol%, 24h, 80 ^{o}C, 95% yield; compared to **1**: 20 mol%, 3 days, 100 ^{o}C, 97% yield). The important increase in reactivity for aminoalkenes bearing a primary amine moiety can clearly be attributed to the fast and irreversible initiation of the calcium precatalyst while the dramatic decrease in reactivity for substrates with secondary amine moieties may arise from the steric hindrance of the two, at least initially, adducted THF molecules, a phenomenon that had already been observed in the comparison between **33** and its THF-solvated analogue **2** (Table 2, entries 29, 33 and 37). This same steric hindrance, however, seemed to have a positive influence on the diastereoselectivity of the cyclisation of 2-amino-5-hexene which favoured the *trans*-2,5-dimethylpyrrolidine product in 91% diastereomeric excess, albeit in very low yield (Table 17, entry 12).

4.2.5   Conclusion and future work

While providing fast and irreversible catalyst initiation, calcium complex **95** is also the first calcium precatalyst to efficiently effect the cyclisation of a terminally alkyl-substituted aminoalkene at room temperature in near quantitative yield. In comparison, lanthanide alkyl precatalysts generally require high temperatures (125°) to achieve the cyclisation of aminoalkenes with unactivated internal olefin moieties,[134, 135] while magnesium phenoxyamine precatalysts (20 mol%) reported by Hultzsch and co-workers performed the cyclisation of 1-amino-2,2-diphenyl-4-hexene at 150 ^{o}C with only moderate yields (47-69%).[152] New group 2 alkyl precatalysts are yet to be designed to accomplish the hydroamination of terminally disubstituted aminoalkenes. Although only preliminary, these results show promising potential for this new series of alkaline earth precatalysts, the first one to provide facile access to highly reactive analogous heteroleptic magnesium, calcium and strontium alkyl species, the full scope of whose catalytic reactivity has yet to be investigated.

Although the heteroleptic magnesium, calcium and strontium complexes **94-96** themselves show no tendency towards ligand lability in solution or during intramolecular hydroamination catalysis, the introduction of smaller anionic co-ligands seems to inevitably induce irreversible Schlenk-type ligand redistribution processes. In

order to avoid these undesirable processes further work may involve introducing more sterically demanding nitrogen-bound substituents onto the BIAN ligand framework.

Although complexes **94-96** present a chiral centre in the C^5 position of the ligand backbone, they form as racemic mixtures. Besides, the chiral centre is too far removed from the coordination sphere of the metal centre to have much influence upon enantioselectivity during catalysis. The introduction of chiral nitrogen-bound substituents onto the BIAN framework would therefore be necessary in order to develop potentially enantioselective alkaline earth precatalysts based upon dearomatised BIAN ligands. A new synthetic route to chiral anilines developed by Coates and co-workers, for example, has enabled the synthesis of the first chiral aryl-BIAN ligands (Figure 73A), which have been successfully used in stereoselective nickel-catalysed polymerisation reactions.[254, 276] The presence of benzylic protons on these ligands, however, could make them unsuitable for reactions with highly basic alkaline earth dialkyls. The difficulty of synthesising chiral alkyl-BIAN ligands was only recently overcome by Hagar *et al.* by using chiral cyclopropylamine precursors (Figure 73B) which prevent the decomposition by isomerisation usually observed in alkyl-BIAN ligands bearing non-cyclic alkyl substituents.[277] Alternatively, asymmetric amido-imine ligands obtained by alkylation in the C^1 position of dipp-BIAN by group 13 trialkyls may also present suitable candidates, as Fedushkin and co-workers reported that both $[\{C^1\text{-Et-(dipp-BIAN)}\}\text{Ga(Et)}_2]$ and $[\{C^1\text{-Me-(dipp-BIAN)}\}\text{In(Me)}_2]$ crystallise as separate isomers, of which the free ligands may be recovered by controlled hydrolysis of the complexes (Figure 73C).[273]

Figure 73. Extent of currently available chiral BIAN or BIAN-derived ligands.
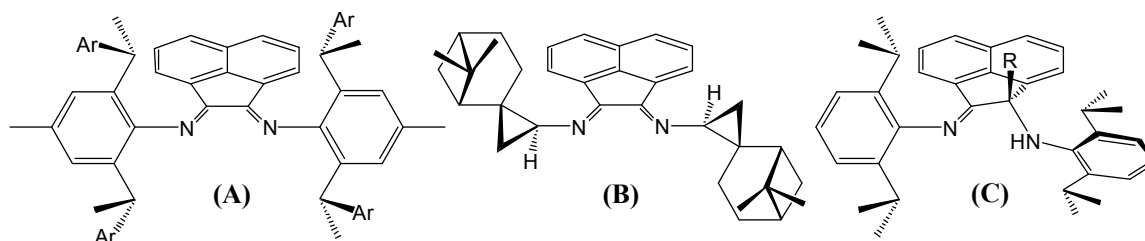
Beyond BIAN ligands, this novel alkylation/dearomatisation chemistry with alkaline earth dialkyl and dibenzyl species may well apply to other neutral ligand precursors with conjugated π-systems. Kiplinger and co-workers, for example, have already described the dearomatisation of terpyridine ligands by lutetium trialkyls.[278] More

recently, Kaneko *et al.* also reported the monoalkylation and dialkylation of Ar-DAB ligands (Ar = 2,6-dimethylphenyl, 2,6-di-*iso*-propylphenyl) by rare earth [M{CH$_2$(SiMe$_3$)}$_3$(THF)$_2$] (M = Sc, Y) complexes to form the amido-imine and diamido complexes respectively.[107] Other potential candidates may include bipyridine- or phenanthroline-based ligands.

Scheme 77. Dearomatisation of pyridine by a homoleptic calcium allyl complex and a heteroleptic magnesium alkyl complex in the presence of phenylsilane.
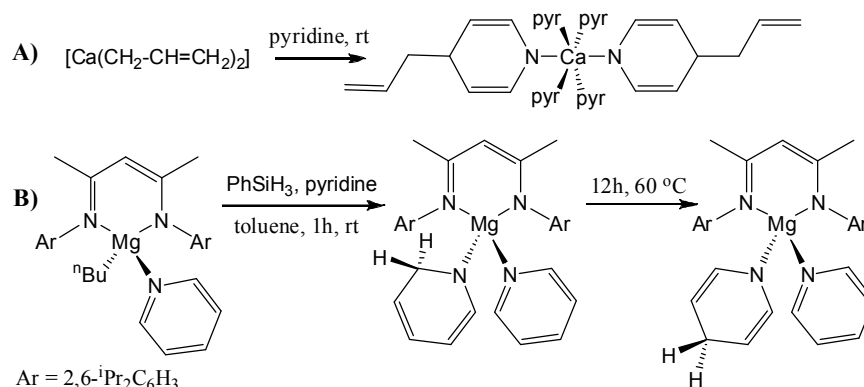
Recent reports by Okuda and co-workers on the alkylation and C-H activation of pyridines with a calcium bis(allyl) complex (Scheme 77A),[279] and by Hill *et al.* on the dearomatisation of pyridine with a *β*-diketiminate-supported magnesium hydride complex (Scheme 77B),[280] also open the possibility of heterocycle coupling which has been recently reported by Diaconescu and co-workers using group 3 and lanthanide benzyl complexes (Scheme 78).

Scheme 78. Pyridine coupling and dearomatisation at group 3 centres.
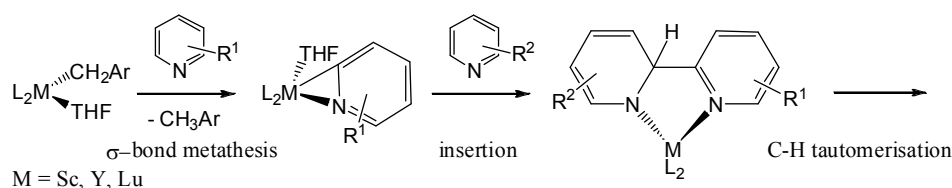
5   General conclusions and perspectives

Although the breakthrough in the development of a well-defined chemistry of the heavier alkaline earth elements originated in similarities with the equally ionic, redox inactive lanthanide (III) d^0 complexes, and a common reactivity pattern based upon σ-bond metathesis and insertion reaction, it is becoming more and more apparent that, rather than simply being lanthanide-mimetic, alkaline earth organometallics have a distinct chemistry of their own. Contrary to the linear trends displayed across the series of lanthanide elements, only marked by slight variations in electropositivity and size, the stark differences in ionic radii, and consequently charge density, across the alkaline earth group from magnesium to barium (Figure 74) also lead to marked differences in reactivity, not only between group 2 and f-elements, but also between the group 2 elements themselves.

Figure 74. Average charge density trends derived from the 6-coordinate ionic radii of the alkaline earth (II) and lanthanide (III) cations.[6]
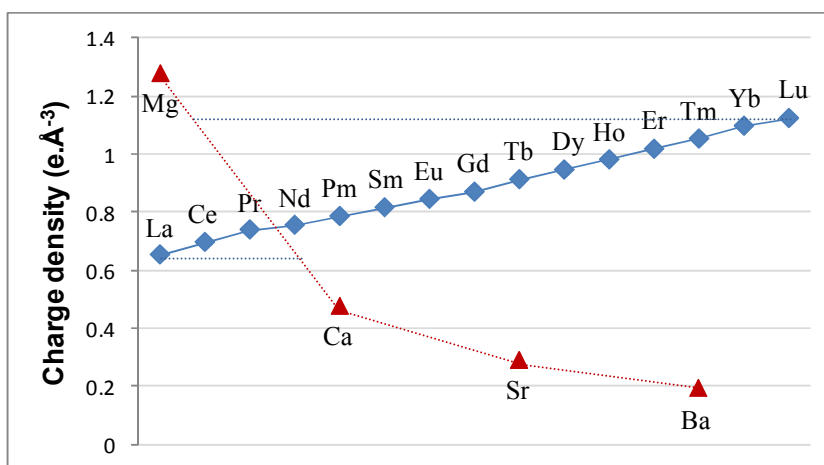

These discrepancies are particularly highlighted by the study of the alkaline earth-mediated intramolecular hydroamination reaction. Instead of a smooth increase in catalytic activity from magnesium to barium, as observed in the lanthanide series from the smallest (lutetium) to the largest (lanthanum) metal centre, catalytic activity increases dramatically from magnesium to calcium, drops again for strontium, and becomes quasi inexistent for barium, a trend which may be explained by the complex interaction between entropic effects, such as substrate access to the catalytic metal centre or the dimerisation of key intermediate species, and charge density effects, such

164

as the polarising capacity of the individual group 2 metal centre. Moreover, the observation of a rate law displaying a first-order decline in [substrate], rather than the zero-order dependence observed in lanthanide-mediated hydroamination/cyclisation reactions, also hints at intrinsic mechanistic differences which will require further computational investigations.

The search for monoanionic ligands capable of stabilising heteroleptic alkaline earth complexes bearing highly reactive alkyl functionalities has led to the discovery of a new dearomatisation/alkylation reactivity providing easy access to the desired group 2 precatalysts. Further work will be required to design new chiral alkaline earth precatalysts based upon this chemistry and to improve kinetic stability against detrimental ligand redistribution processes in solution, especially for the larger group 2 cations.

While the potential of the alkaline earth elements has long been underestimated, the last decade has seen a dramatic increase in the number and variety of group 2-catalysed reactions. The now readily available alkaline earth hydride, alkyl, benzyl and allyl species offer new possibilities for stoichiometric and catalytic reactivity. As this chemistry is still in its infancy, years to come could see a surge in new group 2-mediated heterofunctionalisation reactions (e.g. hydroboration, hydroalkoxylation, hydrothiolation, but also aminoboration, silylboration etc. of unsaturated bonds), functionalisation reactions of aromatic heterocycles, as well as a plethora of more challenging group 2-catalysed dehydrocoupling reactions to form new element-element σ-bonds (e.g. N-P, P-Si, O-Si, Si-Si, perhaps even C-C bonds) as suggested in Figure 75.

Figure 75. Potential catalytic cycles envisaged for new alkaline earth-mediated heterofunctionalisation and dehydrocoupling reactions.

165
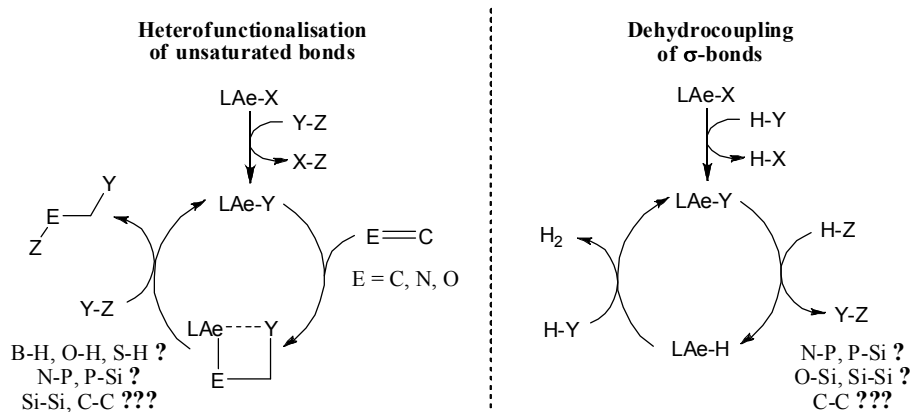
6 Experimental

6.1 General experimental procedures

All reactions dealing with air- and moisture sensitive compounds were carried out under argon atmosphere using standard Schlenk line and glovebox techniques in an MBraun Labmaster glovebox at O_2, H_2O < 0.1 ppm. NMR experiments using air-sensitive compounds were conducted in Youngs tap NMR tubes prepared and sealed in a glovebox under argon. For kinetic analysis samples were frozen to -196 ^{o}C immediately after preparation and defrosted before transfer into the NMR machine. Except if stated otherwise, all NMR data was acquired on a Bruker 300 Ultrashield^{TM} for ^{1}H (300 MHz), ^{13}C{^{1}H} (75.48 MHz) and ^{11}B (96.25 MHz) spectra at room temperature, or on a Bruker 400 Ultrashield^{TM} for variable temperature, kinetics and 2D experiments (^{1}H at 400 MHz and ^{13}C at 100 MHz). Except if stated otherwise all NMR data was acquired at 298 K. ^{1}H/^{13}C NMR spectra were referenced using residual solvent resonances. Infrared analyses of air-sensitive organometallics were conducted using KBr plates pressed under an argon atmosphere, organic compounds were analysed as KBr discs or dichloromethane films. Melting points were determined in sealed capillaries. Elemental analyses of all moisture- and air-sensitive compounds were performed by Stephen Boyer of London Metropolitan Enterprises. X-ray diffraction data was collected at 150 K on a single crystal FR590 Nonius KappaCCD diffractometer, equipped with Oxford Cryosystems, using graphite-monochromated Mo Kα radiation (λ =0.71073 Å), by Dr G. Kociok-Köhn, Dr D. MacDougall or the author at the University of Bath. Data was processed using Nonius Software.[281] Crystal parameters and details on data collection, solution and refinement of all the complexes are presented in the supplementary data section. Structure solution, followed by full-matrix least-squares refinement, was performed using the WINGX-1.70 suite of programs throughout.[282]

6.2 Solvents and reagents

Glassware, Celite and molecular sieves were dried for 24 hours in an oven at 150 °C prior to use.

Solvents: Solvents for air- and moisture-sensitive reactions were provided by an Innovative Technology Solvent Purification System. Hexane, toluene and benzene were used as collected whereas THF and diethyl ether were first dried by distillation over sodium-benzophenone ketyl. All solvents were stored under argon over molecular sieves activated at 150 °C *in vacuo*. C_6D_6, d_8-THF and d_8-toluene were purchased from Fluorochem and dried over molten potassium prior to vacuum transfer into a sealed ampoule and storage in the glovebox under argon.

Inorganic reagents: (Tetrakis(trimethylsilyl))silane (TMSS) was purchased from Goss Scientific Instruments Ltd. and used as received. MgI_2, CaI_2, SrI_2 and BaI_2 were purchased from Sigma-Aldrich and used as received. Solid potassium hexamethyldisilazane was either purchased from Sigma-Aldrich and used as received or synthesised from stirring hexamethyldisilazane with an excess of potassium hydride in toluene at room temperature for 24 hours. 2.5M *n*-Bu-Li in hexanes and $LiAlH_4$ were purchased from Fisher Scientific and used as received.

Amines: All bromo- and chloroalkenes, nitriles and amines were purchased from Sigma-Aldrich and used as received. After drying over CaH_2 all aminoalkenes were distilled *in vacuo* and either vacuum transferred into sealed ampoules or freeze-dried prior to transfer into the glovebox.

Ligand precursors: 1-(*tert*-butyl)imidazole,[208] 1-mesitylimidazole,[219] the *β*-diketiminate ligand precursor [(Dipp)NC(Me)CHC(CMe)NH(Dipp)] (Dipp = 2,6-di-*iso*-propylphenyl),[153] 2,6-diphenylmethyl-*p*-toluidine,[156] the halogenated boranes $Me_3N.BH_2I$,[283] $Me_3N.BH_2Br$, $Me_3N.BHBr_2$ (variation of the procedure reported for $Me_3N.BBr_3$)[284] and Ph_2BBr,[285] the tridentate carbene ligand precursors [HB(Im^{t}Bu)$_3$]Br$_2$ and [HB(ImMes)$_3$]Br$_2$,[207] the bis(imino)pyridine ligand precursor

[2,6-{(Dipp)NCMe}$_2$(C$_5$H$_3$N)][286] and [Dipp-BIAN][251] were all synthesised using literature procedures.

Organometallics: The homoleptic group 2 amides and alkyls [M{N(SiMe$_3$)$_2$}$_2$] (M = Mg **35a**, Ca **35b**, Sr **35c**, Ba **35d**)[142] [M{N(SiMe$_3$)$_2$}$_2$(THF)$_2$] (M = Mg **36a**, Ca **36b**, Sr **36c**, Ba **36d**)[143] and [M{CH(SiMe$_3$)$_2$}$_2$(THF)$_2$] (M = Mg **37a**, Ca **37b**, Sr **37c**, Ba **37d**)[144] were synthesised using literature procedures.

6.3 Equations

Van't Hoff analyses of equilibria

$$\Delta G^{o}(T) = -RT \ln(K_T))$$

$$\Delta G^{o}(T) = \Delta H^{o} - T\Delta S^{o}$$

R = molar gas constant (1.9858775 cal.mol^{-1}.K^{-1})

ΔG^{o} = Gibbs free energy (J.mol^{-1})

ΔH^{o} = free enthalpy (J.mol^{-1})

ΔS^{o} = free entropy (J.mol^{-1}.K^{-1})

K_T = equilibrium constant

T = temperature (K)

Activation energies of NMR fluxional processes

$$k_f = \frac{\pi \Delta v_o}{\sqrt{2}}$$

$$\Delta G^{\ddagger}(T) = -RT_c \ln(k_f)$$

Δv_o = maximum peak to peak separation (s^{-1})

$\Delta G^{\ddagger}$ = Gibbs free energy of activation (J.mol^{-1})

T_c = coalescence temperature (K)

k_f = rate of exchange (s^{-1})

Arrhenius equation

$$\ln(k_T) = -\frac{E_a}{RT} + B$$

Ea = activation energy in (J.mol^{-1})

k_T = reaction rate (s^{-1})

B = constant

Eyring equation

$$\ln(\frac{k_T h}{k_B T}) = -\frac{\Delta H^{\ddagger}}{RT} + \frac{\Delta S^{\ddagger}}{R}$$

$$\Delta G^{\ddagger}(T) = \Delta H^{\ddagger} - T\Delta S^{\ddagger}$$

h = Planck constant (6.626068*10^{-34} m^2.kg.s^{-1})

k$_B$ = Boltzmann constant (1.3806503*10^{-23} m^2.kg.s^{-1}.K^{-1})

$\Delta H^{\ddagger}$ = enthalpy of activation in (J.mol^{-1})

$\Delta S^{\ddagger}$ = entropy of activation in (J.mol^{-1}.K^{-1})

Degree of trigonality of 5-coordinate metal centres[149]

$$\tau = \frac{\beta - \alpha}{60}$$
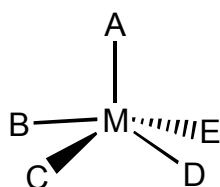
A = axial ligand

β = largest basal angle (B-M-D)

α = second largest basal angle (C-M-E)

Perfect spare pyramidal geometry: $\tau = 0$

Perfect trigonal bipyramidal geometry: $\tau = 1$

6.4   Hydroamination scope methodology (Tables 1 & 2)

In a glovebox, C$_6$D$_6$ or d$_8$-toluene solutions of each aminoalkene (~ 1.0 M) were prepared. For each reaction, 2-20 mol% of the catalyst precursor under study were added into 0.5 mL of aminoalkene solution in a Youngs tap NMR tube and immediately transferred to the 250 MHz NMR spectrometer. The reaction was then regularly monitored by ^{1}H NMR until maximum conversion was reached.

6.5 Kinetic hydroamination studies

6.5.1 General procedure

In a glovebox, d_8-toluene solutions of the precatalysts at 0.016 M (Eyring and Arrhenius analyses) and 0.0112 M (deuteration studies) were prepared with tetrakis(trimethylsilyl)silane (TMSS) at 0.16 M as a reference. For each reaction diprotio or dideuterio (1-allylcyclohexyl)methylamine (61mg, 71 µL, 0.4 mmol for Eyring and Arrhenius analyses; 43 mg, 50 µL, 0.28 mmol for deuteration studies) were pipetted into 0.5 mL of catalyst solution and transferred to a Youngs tap NMR tube. The tube was sealed, removed from the glovebox, immediately frozen with liquid nitrogen and thawed just prior to loading into the NMR spectrometer. ^{1}H NMR spectra were recorded at regular intervals. Substrate consumption was monitored by integration of the internal methane proton of the alkene moiety. Concentrations were calculated over 3 half-lives using TMSS as an internal standard. Data was normalised against the initial substrate concentration [substrate]$_{t=0}$ so that:

$$C_t = \frac{[substrate]_t}{[substrate]_{t=0}}$$

Reaction rates were derived from the plot of $\ln(C_t)$ versus time by using linear trendlines generated by Microsoft Excel software. To obtain Arrhenius and Eyring plots, kinetic analyses were conducted at 4-5 different temperatures, each separated by approximately 5 K. Temperature calibration of the NMR spectrometer was carried out at a gas flow of 535 L.h^{-1} using 80% ethylene glycol in methanol and waiting 15 minutes for temperature equilibration. Thus the following equations were obtained:

Cooling power 5%: $T_{real} = 1.3568\ T_{displayed} - 104.7$

Absence of cooling: $T_{real} = 1.1293\ T_{displayed} - 38.6$

For later reactions using precatalyst **34** a new calibration gave:

Cooling power 5%: $T_{real} = 1.345\ T_{displayed} - 101.6$

For the determination of the order in catalyst, a C_6D_6 solution of the aminoalkene (0.56 M) with an internal TMSS standard at 0.16 M was prepared. For each reaction an approximate amount of precatalyst (2 mg, 4 mg, 6 mg, etc.) was then added to 0.5 mL of the substrate solution and the procedure outlined above repeated. The exact concentration of the precatalyst was measured by integration of the hexamethyldisilazide signal against the internal TMSS standard.

6.5.2 Calculation of standard errors for Eyring plots[287]

Standard errors $\sigma(\Delta H^{\ddagger})$ and $\sigma(\Delta S^{\ddagger})$ were calculated using the least squares method for linear regression outlined below (see e.g. the website *http://mathworld.wolfram.com/LeastSquaresFitting.html*):

$$x_i = \frac{1}{T_i} \qquad \bar{x} = \sum_{i=1}^{n} \frac{1}{T_i} \qquad y_i = \ln(\frac{k_i h}{k_B T_i}) \qquad \bar{y} = \sum_{i=1}^{n} \ln(\frac{k_i h}{k_B T_i})$$

The variance of x (σ^2_x) and y (σ^2_y) and the covariance of x and y ($\mathrm{cov}(x,y)$) are proportional to s_{xx}, s_{yy} and s_{xy} respectively:

$$s_{xx} = \sum_{i=1}^{n} (x_i - \bar{x})^2 \qquad\qquad s_{yy} = \sum_{i=1}^{n} (y_i - \bar{y})^2$$

$$s_{xy} = \sum_{i=1}^{n} (x_i - \bar{x})(y_i - \bar{y})$$

The estimator of the variance (s^2) can be expressed as:

$$s = \sqrt{\frac{s_{yy} - \dfrac{s_{xy}^2}{s_{xx}}}{n-2}}$$

The standard errors $\sigma(\Delta H^{\ddagger})$ and $\sigma(\Delta S^{\ddagger})$ are calculated as follows:

$$\sigma(\Delta H^{\ddagger}) = R \frac{s}{\sqrt{s_{xx}}} \qquad\qquad \sigma(\Delta S^{\ddagger}) = Rs \sqrt{\frac{1}{n} + \frac{\bar{x}^2}{s_{xx}}}$$

6.5.3 Derivation of hydroamination rate law
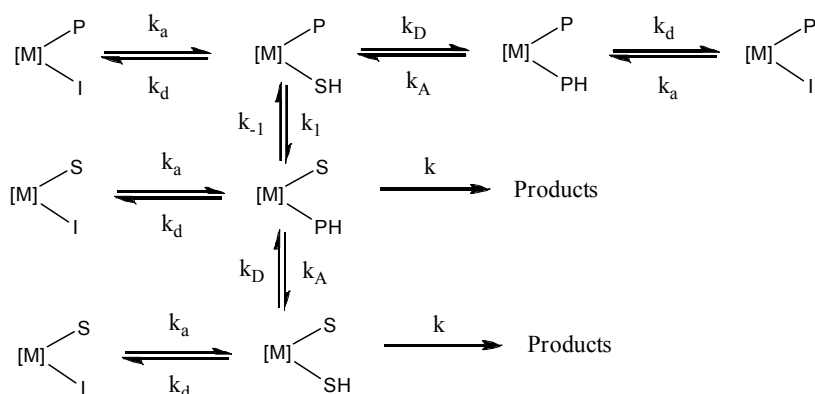
PH = product   SH = substrate   I = non-protic inhibitor e.g. THF

$$rate = k([MSPH] + [MSSH])$$

<u>Condition</u>: rapid pre-equilibria.

A) $k_a[MPI][SH] = k_d[MPSH][I]$

B) $k_a[MSI][PH] = k_d[MSPH][I]$

C) $k_a[MSI][SH] = k_d[MSSH][I]$

D) $k_a[MPI][PH] = k_d[MPPH][I]$

E) $k_D[MPSH][PH] = k_A[MPPH][SH]$

F) $k_D[MSSH][PH] = k_A[MSPH][SH]$

G) $k_1[MPSH] = k_{-1}[MSPH]$

Total catalyst concentration:

$$[cat]_0 = [MSSH] + [MSPH] + [MPSH] + [MPPH] + [MPI] + [MSI]$$

Initial substrate concentration: $[sub]_0 \approx [SH] + [PH]$

Reduced equilibrium constants: $K_S = \dfrac{k_D}{k_A}$ $K_I = \dfrac{k_d}{k_a}$ $K_E = \dfrac{k_{-1}}{k_1}$

172

F) $\quad [MSSH] = \dfrac{k_A}{k_D}[MSPH]\dfrac{[SH]}{[PH]} = \dfrac{1}{K_S}[MSPH]\dfrac{[SH]}{[PH]}$

G) $\quad [MPSH] = \dfrac{k_{-1}}{k_1}[MSPH] = K_E[MSPH]$

E) $\quad [MPPH] = \dfrac{k_D}{k_A}[MPSH]\dfrac{[PH]}{[SH]} = K_S[MPSH]\dfrac{[PH]}{[SH]} = K_S K_E[MSPH]\dfrac{[PH]}{[SH]}$

A) $\quad [MPI] = \dfrac{k_d}{k_a}[MPSH]\dfrac{[I]}{[SH]} = K_I K_E[MSPH]\dfrac{[I]}{[SH]}$

B) $\quad [MSI] = \dfrac{k_d}{k_a}[MSPH]\dfrac{[I]}{[PH]} = K_I[MSPH]\dfrac{[I]}{[PH]}$

$$[cat]_0 = [MSPH](1 + \dfrac{1}{K_S}\dfrac{[SH]}{[PH]} + K_E + K_S K_E\dfrac{[PH]}{[SH]} + K_I K_E\dfrac{[I]}{[SH]} + K_I\dfrac{[I]}{[PH]})$$

$$[cat]_0 = \dfrac{[MSPH]}{K_S[PH][SH]}\{K_S[PH][SH](1 + K_E) + [SH]^2 + K_E K_S^2[PH]^2$$

$$+ K_I K_S K_E[I][PH] + K_I K_S[I][SH]\}$$

$$[cat]_0 = \dfrac{[MSPH]}{K_S[PH][SH]}\{K_S[PH][SH](1 + K_E) + [SH]^2 + K_E K_S^2[PH]^2$$

$$+ K_I K_S[I](K_E[PH] + [SH])\}$$

<u>Hypotheses:</u>

- PH and SH probably have similar binding constants as adducts to the catalyst: $k_A = k_D \rightarrow K_S \approx 1$

$$[cat]_0 \approx \dfrac{[MSPH]}{[PH][SH]}\{[PH][SH](1 + K_E) + [SH]^2 + K_E[PH]^2 + K_I[I](K_E[PH] + [SH])\}$$

$$rate = k([MSPH] + [MSSH]) \approx k[MSPH](1 + \dfrac{[SH]}{[PH]}) = k\dfrac{[MSPH][sub]_0}{[PH]}$$

$$rate \approx \dfrac{k[cat]_0[sub]_0[SH]}{[PH][SH](1 + K_E) + [SH]^2 + K_E[PH]^2 + K_I[I](K_E[PH] + [SH])}$$

- substrate and product amine/amide exchange is roughly equal in both directions
  → $K_E \approx 1$

$$rate \approx \frac{k[cat]_0[sub]_0[SH]}{[PH][SH](1+1)+[SH]^2+[PH]^2+K_I[I]([PH]+[SH])}$$

$$rate \approx \frac{k[cat]_0[sub]_0[SH]}{[sub]_0^2+K_I[I][sub]_0}$$

$$rate = \frac{k[cat]_0[SH]}{[sub]_0+K_I[I]}$$

## 6.6 Study of the intramolecular hydroamination of aminoalkenes

6.6.1 Synthesis of alkaline earth precatalysts

Synthesis of [{(Dipp)NC(Me)CHC(Me)N(Dipp)}Ca{N(SiMe₃)₂}(THF)] (2)[36]
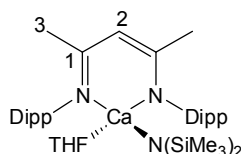
Ligand precursor [(Dipp)NC(Me)CHC(Me)NH(Dipp)] (Dipp = 2,6-di-*iso*-propylphenyl) (3.00 g, 7.17 mmol), calcium iodide (2.11 g, 7.17 mmol) and [KN(SiMe₃)₂] (2.86 g, 14.3 mmol) were stirred over night in a sealed Schlenk flask in 60 mL of THF under argon. The solvent was removed *in vacuo* and the crude product was extracted with 100 mL of hexane. The mixture was stirred for another hour prior to canula filtration away from insoluble KI and concentration until incipient crystallisation. A large crop of colourless crystals was obtained after 1 day at -20 °C (3.4 g, 4.9 mmol, 69%). ^{1}H NMR ppm (C₆D₆): 7.14-7.20 (m, 6H, Ar-*H*), 4.85 (s, 1H, *H-2*), 3.40 (m, 4H, THF), 3.24 (sept, 4H, ^{i}Pr-C*H*Me₂, ^3J = 6.9 Hz), 1.69 (s, 6H, *H-3*), 1.36 (d, 12H, ^{i}Pr-C*H₃*, ^3J = 6.9 Hz), 1.26 (d, 12H, ^{i}Pr-C*H₃*, ^3J = 6.9 Hz), 1.15 (m, 4H, THF), 0.17 (s, 18H, Si(C*H₃*)₃). ^{13}C{^{1}H} NMR ppm (C₆D₆): 166.5 (C-1), 147.4 (*i*-Ar-*C*), 141.5 (*o*-Ar-*C*), 124.7 (*p*-Ar-*C*), 124.1 (*m*-Ar-*C*), 94.2 (C-2), 69.3 (THF), 28.5 (^{i}Pr-*C*HMe₂), 25.5 + 24.9 (^{i}Pr-*C*H₃), 25.3 (THF), 25.0 (C-3), 6.0 (Si(*C*H₃)₃).

Synthesis of [{(Dipp)NC(Me)CHC(Me)N(Dipp)}Ca{N(SiMe₃)₂}] (33)[21, 36, 141]
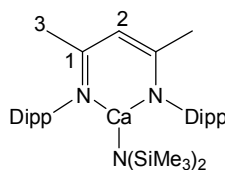
Same procedure as above in Et₂O instead of THF: ligand precursor (1.00 g, 2.39 mmol), calcium iodide (0.70 g, 2.39 mmol) and [KN(SiMe₃)₂] (0.95 g, 4.78 mmol). The isolated ether adduct was dried at 40 °C *in vacuo* for a day to remove the ether. Subsequent recrystallisation in hexane at -20 °C yielded colourless crystals (0.92 g, 1.5 mmol, 62%). ¹H NMR ppm (C₆D₆): 7.13-7.18 (m, 6H, Ar-*H*), 4.77 (s, 1H, *H-2*), 3.12 (sept, 4H, ⁱPr-C*H*Me₂, ³*J* = 6.9 Hz), 1.69 (s, 6H, *H-3*), 1.36 (d, 12H, ⁱPr-C*H₃*, ³*J* = 6.9 Hz), 1.22 (d, 12H, ⁱPr-C*H₃*, ³*J* = 6.9 Hz), 0.05 (s, 18H, Si(C*H₃*)₃). ¹³C{¹H} NMR ppm (C₆D₆): 166.9 (C-1), 145.3 (*i*-Ar-*C*), 141.1 (*o*-Ar-*C*), 125.2 (*p*-Ar-*C*), 124.3 (*m*-Ar-*C*), 91.9 (C-2), 29.9 (ⁱPr-*C*HMe₂), 25.4 + 24.4 (ⁱPr-*C*H₃), 24.7 (C-3), 5.1 (Si(C*H₃*)₃).

Synthesis of [{(Dipp)NC(Me)CHC(Me)N(Dipp)}Sr{N(SiMe₃)₂}(THF)][39]
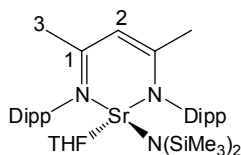
Ligand precursor [(Dipp)NC(Me)CHC(Me)NH(Dipp)] (1.00 g, 2.39 mmol) and [KN(SiMe₃)₂] (1.00 g, 4.77 mmol) were stirred for 5 hours in a sealed Schlenk flask in 30 mL of THF under argon. The solution was added *via* canula to a second Schlenk flask containing a slurry of strontium iodide (0.81 g, 2.39 mmol) in 50 mL of THF. The solution was stirred at room temperature overnight under argon. The solvent was removed *in vacuo* and the crude product extracted with 100 mL of hexane. The mixture was stirred for another hour and allowed to settle prior to canula filtration away from insoluble KI and removal of the solvent. Subsequent recrystallisation in 3 mL of toluene at -20 °C yielded a crop of yellow crystals (1.04 g, 1.4 mmol, 59%). ¹H NMR ppm (C₆D₆): 7.09-7.16 (m, 6H, Ar-*H*), 4.78 (s, 1H, *H-2*), 3.31 (m, 4H, THF), 3.18 (sept, 4H, ⁱPr-C*H*Me₂, ³*J* = 6.9 Hz), 1.69 (s, 6H, *H-3*), 1.32 (d, 12H, ⁱPr-C*H₃*, ³*J* = 6.9 Hz), 1.24 (d, 12H, ⁱPr-C*H₃*, ³*J* = 6.9 Hz), 1.09 (m, 4H, THF), 0.15 (s, 18H, Si(C*H₃*)₃). ¹³C{¹H} NMR ppm (C₆D₆): 165.1 (C-1), 147.4 (*i*-Ar-*C*), 141.0 (*o*-Ar-*C*), 124.3 (*p*-Ar-*C*), 124.1 (*m*-Ar-
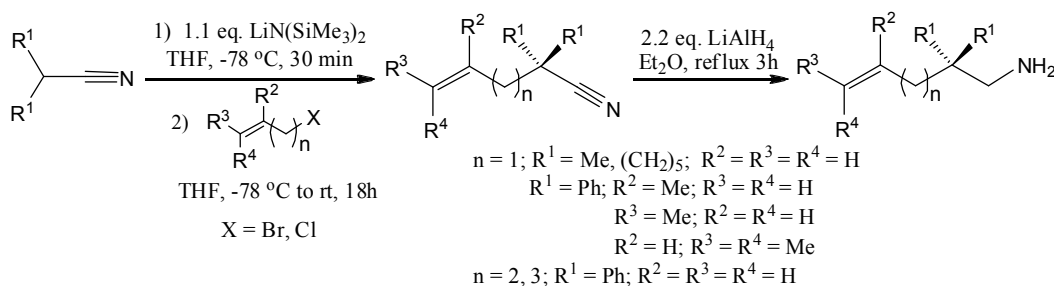
C), 92.6 (C-2), 69.0 (THF), 28.5 (^{i}Pr-*C*HMe$_2$), 25.5 + 25.1 (^{i}Pr-*C*H$_3$), 24.9 (THF), 24.5 (C-3), 5.9 (Si(*C*H$_3$)$_3$).

Synthesis of [Mg{CH(SiMe$_3$)$_2$}$_2$(THF)$_2$] (37a)

THF (30 mL), precooled to -78 °C, was added to a solid mixture of MgI$_2$ (0.70 g, 2.52 mmol) and [K{CH(SiMe$_3$)$_2$}] (1.0 g, 5.04 mmol). The reaction mixture was allowed to warm to room temperature and stirred for 10 hours, at which point all volatiles were removed *in vacuo* to leave a colourless solid. Extraction into hexane, filtration, concentration of the filtrate and storage at -30 °C provided compound **37d** as a colourless crystalline solid (0.60 g, 41%). ^{1}H NMR ppm (C$_6$D$_6$): 3.49 (8H, m, THF), 1.18 (8H, m, THF), 0.30 (36H, s, CH(Si*Me*$_3$)$_2$), -1.54 (2H, s, C*H*(SiMe$_3$)$_2$). Anal. Calc. for C$_{22}$H$_{54}$MgO$_2$Si$_4$ (487.3): C, 54.22; H, 11.17%. Found: C, 54.09; H, 11.07%.

6.6.2   Substrates and products of hydroamination studies

Synthesis of aminoalkenes: General Procedure[54]

n = 1; R^1 = Me, (CH$_2$)$_5$; R^2 = R^3 = R^4 = H
R^1 = Ph; R^2 = Me; R^3 = R^4 = H
R^3 = Me; R^2 = R^4 = H
R^2 = H; R^3 = R^4 = Me
n = 2, 3; R^1 = Ph; R^2 = R^3 = R^4 = H

[LiN(SiMe$_3$)$_2$] was generated *in situ* by addition of a 2.5 M solution of *n*-BuLi in hexanes to a THF solution of hexamethyldisilazane at -78 °C under argon. After 30 minutes one equivalent of the nitrile was added *via* syringe. The yellow solution was stirred at -78 °C for 30 minutes. One equivalent of the bromo- or chloroalkene was then added *via* syringe and the mixture stirred at room temperature overnight. The solution was quenched with 150 mL of water at 0 °C and the organic phase extracted with 3 times 100 mL of Et$_2$O and dried over MgSO$_4$. The solvent was removed *in vacuo* yielding the crude substituted nitrile as a yellow oil. The crude oil was added *via* syringe to a suspension of 2.2 equivalents of LiAlH$_4$ in Et$_2$O at 0 °C under argon. After reflux

for 3 hours the solution was slowly quenched at -78 ºC with a 95:5 THF/water mixture. The solid inorganic residues were filtered on a Büchner funnel and washed with 3 x 100 mL of Et_2O. The filtrates were washed with 200 mL of water, dried over $MgSO_4$ and the solvent removed *in vacuo*, affording a light yellow oil which was either distilled at room pressure or *in vacuo*. The pure aminoalkene was dried for 3 hours over CaH_2 before being either redistilled or vacuum-transferred into a dry ampoule to be used in the glove box.

Synthesis of 1-amino-2,2-diphenyl-4-pentene
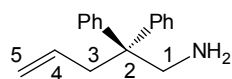
HN(SiMe₃)₂ (4.59 g, 28.5 mmol), 2.5 M solution of *n*-BuLi in hexanes (11.4 mL, 28.5 mmol), diphenylacetonitrile (5.00 g, 25.9 mmol), allyl bromide (2.25 mL, 25.9 mmol), $LiAlH_4$ (2.16 g, 56.9 mmol). The resulting aminoalkene was distilled *in vacuo* as a colourless oil (4.00 g, 16.8 mmol, 65%), b.p. 170 ºC at 0.2 mbar. ^1H NMR ppm (CDCl₃, 250 MHz) of the crude nitrile: 7.18-7.31 (m, 10H, Ph-*H*), 5.60 (ddt, 1H, *H-4*, ^3J = 7.0 Hz, $^3J_{cis}$ = 10.1 Hz, $^3J_{trans}$ = 17.1 Hz), 5.10 (dq, 1H, *H-5$_{trans}$*, ^2J = 1.4 Hz, $^3J_{trans}$ = 17.1 Hz, ^4J = 1.4 Hz), 5.07 (dq, 1H, *H-5$_{cis}$*, ^2J = 1.4 Hz, $^3J_{cis}$ = 10.1 Hz, ^4J = 1.4 Hz), 3.02 (d, 2H, *H-3*, ^3J = 7.0 Hz). ^1H NMR ppm (CDCl₃) of the aminoalkene: 7.10-7.27 (m, 10H, Ph-*H*), 5.34 (ddt, 1H, *H-4*, ^3J = 7.0 Hz, $^3J_{cis}$ = 10.0 Hz, $^3J_{trans}$ = 17.1 Hz), 4.98 (ddt, 1H, *H-5$_{trans}$*, ^2J = 2.3 Hz, $^3J_{trans}$ = 17.1 Hz, ^4J = 1.3 Hz), 4.94 (md, 1H, *H-5$_{cis}$*, $^3J_{cis}$ = 10.0 Hz), 3.28 (s, 2H, *H-1*), 2.88 (dd, 2H, *H-3*, ^3J = 7.0 Hz, ^4J = 1.3 Hz), 0.94 (broad s, 2H, N*H₂*). $^{13}C\{^1H\}$ NMR ppm (CDCl₃): 146.6 (*i*-Ph-*C*), 135.0 (C-4), 128.5 (*m*-Ph-*C*), 128.2 (*o*-Ph-*C*), 126.5 (*p*-Ph-*C*), 118.1 (C-5), 51.8 (C-2), 49.0 (C-1), 41.5 (C-3).
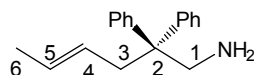
Synthesis of 1-amino-2,2-diphenyl-4-methyl-4-pentene
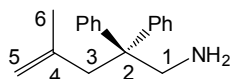
HN(SiMe₃)₂ (4.59 g, 28.5 mmol), 2.5 M solution of *n*-BuLi in hexanes (11.4 mL, 28.5 mmol), diphenylacetonitrile (5.00 g, 25.9 mmol), 3-chloro-2-methyl-1-propene (2.6 mL, 25.9 mmol), $LiAlH_4$ (2.16 g, 56.9 mmol). The resulting aminoalkene was distilled *in vacuo* as a colourless oil (4.31 g, 17.1 mmol, 66%), b.p. 170 ºC at 0.3 mbar. ^1H NMR ppm (CDCl₃, 250 MHz) of the crude nitrile: 7.18-7.33 (m, 10H, Ph-*H*), 4.82 (s, 1H, *H-5$_{trans}$*), 4.66 (s, 1H, *H-5$_{cis}$*), 3.02 (s, 2H, *H-3*), 1.41 (s, 3H, *H-6*). ^1H NMR ppm (CDCl₃)

of the aminoalkene: 7.06-7.20 (m, 10H, Ph-H), 4.72 (dd, 1H, H-5$_{trans}$, ^2J = 2.2 Hz, ^4J = 1.5 Hz), 4.50 (s, 1H, H-5$_{cis}$), 3.14 (s, 2H, H-2), 2.83 (s, 2H, H-3), 0.98 (s, 3H, H-6), 0.83 (broad s, 2H, NH_2). ^{13}C{^{1}H} NMR ppm (CDCl$_3$): 145.9 (i-Ph-C), 141.8 (C-4), 127.3 (m-Ph-C), 126.8 (o-Ph-C), 125.0 (p-Ph-C), 114.2 (C-5), 50.2 (C-2), 46.8 (C-1), 43.0 (C-3), 23.3 (C-6).

Synthesis of trans-1-amino-2,2-diphenyl-4-hexene

HN(SiMe$_3$)$_2$ (4.59 g, 28.5 mmol), 2.5 M solution of n-BuLi in hexanes (11.4 mL, 28.5 mmol), diphenylacetonitrile (5.00 g, 25.9 mmol), 3-bromo-1-propene (2.24 mL, 25.9 mmol), LiAlH$_4$ (2.16 g, 56.9 mmol). The resulting aminoalkene was distilled *in vacuo* as a colourless oil (2.35 g, 9.35 mmol, 36 %), b.p. 180 °C at 0.4 mbar. ^{1}H NMR ppm (CDCl$_3$) of the aminoalkene: 7.14-7.27 (m, 10H, Ph-H); 5.44 (dq, 1H, H-5, ^3J = 6.3 Hz, $^3J_{trans}$ = 21.5 Hz), 4.98-5.11 (m, 1H, H-4), 3.30 (s, 2H, H-1), 2.85 (d, 2H, H-3, ^3J = 7.3 Hz), 1.56 (d, 3H, H-6, ^3J = 6.3 Hz), 0.99 (broad s, 2H, NH_2). ^{13}C{^{1}H} NMR (CDCl$_3$): 146.4 (i-Ph-C), 128.1 (C-4), 128.0 (m-Ph-C), 127.7 (o-Ph-C), 126.4 (p-Ph-C), 125.6 (C-5), 51.5 (C-2), 48.4 (C-1), 39.8 (C-3), 17.8 (C-6).

Synthesis of 1-amino-5-methyl-2,2-diphenyl-4-hexene
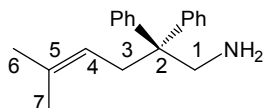
HN(SiMe$_3$)$_2$ (4.59 g, 28.5 mmol), 2.5 M solution of n-BuLi in hexanes (11.4 mL, 28.5 mmol), diphenylacetonitrile (5.00 g, 25.9 mmol), 3-bromo-1,1-dimethyl-1-propene (3.0 mL, 25.9 mmol), LiAlH$_4$ (2.16 g, 56.9 mmol). The resulting aminoalkene was distilled *in vacuo* as a colourless oil (4.50 g, 16.8 mmol, 65%), b.p. 150ºC at 0.2 mbar. ^{1}H NMR ppm (CDCl$_3$) of the aminoalkene: 7.10-7.26 (m, 10H, Ph-H), 4.78 (dt, 1H, H-4, ^3J = 7.1 Hz, $^4J_{trans}$ = 1.1 Hz), 3.24 (s, 2H, H-1), 2.77 (d, 2H, H-3, ^3J = 7.1 Hz), 1.53 (d, 3H, H-7, $^4J_{trans}$ = 1.1 Hz), 1.42 (s, 3H, H-6), 0.95 (broad s, 2H, NH_2). ^{13}C{^{1}H} NMR ppm (CDCl$_3$): 145.4 (i-Ph-C), 133.0 (C-4), 126.9 (m-Ph-C), 126.6 (o-Ph-C), 126.6 (p-Ph-C), 118.8 (C-5), 51.2 (C-2), 48.1 (C-1), 34.2 (C-3), 24.9 (C-7), 16.8 (C-6).

Synthesis of 1-amino-2,2-diphenyl-5-hexene
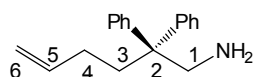
HN(SiMe$_3$)$_2$ (4.59 g, 28.5 mmol), 2.5 M solution of *n*-BuLi in hexanes (11.4 mL, 28.5 mmol), diphenylacetonitrile (5.00 g, 25.9 mmol), 4-bromo-1-butene (2.7 mL, 25.9 mmol), LiAlH$_4$ (2.16 g, 56.9 mmol). The resulting aminoalkene was distilled *in vacuo* as a colourless oil (4.01 g, 16.1 mmol, 62%), b.p. 150 ºC at 0.3 mbar. ^{1}H NMR ppm (CDCl$_3$, 250 MHz) of the crude nitrile: 7.27-7.44 (m, 10H, Ph-*H*), 5.83 (ddt, 1H, *H-5*, ^3J = 6.4 Hz, $^3J_{cis}$ = 10.2 Hz, $^3J_{trans}$ = 16.7 Hz), 5.06 (dq, 1H, *H-6$_{trans}$*, ^2J = 1.6 Hz, $^3J_{trans}$ = 16.7 Hz, ^4J = 1.6 Hz), 5.02 (dq, 1H, *H-6$_{cis}$*, ^2J = 1.6 Hz, $^3J_{cis}$ = 10.2 Hz, ^4J = 1.6 Hz), 2.46-2.52 (m, 2H, *H-4*), 2.16-2.25 (m, 2H, *H-3*). ^{1}H NMR ppm (CDCl$_3$) of the aminoalkene: 7.07-7.22 (m, 10H, Ph-*H*), 5.68 (ddt, 1H, *H-5*, ^3J 6.5 = Hz, $^3J_{cis}$ = 10.2 Hz, $^3J_{trans}$ = 16.8 Hz), 4.86 (dq, 1H, *H-6$_{trans}$*, ^2J = 1.6 Hz, $^3J_{trans}$ = 16.8 Hz, ^4J = 1.6 Hz), 4.81 (md, 1H, *H-6$_{cis}$*, $^3J_{cis}$ = 10.2 Hz), 3.24 (s, 2H, *H-1*), 2.08-2.13 (m, 2H, *H-4*), 1.62-1.70 (m, 2H, *H-3*), 0.84 (broad s, 2H, N*H$_2$*). ^{13}C{^{1}H} NMR ppm (CDCl$_3$): 146.7 (*i*-Ph-*C*), 139.2 (C-5), 128.7 (*m*-Ph-*C*), 128.5 (*o*-Ph-*C*), 126.5 (*p*-Ph-*C*), 114.8 (C-6), 52.2 (C-2), 49.5 (C-1), 36.2 (C-4), 29.0 (C-3).

Synthesis of 1-amino-2,2-diphenyl-6-heptene.
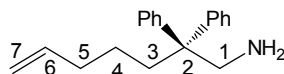
HN(SiMe$_3$)$_2$ (3.00 g, 18.6 mmol), 2.5 M solution of *n*-BuLi in hexanes (7.5 mL, 18.6 mmol), diphenylacetonitrile (3.27 g, 16.9 mmol), 5-bromo-1-pentene (2.0 mL, 16.9 mmol), LiAlH$_4$ (1.41 g, 37.2 mmol). The resulting aminoalkene was distilled *in vacuo* as a colourless oil (2.14 g, 8.1 mmol, 48%), b.p. 150 ºC at 0.2 mbar. ^{1}H NMR ppm (CDCl$_3$, 250 MHz) of the crude nitrile: 7.15-7.31 (m, 10H, Ph-*H*), 5.64 (ddt, 1H, *H-6*, ^3J = 6.7 Hz, $^3J_{cis}$ = 10.2 Hz, $^3J_{trans}$ = 16.9 Hz), 4.91 (dq, 1H, *H-7$_{trans}$*, ^2J = 1.6 Hz, $^3J_{trans}$ = 16.9 Hz, ^4J = 1.6 Hz), 5.07 (md, 1H, *H-7$_{cis}$*, $^3J_{cis}$ = 10.1 Hz), 2.69 (td, 2H, *H-5*, ^3J = 6.7 Hz, ^3J = 4.5 Hz), 2.02 (apparent q, 2H, *H-3*, ^3J = 7.1 Hz), 1.44 (apparent tq, 2H, *H-4*, ^3J = 4.5 Hz). ^{1}H NMR ppm (CDCl$_3$) of the aminoalkene: 7.12-7.29 (m, 10H, Ph-*H*), 5.68 (ddt, 1H, *H-6*, ^3J = 6.7 Hz, $^3J_{cis}$ = 10.2 Hz, $^3J_{trans}$ = 16.9 Hz), 4.92 (dq, 1H, *H-7$_{trans}$*, ^2J = 1.6 Hz, $^3J_{trans}$ = 16.9 Hz, ^4J = 1.6 Hz), 4.88 (md, 1H, *H-7$_{cis}$*, $^3J_{cis}$ = 10.0 Hz), 3.29 (s, 2H, *H-1*), 2.07 (dt, 2H, *H-5*, ^3J = 6.7 Hz, ^3J = 4.5 Hz), 1.98 (apparent q, 2H, *H-3*, ^3J = 4.5 Hz), 1.08 (apparent tq, 2H, *H-4*, ^3J = 4.5 Hz), 0.86 (broad s, 2H, N*H$_2$*). ^{13}C{^{1}H} NMR

ppm (CDCl$_3$): 147.0 (*i*-Ph-*C*), 139.0 (C-6), 128.7 (*m*-Ph-*C*), 128.4 (*o*-Ph-*C*), 126.4 (*p*-Ph-*C*), 115.1 (C-7), 52.2 (C-2), 49.5 (C-1), 36.3 (C-5), 34.6 (C-3), 23.8 (C-4) .

Synthesis of 1-amino-2,2-dimethyl-4-pentene
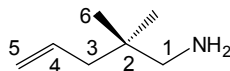
HN(SiMe$_3$)$_2$ (3.93 g, 24.4 mmol), 2.5 M solution of *n*-BuLi in hexanes (9.8 mL, 24.4 mmol), isobutyronitrile (2.0 mL, 22.3 mmol), allyl bromide (1.9 mL, 22.3 mmol), LiAlH$_4$ (2.11 g, 55.7 mmol). The resulting aminoalkene was distilled at room pressure as a colourless oil (1.40 g, 12.5 mmol, 56%), b.p. 130 ºC. ^{1}H NMR ppm (CDCl$_3$, 250 MHz) of the crude nitrile: 5.75 (ddt, 1H, *H-4*, ^3J = 7.3 Hz, $^3J_{cis}$ = 10.3 Hz, $^3J_{trans}$ = 16.9 Hz), 5.10 (md, 1H, *H-5$_{cis}$*, $^3J_{cis}$ = 10.3 Hz), 5.07 (dq, 1H, *H-5$_{trans}$*, ^2J = 1.5 Hz, $^3J_{cis}$ = 16.9 Hz, ^4J = 1.5 Hz), 2.16 (md, 2H, *H-3*, ^3J = 7.3 Hz), 1.22 (s, 6H, *H-6*). ^{1}H NMR ppm (CDCl$_3$) of the aminoalkene: 5.67 (ddt, 1H, *H-4*, ^3J = 7.5 Hz, $^3J_{cis}$ = 11.7 Hz, $^3J_{trans}$ = 16.0 Hz), 4.91 (md, 1H, *H-5$_{cis}$*, $^3J_{cis}$ = 11.7 Hz), 4.89 (md, 1H, *H-5$_{trans}$*, $^3J_{trans}$ = 16.0 Hz), 2.31 (s, 2H, *H-1*), 2.88 (md, 2H, *H-3*, ^3J = 7.5 Hz), 1.69 (broad s, 2H, N*H$_2$*), 0.72 (s, 6H, *H-6*). ^{13}C{^{1}H} NMR ppm (CDCl$_3$): 133.8 (C-4), 115.6 (C-5), 51.2 (C-2), 42.6 (C-1), 33.5 (C-3), 23.2 (C-6).

Synthesis of (1-allylcyclohexyl)methylamine
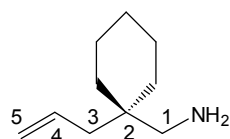
HN(SiMe$_3$)$_2$ (4.59 g, 28.5 mmol), 2.5 M solution of *n*-BuLi in hexanes (11.4 mL, 28.5 mmol), cyclohexanecarbonitrile (3.0 mL, 25.9 mmol), allyl bromide (2.3 mL, 25.9 mmol), LiAlH$_4$ (2.16 g, 56.9 mmol). The resulting aminoalkene was distilled *in vacuo* as a colourless oil (2.51 g, 16.3 mmol, 63%), b.p. 75 ºC at 0.3 mbar. ^{1}H NMR ppm (CDCl$_3$, 298 K, 250 MHz) of the crude nitrile: 5.88 (ddt, 1H, *H-4*, ^3J = 7.4 Hz, $^3J_{cis}$ = 10.3 Hz, $^3J_{trans}$ = 16.8 Hz), 5.19 (md, 1H, *H-5$_{cis}$*, $^3J_{cis}$ = 10.3 Hz), 5.16 (dq, 1H, *H-5$_{trans}$*, ^2J = 1.5 Hz, $^3J_{cis}$ = 16.8 Hz, ^4J = 1.5 Hz), 2.16 (md, 2H, *H-3*, ^3J = 7.4 Hz), 1.90-1.98 (m, 2H, Cy-*H*), 1.51-1.79 (m, 6H, Cy-*H*), 1.18-1.27 (m, 2H, Cy-*H*). ^{1}H NMR ppm (CDCl$_3$) of the aminoalkene: 5.75 (ddt, 1H, *H-4*, ^3J = 7.5 Hz, $^3J_{cis}$ = 10.8 Hz, $^3J_{trans}$ = 16.4 Hz), 5.00 (md, 1H, *H-5$_{cis}$*, $^3J_{cis}$ = 10.8 Hz), 4.99 (md, 1H, *H-5$_{trans}$*, $^3J_{trans}$ = 16.8 Hz), 2.46 (s, 2H, *H-1*), 2.01 (md, 2H, *H-3*, ^3J = 7.5 Hz), 1.98-1.39 (m, 10H, Cy-*H*), 1.13 (broad s, 2H,

N*H₂*). ¹³C{¹H} NMR ppm (CDCl₃): 135.4 (C-4), 117.2 (C-5), 49.2 (*i*-Cy-*C*), 40.2 (C-1), 37.7 (*o*-Cy-*C*), 33.6 (C-3), 26.8 (*m*-Cy-*C*), 22.1 (*p*-Cy-*C*).

*Synthesis of (1-allylcyclohexyl)methylamine-*d₂
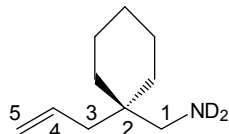
(1-allylcyclohexyl)methylamine (1 g, 6.53 mmol) was stirred in a 1:1 mixture of methanol-*d*/D₂O under argon for a week. After extraction with Et₂O and drying over MgSO4 the solvent was removed *in vacuo*. The resulting crude oil was distilled *in vacuo* yielding a colourless oil (0.89 g, 5.75 mmol, 88%), b.p. 75 °C at 0.3 mbar.

Synthesis of 2-amino-5-hexene
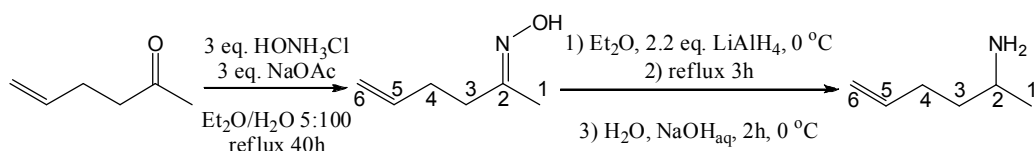
5-hexene-2-one (5 mL, 43.3 mmol), hydroxylamine hydrochloride (9.02 g, 130 mmol) and sodium acetate (10.66 g, 130 mmol) were dissolved in 500 mL of water and 20 mL of Et₂O. The mixture was refluxed for 40h, then extracted into CH₂Cl₂. The organic phase was dried over MgSO₄ and solvent removed *in vacuo*. The crude oil was further distilled *in vacuo* (43 °C, 8.10⁻² mbar) to yield the oxime as a colourless oil (4.81 g, 4.25 mmol, 98%). Both the *(E)* and the *(Z)* isomer could be identified in the NMR in a 60:40 ratio respectively. ¹H NMR ppm (CDCl₃): 8.93 (broad s, 1H, O*H*), 5.74-5.90 (m, 1H, *H-5*), 5.07 (apparent qd, 0.4H, *(Z)-H-6ₜᵣₐₙₛ*, ²*J* = ⁴*J* = 1.7 Hz, ³*Jₜᵣₐₙₛ* = 17.1 Hz,), 5.04 (md, 0.6H, *(E)-H-6ₜᵣₐₙₛ* ³*Jₜᵣₐₙₛ* = 17.1 Hz,), 4.99 (md, 1H, *H-6ᶜⁱˢ*, ³*Jᶜⁱˢ* = 10.1 Hz), 2.47 (m, 0.8H, *(Z)-H-3*), 2.24-2.31 (m, 3.2H, *(E)-H-3 + H-4*), 1.89 (s, 1.8H, *(E)-H-1*), 1.87 (s, 1.2H, *(Z)-H-1*). ¹³C{¹H} NMR ppm (CDCl₃): 158.3 + 157.9 (C-2), 137.4 + 137.2 (C-5), 115.3 + 115.2 (C-6), 35.2 (*(E)*-C-4), 30.3 (*(E)*-C-3), 29.4 (*(Z)*-C-4), 27.9 (*(Z)*-C-3), 19.9 (*(Z)*-C-1), 13.5 (*(E)*-C-1). 5-hexene-2-one oxime (5.76 g, 50.9 mmol) was syringed into a Schlenk flask containing a slurry of LiAlH₄ (3.86 g, 101.8 mmol, 2.2 eq.) at 0 °C. The suspension was refluxed for 2h and allowed to cool to 0 °C before careful quenching with water and 5 mL of a 50% aqueous NaOH solution. The resulting suspension was

filtered and the solid washed with 3 x 10 mL Et$_2$O. The ether was distilled away from the filtrate. Atmospheric distillation at 100 °C yielded the amine as a colourless oil (1.20 g, 12.1 mmol, 24%). ^{1}H NMR ppm (CDCl$_3$): 5.82 (tdd, 1H, *H-5*, ^3J = 6.7 Hz, $^3J_{cis}$ = 10.1 Hz, $^3J_{trans}$ = 17.2 Hz), 5.03 (ddd, 1H, *H-6$_{trans}$*, ^2J = 2.1 Hz, $^3J_{trans}$ = 17.2 Hz, ^4J = 1.7 Hz), 4.95 (tdd, 1H, *H-6$_{cis}$*, ^2J = 2.1 Hz, $^3J_{cis}$ = 10.1 Hz, ^4J = 1.2 Hz), 2.90 (apparent sext, 1H, *H-2*, ^3J = 6.5 Hz), 2.10 (m, 1H, *H-4*), 1.41 (m, 1H, *H-3*), 1.25 (broad s, 2H, N*H$_2$*), 1.07 (d, 3H, *H-1*, ^3J = 6.2 Hz). ^{13}C{^{1}H} NMR ppm (C$_6$D$_6$): 139.5 (C-5), 115.9 (C-6), 47.8 (C-2), 41.0 (C-3), 28.7 (C-4), 23.9 (C-1).

Synthesis of 6-amino-1-pentene
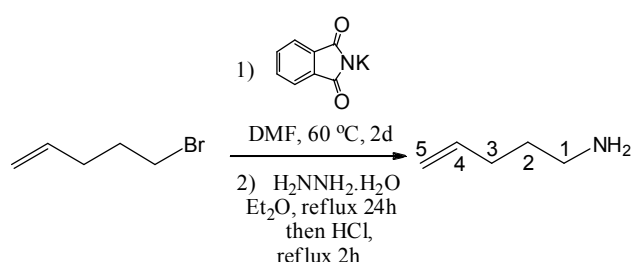
5-bromo-1-pentene (2 mL, 16.9 mmol) and potassium phtalimide (3.13g, 16.9 mmol) were stirred in 30 mL of DMF at 60 °C for 2 days. After filtration, addition of a 1:1 mixture of water and saturated sodium chloride solution, extraction with diethyl ether, drying over MgSO$_4$ and evaporation of all solvent under high vacuum a yellow oil was obtained. After 30 minutes at -20 °C, 6-phtalimide-1-pentene crystallised as an off-white solid (2.77 g, 12.9 mmol, 76%). ^{1}H NMR ppm (CDCl$_3$): 7.70 (dd, 2H, Ph-*H*, ^3J = 5.5 Hz, ^4J = 3.0 Hz), 7.59 (dd, 2H, Ph-*H*, ^3J = 5.5 Hz, ^4J = 3.0 Hz), 5.60 (tdd, 1H, *H-2*, ^3J = 7.3 Hz, $^3J_{cis}$ = 10.4 Hz, $^3J_{trans}$ = 16.7 Hz), 4.92 (ddd, 1H, *H-1$_{trans}$*, ^2J = 1.7 Hz, $^3J_{trans}$ = 16.7 Hz, ^4J = 1.7 Hz), 4.84 (ddd, 1H, *H-1$_{cis}$*, ^2J = 1.7 Hz, $^3J_{cis}$ = 10.4 Hz, ^4J = 4.8 Hz), 3.56 (t, 2H, *H-5*, ^3J = 7.3 Hz), 1.97 (m, 2H, *H-3*), 1.66 (m, 2H, *H-4*). ^{13}C{^{1}H} NMR ppm (CDCl$_3$): 168.0 (*C*=O), 137.0 (C-4), 133.6 (Ph-*C*), 131.8 (Ph-*C*), 122.8 (Ph-*C*), 114.9 (C-5), 37.2 (C-1), 30.6 (C-3), 27.3 (C-2). 6-phthalimide1-pentene (2.77g, 12.9 mmol) and hydrazine monohydrate (0.66 g, 32.3 mmol) were refluxed in ethanol for 24h. HCl 36% in water (15 mL) was added dropwise and the mixture refluxed for another 2h. After filtration, the solvent was removed from the filtrate to yield the hydrochloride salt as a crystalline solid. The crude solid was dissolved in water, basified with NaOH and extracted with Et$_2$O. Distillation of the ether at atmospheric pressure yielded 6-amino-1-pentene as a crude yellow oil which was distilled at atmospheric pressure at 100 °C (220 mg, 2.58 mmol, 20 %). ^{1}H NMR ppm (CDCl$_3$): 5.80 (ddd, 1H,

H-4, ^3J = 6.9 Hz, $^3J_{cis}$ = 12.1 Hz, $^3J_{trans}$ = 17.2 Hz), 5.01 (d, 1H, $^3J_{trans}$ = 17.2 Hz), 4.95 (d, 1H, $^3J_{cis}$ = 12.1 Hz), 2.70 (t, 2H, *H-1*, ^3J = 7.0 Hz), 2.13 (dt, 2H, *H-3*, ^3J = 7.2, 6.8, Hz), 1.54 (tt, 2H, *H-2*, ^3J = 7.2, 7.0 Hz), 1.20 (s, 2H, N*H*). $^{13}C\{^1H\}$ NMR (C_6D_6): 139.2 (C-4), 114.9 (C-5), 42.0 (C-1), 33.6 (C-3), 29.8 (C-2).

Synthesis of N-allyl-6-amino-1-pentene
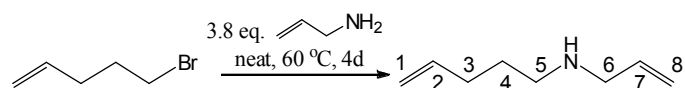
5-bromo-1-pentene (1.25 mL, 10.5 mmol) and an excess of allylamine (3 mL, 39.9 mmol) was stirred in a sealed ampoule under argon at 60 °C for 4 days. After addition of water, extraction with diethyl ether, drying over magnesium sulphate and evaporation of the solvent and the excess allylamine, the crude product was dried over CaH_2 and vacuum transferred into a sealed ampoule, affording a colourless oil (0.89 g, 7.11 mmol, 68%).^1H NMR ppm (CDCl$_3$): 5.73-5.98 (m, 2H, *H-2/7*), 5.09 (md, 1H, *H-1/8$_{trans}$*, $^3J_{trans}$ = 17.5 Hz), 5.00 (md, 1H, *H-1/8$_{cis}$*, $^3J_{cis}$ = 10.2 Hz), 4.94 (md, 1H, *H-1/8$_{trans}$*, $^3J_{trans}$ = 17.2 Hz), 4.88 (md, 1H, *H-1/8$_{cis}$*, $^3J_{cis}$ = 10.0 Hz), 3.24 (dt, 2H, *H-6*, ^3J = 6.0 Hz, ^4J = 1.3 Hz), 2.62 (t, 2H, *H-5*, ^3J = 7.2 Hz), 2.00 (m, 2H, *H-3*), 1.52 (m, 2H, *H-4*), 1.26 (broad s, 1H, N*H*). $^{13}C\{^1H\}$ NMR ppm (CDCl$_3$): 138.4 (C-2/7), 137.0 (C-2/7), 115.6 (C-1/8), 114.5 (C-1/8), 52.4 (C-6), 48.8 (C-5), 31.5 (C-3), 29.2 (C-4).

*Synthesis of N-benzyl-(1-allylcyclohexyl)methylamine*
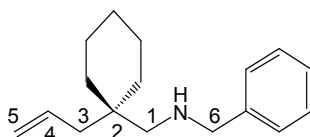
(1-allylcyclohexyl)methylamine (1 g, 6.53 mmol) and a slight excess of benzaldehyde (0.77 g, 7.26 mmol) were stirred at room temperature for 5h. An excess of NaBH$_4$ (0.41 g, 10.8 mmol) was added and the mixture stirred overnight. After treating with water and 20 mL of a 1M aqueous solution of NaOH the reaction mixture was extracted twice with CH$_2$Cl$_2$, the combined organic fractions dried over MgSO$_4$ and the solvent removed *in vacuo*. Distillation *in vacuo* yielded the desired aminoalkene as a colourless oil (1.08 g, 4.44 mmol, 68 %). ^1H NMR ppm (CDCl$_3$): 7.19-7.32 (m, 5H, Ph-*H*), 5.79 (tdd, 1H, *H-4*, ^3J = 7.6, $^3J_{cis}$ = 10.0, $^3J_{trans}$ = 16.9 Hz), 4.95-5.02 (m, 2H, *H-5*), 3.77 (s, 2H, *H-6*), 2.41 (s, 2H, *H-1*), 2.11-2.13 (m, 2H, *H-3*), 1.28-1.41 (m, 10H, Cy-*H*), 1.13 (broad s, 1H, N*H*). $^{13}C\{^1H\}$ NMR ppm (CDCl$_3$): 141.3 (*i*-Ph-*C*), 135.6 (C-4), 128.6 (m-

Ph-*C*), 128.2 (*o*-Ph-*C*), 126.9 (*p*-Ph-*C*), 116.9 (C-5), 56.1 (C-6), 55.1 (C-1), 40.9 (C-3), 36.9 (Cy-*C*), 34.2 (C-2), 26.8 (Cy-*C*), 21.8 (Cy-*C*).

### 6.6.3 Synthesis of cyclised amines: General Procedure

All NMR spectra of cyclised amines were recorded from *in situ* NMR scale catalytic hydroamination/cyclisation reactions of the corresponding aminoalkene with the most appropriate group 2 catalyst.

Synthesis of 2-methyl-4,4-dimethylpyrrolidine
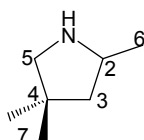
^{1}H NMR ppm (C$_6$D$_6$): 3.08 (m, 1H, *H-2*), 2.62 (dd, 1H, *H-5*, ^2J = 10.0 Hz, ^3J = 5.4 Hz), 2.47 (dd, 1H, *H-5*, ^2J = 10.0, ^3J = 7.4 Hz), 1.48 (dd, 1H, *H-3*, ^2J = 12.2 Hz, ^3J = 6.7 Hz), 1.74 (broad s, 1H, NH), 1.04 (d, 3H, *H-6*, ^3J = 6.2 Hz), 0.97 + 0.92 (two s, 3H each, *H-7*), 0.94 (m, 1H, *H-3*). ^{13}C{^{1}H} NMR ppm (C$_6$D$_6$): 56.8 (C-5), 55.0 (C-2), 47.1 (C-3), 39.3 (C-4), 27.2 (C-7), 18.8 (C-6).

*Synthesis of 2-methyl-4,4-diphenylpyrrolidine*
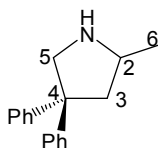
^{1}H NMR ppm (C$_6$D$_6$): 6.96-7.20 (m, 10H, Ph-*H*), 3.50 + 3.42 (two d, 1H each, *H-5*, ^2J = 11.1 Hz), 3.18 (m, 1H, *H-2*), 2.39 (ddd, 1H, *H-3*, ^2J = 12.6 Hz, ^3J = 6.8 Hz, ^4J = 0.8 Hz), 1.82 (dd, 1H, *H-3*, ^2J = 12.6 Hz, ^3J = 8.5 Hz), 1.40 (broad s, 1H, N*H*), 0.99 (d, 3H, *H-6*, ^3J = 6.4 Hz). ^{13}C{^{1}H} NMR ppm (C$_6$D$_6$): 148.4 + 147.9 (i-Ph-*C*), 128.6 + 128.5 (*m*-Ph-*C*), 127.5 + 127.4 (*o*-Ph-*C*), 126.2 + 126.1 (*p*-Ph-*C*), 58.7 (C-5), 57.3 (C-4), 53.5 (C-2), 47.4 (C-3), 22.5 (C-6).

*Synthesis of 2-methyl-4,4-cyclohexylpyrrolidine*
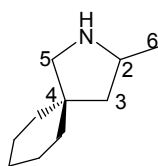
^{1}H NMR ppm (C$_6$D$_6$): 3.01 (m, 1H, *H-2*), 2.75 (dd, 1H, *H-5*, ^2J = 10.4 Hz, ^3J = 4.9 Hz), 2.52 (dd, 1H, *H-5*, ^2J = 10.4 Hz, ^3J = 7.8 Hz), 1.55 (dd, 1H, *H-3*, ^2J = 12.4 Hz, ^3J = 6.7 Hz), 1.23-1.37 (m, 10H, Cy-*H*), 1.17 (broad s, 1H, N*H*), 1.05 (d, 3H, *H-6*, ^3J = 6.2 Hz), 0.87 (dd, 1H, *H-3*, ^2J = 12.4 Hz, ^3J = 9.0 Hz) . ^{13}C{^{1}H} NMR ppm (C$_6$D$_6$): 59.8 (C-5), 54.3 (C-2), 47.9 (C-3), 44.0 (C-4), 39.0 (Cy-*C*), 37.6(Cy-*C*), 26.5 (Cy-*C*), 24.3 (Cy-*C*), 24.1 (Cy-*C*), 22.0 (C-6).

Synthesis of N-*benzyl-2-methyl-4,4-cyclohexylpyrrolidine*
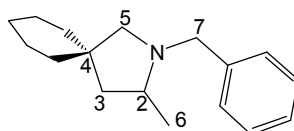
^{1}H NMR ppm (d$_8$-tol): 7.30 (d, 2H, *o*-Ph-*H*, ^3J = 7.3 Hz), 7.16 (t, 2H, *m*-Ph-*H*, ^3J = 7.3 Hz), 7.07 (d, 1H, *p*-Ph-*H*, ^3J = 7.3 Hz), 3.90 (d, 1H, *H-7*, ^2J = 13.5 Hz) 2.90 (d, 1H, *H-7*, ^2J = 13.5 Hz) , 2.76 (d, 1H, *H-5*, ^2J = 9.1 Hz), 2.35 (m, 1H, *H-2*), 1.73 (d, 1H, *H-5*, ^2J = 9.1 Hz), 1.61 (dd, 1H, *H-3*, ^2J = 12.2 Hz, ^3J = 7.2 Hz), 1.21-1.35 (m, 10H, Cy-*H*), 1.20 (dd, 1H, *H-3*, ^2J = 12.2 Hz, ^3J = 9.0 Hz), 1.06 (d, 3H, *H-6*, ^3J = 5.8 Hz) . ^{13}C{^{1}H} NMR ppm (d$_8$-tol): 140.9 (*i*-Ph-*C*), 128.6 (*o*-Ph-*C*), 128.3 (*m*-Ph-*C*), 126.7 (*p*-Ph-*C*), 59.4 (C-5), 58.3 (C-4), 39.5 (C-2), 38.6 (C-7), 26.4 (C-3), 25.1 (Cy-*C*), 24.0 (Cy-*C*), 23.7 (Cy-*C*), 19.7 (C-6).

Synthesis of 2,2-dimethyl-4,4-diphenylpyrrolidine
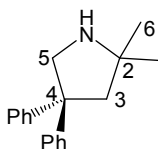
^{1}H NMR ppm (C$_6$D$_6$): 6.96-7.22 (m, 10H, Ph), 3.53 (d, 2H, *H-5*, ^3J = 7.7 Hz), 2.34 (s, 2H, *H-3*), 1.28 (t, 1H, N*H*, ^3J = 7.7 Hz), 1.03 (s, 6H, *H-6*). ^{13}C{^{1}H} NMR ppm (C$_6$D$_6$): 148.6 (i-Ph-*C*), 128.5 (*m*-Ph-*C*), 127.5 (*o*-Ph-*C*), 126.0 (*p*-Ph-*C*), 59.2 (C-5), 58.3 (C-4), 58.0 (C-2), 52.7 (C-3), 31.0 (C-6).

Synthesis of 2-ethyl-4,4-diphenylpyrrolidine
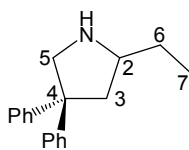
^{1}H NMR ppm (C$_6$D$_6$): 6.98-7.19 (m, 10H, Ph-*H*), 3.47 (ddd, 1H, *H-5*, ^2J = 10.9 Hz, ^3J = 6.3 Hz, ^4J = 1.4 Hz), 3.26 (dd, 1H, *H-5*, ^2J = 10.9 Hz, ^3J = 8.7 Hz), 2.93 (m, 1H, *H-2*), 2.48 (ddd, 1H, *H-3*, ^2J = 12.4 Hz, ^3J = 6.5 Hz, ^4J = 1.4 Hz), 1.82 (dd, 1H, *H-3*, ^2J = 12.4 Hz, ^3J = 9.1 Hz), 1.60 (broad s, 1H, N*H*), 1.46 (qm, 2H, *H-6*, ^3J = 7.4 Hz), 0.85 (t, 3H, *H-7*, ^3J = 7.4 Hz). ^{13}C{^{1}H} NMR ppm (C$_6$D$_6$): 148.7 (i-Ph-*C*), 129.8 (*m*-Ph-*C*), 127.5 (*o*-Ph-*C*), 126.2 (*p*-Ph-*C*), 59.6 (C-2), 58.3 (C-5), 56.9 (C-4), 45.5 (C-3), 17.9 (C-6), 11.7 (C-7).

Synthesis of 2-methyl-5,5-diphenylpiperidine
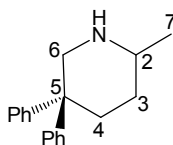
^{1}H NMR ppm (C$_6$D$_6$): 7.44 (dm, 2H, *p*-Ph-*H*), 6.99-7.22 (m, 8H, *o/m*-Ph-*H*), 3.77 (dt, 1H, *H-6*, ^2J = 12.9 Hz, ^3J = 3.0 Hz), 2.92 (dd, 1H, *H-6*, ^2J = 12.9 Hz, ^3J = 6.7 Hz), 2.54 (dtq, 1H, *H-2*, ^3J = 2.6 Hz, ^3J = 6.3 Hz, ^3J = 6.4 Hz), 2.47 (dq, 1H, *H-4*, ^2J = 13.1 Hz, ^3J = 3.2 Hz), 2.07 (dt, 1H, *H-4*, ^2J = 13.1 Hz, ^3J = 3.4 Hz), 1.40 (dq, 1H, *H-3*, ^2J = 13.0 Hz, ^3J = 3.0 Hz), 1.06-1.19 (ddt, 1H, *H-3*, ^2J = 13.0 Hz, ^3J = 11.0 Hz, ^3J = 3.2 Hz), 0.94 (broad s, 1H, N*H*), 0.91 (d, 3H, *H-7*, ^3J = 6.3 Hz). ^{13}C{^{1}H} NMR ppm (C$_6$D$_6$): 149.8 (i-Ph-*C*), 129.2 (*m*-Ph-*C*), 128.6 (*o*-Ph-*C*), 127.0 (*p*-Ph-*C*), 56.7 (C-6), 52.5 (C-2), 45.6 (C-5), 36.2 (C-4), 31.4 (C-3), 22.6 (C-7).

*Synthesis of 2-methyl-6,6-diphenylhexahydroazepine*
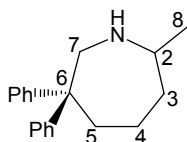
^{1}H NMR ppm (d$_8$-tol): 7.41 (dm, 2H, *p*-Ph), 7.10-7.28 (m, 8H, *o/m*-Ph), 3.81 (dd, 1H, *H-7*, ^2J = 14.5 Hz, ^3J = 7.2 Hz), 2.91 (dd, 1H, *H-7*, ^2J = 14.5 Hz, ^3J = 2.7 Hz), 2.58 (m, 1H, *H-6*), 2.55 (dd, 1H, *H-5*, ^2J = 14.4 Hz, ^3J = 8.0 Hz), 2.17-2.26 (m, 1H, *H-3*), 1.66-1.74 (m, 1H, *H-5*), 1.46-1.54 (m, 1H, *H-4*), 0.22-1.32 (m, 2H, *H-3 + H-4*), 1.10 (broad s, 1H, N*H*), 1.04 (d, 3H, *H-8*, ^3J = 6.3 Hz. ^{13}C{^{1}H} NMR ppm (d$_8$-tol): 151.9 + 149.2 (*i*-

Ph-*C*), 128.3 + 128.1 (*m*-Ph-*C*), 128.0 (*o*-Ph-*C*), 125.9 + 125.6 (*p*-Ph-*C*), 59.8 (C-1), 57.9 (C-2), 52.4 (C-6), 40.9 (C-5), 40.0 (C-3), 23.7 (C-4), 23.6 (C-8).

*Synthesis of 1-allyl-2-methylpyrrolidine*
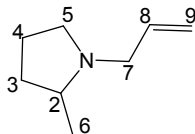
^{1}H NMR ppm (C$_6$D$_6$): 5.93 (dddd, 1H, *H-8*, $^3J_{trans}$ = 17.2 Hz, $^3J_{cis}$ = 10.2 Hz, ^3J = 7.6 Hz, ^3J = 4.8 Hz), 5.15 (ddt, 1H, *H-9*$_{trans}$, ^2J = 2.0 Hz, $^3J_{trans}$ = 17.2 Hz, ^4J = 1.8 Hz), 4.99 (ddt, 1H, *H-9*$_{cis}$, ^2J = 2.0 Hz, $^3J_{cis}$ = 10.2 Hz, ^4J = 0.9 Hz), 3.40 (ddt, 1H, *H-7*, ^2J = 13.5 Hz, ^3J = 4.8 Hz, ^4J = 1.8 Hz), 3.06 (m, 1H, *H-1*), 2.59 (ddt, *H-7*, ^2J = 13.5 Hz, ^3J = 7.6 Hz, ^4J = 0.9 Hz), 2.16 (m, 1H, *H-2*), 1.99 (m, 1H, *H-5*), 1.68-1.79 (m, 1H, *H-3*), 1.56-1.68 (m, 1H, *H-4*), 1.39-1.52 (m, 1H, *H-4*), 1.22-1.39 (m, 1H, *H-3*), 1.02 (d, 3H, *H-6*, ^3J = 6.0 Hz). ^{13}C{^{1}H} NMR ppm (C$_6$D$_6$): 137.7 (C-8), 115.7 (C-9), 59.5 (C-2), 57.2 (C-7), 54.3 (C-5), 33.4 (C-3), 22.1 (C-4), 19.5 (C-6).

*Synthesis of N-(2-methylpent-2-enylidene)pent-4-en-1-amine*
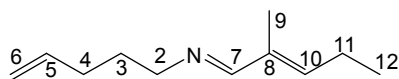
^{1}H NMR ppm (CDCl$_3$): 8.32 (s, 0.09H, *H-7*$_{cis}$), 7.77 (s, 0.09H, *H-7*$_{trans}$), 5.82 (m, 1H, *H-5*), (dm, 1H, *H-10*, ^3J = Hz) 4.98 (dm, 1H, *H-6*$_{trans}$, $^3J_{trans}$ = 17.5 Hz), 4.95 (dm, 1H, *H-6*$_{cis}$, $^3J_{cis}$ = 10.3 Hz), 3.50 + 3.46 (two aparent t, 0.18H + 1.82H, *H-2*, ^3J = 6.9 Hz), 2.29 + 2.24 (two apparent quint., 0.18H + 1.82H, *H-11*, ^3J = 7.5 Hz), 2.07 (apparent q, 2H, *H-4*, ^3J = 6.6 Hz), 1.87 (s, 0.27H, *H-9*$_{cis}$), 1.83 (s, 2.73H, *H-9*$_{trans}$), 1.71 (apparent quint., 2H, *H-3*, ^3J = 6.8 Hz), 1.04 + 1.03 (two t, 2.73H + 0.27H, *H-12*, ^3J = 7.5 Hz). ^{13}C{^{1}H} NMR ppm (CDCl$_3$): 165.8 (C-7), 143.2 (C-10), 138.5 (C-5), 135.2 (C-8), 114.6 (C-6), 60.6 (C-2), 31.4 (C-4), 30.14 (C-3), 21.7 (C-11), 13.5 (C-12), 11.4 (C-9). ESI-MS: [M-H]$^+$ = 166.16.

Synthesis of 2,5-dimethylpyrrolidine
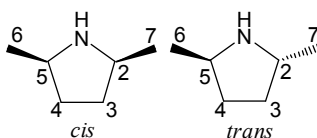
^{1}H NMR ppm (C$_6$D$_6$) *trans*: 3.09-3.22 (m, 2H, *H-2/5*), 1.63-1.82 (m, 2H, *H-3/4*), 1.04-1.15 (m, 2H, *H-3/4*), 0.99 (d, 6H, *H-6/7*), 0.87 (broad s, 1H, N*H*); *cis*: 2.87-2.99 (m, 2H, *H-2/5*), 1.63-1.82 (m, 2H, *H-3/4*), 1.04-1.15 (m, 2H, *H-3/4*), 1.00 (d, 6H, *H-6/7*), 0.87 (broad s, 1H, N*H*). ^{13}C{^{1}H} NMR ppm (C$_6$D$_6$) *trans*: 53.4 (C-2/5), 35.1 (C-3/4), 22.7 (C-6/7); *cis*: 54.9 (C-2/5), 33.9 (C-3/4), 22.1 (C-6/7).

6.6.4 Stoichiometric reactions
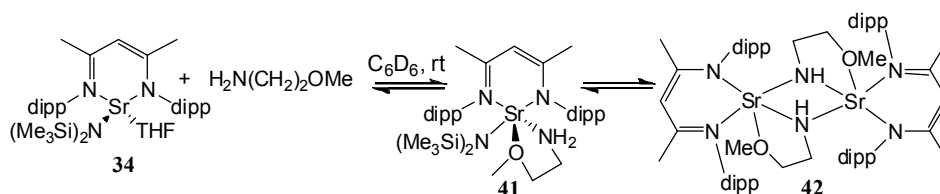
2-methoxyethylamine (5.9 µL, 67.8 µmol) was added to 0.5 mL of C$_6$D$_6$ solution of **34** (50 mg, 67.8 µmol) at room temperature. A ^{1}H NMR spectrum recorded after 25 minutes at room temperature showed a 70:25:5 mixture of **41**, a potentially dimeric strontium methoxyethylamide complex **42** and the known homoleptic complex [{ArNC(Me)CHC(Me)NAr}$_2$Sr(THF)].

Synthesis of [{ArNC(Me)CHC(Me)Ar}Sr{N(SiMe$_3$)$_2$}{H$_2$N(CH$_2$)$_2$OMe}] (41)
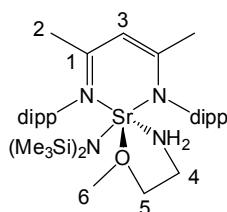
^{1}H NMR ppm (C$_6$D$_6$): 7.02-7.11 (m, 6H, Ar-*H*), 4.89 (s, 1H, *H-4*), 3.55 (m, 7H, THF + *H-6*), 3.36 (broad sept, 4H, ^{i}Pr-C*H*), 2.33 (broad t, 2H, *H-5, ^3J = 4.4 Hz), 1.76 (broad t, 2H, *H-3, ^3J = 4.4 Hz), 1.70 (s, 6H, *H-2*), 1.27 (broad d, 24H, ^{i}Pr-C*H$_3$*), 0.32 (s, 18H, Si(C*H$_3$*)$_3$), -0.07 (broad t, 2H, N*H$_2$*). ^{13}C NMR ppm (d$_8$-tol): 159.8 (C-1), 151.3 (*i*-Ar-C), 139.5 (*o*-Ar-C), 123.2 (*m*-Ar-C), 120.6 (*p*-Ar-C), 91.0 (C-3), 73.1 (C-5), 57.8 (C-6), 41.3 (C-4), 27.6 (^{i}Pr-*CH*), 24.5 (^{i}Pr-*CH$_3$*), 24.0 (C-2), 1.3 (Si(C*H$_3$*)$_3$). Anal. calc. for

$C_{38}H_{88}N_4OSi_2Sr$ (760.9): C, 61.61; H, 9.25; N, 7.56%. Found: C, 61.68; H, 9.29; N, 7.47%.
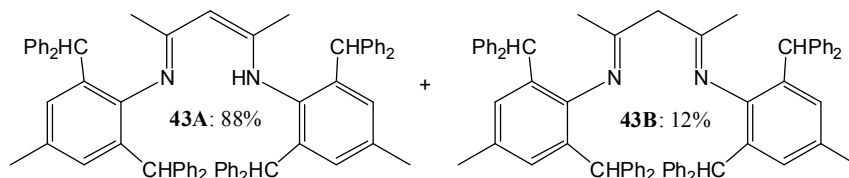
Identification of the amine/amide exchange product 42
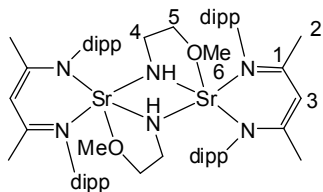
^{1}H NMR ppm (C_6D_6): 7.02-7.11 (m, 6H, Ar-*H*), 4.74 (s, 1H, *H-3*), 3.55 (m, 7H, THF + *H-6*), 3.23 (sept, 4H, ^{i}Pr-C*H*, ^3J = 6.8 Hz), 2.79 (broad s, 2H, *H-5*), 2.67 (broad s, 2H, *H-4*), 2.08 (s, 6H, *H-2*), 1.22 + 1.11 (two d, 12H each, ^{i}Pr-C*H$_3$*, ^3J = 6.8 Hz), 0.09 (s, 18H, HN(Si*Me$_3$*)$_2$), -1.75 (broad s, 1H, N*H*).

### 6.6.5   Reactions with the bulky β-diketiminate ligand 43

Synthesis of ligand precursor 43

2,4-pentanedione (1.37 g, 13.6 mmol) and 2,6-diphenylmethyl-*p*-toluidine (12 g, 27.3 mmol) were refluxed with *p*-toluenesulfonic acid (5.19 g, 27.3 mmol) in toluene under Dean-Stark conditions for five days. Upon cooling of the resulting brown mixture a cream-coloured solid precipitated, which was filtered, neutralised with 500 mL of a 5% aqueous NaOH solution and extracted into 800 mL of CH_2Cl_2. After drying over $MgSO_4$ the solvent was removed *in vacuo* yielding an off-white solid which was purified by flash chromatography with a 50:50 hexane/THF mixture. Crystallisation from hot chloroform afforded compound **43** as colourless needles (6.70 g, 7.11 mmol, 52%). ^{1}H NMR ppm (CDCl$_3$), amino-imine **43A** (88%): 12.11 (s, 1H, N*H*), 7.26-7.28 (m, 16H, Ph-*H*), 7.00-7.05 (m, 24H, Ph-*H*), 6.85 (s, 4H, *H-6*), 5.95 (s, 4H, *H-8*), 4.18 (s, 1H, *H-2*), 2.24 (s, 6H, *H-9*), 0.25 (s, 6H, *H-3*); diimine **43B** (12%): 7.08-7.23 (m, 40H, Ph-*H*), 6.69 (s, 4H, *H-6*), 5.42 (s, 4H, *H-8*), 3.07 (s, 2H, *H-2*), 2.17 (s, 6H, *H-9*), 0.56 (s,

6H, *H-3*). ^{13}C{^{1}H} NMR ppm (CDCl$_3$), amino-imine **43A**: 164.0 (C-1), 144.8 (C-4), 142.3 (*i*-Ph-*C*), 138.6 (C-7), 133.4 (C-5), 130.0 (*m*-Ph-*C*), 129.4 (*m*-Ph-*C*), 128.2 (*o*-Ph-*C*), 128.0 (*o*-Ph-*C*), 126.1 (C-6), 125.8 (*p*-Ph-*C*), 94.8 (C-2), 52.1 (C-8), 21.5 (C-3), 19.5 (C-9); diimine **43B**: 164.0 (C-1), 144.0 (C-4), 141.2 (*i*-Ph-*C*), 138.6 (C-7), 132.5 (C-5), 129.9 (*m*-Ph-*C*), 129.3 (*m*-Ph-*C*), 128.3 (*o*-Ph-*C*), 127.9 (*o*-Ph-*C*), 126.1 (C-6), 125.9 (*p*-Ph-*C*), 77.0 (C-2), 51.5 (C-8), 21.5 (C-3), 19.5 (C-9). ESI-MS: [M-H]$^+$ = 944.48. Anal. calc. for C$_{71}$H$_{62}$N$_2$ (943.3): C, 90.41; H, 6.63; N, 2.97%. Found: C, 90.36; H, 6.58; N, 2.94%.

*Synthesis of ligand magnesium complex 44*
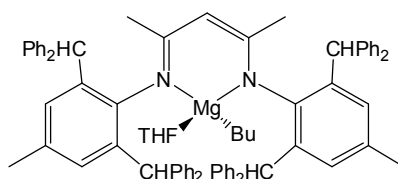
MgBu$_2$ (0.318 mL of a 1 M solution in heptane, 0.318 mmol) and ligand precursor **43** (300 mg, 0.318 mmol) were heated in THF at 60 $^{\circ}$C for 2 hours. The solvent was removed *in vacuo* and the crude product recrystallised at room temperature from a 10:1 toluene/THF mixture to yield pale yellow crystals (270 mg, 0.246 mmol, 77%). ^{1}H NMR ppm (C$_6$D$_6$): 7.40 (dd, 16H, Ph-*H*, ^3J = 6.8, 5.4 Hz), 7.23 (s, 4H, *H-6*), 7.16-7.21 (m, 20H, Ph-*H*), 7.10 (t, 4H, Ph-*H*, ^3J = 7.3 Hz), 7.00 (t, 4H, Ph-*H*, ^3J = 7.3 Hz), 5.95 (s, 4H, *H-8*), 4.67 (s, 1H, *H-2*), 3.74 (m, 4H, THF), 1.96 (s, 6H, *H-9*), 1.41-1.46 (m, 8H, THF + Bu-(C*H*$_2$)$_2$), 1.09 (t, 3H, Bu-C*H*$_3$, ^3J = 6.7 Hz), 1.03 (s, 6H, *H-2*), -0.43-(-0.38) (m, 2H, Mg-C*H*$_2$). ^{13}C{^{1}H} NMR ppm (C$_6$D$_6$): 171.0 (C-1), 145.1 (C-4), 144.5 (*i*-Ph-*C*), 143.2 (*i*-Ph-*C*), 134.0 (C-7), 130.4 (*m*-Ph-*C*), 130.2 (C-5), 129.9 (*m*-Ph-*C*), 128.9 (*m*-Ph-*C*), 128.7 (*m*-Ph-*C*), 128.5 (C-6), 128.3 (*o*-Ph-*C*), 128.1 (*o*-Ph-*C*), 128.0 (*o*-Ph-*C*), 127.9 (*o*-Ph-*C*), 126.9 (*p*-Ph-*C*), 126.7 (*p*-Ph-*C*), 96.2 (C-2), 52.8 (C-8), 32.0 + 31.9 (Bu-(*C*H$_2$)$_2$), 23.3 (C-3), 21.4 (THF), 21.2 (C-9), 14.2 (Bu-*C*H$_3$), 6.5 (Mg-*C*H$_2$). Anal. calc. for C$_{79}$H$_{78}$MgN$_2$O (1095.8): C, 86.59; H, 7.17; N, 2.56%. Found: C, 86.62, H, 7.09, N 2.52%.

6.7   Synthesis and characterisation of bis(carbene)borate compounds

## 6.7.1   *Synthesis of dihydro-bis(imidazole)boronium salts: General Procedure*

Two equivalents of the imidazole and one equivalent of $Me_3N.BH_2X$ (X = Br, I) were refluxed in 20 mL of dry chlorobenzene at 133 °C under argon for 3-5 hours (X = I) or 10-15 hours (X = Br). Upon cooling to room temperature a white precipitate formed. After removal of the solvent *in vacuo,* the crude white solid was recrystallised and dried *in vacuo* for several hours before transfer into the glove box.

*Synthesis of [$H_2B(Im^tBu)_2$]I (**58**)*
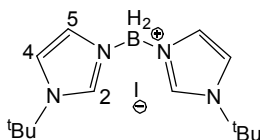
1-(*tert*-butyl)imidazole (6.00 g, 48.32 mmol) and $Me_3NB.H_2I$ (4.80 g, 24.16 mmol). Recrystallised from water as a colourless solid (7.72 g, 19.89 mmol, 82%), mp 135°C. ^{1}H NMR ppm (CDCl$_3$): 9.21 (s, 1H, *H-2*), 7.16 (d, 1H, *H-5*, ^3J 1.8 Hz), 7.12 (d, 1H, *H-4*, ^3J 1.8 Hz), 1.70 (s, 9H, C*H$_3$*), B*H$_2$* signal broadened into baseline. ^{13}C{^{1}H} NMR ppm (CDCl$_3$): 138.3 (C-2), 130.0 (C-5), 126.0 (C-4), 59.2 (*C*(CH$_3$)$_3$), 30.9 (*CH$_3$*). ^{11}B NMR ppm (CDCl$_3$): -7.60 (broad s, *B*H$_2$). IR (Nujol): v_{B-H} 2434 cm^{-1}, br. Anal. Calc. for C$_{14}$H$_{26}$BIN$_4$ (388.1): C, 43.33; H, 6.75; N, 14.44%. Found: C, 43.0; H, 6.70; N, 14.0%.

*Synthesis of [$H_2B(Im^tBu)_2$]Br (**59**)*
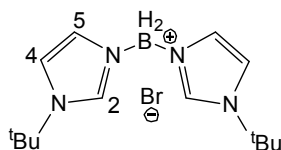
1-(*tert*-butyl)imidazole (2.00 g, 16.11 mmol) and $Me_3N.BH_2Br$ (1.25 g, 8.05 mmol). Recrystallised from CH$_2$Cl$_2$ as a colourless solid (2.92 g, 8.2 mmol, 100%), mp 110°C. ^{1}H NMR ppm (CDCl$_3$): 9.49 (t, 1H, *H-2*, ^4J = 1.5 Hz), 7.15 (t, 1H, *H-5*, ^3J = 1.5 Hz), 7.08 (t, 1H, *H-4*, ^3J = 1.5 Hz), 1.70 (s, 9H, C*H$_3$*), B*H$_2$* signal broadened into baseline. ^{13}C{^{1}H} NMR ppm (CDCl$_3$): 130.1 (C-2), 129.0 (C-5), 126.0 (C-4), 59.0 (*C*(CH$_3$)$_3$), 30.8 (*CH$_3$*). ^{11}B NMR ppm (CDCl$_3$): -9.09 (broad s, *B*H$_2$). IR (Nujol): v_{B-H} 2434 cm^{-1}, br.

Anal. Calc. for $C_{14}H_{26}BBrN_4$ (340.1): C, 49.2; H, 7.53; N 16.67%. Found: C, 49.30; H, 7.68; N, 16.43%.

Synthesis of [H₂B(ImMes)₂]I (60)
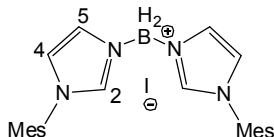
1-mesitylimidazole (2.00 g, 10.74 mmol) and $Me_3N.BH_2I$ (1.07 g, 5.37 mmol). Recrystallised from $CHCl_3$ as a colourless solid (2.35 g, 4.56 mmol, 85%), mp 172°C. ^1H NMR ppm ($CDCl_3$): 9.20 (s, 1H, *H-2*), 7.60 (s, 1H, *H-5*), 7.05 (s, 1H, *H-4*), 6.98 (s, 2H, *m*-Mes-*H*), 2.33 (s, 3H, *p*-C*H₃*), 2.04 (s, 6H, *o*-C*H₃*), B*H₂* signal broadened into baseline. $^{13}C\{^1H\}$ NMR ppm ($CDCl_3$): 141.1 (C-2), 140.2 (*i*-Mes-*C*), 134.8 (*m*-Mes-*C*), 130.1 (*p*-Mes-*C*), 126.8 (C-5), 123.2 (*o*-Mes-*C*), 115.1 (C-4), 21.5 (*p*-C*H₃*), 18.2 (*o*-C*H₃*). ^{11}B NMR ppm ($CDCl_3$): -6.10 (broad s, B*H₂*). IR (Nujol): v_{B-H} 2444 cm^{-1}, br. Anal. Calc. for $C_{24}H_{30}BIN_4$ (512.2): C, 56.27; H, 5.90; N, 10.94%. Found: C, 56.7; H, 5.89; N, 10.7%.

Synthesis of [H₂B(ImMes)₂]Br (61)
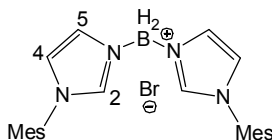
1-mesitylimidazole (2.00 g, 10.74 mmol) and $Me_3N.BH_2Br$ (0.82 g, 5.37 mmol). Crystallised from $CHCl_3$ as a colourless solid (1.30 g, 2.79 mmol, 52%), mp 190-192°C. ^1H NMR ppm ($CDCl_3$): 9.55 (s, 1H, *H-2*), 7.60 (s, 1H, *H-5*), 7.00 (s, 1H, *H-4*), 6.97 (s, 2H, *m*-Mes-*H*), 2.32 (s, 3H, *p*-C*H₃*), 2.04 (s, 6H, *o*-C*H₃*), B*H₂* signal broadened into baseline. $^{13}C\{^1H\}$ NMR ppm ($CDCl_3$): 140.4 (C-2), 140.3 (*i*-Mes-*C*), 134.3 (*m*-Mes-*C*), 129.4 (*p*-Mes-*C*), 126.1 (C-5), 122.1 (*o*-Mes-*C*), 114.4 (C-4), 20.9 (*p*-C*H₃*), 17.4 (*o*-C*H₃*). ^{11}B NMR ppm ($CDCl_3$): -7.90 (broad s, B*H₂*). IR (Nujol): v_{B-H} 2441 cm^{-1}, br. Anal. Calc. for $C_{24}H_{30}BBrN_4$ (465.2): C, 61.91; H, 6.50; N, 12.04%. Found: C, 61.7; H, 6.48; N, 11.9%.

Synthesis of [Ph₂B(ImᵗBu)₂]Br
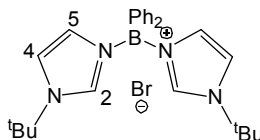
1-(*tert*-butyl)imidazole (2.04 g, 16.40 mmol) and diphenylbromoborane (2.00 g, 8.20 mmol) were weighed out into separate Schlenk flasks and dissolved in toluene. The boronium salt instantly precipitated upon addition of the imidazole to the borane *via* canula. The mixture was refluxed at 120 °C for 1 hour, cooled down and the air-stable precipitate dried over a Büchner funnel. The crude product was recrystallised from a 10:1 mixture of CH_2Cl_2 and Et_2O at -20 °C, yielding a colourless solid (2.14 g, 5.82 mmol, 71%), mp 169-172°C. ^{1}H NMR ppm ($CDCl_3$): 8.20 (s, 2H, *H-2*), 7.34 (t, 2H, *H-5*, ^3J = 1.8 Hz), 7.17-7.23 (m, 4H, *m*-Ph-*H*), 7.19 (s, 2H, *H-4*), 7.03-7.06 (m, 6H, *o/p*-Ph-*H*), 1.59 (s, 18H, C*H₃*). ^{13}C{^{1}H} NMR ppm ($CDCl_3$): 140.5 (C-*2*), 134.7 (C-5), 132.2 (*i*-Ph-*C*), 126.6 (*m*-Ph-*C*), 126.0 (*p*-Ph-*C*), 124.5 (*o*-Ph-*C*), 118.0 (C-4), 57.7 (*C*(CH₃)₃), 28.9 (*C*H₃). ^{11}B NMR ppm ($CDCl_3$): 1.97 (s, *B*Ph₂).

6.7.2 Synthesis of bis(imidazolin-2-ylidene-1-yl)borate alkaline earth complexes: General Procedure

In a glovebox, the appropriate bis(imidazole)boronium salt, calcium- or strontium iodide and potassium bis(trimethylsilyl)amide were weighed out at a 1:1:2 or 3 ratio into a dry Schlenk flask. 15 mL of dry THF were added under argon at -78 °C. The solution was stirred at room temperature overnight. The solvent was removed *in vacuo* and the crude product extracted with hexane. The mixture was stirred for another hour prior to canula filtration away from insoluble KI and concentration of the filtrate to incipient crystallisation. Crystals were obtained after 3-7 days at -20 ºC. All X-ray structures were obtained from crystals selected under a cryogenic flow of nitrogen due to their extreme temperature-sensitivity.

Synthesis of [{H₂B(Im^tBu)₂}Ca{N(SiMe₃)₂}(THF)] (62)
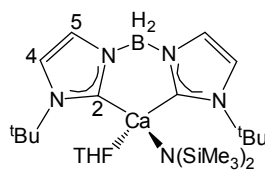
a) **59** (2.08 g, 6.12 mmol), calcium iodide (1.79 g, 6.12 mmol) and [KN(SiMe₃)] (3.66 g, 18.38 mmol): pale yellow transparent solid, very air- and temperature-sensitive, oily at 21 °C, crystallised after 4 days at -16 °C (0.55g, 1.03 mmol, 16.8%). b) **58** (2.00 g, 5.15 mmol), calcium iodide (1.51 g, 5.15 mmol) and [KN(SiMe₃)₂] (3.08 g, 15.46 mmol): off-white powder (1.55 g, 2.90 mmol, 56%). ^{1}H{^{11}B} NMR ppm (C₆D₆): 7.23 (d, 1H, *H-5*, ^3J = 1.5 Hz), 7.13 (s, 1H, *H-5*), 6.59 (d, 1H, *H-4*, ^3J = 1.5 Hz), 6.52 (s, 1H, *H-4*), 4.31 (broad, 2H, B*H₂*), 3.63 (m, 4H, THF), 1.36 (m, 4H, THF), 1.31 (s, 18H, C(C*H₃*)₃), 0.45 (s, 18H, Si(C*H₃*)₃). ^{13}C{^{1}H} NMR ppm (C₆D₆):195.0 (C-2), 125.0, (C-5), 114.4 (C-4), 68.6 (THF), 54.8 (THF), 31.1 (*C*(CH₃)₃), 25.0 (C(*C*H₃)₃), 2.3 (Si(*C*H₃)₃). ^{11}B{^{1}H} NMR ppm (C₆D₆): -5.8 (B*H₂*). In d₈-toluene, the imidazol-2-ylidene ^{1}H and ^{13}C{^{1}H} NMR signals split at low temperatures. IR (Nujol): ν_{B-H} 2385, 2252 cm^{-1}. Anal. Calc. for C₂₄H₅₂BCaN₅OSi₂ (533.8): C, 54.00; H, 9.82; N, 13.12%. Found: C, 54.09; H, 9.41; N, 13.23%.

Synthesis of [{H₂B(Im^tBu)₂}Sr{N(SiMe₃)₂}(THF)₂] (63)
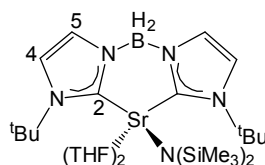
58 (1.00 g, 2.58 mmol), strontium iodide (0.88 g, 2.58 mmol) and [KN(SiMe₃)₂] (1.54 g, 7.73 mmol): large crop of colourless crystals after 1 day at -20 ºC (1.85 g, 1.98 mmol, 76%), mp 137-140 ºC. X-ray crystallography and NMR showed presence of hexane in the lattice. ^{1}H{^{11}B} NMR ppm (C₆D₆): 7.23 (broad s, 2H, *H-5*), 6.62 (s, 2H, *H-4*), 4.31 (broad, 2H, B*H₂*), 3.59 (m, 8H, THF), 1.35 (s, 18H, C(C*H₃*)₃), 1.30 (m, 8H, THF), 0.86-0.94 (m, hex), 0.37 (s, 18H, Si(C*H₃*)₃). ^{13}C{^{1}H} NMR ppm (C₆D₆): 201.5 (C-2), 126.0 (C-5), 115.2 (C-4), 69.0 (THF), 55.5 (*C*(CH₃)₃), 32.3 (C(*C*H₃)₃), 30.3 (hex), 25.8 (THF), 23.4 (hex), 14.7 (hex), 5.9 (Si(*C*H₃)₃). ^{11}B{^{1}H} NMR ppm (C₆D₆): -5.71 (B*H₂*). IR (Nujol): ν_{B-H} 2363, 2252 cm^{-1}. Anal. Calc. for C₂₉.₅H₆₁.₅BN₅O₂Si₂Sr (937.8): C, 52.63; H, 9.21; N, 10.41%. Found: C, 52.75; H, 9.43; 10.33.

Synthesis of [{H₂B(Im^tBu)₂}₂Ca(THF)] (64)
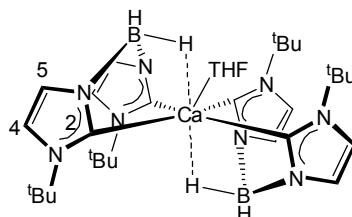
Redistribution product from the attempted synthesis of [{H₂B(Im^tBu)₂}CaI(THF)]: **58** (0.50 g, 1.29 mmol), calcium iodide (0.38 g, 1.29 mmol) and [KN(SiMe₃)₂] (0.51 g, 2.58 mmol): colourless crystals after 3 days at -20 ºC (0.20 g, 49% based on CaI₂). ¹H{¹¹B} NMR ppm (C₆D₆): 7.26 (d, 4H, *H-5*, ³*J* = 1.5 Hz), 6.60 (d, 4H, *H-4*, ³*J* = 1.5 Hz), 4.44 (broad, 2H, B*H₂*), 3.59 (m, 4H, THF), 1.38 (m, 4H, THF), 1.36 (s, 36H, C(C*H₃*)₃). ¹³C{¹H} NMR ppm (C₆D₆): 195.0 (C-2), 124.0 (C-5), 113.3 (C-4), 66.7 (THF), 53.8 (*C*(CH₃)₃), 30.0 (C(*CH₃*)₃), 24.3 (THF). ¹¹B{¹H} NMR ppm (C₆D₆): -5.42 (*B*H₂). IR (Nujol): ν_B-H 2363, 2255 cm⁻¹.

Synthesis of [{H₂B(Im^tBu)₂}₂Ca{N-(Im^tBu)}] (64')
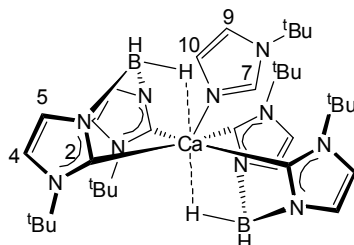
Result of the rational synthesis of [{H₂B(Im^tBu)₂}₂Ca(THF)]: **58** (0.50 g, 1.29 mmol), calcium iodide (0.19 g, 0.64 mmol) and [KN(SiMe₃)₂] (0.51 g, 2.58 mmol): colourless crystals (0.19 g, 0.28 mmol, 44 %). ¹H{¹¹B} ppm NMR (C₆D₆): 7.46 (broad s, 1H, *H-7*), 7.38 (d, 4H, *H-5*, ³*J* = 1.5 Hz,), 7.13 (s, 1H, *H-10*), 6.70 (d, 4H, *H-4*, ³*J* = 1.5 Hz), 6.36 (s, 1H, *H-9*), 4.45 (broad, 2H, B*H₂*), 1.34 (s, 36H, ligand C(C*H₃*)₃), 0.84 (9H, s, co-ligand C(C*H₃*)₃). ¹³C{¹H} NMR ppm (C₆D₆): 198.0 (C-2), 134.9 (C-7), 126.3 (C-10), 124.3 (C-4), 114.0 (C-9), 113.0 (C-5), 53.9 (ligand *C*(CH₃)₃), 52.7 (co-ligand *C*(CH₃)₃), 29.9 (ligand C(*CH₃*)₃), 28.6 (co-ligand C(*CH₃*)₃). ¹¹B{¹H} NMR ppm (C₆D₆): -5.11 (*B*H₂).

Synthesis of [{H₂B(Im^tBu)₂}₂Sr(THF)₂] (65)

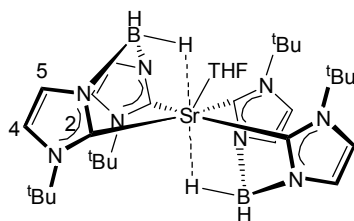Redistribution product of the synthesis of [{H$_2$B(Im^{t}Bu)$_2$}SrI(THF)]: **58** (0.50 g, 1.29 mmol), strontium iodide (0.44 g, 1.29 mmol) and [KN(SiMe$_3$)$_2$] (0.51 g, 2.58 mmol): colourless crystals after 3 days at -20 ºC (0.21 g, 43%). ^{1}H{^{11}B} NMR ppm (C$_6$D$_6$): 7.29 (d, 4H, *H-5*, ^3J = 1.5 Hz), 6.63 (d, 4H, *H-4*, ^3J = 1.5 Hz), 4.44 (broad, 2H, B*H$_2$*) 3.67 (m, 4H, THF), 1.30 (s, 36H, C(C*H$_3$*)$_3$), 1.30 (m, 4H, THF). ^{13}C{^{1}H} NMR ppm (C$_6$D$_6$): 198.9 (C-2), 124.3 (C-5), 113.1 (C-4), 67.2 (THF), 53.7 (*C*(CH$_3$)$_3$), 30.0 (C(*C*H$_3$)$_3$), 24.2 (THF). ^{11}B{^{1}H} NMR ppm (C$_6$D$_6$): -5.64 (*B*H$_2$).

Synthesis of [{H₂B(ImMes)₂}Ca{N(TMS)₂}(THF)] (66)
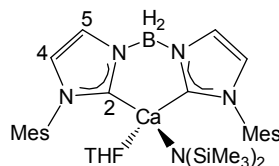
60 (0.50 g, 0.98 mmol) and **36b** (0.74 g, 1.46 mmol) were stirred in cold THF overnight. Extraction with hexane yielded a light pink powder (0.14 g, 0.49 mmol, 50 %). ^{1}H{^{11}B} NMR ppm (C$_6$D$_6$): 7.21 (d, 2H, *H-5*, ^{3}J = 1.5 Hz), 6.77 (s, 4H, *m*-Mes-*H*), 6.27 (d, 2H, *H-4*, ^{3}J = 1.5 Hz), 4.41 (broad, 2H, B*H$_2$*), 3.52 (m, 4H, THF), 2.12 (s, 6H, *p*-C*H$_3$*), 1.93 (s, 12H, *o*-C*H$_3$*), 1.14 (m, 4H, THF), 0.12 (s, 18H, TMS). ^{13}C{^{1}H} NMR ppm (C$_6$D$_6$): 196.0 (C-2), 137.1 (*i*-Mes-*C*), 136.2 (*p*-Mes-*C*), 135.0 (*o*-Mes-*C*), 128.2 (*m*-Mes-*C*), 123.6 (C-5), 117.7 (C-4), 67.6 (THF), 23.7 (THF), 19.6 (*p*-C*H$_3$*), 16.4 (*o*-C*H$_3$*), 3.9 (Si(C*H$_3$*)$_3$). ^{11}B{^{1}H} NMR ppm (C$_6$D$_6$): -5.87 (*B*H$_2$).

Synthesis of [Ph₂B(Im^{t}Bu)]₂ (81)
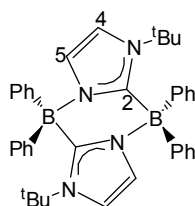
Only isolable product of the reaction of [Ph$_2$B(Im^{t}Bu)$_2$Br] and [Ca{N(SiMe$_3$)$_2$}$_2$(THF)$_2$] in 1:1.5 ratio at -78 °C in THF. Reaction mixture turned brown at room temperature and yielded [Ph$_2$B(Im^{t}Bu)]$_2$ as colourless crystals from toluene after 10 days at -20 °C. ^{1}H{^{11}B} NMR ppm (C$_6$D$_6$): 7.59 (dd, 4H, *o*-Ph-*H*, ^3J = 8.1 Hz, ^4J = 1.5 Hz), 7.19-7.29 (m, 6H, *m/p*-Ph-*H*), 6.91 (d, 1H, *H-5*, ^3J = 1.8 Hz), 6.45 (d, 1H, *H-4*, ^3J = 1.8 Hz), 0.74 (s, 9H, C(C*H$_3$*)$_3$). ^{13}C{^{1}H} NMR ppm (d$_8$-tol): 182.9 (C-2), 136.6 (*i*-Ph-*C*), 129.7 (*o*-Ph-*C*), 128.9 (*p*-Ph-*C*), 127.8 (*m*-Ph-*C*), 126.0 (C-5), 124.3 (C-4), 59.2 (*C*(CH$_3$)$_3$), 31.7 (C(*C*H$_3$)$_3$). ^{11}B{^{1}H} NMR ppm (d$_8$-tol): -2.53 (*B*Ph$_2$). Anal. Calc. for C$_{38}$H$_{42}$B$_2$N$_4$ (576.4): C, 79.18; H, 7.34; N, 9.72%. Found: C, 79.13; H, 7.29; N, 9.72%.

6.7.3 Stoichiometric reactions

Synthesis of [{H₂B(Im^{t}Bu)₂}Ca{NHCH₂Ph}(THF)] (70)
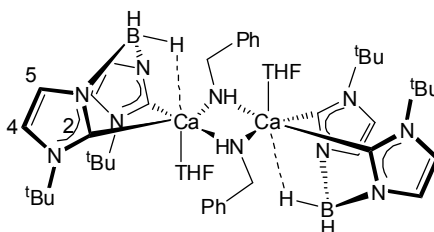
NMR scale reaction in C$_6$D$_6$: benzylamine (8.19 µL, 75 µmol) and **62** (40 mg, 75 µmol). The solution instantly turned crimson. ^{1}H NMR data showed complete conversion within the first point of analysis. By comparison with the known structure of *β*-diketiminato analogue the compound is expected to be dimeric. Due to slow protonation of the ligand by the amine, however, the compound could not be isolated. ^{1}H{^{11}B} NMR ppm (C$_6$D$_6$): 7.20 (s, 2H, *H-5*), 6.87-7.03 (m, 5H, Ph-*H*), 6.57 (s, 2H, *H-4*), 4.45 (broad s, 2H, B*H$_2$*), 3.55 (broad, 2H, NHC*H$_2$*Ph), 3.48 (m, 4H, THF), 1.24 (m, 4H, THF), 1.20 (s, 18H, C(C*H$_3$*)$_3$), 0.11 (s, 18H, HN(Si(C*H$_3$*)$_3$)$_2$), -1.25 (broad s, N*H*). ^{13}C{^{1}H} NMR ppm (C$_6$D$_6$): 198.0 (C-2), 144.3 (*i*-Ph-*C*), 129.5 (*m*-Ph-*C*), 127.3 (*o*-Ph-*C*), 127.2 (*p*-Ph-*C*), 126.1 (C-5), 115.0 (C-4), 68.4 (THF), 55.6 (*C*(CH$_3$)$_3$), 45.8

(NHCH_2Ph), 31.7 (C(CH$_3$)$_3$), 26.1 (THF), 3.0 (HN(Si(CH$_3$)$_3$)$_2$). ^{11}B{^{1}H} NMR ppm (C$_6$D$_6$): -5.68 (BH$_2$).

Synthesis of [{H$_2$B(Im^{t}Bu)$_2$}Ca{NH(CH$_2$)$_2$OMe}] (71)
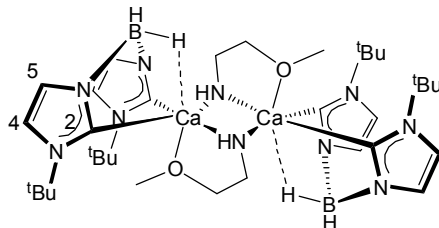
NMR scale reaction in C$_6$D$_6$: 2-methoxyethylamine (12.6 µL, 144 µmol) and **62** (80 mg, 144 µmol): the solution instantly turned orange. ^{1}H NMR data showed complete conversion within the first point of analysis. By comparison with the known structure of *β*-diketiminato analogue the compound is expected to be dimeric. Due to slow protonation of the ligand by the amine, however, the compound could not be isolated. ^{1}H{^{11}B} NMR ppm (C$_6$D$_6$): 7.30 (s, 2H, *H-5*), 7.57 (s, 2H, *H-4*), 3.57 (m, 4H, free THF), 4.40 (broad, 2H, BH$_2$), 3.01 (broad m, 5H, CH$_3$OCH$_2$) 1.41 (m, 4H, free THF), 1.32 (s, 18H, C(CH$_3$)$_3$), 0.85 (s, 2H, NHCH$_2$), -0.89 (broad s, 1H, NH). ^{13}C{^{1}H} NMR ppm (C$_6$D$_6$): 199.3 (C-2), 126.1 (C-5), 114.8 (C-4), 55.8 (OCH$_2$), 54.7 (THF), 31.6 (OCH$_3$), 30.3 (C(CH$_3$)$_3$), 26.1 (C(CH$_3$)$_3$). ^{11}B{^{1}H} NMR ppm (C$_6$D$_6$): -5.71 (BH$_2$).

6.8 Synthesis and characterisation of tris(carbene)borate compounds

6.8.1 Synthesis of tris(imidazolin-2-ylidene-1-yl)borate alkaline earth amides and iodides: General Procedure

In a glovebox, the appropriate tris(imidazole)boronium salt, calcium-, strontium- or barium iodide and potassium (bis(trimethylsilyl))amide were weighed out at a 1:1:3 or 4 ratio into a dry Schlenk flask. 15 mL of dry THF were added under argon at -78 °C. The solution was stirred at room temperature overnight. The solvent was removed *in vacuo* and the crude product extracted with toluene. The mixture was stirred for another hour prior to canula filtration away from insoluble KI and concentration of the filtrate to incipient crystallisation. Crystals were obtained after 3-7 days at -20 ºC. All X-ray

structures were obtained from crystals selected under a cryogenic flow of nitrogen due to their extreme temperature-sensitivity.

Synthesis of [{HB(Im^{t}Bu)$_3$}Ca{N(SiMe$_3$)$_2$}] (73)
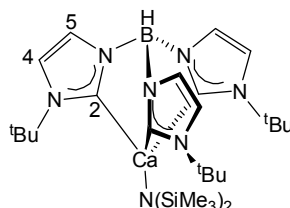
[HB(Im^{t}Bu)$_3$]Br$_2$ (**72** 0.5 g, 0.92 mmol), calcium iodide (0.27 g, 0.92 mmol), [KN(SiMe$_3$)$_2$] (0.73 g, 3.67 mmol): off-white powder (0.52 g, 0.89 mmol, 97 %). ^{1}H{^{11}B} NMR ppm (d$_8$-tol): 7.33 (s, 3H, *H-5*), 6.65 (s, 3H, *H-4*), 4.97 (broad, 1H, B*H*), 1.37 (s, 27H, C(C*H$_3$*)$_3$), 0.27 (broad, 18H, Si(C*H$_3$*)$_3$). ^{13}C{^{1}H} NMR ppm (d$_8$-tol): 198.5 (C-2), 127.3 (C-5), 113.9 (C-4), 55.8 (*C*(CH$_3$)$_3$), 31.2 (C(*C*H$_3$)$_3$), 2.6 (Si(*C*H$_3$)$_3$). ^{11}B{^{1}H} NMR ppm (d$_8$-tol): 2.53 (*B*H). Anal. Calc. for C$_{27}$H$_{52}$BCaN$_7$Si$_2$ (581.8): C, 55.74; H, 9.01; N, 16.85%. Found: C, 55.69; H, 8.96; N, 16.91%.

Synthesis of [Ca{N(SiMe$_3$)$_2$}{N-(Im^{t}Bu)$_2$}] (80)
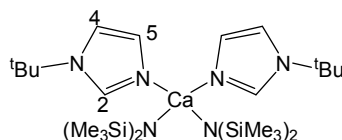
10% by-product of the synthesis of **73**, isolated in the first crystallisation fraction. ^{1}H NMR ppm (d$_8$-tol): 8.02 (broad s, 1H, *H-2*), 6.98 (broad s, 1H, *H-5*), 6.42 (broad s, 1H, *H-4*), 1.03 (s, 9H, C(C*H$_3$*)$_3$), 0.44 (s, 18H, Si(C*H$_3$*)$_3$). ^{13}C{^{1}H} NMR ppm (d$_8$-tol): 135.7 (C-2), 124.9 (C-5), 114.8 (C-4), 53.5 (*C*(CH$_3$)$_3$), 28.7 (C(*C*H$_3$)$_3$), 4.8 (Si(*C*H$_3$)$_3$).

Synthesis of [{HB(Im^{t}Bu)$_3$}Sr{N(SiMe$_3$)$_2$}{N-(Im^{t}Bu)}] (74)
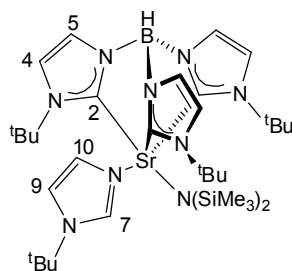
72 (1.00 g, 1.84 mmol), strontium iodide (0.62 g, 1.84 mmol), [KN(SiMe$_3$)$_2$] (1.46 g, 7.34 mmol): colourless crystals (0.55 g, 0.73 mmol, 53% based on [HB(Im^{t}Bu)$_3$]Br$_2$).

X-ray crystallography and NMR showed presence of toluene in the lattice. ^{1}H{^{11}B} NMR ppm (d$_8$-tol, 298 K): 7.47 (broad s, 1H, *H-7*), 7.33 (d, 3H, *H-5*, ^{3}J = 1.5 Hz), 7.19 (broad s, 1H, *H-10*), 6.65 (d, 3H, *H-4*, ^{3}J = 1.5 Hz), 6.55 (broad s, 1H, *H-9*), 5.00 (broad, 1H, B*H*), 1.39 (s, 27H, ligand C(C*H₃*)₃), 0.99 (s, 9H, co-ligand C(C*H₃*)₃), 0.27 (s, 18H, Si(C*H₃*)₃). ^{13}C{^{1}H} NMR ppm (d$_8$-tol, 298 K): 201.5 (C-2), 137.1 (C-7), 129.3 (C-10), 127.6 (C-5), 113.6 (C-4/9), 55.7 (ligand + co-ligand *C*(CH₃)₃), 31.2 (ligand C(*C*H₃)₃), 30.0 (co-ligand C(*C*H₃)₃), 2.59 (Si(*C*H₃)₃). ^{11}B{^{1}H} NMR ppm (d$_8$-tol, 298 K): 3.35 (*B*H). Anal. Calc. for C$_{34}$H$_{64}$BN$_9$Si$_2$Sr (753.5): C, 54.19; H, 8.56; N, 16.73%. Found: C, 54.29; H, 8.56; N, 16.79%.

Synthesis of [{HB(Im^{t}Bu)₃}Sr{N(SiMe₃)₂}(THF)] (74')
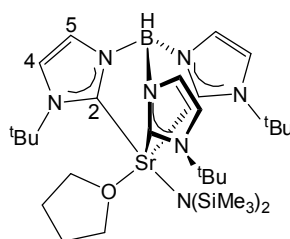
72 (1.33 g, 2.45 mmol), strontium iodide (0.31 g, 0.92 mmol), [KN(SiMe₃)₂] (0.73 g, 3.67 mmol), filtration through filter canula only, all glassware prewashed with a basic 2-propanol solution of potassium hydroxide before drying 1 day at 150 °C: colourless crystals after 1 day at -20 °C (0.26 g, 0.37 mmol, 40% based on SrI₂). A second crystallisation fraction yielded 0.15 g of **74**. ^{1}H{^{11}B} NMR ppm (d$_8$-tol): 7.20 (d, 3H, *H-5*, ^{3}J = 1.2 Hz), 6.48 (d, 3H, *H-4*, ^{3}J=1.2 Hz), 4.86 (broad, 1H, BH), 3.55 (m, 4H, THF), 1.39 (m, 4H, THF), 1.37 (s, 27H, C(C*H₃*)₃), 0.40 (s, 18H, Si(C*H₃*)₃). ^{13}C{^{1}H} NMR ppm (d$_8$-tol): 198.7 (C-2), 126.8 (C-5), 113.8 (C-4), 68.3 (THF), 55.3 (*C*(CH₃)₃), 31.3 (C(*C*H₃)₃), 25.5 (THF), 6.7 (Si(*C*H₃)₃). ^{11}B{^{1}H} NMR ppm (d$_8$-tol): 2.40 (*B*H). Anal. Calc. for C$_{31}$H$_{60}$BN$_7$OSi$_2$Sr (701.5): C, 53.08; H, 8.62; N, 13.98%. Found: C, 52.99; H, 8.55; N, 13.88%.

Synthesis of [{HB(Im^{t}Bu)$_3$}Ba{N(SiMe$_3$)$_2$}{N-(Im^{t}Bu)}$_{1.5}$] (75)
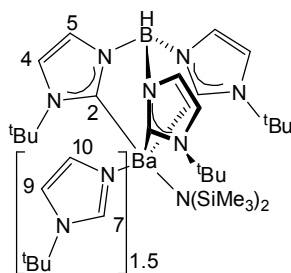
72 (1.00 g, 1.84 mmol), barium iodide (0.72 g, 1.84 mmol), [KN(SiMe$_3$)$_2$] (1.46 g, 7.34 mmol): colourless crystals in an oily mass of free 1-*tert*-butylimidazole (0.77 g, 0.89 mmol, 48% based on BaI$_2$). In solution each barium centre is solvated by two 1-*tert*-butylimidazole fragments due to the presence of free imidazole around the crystals. ^{1}H{^{11}B} NMR ppm (d$_8$-tol): 7.34 (broad s, 2H, *H-7*), 7.30 (s, 3H, *H-5*), 6.98 (s, 2H, *H-10*), 6.54 (s, 3H, *H-4*), 6.42 (s, 2H, *H-9*), 4.98 (broad, 1H, B*H*), 2.12 (m, tol), 1.30 (s, 27H, ligand C(C*H$_3$*)$_3$), 0.97 (s, 18H, co-ligand C(C*H$_3$*)$_3$), 0.51 (Si(C*H$_3$*)$_3$). ^{13}C{^{1}H} NMR ppm (d$_8$-tol): 205.9 (C-2), 147.5 (C-7), 135.5 (C-10), 126.5 (C-5), 115.5 (C-9), 113.1 (C-4), 55.0 (ligand *C*(CH$_3$)$_3$), 53.9 (co-ligand *C*(CH$_3$)$_3$), 31.2 (ligand C(*C*H$_3$)$_3$), 29.7 (co-ligand C(*C*H$_3$)$_3$), 6.5 (Si(*C*H$_3$)$_3$). Multiple attempts to obtain elemental analysis data of **75** failed due to the extreme air-, moisture- and temperature-sensitivity of the crystals.

Synthesis of [{HB(Im^{t}Bu)$_3$}CaI{N-(Im^{t}Bu)}] (76)
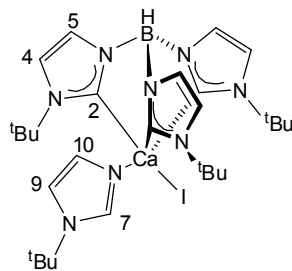
72 (0.5 g, 0.92 mmol), calcium iodide (0.27 g, 0.92 mmol), [KN(SiMe$_3$)$_2$] (0.55 g, 2.76 mmol): off-white powder after 2 days at -20 ºC (0.42 g, 0.62 mmol, 68%). ^{1}H{^{11}B} NMR ppm (d$_8$-tol): 7.91 (broad s, 1H, *H-7*), 7.19 (d, 3H, *H-5*, ^3J = 1.5 Hz), 6.55 (broad s, 1H, *H-10*), 6.44 (d, 3H, *H-4*, ^3J = 1.5 Hz), 6.10 (broad s, 1H, *H-9*), 4.88 (broad, 1H, B*H*), 1.31 (s, 27H, ligand C(C*H$_3$*)$_3$), 0.84 (s, 9H, co-ligand ligand C(C*H$_3$*)$_3$). ^{13}C{^{1}H} NMR ppm (d$_8$-tol): 195.5 (C-2), 129.0 (C-7), 125.4 (C-10), 125.0 (C-5), 115.3 (C-9), 113.4 (C-4), 54.3 (ligand +co-ligand *C*(CH$_3$)$_3$), 29.9 (ligand C(*C*H$_3$)$_3$), 28.8 (co-ligand

C(CH$_3$)$_3$). ^{11}B{^{1}H} NMR ppm (d$_8$-tol): 1.7 (*B*H). Anal. Calc. for C$_{28}$H$_{46}$BCaNI$_8$ (672.5): C, 50.01; H, 6.89; N, 16.66%. Found: C, 49.93; H, 6.87; N, 16.58%.

Synthesis of [{HB(Im^{t}Bu)$_3$}CaI(THF)] (76')
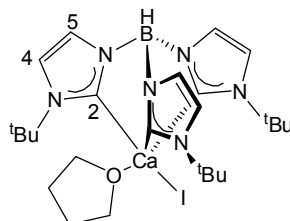
5-10% by-product of the synthesis of **76** detected in the ^{1}H NMR spectrum of the crude. Although colourless single crystals were isolated for X-ray crystallography, sufficient pure material was not available for NMR or elemental analysis.

6.8.2 Synthesis of tris(imidazolyl-2-ylidenyl)borate alkaline earth compounds 77 and 78: General Procedure:

In a glove-box, **72** and **36b** or **36c** were weighed at a 1:1.5 ratio into a dry Schlenk flask. Dry THF was added at -78 °C and the mixture was left to stir at room temperature overnight. The solvent was removed *in vacuo* and the crude product extracted with toluene. The mixture was stirred for another hour prior to canula filtration away from insoluble KI and concentration of the solution to incipient crystallisation. After 3-5 days at -20 ºC, the mother liquor was filtered into a second Schlenk flask and the transparent crystals completely dried on vacuum line.

Synthesis of [{HB(Im^{t}Bu)$_3$}CaBr]$_2$ (77)
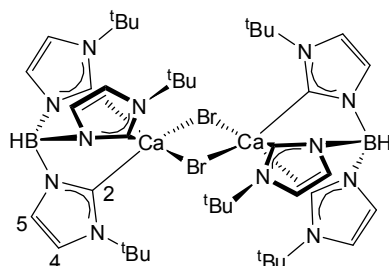
72 (0.5 g, 0.92 mmol) and **36b** (0.70 g, 1.38 mmol): colourless crystals after 2 days at -20 ºC (0.32 g, 0.64 mmol, 69%). ^{1}H{^{11}B} NMR ppm (d$_8$-tol): 7.24 (d, 3H, *H-5*, ^3J = 1.2

Hz), 6.53 (d, 3H, *H-4*, ^3J = 1.2 Hz), 4.94 (broad, 1H, B*H*), 1.54 (s, 27H, C(C*H$_3$*)$_3$). ^{13}C{^{1}H} NMR ppm (d$_8$-tol): 199.4 (C-2), 125.9 (C-5), 114.0 (C-4), 55.9 (*C*(CH$_3$)$_3$), 32.2 (C(*C*H$_3$)$_3$). ^{11}B{^{1}H} NMR ppm (d$_8$-tol): 1.91 (*B*H). Anal. Calc. for C$_{21}$H$_{34}$BBrCaN$_6$ (501.3): C, 50.31; H, 6.84; N, 16.76%. Found: C, 50.28; H, 6.76; N, 16.67%.

Synthesis of [{HB(Im^{t}Bu)$_3$}$_2$Sr] (78)
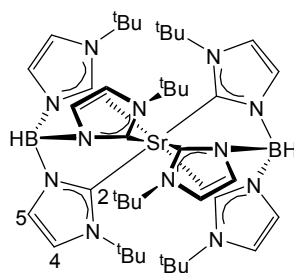
Redistribution product from the attempted synthesis of [{HB(Im^{t}Bu)$_3$}SrBr]$_2$: **72** (0.5 g, 0.92 mmol) and **36c** (0.76 g, 1.38 mmol): colourless crystals after 4 days at -20 °C (0.21 g, 0.25 mmol, 54% based on ligand). ^{1}H{^{11}B} NMR ppm (d$_8$-tol): 7.25 (d, 3H, *H-5*, ^3J = 1.5 Hz), 6.57 (d, 3H, *H-4*, ^3J = 1.5 Hz), 4.92 (s, 1H, B*H*), 1.31 (s, 27H, C(C*H$_3$*)$_3$). ^{13}C{^{1}H} NMR ppm (d$_8$-tol): 201.6 (C-2), 128.1 (C-5), 113.8 (C-4), 55.7 (*C*(CH$_3$)$_3$), 31.3 (C(*C*H$_3$)$_3$). ^{11}B{^{1}H} NMR ppm (d$_8$-tol): 3.84 (*B*H). Anal. Calc. for C$_{42}$H$_{68}$B$_2$N$_{12}$Sr (850.3): C, 59.33; H, 8.06; N, 19.77%. Found: C, 59.27; H, 8.14; N, 19.69%.

6.9 Dearomatisation and deprotonation of a bis(imino)pyridine ligand by group 2 dialkyls

Synthesis of [{2,6-(Dipp-NCCH$_2$)$_2$(C$_5$H$_3$N)}Mg(THF)$_2$] (86a)
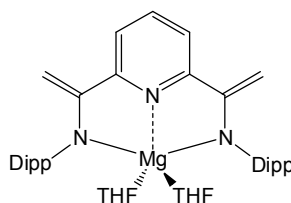
50 mg of **37a** (102.6 μmol) and 49 mg of ligand precursor **82** (102.6 μmol) were dissolved in C$_6$D$_6$. First slightly pink then slowly turning dark green, the reaction was followed by NMR at 60 °C temperature and reached completion after 1.5 days (NMR yield: 98%, colour: orange). Yellow crystals suitable for X-ray crystallography were isolated by recrystallisation from hexane at -30 °C (52 mg, 78%), m.p. 110 °C. ^{1}H NMR

ppm (C$_6$D$_6$): 7.56 (d, 2H, *m*-pyr-*H*, ^3J = 8.4 Hz), 7.25 (d, 4H, *m*-Ar-*H*, ^3J = 7.2 Hz), 7.27-7.18 (m, 2H, *p*-Ar-*H*), 7.09 (d, 1H, *p*-pyr-*H*, ^3J = 8.4 Hz), 4.66 (s, 2H, C=C*H$_2$*), 3.67 (s, 2H, C=C*H$_2$*), 3.56 (sept, 4H, ^{i}Pr-C*H*Me$_2$, ^3J = 6.7 Hz), 3.19 (m, 4H, THF), 1.46 (d, 12H, ^{i}Pr-C*H$_3$*, ^3J = 6.7 Hz), 1.17 (d, 12H, ^{i}Pr-C*H$_3$*, ^3J = 6.7 Hz), 1.06 (m, 4H, THF). ^{13}C{^{1}H} NMR ppm (C$_6$D$_6$): 155.9 (N-*C*=CH$_2$), 155.7 (N-*C*=CH$_2$) 152.7 (*i*-Ar-*C*), 145.7 (*o*-Ar-*C*), 137.5 (*p*-pyr-*C*), 124.0 (*m*-Ar-*C*), 123.4 (*p*-Ar-*C*), 117.5 (*m*-pyr-*C*), 79.3 (C=*C*H$_2$), 70.0 (THF), 28.4 (^{i}Pr-*C*HMe$_2$), 26.8 + 25.4 (^{i}Pr-*C*H$_3$), 25.2 (THF). IR (KBr): 3042, 2955, 2865, 1644, 1580, 1565, 1472, 1431, 1379, 1359, 1312, 1251, 1201, 1161, 1103, 1082, 1030, 995, 928, 885, 870, 815, 800, 771, 742, 693, 670,646. Anal. Calc. for C$_{41}$H$_{57}$MgN$_3$O$_2$ (648.2): C, 75.97; H, 8.86: N, 6.48%. Found: C, 75.87; H, 8.81: N, 6.51%.

*Monodeprotonated intermediate **85a** observed by NMR*
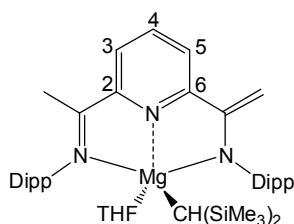
^{1}H NMR ppm (C$_6$D$_6$): 7.66 (dd, 1H, pyr-*H-5*, ^3J = 6.5 Hz, ^4J = 2.7 Hz), 6.88-6.94 (m, 2H, pyr-*H-3* + pyr-*H-4*), 4.60 (s, 1H, C=C*H$_2$*), 3.99 (s, 1H, C=C*H$_2$*), 3.54, 2.80 (2 septuplets, 2H:2H, ^{i}Pr-C*H*Me$_2$, ^3J = 6.5 Hz), 1.72 (s, 3H, N=CC*H$_3$*), 1.47, 1.43, 1.32, 0.94 (4 doublets, 6H:6H:6H:6H, ^{i}Pr-C*H$_3$*, ^3J = 6.5 Hz) 0.04 (s, 18H, CH(Si*Me$_3$*)$_2$), -1.57 (1H, s, C*H*(SiMe$_3$)$_2$).

*Synthesis of [{2,6-(Dipp-NCCH$_2$)$_2$(C$_5$H$_3$N)}Ca(THF)$_2$](**86b**)*
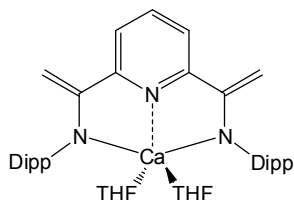
50 mg of **37b** (99.4 μmol) and 48 mg of ligand precursor **82** (99.4 μmol) were dissolved in C$_6$D$_6$. First dark green, the reaction mixture slowly turned yellow-green. The reaction was followed by NMR at room temperature and reached completion after 1.5 days (NMR yield: 98%). Orange crystals suitable for X-ray crystallography were isolated by recrystallisation from hexane at room temperature (55 mg, 83%), m.p. 112-114 °C. ^{1}H

NMR ppm (C$_6$D$_6$): 7.72 (d, 2H, *m*-pyr-*H*, ^3J = 8.0 Hz), 7.26 (d, 4H, *m*-Ar-*H*, ^3J = 7.2 Hz), 7.10-7.17 (m, 3H, *p*-pyr-*H* + *p*-Ar-*H*), 4.59 (s, 2H, C=C*H$_2$*), 3.65 (s, 2H, C=C*H$_2$*), 3.59 (sept, 4H, ^{i}Pr-C*H*Me$_2$, ^3J = 6.8 Hz), 3.12 (m, 4H, THF), 1.48 (d, 12H, ^{i}Pr-C*H$_3$*, ^3J = 6.8 Hz), 1.15 (d, 12H, ^{i}Pr-C*H$_3$*, ^3J = 6.8 Hz), 1.12 (m, 4H, THF). ^{13}C{^{1}H} NMR ppm (C$_6$D$_6$): 159.3 + 158.1 (N-*C*=CH$_2$) 151.3 (*i*-Ar-*C*), 144.7 (*o*-Ar-*C*), 136.5 (*p*-pyr-*C*), 123.5 (*m*-Ar-*C*), 122.2 (*p*-Ar-*C*), 118.4 (*m*-pyr-*C*), 76.5 (C=*C*H$_2$, identified by HMQC), 68.6 (THF), 28.2 (^{i}Pr-*C*HMe$_2$), 25.9 + 25.5 (^{i}Pr-*C*H$_3$), 25.2 (THF). IR (KBr): 3049, 2955, 2863, 1638, 1585, 1559, 1461, 1429, 1385, 1363, 1315, 1252, 1211, 1163, 1109, 1059, 1030, 992, 932, 884, 859, 818, 793, 770, 755, 748, 725, 672, 637. Anal. Calc. for C$_{41}$H$_{57}$CaN$_3$O$_2$: (664.0): C, 74.16; H, 8.65: N, 6.33%. Found: C, 74.06; H, 8.63; N, 6.36.

*Symmetric dearomatised intermediate **83b** observed by NMR*
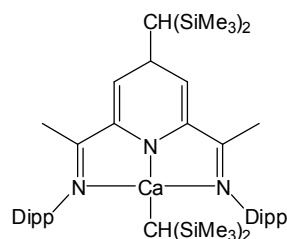
^{1}H NMR ppm (C$_6$D$_6$, 298 K): 5.00 (d, 2H, *m*-pyr-*H*, ^3J = 3.2 Hz), 4.69 (broad, 1H, *p*-pyr-*H*), 1.84 (s, 6H, N=CC*H$_3$*), 0.32 (pyr-C*H*(SiMe$_3$)$_2$), identified by COSY), −1.84 (s, 1H, CaC*H*(SiMe$_3$)$_2$).

*Asymmetric dearomatised intermediate **84b** observed by NMR*
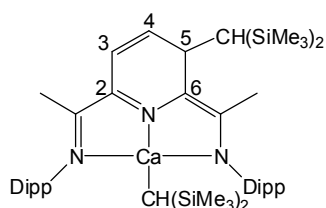
^{1}H NMR ppm (C$_6$D$_6$): 6.44 (d, 1H, pyr-*H-3*, ^3J = 10.1 Hz), 5.32 (dd, 1H, pyr-*H-4*, ^3J = 10.1 Hz, 4.9 Hz), 4.57 (broad, 1H, pyr-*H-5*), 1.80 and 1.77 (2 singlets, 3H each, N=CC*H$_3$*), 0.30 (pyr-C*H*(SiMe$_3$)$_2$, identified by COSY), -1.82 (1H, s, CaC*H*(SiMe$_3$)$_2$).

*Monodeprotonated intermediate **85b** observed by NMR*
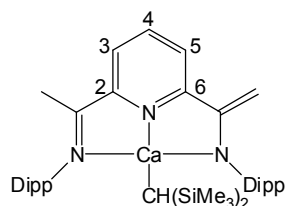
^{1}H NMR ppm (C$_6$D$_6$): 7.88 (d, 1H, pyr-*H-3*, ^3J = 8.1 Hz), 7.18 (m, 1H, pyr-*H-4*), 6.88 (d, 1H, pyr-*H-5*, ^3J = 7.5 Hz), 3.94 and 3.64 (two s, 1H each, C=C*H$_2$*), 1.68 (s, 3H, N=CC*H$_3$*), −1.82 (s, 1H, CaC*H*(SiMe$_3$)$_2$).

*Synthesis of [{2,6-(Dipp-NCCH$_2$)$_2$(C$_5$H$_3$N)}Sr(THF)]$_6$ (**86c**)*
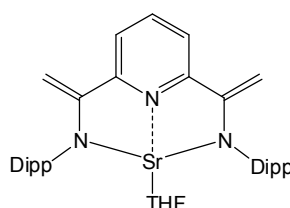
50 mg of **37c** (90.8 µmol) and 44 mg of ligand precursor **82** (90.8 µmol) were dissolved in C$_6$D$_6$. First dark blue, the reaction mixture quickly turned bright green. The reaction was followed by NMR at room temperature and reached completion after 4 hours (NMR yield: 95%). Bright red crystals suitable for X-ray crystallography were isolated by recrystallisation from hexane at room temperature (41 mg, 71%), m.p. 116 °C. ^{1}H NMR (C$_6$D$_6$): 7.76 (d, 2H, *m*-pyr-*H*, ^3J = 8.0 Hz), 7.26 (d, 4H, *m*-Ar-*H*, ^3J = 7.2 Hz), 7.04-7.18 (m, 3H, *p*-pyr-*H* + *p*-Ar-*H*), 4.53 (s, 2H, C=C*H$_2$*), 3.59 (s, 2H, C=C*H$_2$*), 3.57 (sept, 4H, ^{i}Pr-C*H*Me$_2$, ^3J = 6.8 Hz), 3.15 (m, 4H, THF), 1.47 (d, 12H, ^{i}Pr-C*H$_3$*, ^3J = 6.8 Hz), 1.16 (m, 4H, THF), 1.15 (d, 12H, ^{i}Pr-C*H$_3$*, ^3J = 6.8 Hz). ^{13}C{^{1}H} NMR ppm (C$_6$D$_6$): 160.1 (N-*C*=CH$_2$), 158.6 (N-*C*=CH$_2$) 151.4 (*i*-Ar-*C*), 144.4 (*o*-Ar-*C*), 136.2 (*p*-pyr-*C*), 123.6 (*m*-Ar-*C*), 121.8 (*p*-Ar-*C*), 118.8 (*m*-pyr-*C*), 75.8 (C=*C*H$_2$), 68.2 (THF), 28.2 (^{i}Pr-*C*HMe$_2$), 25.9 + 25.7 (^{i}Pr-C*H$_3$*), 25.4 (THF). IR (KBr): 3047, 2958, 2859, 1644, 1587, 1561, 1527, 1460, 1425, 1378, 1356, 1311, 1248, 1207, 1166, 1099, 1052, 1023, 998, 941, 855, 824, 795, 776, 760, 744, 732, 694, 665. Anal. Calc. for C$_{37}$H$_{49}$N$_3$OSr: (639.4): C, 69.50; H, 7.72; N, 6.57%. Found: C, 69.28; H, 7.83; N, 6.17%.

*Symmetric dearomatised intermediate **83c** observed by NMR*

^{1}H NMR ppm (C$_6$D$_6$, 298 K): 5.00 (d, 2H, *m*-pyr, ^3J = 3.2 Hz), 4.72 (m, 1H, *p*-pyr), 1.86 (s, 6H, N=CCH_3), 0.30 (pyr-CH(SiMe$_3$)$_2$, identified by COSY), -1.83 (s, 1H, SrCH(SiMe$_3$)$_2$).

*Asymmetric dearomatised intermediate **84c** observed by NMR*
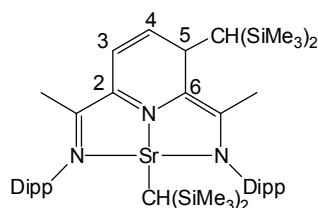
^{1}H NMR ppm (C$_6$D$_6$, 298 K): 6.22 (d, 1H, pyr-*H-3*, ^3J = 9.6 Hz), 5.34 (dd, 1H, pyr-*H-4*, ^3J = 9.6 Hz, 5.8 Hz), 4.34 (md, 1H, pyr-*H-5*, ^3J = 5.8 Hz), 1.80 and 1.72 (2 singlets, 3H each, N=CCH_3), 0.28 (pyr-CH(SiMe$_3$)$_2$, identified by COSY), −1.98 (1H, s, SrCH(SiMe$_3$)$_2$).

*Monodeprotonated intermediate **85c** observed by NMR*
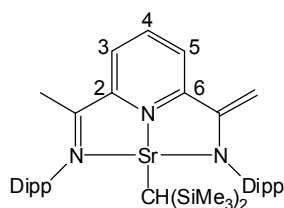
^{1}H NMR ppm (C$_6$D$_6$): 7.93 (d, 1H, pyr-*H-5*, ^3J = 8.3 Hz), 7.35 (m, 1H, pyr-*H-4*), 6.85 (d, 1H, pyr-*H-5*, ^3J = 7.6 Hz), 4.48 (s, 1H, C=CH_2), 3.86 (s, 1H, C=CH_2), 1.66 (s, 3H, N=CCH_3), -1.88 (s, 1H, SrCH(SiMe$_3$)$_2$).

Synthesis of [{2,6-(Dipp-NCCH₂)₂(C₅H₃N)}Ba(THF)]₆ (86d)
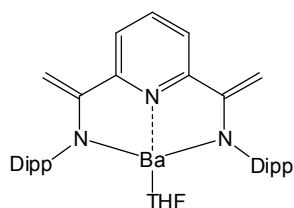
50 mg of **37d** (83.3 μmol) and 40 mg of ligand precursor **82** (83.3 μmol) were dissolved in C_6D_6. Instantly dark blue, the reaction mixture slowly turned brown-green, then dark brown. The reaction was followed by NMR at room temperature. All ligand was instantly consumed to form a dark blue intermediate which was then slowly transformed within 8 hours into the desired dark red product (NMR yield: 98%). Dark red crystals suitable for X-ray crystallography were isolated by recrystallisation from hexane at room temperature (42 mg, 73%), m.p. 132 ℃. ^{1}H NMR ppm (C_6D_6): 7.74 (d, 2H, *m*-pyr-*H*, ^3J = 8.0 Hz), 7.28 (d, 4H, *m*-Ar-*H*, ^3J = 7.2 Hz), 7.06-7.22 (m, 3H, *p*-pyr-*H* + *p*-Ar-*H*), 4.43 (s, 2H, C=C*H₂*), 3.45 (s, 2H, C=C*H₂*), 3.45 (sept, 4H, ^{i}Pr-C*H*Me₂, ^3J = 6.8 Hz), 3.26 (m, 4H, THF), 1.46 (d, 12H, ^{i}Pr-C*H₃*, ^3J = 6.8 Hz), 1.26 (m, 4H, THF), 1.15 (d, 12H, ^{i}Pr-C*H₃*, ^3J = 6.8 Hz). ^{13}C{^{1}H} NMR ppm (C_6D_6): 160.8 (N-*C*=CH₂), 158.8 (N-*C*=CH₂) 149.7 (*i*-Ar-*C*), 144.6 (*o*-Ar-*C*), 136.0 (*p*-pyr-*C*), 123.7 (*m*-Ar-*C*), 121.8 (*p*-Ar-*C*), 119.0 (*m*-pyr-*C*), 74.9 (C=*C*H₂), 67.9 (THF), 28.2 (^{i}Pr-*C*HMe₂), 26.0 + 25.8 (^{i}Pr-C*H₃*), 25.6 (THF). IR (KBr): 3047, 2955, 2860, 1638, 1581, 1559, 1530, 1461, 1432, 1382, 1356, 1321, 1249, 1201, 1169, 1100, 1055, 1027, 1005, 935, 878, 853, 824, 799, 774, 758, 742, 723, 698, 663. Anal. Calc. for $C_{37}H_{49}BaN_3O$ (689.3): C, 64.49; H, 7.17; N, 6.10%. Found: 64.38; H, 7.14; N, 6.04%.

*Symmetric dearomatised intermediate **83d** observed by NMR*
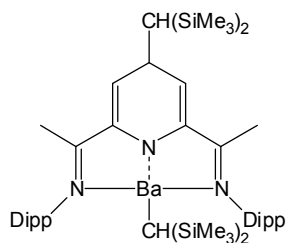
^{1}H NMR ppm (C_6D_6): 5.99 (d, 2H, *m*-pyr-*H*, ^3J = 3.6 Hz), 4.65 (dd, 1H, *p*-pyr-*H*, ^3J = 3.6 Hz, 7.0 Hz), 1.89 (s, 6H, N=CC*H₃*), 0.31 (pyr-C*H*(SiMe₃)₂), identified by COSY), -1.74 (s, 1H, BaC*H*(SiMe₃)₂).

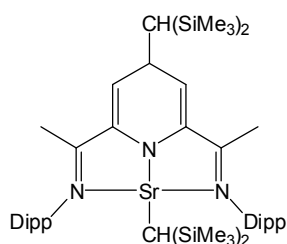*Asymmetric dearomatised intermediate **84d** observed by NMR*
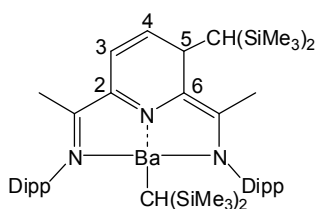
^{1}H NMR ppm (C$_6$D$_6$): 6.25 (d, 1H, pyr-*H-3*, ^3J = 9.6 Hz), 5.35 (dd, 1H, pyr-*H-4*, ^3J = 9.6 Hz, 5.9 Hz), 4.36 (dd, 1H, pyr-*H-5*, ^3J = 5.9 Hz, 2.9 Hz), 3.21, 3.12, 3.01 (3 septuplets, 1H:1H:2H, ^{i}Pr-C*H*Me$_2$, ^3J = 6.5 Hz), 1.82, 1.75 (2 singlets, 3H each, N=CC*H$_3$*), 0.29 (pyr-C*H*(SiMe$_3$)$_2$, identified by COSY), -1.87 (1H, s, BaC*H*(SiMe$_3$)$_2$).

*Synthesis of [2,6-(Dipp-N=CEt)$_2$(C$_5$H$_3$N)] (**87**)*
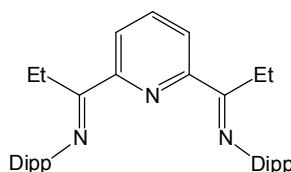
Methyl iodide (260 μL, 4.16 mmol) was added to a toluene solution of calcium complex **86b** (690 mg, 1.04 mmol). The orange mixture was heated at 60 ^{o}C for two days. The resultant colourless suspension was extracted with CH$_2$Cl$_2$ and the organic phase dried over MgSO$_4$ before removal of the solvent *in vacuo*, yielding a crude pale yellow solid which was recrystallised from cold CH$_2$Cl$_2$ (0.47 g, 0.92 mmol, 89%). ^{1}H NMR ppm (CDCl$_3$): 8.41 (d, 2H, *m*-pyr-*H*, ^3J = 7.5 Hz), 7.29 (t, 1H, *p*-pyr-*H*, ^3J = 7.5 Hz), 6.99-7.13 (m, 6H, Ar-*H*), 2.87 (sept, 4H, ^{i}Pr-C*H*Me$_2$, ^3J = 7.0 Hz), 2.76 (q, 4H, Et-C*H$_2$*, ^3J = 7.7 Hz), 1.14 + 1.16 (two overlapping d, 24H, ^3J = 7.0 Hz), 0.97 (t, 6H, Et-C*H$_3$*, ^3J = 7.7 Hz). ^{13}C{^{1}H} NMR ppm (CDCl$_3$): 170.5 (N=*C*), 154.9 (*o*-pyr-*C*), 146.6 (*i*-Ar-*C*), 137.3 (*p*-pyr-*C*), 135.6 (*o*-Ar-*C*), 124.1 (*m*-pyr-*C*), 123.3 (*m*-Ar-*C*), 123.2 (*p*-Ar-*C*), 28.7 (^{i}Pr-C*H*Me$_2$), 23.7 (^{i}Pr-*C*H$_3$), 22.2 (Et-*C*H$_2$), 11.1 (Et-*C*H$_3$). Anal. Calc. for C$_{35}$H$_{47}$N$_3$ (509.8): C, 82.46; H, 9.29; N, 8.24%. Found: C, 81.20; H, 9.15: N, 8.10%.

Synthesis of [{2,6-(Dipp-NC=CHMe)₂(C₅H₃N)}Sr(THF)₂] (91)
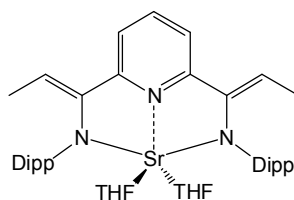
33 mg of **37c** (58.9 μmol) and 30 mg of ligand precursor **87** (58.9 μmol) were dissolved in C$_6$D$_6$. The solution instantly turned dark blue and ^{1}H NMR data showed complete conversion of the starting materials to a 1:2 mixture of the dearomatised complexes **88** and **89** respectively. The deep blue colour slowly faded into dark green and then dark red over a period of 3 days at room temperature, ultimately yielding compound **91** as a dark red compound (NMR yield 95%). ^{1}H NMR ppm (C$_6$D$_6$): 7.55 (d, 2H, *m*-pyr-*H*, ^3J = 7.9 Hz), 7.25 (d, 4H, *m*-Ar-*H*, ^3J = 7.3 Hz), 7.23 (t, 1H, *p*-pyr-*H*, ^3J = 7.9 Hz), 7.01 (t, 2H, *p*-Ar-*H*, ^3J = 7.3 Hz), 3.95 (q, 2H, C=C*H*CH₃, ^3J = 7.7 Hz), 3.60 (sept, 2H, ^{i}Pr-C*H*Me₂, ^3J = 7.0 Hz), 3.14-3.30 (m, 10H, ^{i}Pr-C*H*Me₂ + THF), 2.16 (d, 6H, C=CHC*H₃*, ^3J = 7.7 Hz), 1.43 (d, 12H, ^{i}Pr-C*H₃*, ^3J = 7.0 Hz), 1.19-1.21 (m, 20H, ^{i}Pr-C*H₃* + THF).

*Symmetric dearomatised intermediate **88** observed by NMR*
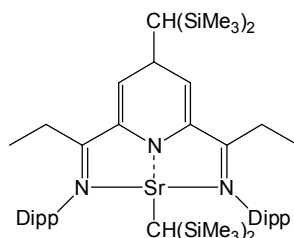
^{1}H NMR ppm (C$_6$D$_6$): 6.99-7.15 (m, 6H, Ar-*H*), 5.03 (d, 2H, *m*-pyr-*H*, ^3J = 3.4 Hz), 4.78 (dd, 1H, *p*-pyr-*H*, ^3J = 5.3, 3.4 Hz), 3.60 + 3.65 (two overlapping sept, 2H, ^{i}Pr-C*H*Me₂, ^3J = 7.3 Hz), 2.95 + 2.99 (two overlapping sept, 2H, ^{i}Pr-C*H*Me₂, ^3J = 7.3 Hz), 2.14 (q, 4H, Et-C*H₂*, ^3J = 7.7 Hz), 1.16-1.26 + 1.42-1.46 (two m, 24H, ^{i}Pr-C*H₃*), 1.10 (t, 6H, Et-C*H₃*, ^3J = 7.7 Hz), 0.39 (broad d, 1H, C-C*H*(SiMe₃)₂), 0.33 + 0.27 (two s, 18H each, Si*Me₃*), -1.89 (s, 1H, Sr-C*H*(SiMe₃)₂).

*Asymmetric dearomatised intermediate **88** observed by NMR*
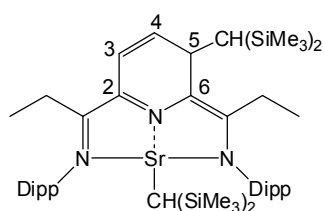
^{1}H NMR ppm (C$_6$D$_6$): 6.99-7.15 (m, 6H, Ar-*H*), 6.18 (d, 1H, *H-3*, ^3J = 10.2 Hz), 5.31 (dd, 1H, *H-4*, ^3J = 10.2, 5.7 Hz), 4.31 (dd, 1H, *H-5*, ^3J = 5.7, 1.8 Hz), 3.21 + 3.26 (two overlapping sept, 2H, ^{i}Pr-C*H*Me$_2$, ^3J = 6.6 Hz), 3.09 (sept, 1H, ^{i}Pr-C*H*Me$_2$, ^3J = 6.6 Hz), 2.81 (sept, 1H, ^{i}Pr-C*H*Me$_2$, ^3J = 7.2 Hz), 2.21 + 2.26 (two overlapping q, 4H, Et-C*H$_2$*, ^3J = 7.5 Hz), 1.16-1.26 + 1.42-1.46 (two m, 24H, ^{i}Pr-C*H$_3$*), 0.85 + 0.92 (two t, 3H each, Et-C*H$_3$*, ^3J = 7.5 Hz), 0.50 (broad s, 1H, C-C*H*(SiMe$_3$)$_2$), 0.17 + 0.27 (two s, 18H each, Si*Me$_3$*), -2.19 (s, 1H, Sr-C*H*(SiMe$_3$)$_2$).

*Monodeprotonated intermediate **89** observed by NMR*
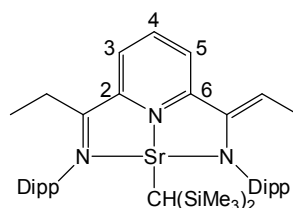
^{1}H NMR ppm (C$_6$D$_6$): 7.76 (d, 1H, *H-3*, ^3J = 7.9 Hz), 7.20 (t, 1H, *H-4*, ^3J = 7.9 Hz), 6.53 (d, 1H, *H-5*, ^3J = 7.9 Hz), 2.89-3.83 (m, ^{i}Pr-C*H*Me$_2$ + C=C*H*Me), 2.42 (q, 2H, Et-C*H$_2$*, ^3J = 8.8 Hz), 2.21 (d, 3H, C=CHC*H$_3$*, ^3J = 7.7 Hz), 1.08-1.28 (m, ^{i}Pr-C*H$_3$*), 0.98 (t, 3H, Et-C*H$_3$*, ^3J = 8.8 Hz), -2.18 (s, 1H, Sr-C*H*(SiMe$_3$)$_2$).

6.10   Dearomatisation of dipp-BIAN by group 1 and 2 alkyls

Numbering scheme for all compounds:
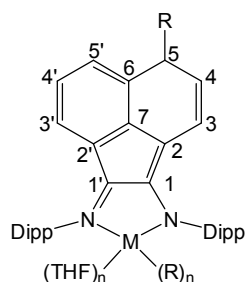
Synthesis of [{(C⁵-CH(SiMe₃)₂)(dipp-BIAN)}K]₂ (93)
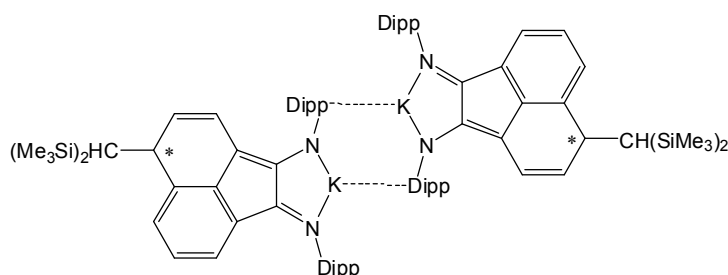
25 mg of [KCH(SiMe₃)₂] (99.8 μmol) and 50 mg of dipp-BIAN (99.8 μmol) were dissolved in C_6D_6. The reaction mixture turned instantly dark green (NMR yield >99%). Green crystals suitable for X-ray crystallography could be isolated upon crystallisation from toluene at room temperature. The reaction was later scaled up in toluene with [KCH(SiMe₃)₂] (396 mg, 2.00 mmol) and dipp-BIAN (1.00 g, 2.00 mmol), 95% isolated yield (1.32 g, 1.90 mmol). ^{1}H NMR ppm (C_6D_6): 7.00-7.21 (m, 6H, Ar-*H*), 6.51 (d, 1H, *H-3'*, ^3J = 7.5 Hz), 6.03 (t, 1H, *H-4'*, ^3J = 7.5 Hz), 5.65 (d, 1H, *H-5'*, ^3J = 7.5 Hz), 5.60 (d, 1H, *H-3*, $^3J_{cis}$ = 9.8 Hz), 4.65 (dd, 1H, *H-4*, $^3J_{cis}$ = 9.8 Hz, ^3J = 4.1 Hz) , 4.41 (broad, 1H, *H-5*), 3.59-3.60 (m, 2H, ^{i}Pr-C*H*Me₂), 3.06 + 2.98 (two sept, 1H each, ^{i}Pr-C*H*Me₂, ^3J = 6.7 Hz), 1.51 + 1.44 (two d, 3H each, ^{i}Pr-C*H₃*, ^3J = 6.7 Hz), 1.23 + 1.17 + 1.13 (three d, 9H: 3H: 6H, ^{i}Pr-C*H₃*, ^3J = 6.7 Hz), 0.55 (s, 1H, C-C*H*(SiMe₃)₂), 0.18 + 0.04 (two s, 9H each, C-CH(Si*Me₃*)₂). ^{13}C{^{1}H} NMR ppm (C_6D_6): 175.7 (*C-1'*), 153.9, 152.5, 148.7, 148.5, 141.8, 141.6, 136.6, 136.4, 129.9, 128.2, 127.9, 125.4, 124.4, 124.2, 123.7 (*C-5' + C-3*), 123.1, 123.0, 122.9, 121.2 (*C-4'*), 120.4, 116.8 (*C-4*), 102.7, 38.5 (*C-5*), 29.1 + 28.9 + 28.6 + 28.5 (^{i}Pr-*C*HMe₂), 25.2 (C-*C*H(SiMe₃)₂), 24.9 + 24.7 + 24.6 + 24.4 + 23.9 + 23.8 (^{i}Pr-*C*H₃), 2.3 + 2.1 (C-CH(Si*Me₃*)₂). Anal. Calc. for C₄₃H₅₉KN₂Si₂ (699.2): C, 73.86; H, 8.51; N, 4.01%. Found: C, 73.79; H, 8.59; N, 3.96%.

Synthesis of [{(C⁵-CH(SiMe₃)₂)(dipp-BIAN)}Mg{CH(SiMe₃)₂}(THF)] (94)
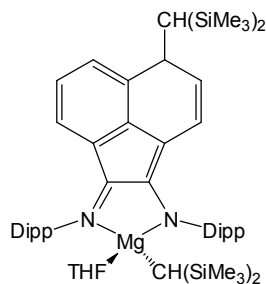
50 mg of **37a** (103.9 μmol) and 52 mg of dipp-BIAN (103.9 μmol) in C_6D_6. The reaction mixture was heated at 60 °C over night and slowly turned dark green. ^{1}H NMR

data showed the clean formation of complex **94** as the sole product of the reaction (NMR yield 100%). The reaction was scaled up (**37a** 271 mg, 0.599 mmol; dipp-BIAN 300 mg, 0.599 mmol), heated for 24 hours at 60 $^{\circ}$C in toluene before the solvent was removed *in vacuo*. Due to failure to recrystallise the crude solid from minimal amount of pentane, even after months of storage at -30 $^{\circ}$C, complex **94** was used as a crude green solid, whose purity was confirmed by NMR and elemental analysis data. ^{1}H NMR ppm (C_6D_6): 7.15-7.25 (m, 6H, Ar-*H*), 6.45 (d, 1H, *H-3'*, ^3J = 7.7 Hz), 6.05 (t, 1H, *H-4'*, ^3J = 7.7 Hz), 5.47 (dd, 1H, *H-3*, $^3J_{cis}$ = 10.2 Hz, ^4J = 2.3 Hz), 5.44-5.47 (m, 1H, *H-5'*), 5.05 (dd, 1H, *H-4*, $^3J_{cis}$ = 10.2, ^3J = 4.4Hz), 4.07 (m, 1H, *H-5*), 3.78 (broad m, THF), 3.55 + 3.11 (two sept, 2H each, [i]Pr-C*H*Me$_2$, ^3J = 6.8 Hz), 1.41-1.44 (m, 14H, [i]Pr-C*H$_3$* + THF), 1.39 + 1.36 + 1.31 + 1.29 + 1.16 + 1.13 (six d, 3H each, [i]Pr-C*H$_3$*, ^3J = 6.8 Hz)), 0.46 (d, 1H, C-C*H*(SiMe$_3$)$_2$, ^3J = 1.6 Hz), 0.00 (s, 18H, Mg-CH(Si*Me$_3$*)$_2$), 0.01 + -0.03 (two s, 9H each, C-CH(Si*Me$_3$*)$_2$), -1.59 (s, 1H, Mg-C*H*(SiMe$_3$)$_2$). ^{13}C{^{1}H} NMR ppm (C_6D_6): 181.9 (*C-1'*), 149.5, 148.8, 148.2, 146.5, 144.5, 139.5, 139.4, 133.1, 133.0 (*C-3'*), 131.8, 127.2, 126.0, 125.8 (*C-4*), 125.2, 124.9, 124.8 (*C-5'*), 124.6, 124.5, 124.0, 123.4 (*C-4'*), 122.6 (*C-3*), 122.1, 111.8 (*C-2*), 68.9 (THF, very broad), 38.4 (*C-5*), 29.1 + 28.9 + 28.6 + 28.6 ([i]Pr-*C*HMe$_2$), 25.9 + 25.33 + 25.29 + 25.27 + 25.1 + 24.9 + 24.8 + 24.7 ([i]Pr-*C*H$_3$), 23.9 (THF), 22.7 (C-*C*H(SiMe$_3$)$_2$), 5.6 (Mg-CH(Si*Me$_3$*)$_2$), 2.1 + 1.0 (C-CH(Si*Me$_3$*)$_2$), -3.1 (Mg-*C*H(SiMe$_3$)$_2$). Anal. Calc. for $C_{54}H_{86}MgN_2OSi_4$ (915.9): C, 70.81; H, 9.46; N, 3.06%. Found: C, 70.79; H, 9.36; N, 2.95%.

*Synthesis of [{(C[5]-CH(SiMe$_3$)$_2$)(dipp-BIAN)}Ca{CH(SiMe$_3$)$_2$}(THF)$_2$] (**95**)*
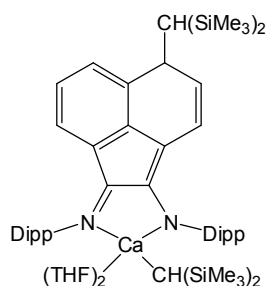
50 mg of **37b** (99.8 μmol) and 50 mg of dipp-BIAN (99.8 μmol) were dissolved in C_6D_6. The reaction mixture turns instantly dark green. ^{1}H NMR data showed the clean formation of complex **95** as the sole product of the reaction (NMR yield 100%). The reaction was scaled up (**37b** 1.00 g, 2 mmol; dipp-BIAN 1.00 g, 2 mmol), stirred for 10 minutes at room temperature in toluene before the solvent was removed *in vacuo*. Due to failure to recrystallise the crude solid from minimal amount of pentane, even after

months of storage at -30 °C, complex **95** was used as a crude dark green solid, whose purity was confirmed by NMR and elemental analysis data. ^{1}H NMR ppm (C$_6$D$_6$): 7.15-7.26 (m, 6H, Ar-*H*), 6.46 (d, 1H, *H-3'*, ^3J = 7.7 Hz), 6.06 (t, 1H, *H-4'*, ^3J = 7.7 Hz), 5.43-5.47 (m, 2H, *H-5'* + *H-3*), 4.96 (dd, 1H, $^3J_{cis}$ = 10.2, ^3J = 4.4 Hz), 4.12 (m, 1H, *H-5*), 3.62 (sept, 2H, ^{i}Pr-C*H*Me$_2$, ^3J = 6.8 Hz), 3.51 (broad m, THF), 3.24 (sept, 2H, ^{i}Pr-C*H*Me$_2$, ^3J = 6.7 Hz), 1.49 (d, 6H each, ^{i}Pr-C*H$_3$*, ^3J = 6.7 Hz), 1.41 + 1.34 (two d, 3H each, ^{i}Pr-C*H$_3$*, ^3J = 6.8 Hz), 1.18-1.31 (m, 20H, THF + ^{i}Pr-C*H$_3$*), 0.48 (d, 1H, C-C*H*(SiMe$_3$)$_2$, ^3J = 1.6 Hz), 0.21 (s, 18H, Ca-CH(Si*Me$_3$*)$_2$), 0.04 + 0.00 (two s, 9H each, C-CH(Si*Me$_3$*)$_2$), -1.72 (s, 1H, Ca-C*H*(SiMe$_3$)$_2$). ^{13}C{^{1}H} NMR ppm (C$_6$D$_6$): 181.7 (*C-1'*), 150.1, 149.7, 148.2, 146.1, 143.3, 142.7, 138.8, 137.0, 132.5 (*C-3'*), 131.2, 126.4, 126.2, 124.5, 124.5 (*C-3*), 124.4, 124.0, 123.8, 123.5 (*C-4*), 123.1, 122.7 (*C-5'*), 122.6 (*C-4'*), 110.7 (*C-2*), 69.6 (THF, very broad), 38.3 (*C-5*), 29.3 + 29.2 + 28.9 + 28.5 (^{i}Pr-C*H*Me$_2$), 26.0 + 25.6 + 25.3 + 25.2 + 25.2 + 24.7 + 24.4 + 24.3 (^{i}Pr-C*H$_3$*), 25.3 (THF), 23.4 (C-*C*H(SiMe$_3$)$_2$), 14.3 (Ca-*C*H(SiMe$_3$)$_2$), 6.1 (Ca-CH(Si*Me$_3$*)$_2$), 2.1 + 1.0 (C-CH(Si*Me$_3$*)$_2$). Anal. Calc. for C$_{58}$H$_{94}$CaN$_2$O$_2$Si$_4$ (1003.8): C, 69.40; H, 9.44; N, 2.79%. Found: C, 69.34; H, 9.34; N, 2.73%.

*Synthesis of [{(C^5-CH(SiMe$_3$)$_2$)(dipp-BIAN)}Sr{CH(SiMe$_3$)$_2$}(THF)$_2$] (**96**)*
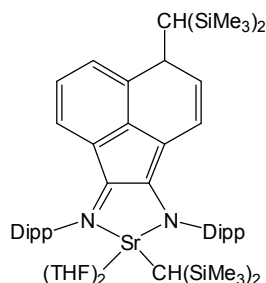
50 mg of **37c** (90.8 μmol) and 45 mg of dipp-BIAN (90.8 μmol) were dissolved in C$_6$D$_6$. The reaction mixture turns instantly dark green. ^{1}H NMR data showed the clean formation of complex **96** as the sole product of the reaction (NMR yield 100%). The reaction was scaled up (**37b** 551 mg, 1 mmol; dipp-BIAN 0.50 g, 1 mmol), stirred for 10 minutes at room temperature in toluene before the solvent was removed *in vacuo*. Due to failure to recrystallise the crude solid from minimal amount of pentane, even after months of storage at -30 °C, complex **96** was used as a crude dark green solid, whose purity was confirmed by NMR and elemental analysis data. ^{1}H NMR ppm (C$_6$D$_6$): 6.97-7.16 (m, 6H, Ar-*H*), 6.45 (d, 1H, *H-3'*, ^3J = 7.7 Hz), 6.06 (t, 1H, *H-4'*, ^3J = 7.7 Hz), 5.41 (dd, 1H, *H-3*, $^3J_{cis}$ = 10.2 Hz, ^4J = 2.1 Hz), 5.40-5.42 (m, 1H, *H-5'*), 4.89

214

(dd, 1H, *H-4*, $^3J_{cis}$ = 10.2, ^3J =4.6 Hz), 4.15 (m, 1H, *H-2*), 3.68 (sept, 2H, ^{i}Pr-C*H*Me$_2$, ^3J = 6.8 Hz), 3.37 (broad m, THF), 3.27 (sept, 2H, ^{i}Pr-C*H*Me$_2$, ^3J = 6.7 Hz), 1.53 + 1.52 (two d, 3H each, ^{i}Pr-C*H$_3$*, ^3J = 6.7 Hz), 1.38 + 1.36 (two d, 3H each, ^{i}Pr-C*H$_3$*, ^3J = 6.8 Hz), 1.25-1.31 (m, 20H, ^{i}Pr-C*H$_3$* + THF), 0.49 (d, 1H, C-C*H*(SiMe$_3$)$_2$, ^3J = 1.6 Hz), 0.30 (s, 18H, Sr-CH(Si*Me$_3$*)$_2$), 0.06 + -0.01 (two s, 9H each, C-CH(Si*Me$_3$*)$_2$), -1.86 (s, 1H, Sr-C*H*(SiMe$_3$)$_2$). ^{13}C{^{1}H} NMR ppm (C$_6$D$_6$): 181.1 (*C-1'*), 151.1, 150.2, 149.0, 146.9, 143.3, 142.6, 138.6, 138.4, 132.4 (*C-3'*), 131.0, 126.3, 125.9, 124.5 (*C-5'*), 124.2, 124.3, 123.7, 123.1, 123.0, 122.9 (*C-3*), 122.5 (*C-4*), 122.2 (*C-4'*), 109.5 (*C-2*), 69.4 (THF, very broad), 38.4 (*C-5*), 29.5 + 29.3 + 29.0 + 28.6 (^{i}Pr-*C*HMe$_2$), 26.0 + 25.7 + 25.4 + 25.3 + 25.2 + 24.9 + 24.4 + 24.3 (^{i}Pr-*C*H$_3$), 25.3 (THF), 23.6 (C-*C*H(SiMe$_3$)$_2$), 19.1 (Sr-CH(Si*Me$_3$*)$_2$), 6.4 (Sr-CH(Si*Me$_3$*)$_2$), 2.2 + 1.1 (C-CH(Si*Me$_3$*)$_2$). Anal. Calc. for C$_{58}$H$_{94}$N$_2$O$_2$Si$_4$Sr (1051.3): C, 66.26; H, 9.01; N, 2.66%. Found: C, 66.33; H, 8.97; N, 2.70%.

Synthesis of [{(C^5-CH(SiMe$_3$)$_2$)(dipp-BIAN)}Ba{CH(SiMe$_3$)$_2$}(THF)$_2$] (97)
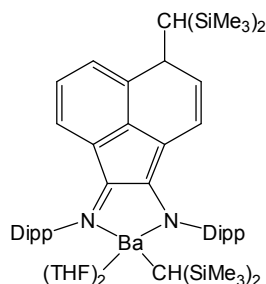
50 mg of **37d** (83.3 µmol) and 42 mg of dipp-BIAN (83.3 µmol) were dissolved in C$_6$D$_6$. The reaction mixture turns instantly dark green. ^{1}H NMR shows presence of three components among which the heteroleptic barium alkyl complex **97** (70%) and the homoleptic barium complex **98** (20%). Upon recrystallisation of the crude mixture from toluene at -30 °C for a week, orange crystals of compound **99** suitable for X-ray diffraction analysis were isolated from the reaction mixture. The amount of **99** which was isolated was, however, insufficient for the acquisition of both NMR and elemental analysis data. Although attempts to separate **97** and **98** by recrystallisation failed preventing the acquisition of elemental analysis data, compound **98** could be synthesised in high purity by independent methods (*vide infra*). ^{1}H NMR ppm (C$_6$D$_6$) for **97**: 7.08-7.23 (m, 6H, Ar-*H*), 6.48 (d, 1H, *H-3'*, ^3J = 7.7 Hz), 6.08 (t, 1H, *H-4'*, ^3J = 7.7 Hz), 5.47-5.51 (m, 2H, *H-5'* + *H-4*), 4.88 (dd, 1H, *H-4*, $^3J_{cis}$ = 10.2, ^3J = 4.4Hz), 4.21 (m, 1H, *H-5*), 3.69 (sept, 2H, ^{i}Pr-C*H*Me$_2$, ^3J = 6.8 Hz), 3.32 (broad m, 8H, THF),

3.27 (sept, 2H, ^{i}Pr-CHMe$_2$, ^3J = 6.7 Hz), 1.53 + 1.49 (two d, 3H each, ^{i}Pr-CH_3, ^3J = 6.7 Hz), 1.37 + 1.34 (two d, 3H each, ^{i}Pr-CH_3, ^3J = 6.8 Hz), 1.22-1.32 (m, 20H, THF + ^{i}Pr-CH_3), 0.50 (d, 1H, C-CH(SiMe$_3$)$_2$, ^3J = 1.6 Hz), 0.29 (s, 18H, Ba-CH(SiMe_3)$_2$), 0.09 + 0.04 (two s, 9H each, C-CH(SiMe_3)$_2$), -1.73 (broad s, 1H, Ba-CH(SiMe$_3$)$_2$). ^{13}C{^{1}H} NMR ppm (C$_6$D$_6$): 179.9 (*C-1'*), 150.8, 149.8, 148.8, 147.0, 143.2, 142.7, 138.0, 135.7, 132.2 (*C-3'*), 131.1, 126.1, 125.6, 124.4 (*C-5'*), 124.2, 124.0, 123.9, 123.8, 123.6, 123.2, 122.9 (*C-3*), 122.6 (*C-4*), 122.0 (*C-4'*), 107.5 (*C-2*), 68.3 (THF, very broad), 38.4 (*C-5*), 33.8 (Ba-CH(SiMe_3)$_2$), 29.6 + 29.5 + 29.0 + 28.8 (^{i}Pr-CHMe$_2$), 25.6 + 25.5 + 25.2 + 25.1 + 25.0 + 24.9 + 24.5 + 24.3 (^{i}Pr-CH$_3$), 25.4 (THF), 23.8 (C-CH(SiMe$_3$)$_2$), 6.1 (Ba-CH(SiMe$_3$)$_2$), 2.2 + 1.4 (C-CH(SiMe_3)$_2$).

Independent syntheses of [{(C^5-CH(SiMe$_3$)$_2$)(dipp-BIAN)}$_2$Ba (THF)$_2$] (98)
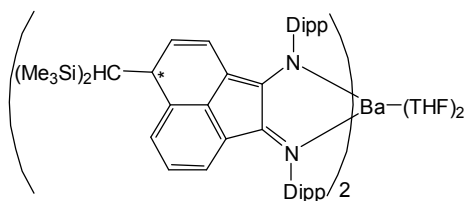
a) 15 mg of **37d** (25.0 μmol) and 25 mg of dipp-BIAN (50 μmol) were dissolved in d$_8$-toluene at room temperature. After 10 minutes the solution had turned a homogeneous dark green. ^{1}H NMR data showed the clean formation of **98** as the sole product of the reaction. b) [KCH(SiMe$_3$)$_2$] (300 mg, 1.50 mmol) and **37d** (455 mg, 0.75 mmol) were stirred in THF at room temperature for 24 hours prior to removal of the solvent *in vacuo* and extraction into toluene. Removal of the solvent yielded complex **98** as a crude dark green solid whose ^{1}H NMR spectrum was reminiscent of that obtained from the reaction described in a). ^{1}H NMR ppm (d$_8$-tol): 6.84-7.32 (m, 12H, Ar-H), 6.46 (d, 2H, *H-3'*, ^3J = 7.7 Hz), 6.00 (t, 2H, *H-4'*, ^3J = 7.7 Hz), 5.34 (dd, 2H, *H-5'*, ^3J = 7.7 Hz, ^4J = 4.2 Hz), 5.17 (dd, 2H, *H-3*, $^3J_{cis}$ = 10.2 Hz, ^4J =1.5 Hz), 4.77 (dd, 2H, *H-4*, $^3J_{cis}$ = 10.2, ^3J = 4.3 Hz), 4.16 (broad s, 2H, *H-5*), 3.46-3.62 (m, 12H, THF + ^{i}Pr-CHMe$_2$), 3.09 (sept, 4H, ^{i}Pr-CHMe$_2$, ^3J = 6.6 Hz), 1.45 (m, 8H, THF), 1.38 + 1.35 (two d, 6H each, ^{i}Pr-CH_3, ^3J = 6.7 Hz), 1.24 (d, 6H, ^{i}Pr-CH_3, ^3J = 6.8 Hz), 1.03-1.14 (m, 30H, ^{i}Pr-CH_3), 0.49 (broad s, 2H, CH(SiMe$_3$)$_2$, ^3J = 1.6 Hz), 0.02 + -0.04 (two s, 9H each, SiMe_3). ^{13}C{^{1}H} NMR ppm (d$_8$-tol): 180.3 (*C-1'*), 151.0, 150.70, 150.69, 149.9, 147.69, 147.64, 143.7, 143.25, 143.22, 138.73, 138.70, 138.61, 138.56, 138.15, 138.23, 137.47, 137.57, 132.5, 131.1, 126.7, 126.0, 124.9, 124.65, 124.71, 124.6, 123.77, 123.73, 123.5, 122.3, 122.1, 109.22,

109.19, 68.0 (THF, broad), 38.8 (*C-5*), 29.9 + 29.7 + 29.5 + 29.1 +28.8 (^{i}Pr-*C*HMe$_2$),
26.24 + 26.18 + 26.11 + 25.9 + 25.5 + 24.4 + 23. 8 (^{i}Pr-*C*H$_3$), 25.1 (THF), 23.4 + 23.2
(*C*H(SiMe$_3$)$_2$), 2.8 + 1.3 (Si*Me$_3$*).

*Independent syntheses of [{(C^5-CH(SiMe$_3$)$_2$)(dipp-BIAN)}$_2$Ca (THF)] (**100**)*
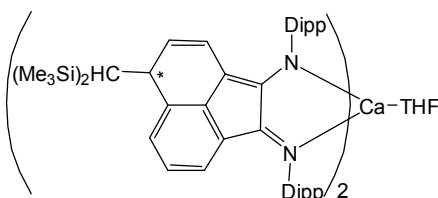
[KCH(SiMe$_3$)$_2$] (300 mg, 1.50 mmol) and **37b** (379 mg, 0.75 mmol) were stirred in
THF at room temperature for 24 hours prior to removal of the solvent *in vacuo* and
extraction into hexane. Removal of the solvent yielded complex **100** as a crude dark
green solid which was recrystallised from a 10:1 toluene/THF mixture at -30 $^{\circ}$C over
several days, yielding complex **100** as dark green solid (265 mg, 25%) in a first fraction
and green crystals in a second one. Due to apparent fluxional behaviour in solution ^{1}H
NMR peaks were extremely broad and ^{13}C{^{1}H} NMR signals too weak for analysis. ^{1}H
NMR (C$_6$D$_6$): 6.99-7.25 (m, 12H, Ar-*H*), 6.45 (broad d, 2H, *H-3'*, ${}^{3}J$ = 7.7 Hz), 6.05
(broad t, 2H, *H-3'*, ${}^{3}J$ = 7.7 Hz), 5.23-5.38 (broad m, 4H, *H-3/4*), 4.99 (broad d, 2H, *H-5'*, ${}^{3}J$ = 7.7 Hz), 4.18 (s, 2H, *H-5*), 3.60 (broad m, 4H, THF), 2.99-3.44 (broad m, 8H,
^{i}Pr-C*H*Me$_2$), 0.68-1.34 (broad m, 52H each, ^{i}Pr-C*H$_3$* + THF), 0.51 (broad s, 1H, C-C*H*(SiMe$_3$)$_2$), 0.05 + -0.04 (two broad s, 9H each, C-CH(Si*Me$_3$*)$_2$). Anal. Calc. for
C$_{90}$H$_{126}$CaN$_4$OSi$_4$ (1432.4): %C, 75.46; H, 8.87; N, 3.91%. Found: C, 75.29; H, 8.74; N,
3.84%.

*Synthesis of [{(C^5-CH(SiMe$_3$)(2-NMe$_2$-Ph))(dipp-BIAN)}K]$_6$ (**101**)*
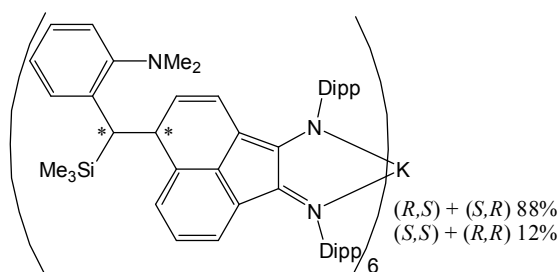
[K{CH(SiMe$_3$)(2-NMe$_2$-Ph)}] (25 mg, 83.5 µmol) and dipp-BIAN (42 mg, 83.5 µmol)
were dissolved in d$_8$-toluene. The solution instantly turned dark green. Crystallisation
after one day at room temperature afforded dark green crystals of the (*R,S*) + (*S,R*)

diastereomer of complex **101** (51 mg, 68.3 μmol 82%). ^{1}H NMR ppm (d$_8$-tol) of the major (*R,S*) + (*S,R*) diastereomer (88%): 6.88-7.20 (m, 10H, Ar-*H*), 6.04 (d, 1H, *H-3'*, ^3J = 7.7 Hz), 5.60 (t, 1H, *H-4'*, ^3J = 7.7 Hz), 5.44-5.50 (m, 2H, *H-3/5'*), 4.63-4.67 (m, 1H, *H-4*), 3.81 (broad s, 1H, *H-5*), 3.49 (sept, 2H, ^{i}Pr-C*H*Me$_2$, ^3J = 6.7 Hz), 3.35 (s, 1H, C*H*(SiMe$_3$)), 2.95 (sept, 1H, ^{i}Pr-C*H*Me$_2$, ^3J = 6.6 Hz), 2.85 (broad m, 1H, ^{i}Pr-C*H*Me$_2$), 2.33 (s, 6H, N*Me$_2$*), 1.52 (d, 3H, ^{i}Pr-C*H$_3$*, ^3J = 6.6 Hz), 1.30-1.44 (m, 6H, ^{i}Pr-C*H$_3$*), 0.98-0.19 (m, 12H, ^{i}Pr-C*H$_3$*), 0.81 (d, 3H, ^{i}Pr-C*H$_3$*, ^3J = 6.7 Hz), -0.03 (s, 9H, Si*Me$_3$*); minor (*R,R*) + (*S,S*) diastereomer (12%): 6.66 (d, 1H, *H-3'*, ^3J = 7.7 Hz), 5.85-5.88 (m, 1H, *H-4'*), 3.46-3.49 (m, 1H, *H-3/5'*), 4.78 (broad d, 1H, *H-4*, $^3J_{cis}$ = 10.1 Hz), 3.81 (broad s, 1H, *H-5*), 3.53 (m, 2H, ^{i}Pr-C*H*Me$_2$ + C*H*(SiMe$_3$), identified by COSY), 2.95 + 2.85 (two broad sept, 1H each, ^{i}Pr-C*H*Me$_2$), 2.45 (s, 6H, N*Me$_2$*), 0.99-1.57 (m, 24H, ^{i}Pr-C*H$_3$*), 0.00 (s, 9H, Si*Me$_3$*). ^{13}C{^{1}H} NMR ppm (d$_8$-tol), mixture of both diastereomers: 174.1 (C-1), 153.2, 152.6, 148.0, 141.1, 140.8, 140.1, 137.8, 137.7, 137.6, 137.2, 137.1, 136.1, 135.1, 132.1 (C-3'), 128.1, 125.3, 123.8, 123.7, 123.5, 123.0 (C-3/5'), 122.5 (C3/5'), 120.7, 119.3 (C-4'), 111.8 (C-4), 45.1 (N*Me$_2$*), 42.1 (C-5), 40.1 (*C*H(SiMe$_3$)), 29.2 +29.1 + 28.8 + 28.4 (^{i}Pr-*C*HMe$_2$), 25.7 + 25.2 + 25.1 + 24.5 + 24.4 + 24.2 + 23.5 + 23.4 + 23.2 (^{i}Pr-C*H$_3$*), -0.04 (Si*Me$_3$*). Anal. Calc. for C$_{288}$H$_{360}$K$_6$N$_{18}$Si$_6$ (4477.14): %C, 77.26; H, 8.10; N, 5.63. Found: %C, 77.22; H, 8.19; N, 5.58.

6.11 ^{1}H NMR spectra of compounds lacking elemental analysis data and/or crystal structures

Figure 76. ^{1}H NMR spectrum of complex **64**.
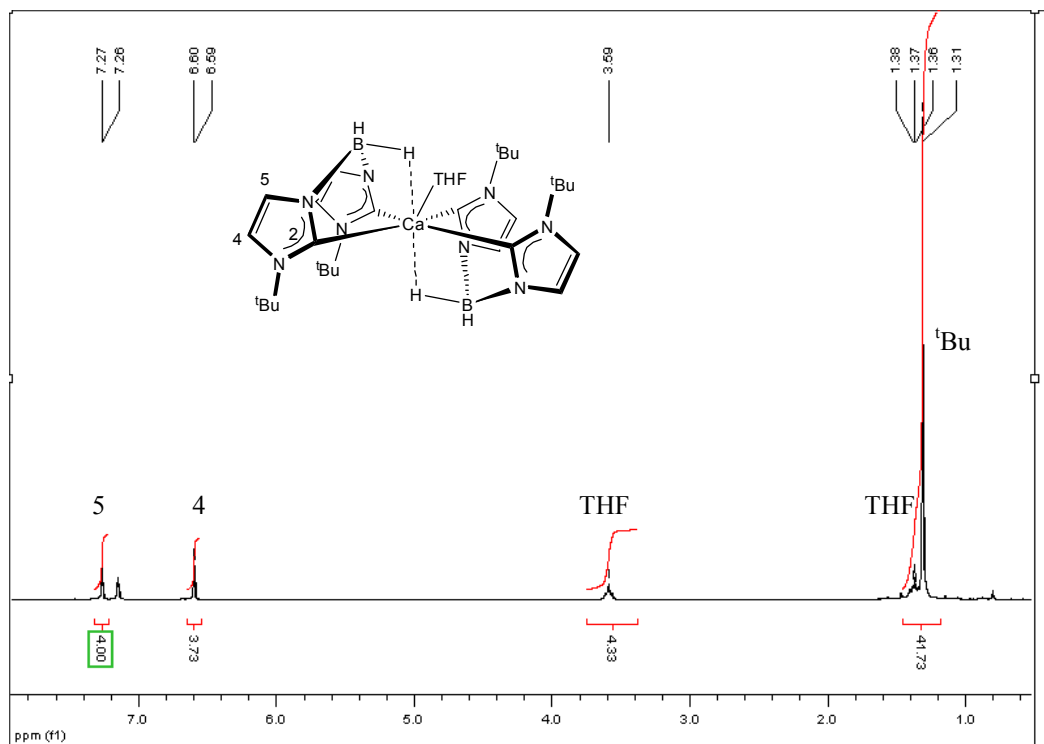
Figure 77. ^{1}H NMR spectrum of complex **65**.
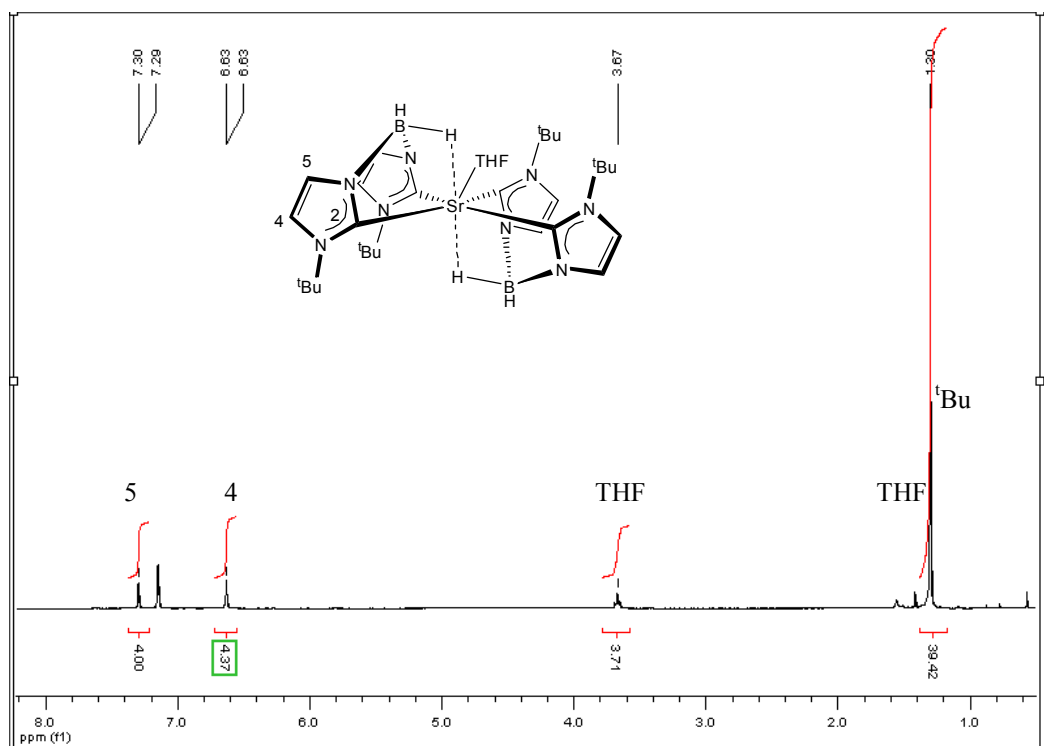
Figure 78. ^{1}H NMR spectrum of complex **66**.
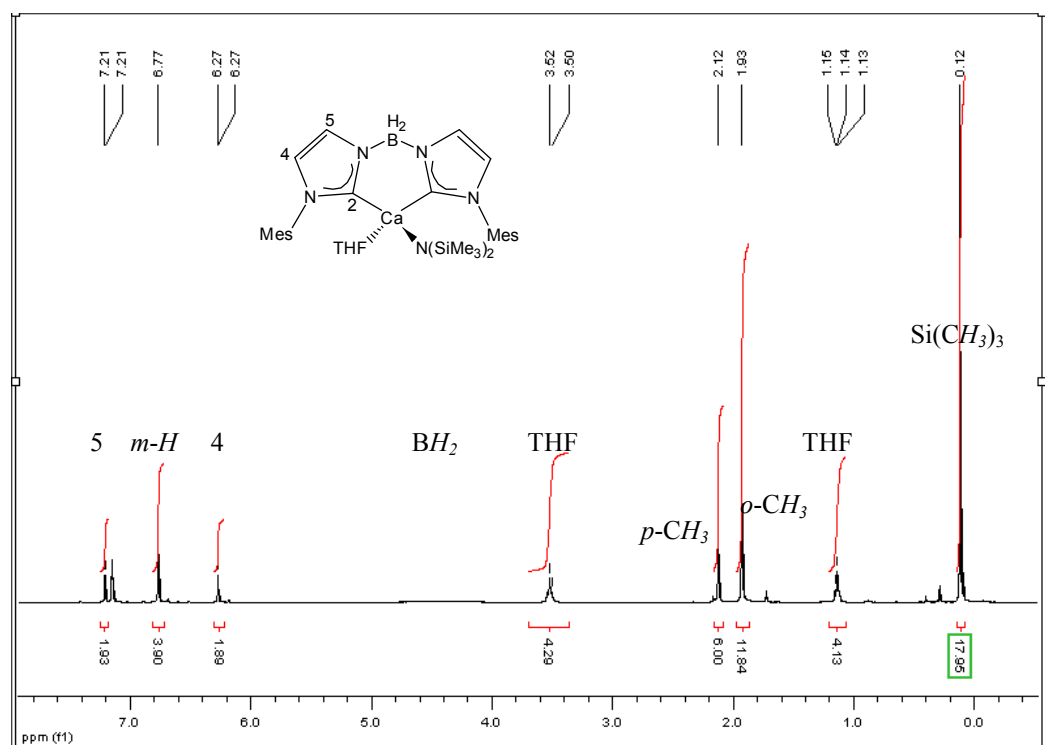
Figure 79. ^{1}H NMR spectrum of complex **75**.
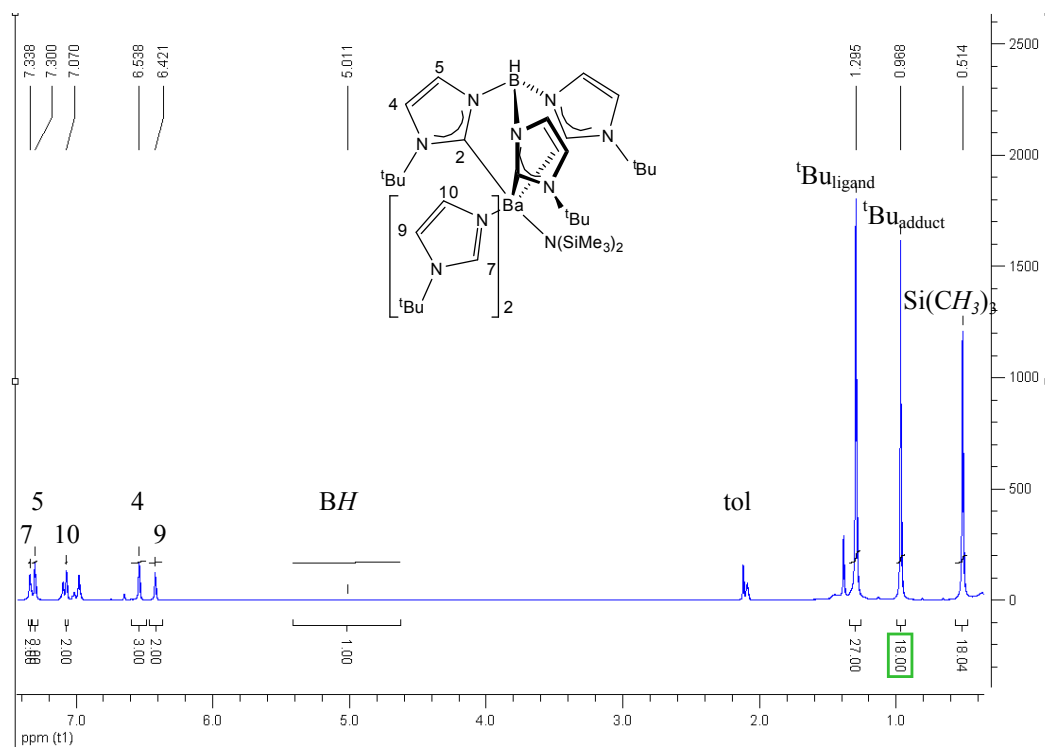
Figure 80. ^{1}H NMR spectrum of complex **94**.
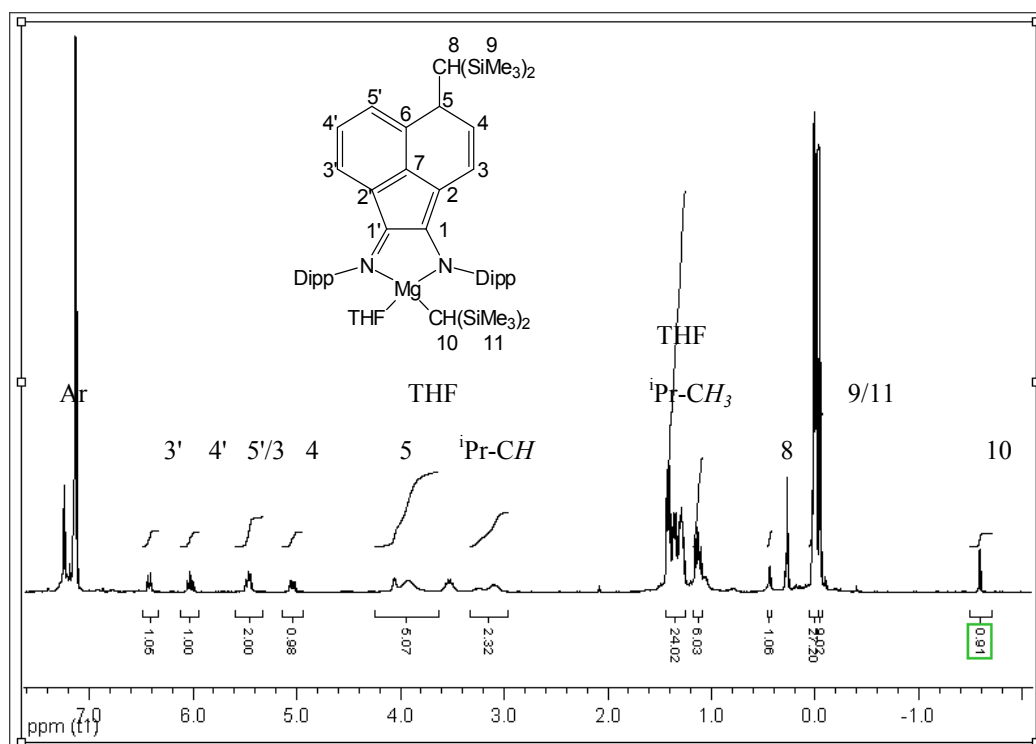
Figure 81. ^{1}H NMR spectrum of complex **96**.
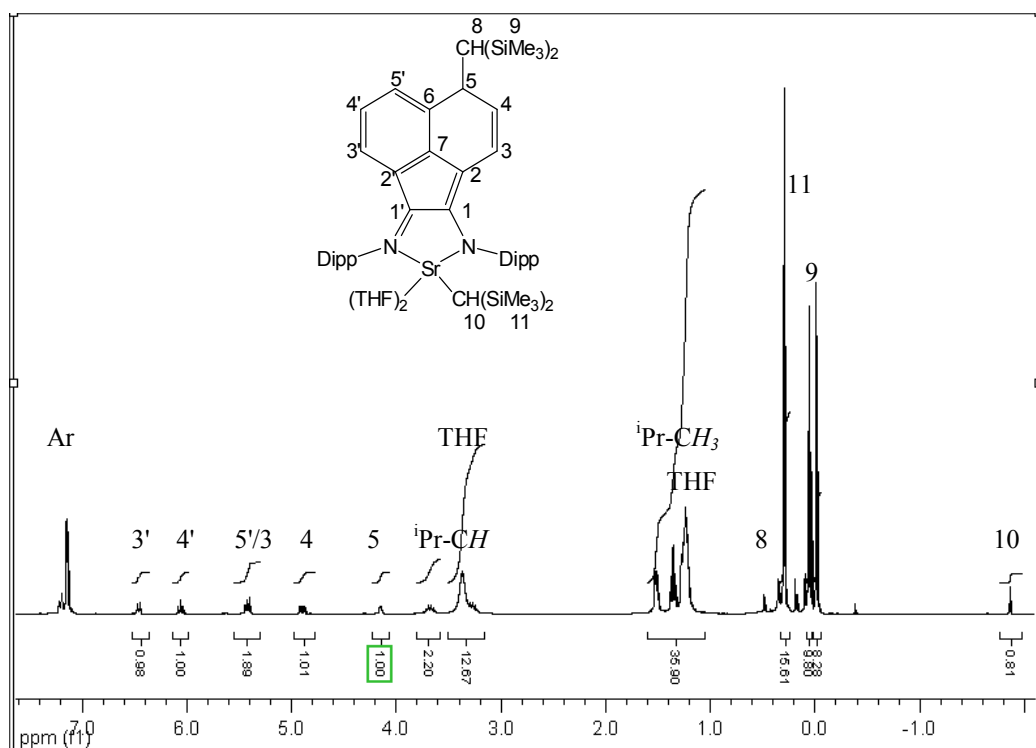
6.12 X-ray crystallography data

	37a	41	43	44
Molecular formula	$C_{22}H_{54}MgO_2Si_4$	$C_{41}H_{71}N_4OSi_2Sr$	$C_{144.30}H_{126.30}Cl_{6.90}N_4$	$C_{86}H_{86}MgN_2O$
Formula weight (g mol^{-1})	487.32	779.82	2161.00	1187.88
Crystal system	Monoclinic	Monoclinic	Monoclinic	Monoclinic
Space group	C 2/c	P 2$_1$/n	P 2$_1$	P 2$_1$
a (Å)	18.1694(4)	11.7396(2)	14.8918(2)	13.9290(5)
b (Å)	9.5586(2)	18.1629(3)	22.3244(4)	15.8762(7)
c (Å)	18.6690(5)	22.0002(3)	18.9375(3)	15.5792(7)
α (deg)	90	90	90	90
β (deg)	109.4520(10)	105.0920(10)	109.1590(10)	96.364(2)
γ (deg)	90	90	90	90
V (Å^3)	3057.25(12)	4529.20(12)	5947.07(16)	3423.9(2
Z	4	4	2	2
μ (mm^{-1})	0.230	1.276	0.218	0.075
ρ (g cm^{-3})	1.059	1.144	1.207	1.152
θ range (°)	5.20 to 27.50	4.93 to 27.48	3.46 to 25.04	4.07 to 25.08
Measured/independent reflections/ R_{int}	21287 / 3470 / 0.0651	63038 / 10311 / 0.0577	87101 / 20791 / 0.0719	35511 / 11921 / 0.1168
R_1,[a] wR_2 [$I > 2\sigma(I)$][b]	0.0397, 0.1038	0.0337, 0.0752	0.0682, 0.1738	0.0658, 0.1330
R_1,[a] wR_2 (all data)[b]	0.0503, 0.1107	0.0529, 0.0831	0.0906, 0.1912	0.1202, 0.1581

41. The asymmetric unit contains one molecule of benzene solvent.

43. The asymmetric unit contains two independent molecules of the ligand and three independent molecules of solvent CHCl$_3$. The N-*H* hydrogens have been located in the difference Fourier map and were freely refined with idealised bond length. Due to solvent loss all CHCl$_3$ molecules have an occupation factor of 70-80%. One of the solvent molecules presents a disorder in one Cl atom in a 1:1 ratio. Bond lengths in this disorder have been restrained.

44. Each asymmetric unit contains one Mg complex and one molecule of toluene which is disordered over two sites in the ratio 56:44. Bond lengths of the two CH$_3$ groups had to be restrained. In the adducted THF molecule, atom C(79) presents a disorder over two sites in a 75:25 ratio. The bond length C(78)-C(79A) had to be restrained.

	58	**60**	**63**	**64**
Molecular formula	$C_{14}H_{26}BIN_4$	$C_{24}H_{30}BIN_4$	$C_{29.50}H_{61.50}BN_5O_2Si_2Sr$	$C_{32}H_{56}B_2CaN_8O$
Formula weight (g mol^{-1})	388.10	512.23	672.95	630.55
Crystal system	Monoclinic	Monoclinic	Tetragonal	Orthorhombic
Space group	P 2$_1$/c	P2$_1$/m	P 4$_2$/n	P b c a
a (Å)	11.9656(2)	8.2566(1)	20.54500(10)	16.0309(3)
b (Å)	10.06550(10)	19.2495(3)	20.54500(10)	19.9759(4)
c (Å)	15.1879(2)	8.8410(1)	18.9151(2)	23.0604(5)
α (deg)	90	90	90	90
β (deg)	96.4050(10)	115.216(1)	90	90
γ (deg)	90	90	90	90
V (Å^3)	1817.81(4)	1271.25(3)	7984.01(10)	7384.7(3)
Z	4	2	8	8
μ (mm^{-1})	1.759	1.276	1.440	0.205
ρ (g cm^{-3})	1.418	1.338	1.120	1.134
θ range (^{o})	3.03 to 30.00	3.53 to 30.01	3.67 to 27.49	3.81 to 24.21
Measured/indepen-dent reflections/ R_{int}	34042 / 5294 / 0.0409	25876 / 3804 / 0.0413	132210 / 9125 / 0.0736	92909 / 5875 / 0.2578
R_1,[a] wR_2 [$I > 2\sigma(I)$][b]	0.0682, 0.1256	0.0269, 0.0597	0.0566, 0.1267	0.0609, 0.1191
R_1,[a] wR_2 (all data)[b]	0.0921, 0.1397	0.0351, 0.0632	0.0928, 0.1493	0.1067, 0.1410

63. The complex contains one disordered (80:20) THF co-ligand. Each molecule of the complex co-crystallises with 1/4 of solvent which could be modelled either as hexane or THF, disordered about a centre of inversion. NMR spectroscopy indicated that hexane was present.

64. The sample consisted of low melting crystals which were selected using a modified cryogenic device, similar to that described by Veith and Baerninghausen.[288] Weak diffraction resulted in a high R_{int}. The compound contains one THF co-ligand showing a 1:1 disorder in C(32).

	67	**74**	**75**	**76′**
Molecular formula	$C_{63}H_{80}B_2Ca_2I_2N_8O_2$	$C_{48}H_{80}BN_9Si_2Sr$	$C_{89}H_{156}B_2Ba_2N_{20}Si_4$	$C_{25}H_{42}BCaIN_6O$
Formula weight (g mol^{-1})	1336.93	937.82	1915.00	758.64
Crystal system	Triclinic	Orthorhombic	Monoclinic	Monoclinic
Space group	P $\bar{1}$	P c a b	P 2_1/n	P 2_1/c
a (Å)	12.7284(4)	19.16240(10)	22.00420(10)	18.4848(16)
b (Å)	15.4087(6)	20.46130(10)	13.95240(10)	10.5873(9)
c (Å)	18.6707(8)	27.5283(2)	34.0515(2)	20.6304(15)
α (deg)	88.9100(10)	90	90	90
β (deg)	84.7710(10)	90	91.5650(10)	93.155(5)
γ (deg)	65.664(2)	90	90	90
V (Å^3)	3321.9(2)	10793.50(11)	10450.30(11)	4031.3(6)
Z	2	8	4	4
μ (mm^{-1})	1.147	1.082	0.845	0.95
ρ (g cm^{-3})	1.337	1.154	1.217	1.25
θ range (º)	3.67 to 24.94	3.12 to 27.49	3.52 to 27.47	3.47 to 26.02
Measured/independent reflexions/ R_{int}	30202 / 11375 / 0.1265	176037 / 12336 / 0.1222	135871 / 23755 / 0.0801	24028 / 7870 / 0.060
R_1,[a] wR_2 [I > 2σ(I)][b]	0.1107, 0.2617	0.0467, 0.0909	0.0399, 0.0797	0.059, 0.123
R_1, wR_2 (all data)[b]	0.1665, 0.2925	0.0848, 0.1051	0.0724, 0.0900	0.090, 0.138

67. The asymmetric unit consists of two molecules of the calcium iodide dimer and one solvent molecule of toluene. Both THF groups binding to Ca show potential disorder which could not be resolved due to the very weak dataset. The B-*H* hydrogens were located in the difference Fourier map but could not be refined freely because of the poor dataset.

74. The complex co-crystallises with two molecules of toluene, of which the second presents a potential disorder (C(42)-C(48)). Resolving the disorder, however, did not lead to a better result.

75. The complex co-crystallises with two molecules of toluene solvent. One of the *tert*-butylimidazole co-ligands presents a disorder (35:65) in two of the CH_3 groups of the *tert*-butyl substituent.

76′. The complex co-crystallises with two molecules of toluene solvent, one of which is disordered about a centre of inversion, the other one over two sites in a 36:64 ratio. The THF co-ligand presents a disorder (49:51) in C(23) and C(24).

	77	78	79	80	81
Molecular formula	$C_{70}H_{100}B_2Br_2Ca_2N_{12}$	$C_{70}H_{100}B_2N_{12}Sr$	$C_{100}H_{112}B_2N_{12}O_4Sr_2$	$C_{26}H_{60}CaN_6Si_4$	$C_{52}H_{58}B_2N_4$
Formula weight (g mol^{-1})	1371.22	1218.86	1742.88	609.24	760.64
Crystal system	Triclinic	Monoclinic	Triclinic	Monoclinic	Monoclinic
Space group	P $\bar{1}$	C 2/c	P $\bar{1}$	P2$_1$/a	C 2/c
a (Å)	10.81420(10)	25.2604(6)	13.0315(3)	16.6547(3)	17.5721(5)
b (Å)	12.53040(10)	11.2390(2)	14.9297(4)	10.5277(2)	11.7891(3)
c (Å)	14.9414(2)	25.2461(6)	15.1218(4)	22.7316(4)	21.3849(4)
α (deg)	69.7990(10)	90	98.9760(10)	90	90
β (deg)	88.4830(10)	105.2890(10)	114.247(2)	106.132(1)	103.475(2)
γ (deg)	77.9470(10)	90	111.9350(10)	90	90
V (Å^3)	1855.92(3)	6913.7(3)	2315.81(10)	3828.72(12)	4308.13(18)
Z	1	4	1	4	4
μ (mm^{-1})	1.277	0.828	1.209	0.312	0.067
ρ (g cm^{-3})	1.227	1.171	1.250	1.057	1.173
θ range (°)	3.01 to 30.01	3.34 to 27.45	4.02 to 24.99	3.90 to 26.50	3.97 to 27.47
Measured / independent reflections / R_{int}	51329 / 10759 / 0.0578	26486 / 7654 / 0.1566	27544 / 8086 / 0.1060	29884 / 7866 / 0.0625	27498 / 4879 / 0.0964
R_1,[a] wR_2 [$I > 2\sigma(I)$][b]	0.0452, 0.1062	0.0600, 0.1435	0.0600, 0.1244	0.0490, 0.1172	0.0487, 0.1187
R_1,[a] wR_2 (all data)[b]	0.0710, 0.1189	0.0992, 0.1699	0.1087, 0.1474	0.0717, 0.1317	0.0718, 0.1352

77. The complex co-crystallises with two molecules of toluene solvent.

78. The crystals lost solvent during data collection, hence the bad R_{int}. It was not possible to use all collected data for integration which led to a lower completeness of data (97%). Each asymmetric unit consists of 1/2 molecule of the homoleptic Sr complex and two molecules of toluene in three positions. One toluene molecule is located on a two-fold axis. Another is disordered about a centre of inversion with 50% occupation factor. For the third one, heavily disordered over four positions in a 50:15:15:20 ratio, carbon atoms were fitted to a regular hexagon and refined isotropically.

79. The dimer co-crystallises with two molecules of toluene. The two bridging oxygen atoms are disordered over three positions in a 2:3:3 ratio.

81. The compound co-crystallises with one molecule toluene solvent disordered in a 1:3 ratio.

	86a	86b	86c	86d
Molecular formula	$C_{41}H_{57}MgN_3O_2$	$C_{41}H_{57}CaN_3O_2$	$C_{258}H_{330}N_{18}O_6Sr_6$	$C_{258}H_{330}Ba_6N_{18}O_6$
Formula weight ($g\ mol^{-1}$)	648.21	663.98	4305.12	4603.44
Crystal system	Monoclinic	Monoclinic	Cubic	Cubic
Space group	P 2_1/n	P 2_1/n	P a $\bar{3}$	P a $\bar{3}$
a (Å)	11.3851(2)	11.5654(3)	28.6787(3)	28.7452(3)
b (Å)	17.0663(4)	17.1777(5)	28.6787(3)	28.7452(3)
c (Å)	19.7459(5)	19.9552(6)	28.6787(3)	28.7452(3)
α (deg)	90	90	90	90
β (deg)	101.9072	102.483(2)	90	90
γ (deg)	90	90	90	90
V (Å^3)	3754.10(15)	3870.72(19)	23587.3(4)	23751.8
Z	4	4	4	4
μ (mm^{-1})	0.085	0.199	1.406	1.038
ρ ($g\ cm^{-3}$)	1.147	1.139	1.212	1.287
θ range (^{o})	4.67 to 27.50	5.40 to 27.49	3.01 to 25.02	3.61 to 25.03
Measured/independent reflections/ R_{int}	45139 / 8530 / 0.0967	45280 / 8750 / 0.1412	74769 / 6706 / 0.1521	202576 / 6961 / 0.1544
R_1,[a] wR_2 [$I > 2\sigma(I)$][b]	0.0615, 0.1477	0.0565, 0.1251	0.0472, 0.0827	0.0692, 0.1701
R_1,[a] wR_2 (all data)[b]	0.0997, 0.1730	0.1119, 0.1522	0.0892, 0.0962	0.1115, 0.1947

86c. The asymmetric unit contains one molecule of the Sr complex and one benzene solvent molecule. C(14)-Sr interactions lead to a hexameric structure. One of the *iso*-propyl substituents presents a 1:1 disorder in C(32).

86d. The asymmetric unit contains one molecule of the Ba complex and one benzene solvent molecule. C(14)-Ba interactions lead to a hexameric structure. The THF co-ligand presents a potential disorder in C(42) but solving the disorder gave no improvement.

	93	99	100	101
Molecular formula	$C_{100}H_{134}K_2N_4Si_4$	$C_{86}H_{118}N_4Si_4$	$C_{100}H_{140}CaN_4O_2Si_4$	$C_{288}H_{360}K_6N_{18}Si_6$
Formula weight (g mol^{-1})	1582.67	1320.20	1582.60	4477.08
Crystal system	Triclinic	Trigonal	Triclinic	Cubic
Space group	P $\bar{1}$	P 3_1 2 1	P $\bar{1}$	I a $\bar{3}$
a (Å)	12.8884(5)	13.7376(4)	17.3947(6)	39.6750(7)
b (Å)	13.4573(5)	13.7376(4)	18.2532(9)	39.6750(7)
c (Å)	15.4273(6)	37.1695(13)	19.0363(9)	39.6750(7)
α (deg)	110.607(2)	90	116.153(2)	90
β (deg)	96.794(3)	90	108.911(2)	90
γ (deg)	97.900(2)	120	91.946(2)	90
V (Å^3)	2440.37(16)	6074.9(3)	5020.1(4)	62452.6(19)
Z	1	3	2	8
μ (mm^{-1})	0.191	0.118	0.156	0.154
ρ (g cm^{-3})	1.077	1.083	1.047	0.952
θ range (º)	6.40 to 25.00	2.97 to 25.05	4.81 to 25.05	2.99 to 25.02
Measured/independent reflexions/ R_{int}	27778 / 8336 / 0.0641	28082 / 7053 / 0.0931	79347 / 17520 / 0.1864	55758 / 9182 / 0.1026
R_1,[a] wR_2 [I > 2σ(I)][b]	0.0704, 0.1528	0.0684, 0.1120	0.0975, 0.2301	0.1001, 0.2422
R_1,[a] wR_2 (all data)[b]	0.0990, 0.1706	0.1416, 0.1325	0.2083, 0.2979	0.1786, 0.2848

93. The dimer co-crystallises with one molecule of toluene solvent.

100. The crystal was very small and weakly diffracting, hence the high R_{int}. The asymmetric unit contains the complex and three solvent molecules. Two half-occupied THF (bond lengths in the THF containing O(3) had to be restrained) and one benzene molecule disordered over two sites in a 63:37 ratio. Atoms of the benzene unit have been refined isotropically. All methyl groups of the $CH(SiMe_3)_2$ substituent containing Si(1) and Si(2) present a rotational disorder in a 42:58 ratio.

101. The asymmetric unit contains 1/6 of a hexameric arranged K complex. It further contains one toluene solvent molecule with 50% occupation factor which is disordered over a two-fold axis. Another toluene molecule is disordered about a three-fold axis with an occupation factor of 33%. A trace of a further solvent molecule was located over a three-fold axis but could not properly be solved. The very large crystal diffracted well at low angles but presented a decline in intensity above $2\theta = 35º$. Therefore the solvent disorders could not be solved satisfactory. The PLATON programme SQUEEZE was employed to take care of the solvent-containing voids. Checkcif detected a potential disorder in one of the *iso*-propyl groups (C(39)-C(41)). Due to the lack of high angle intensity data this could not be solved properly.

6.13 Kinetic data for hydroamination catalysis

NB: The temperatures quoted here are those displayed by the internal probe of the NMR spectrometer. For real temperatures derived from displayed temperatures, refer to the equations in section 6.5.1.

Kinetic analyses for the cyclisation of (1-allylcyclohexyl) methylamine (0.80 M, 0.5 mL) with **35b** (2 mol%)

$y = -0.0048x - 0.0097$
$R^2 = 0.9994$

$y = -0.0348x - 0.0265$
$R^2 = 0.9996$

$y = -0.0186x + 0.0023$
$R^2 = 0.9999$

$y = -0.0123x - 0.0149$
$R^2 = 0.9996$
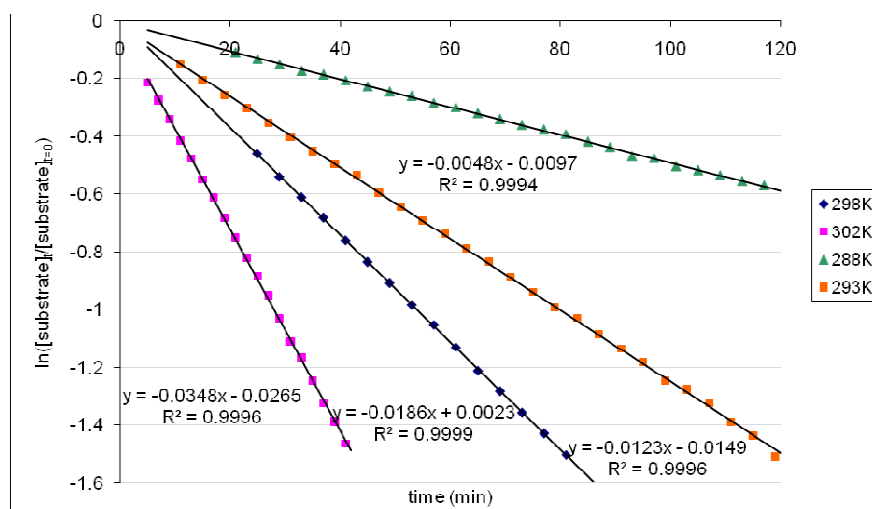
288-293 K: cooling power 5%
298-302 K: no cooling

Kinetic analyses for the cyclisation of (1-allylcyclohexyl) methylamine (0.80 M, 0.5 mL) with **35c** (2 mol%)

$y = -0.0185x + 0.0334$
$R^2 = 0.9959$

$y = -0.0349x + 0.0055$
$R^2 = 0.9965$

$y = -0.0662x - 0.0319$
$R^2 = 0.9969$

$y = -0.1223x - 0.0817$
$R^2 = 0.9973$
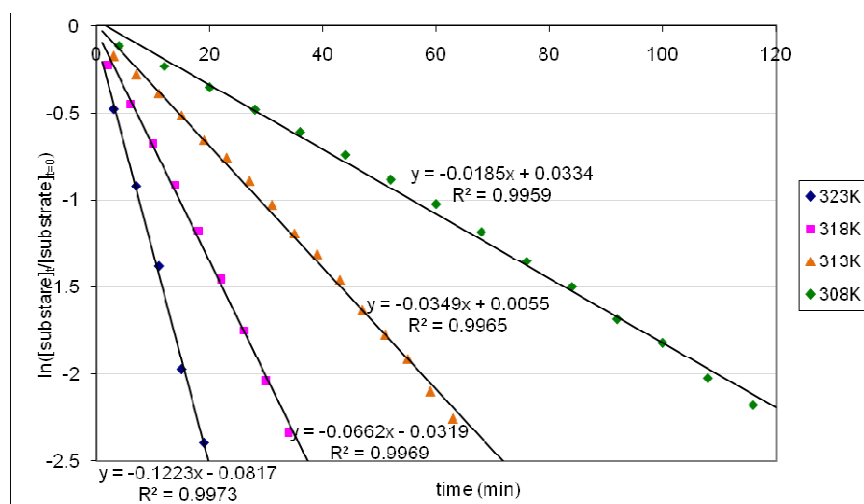
308-323 K: no cooling

228

Kinetic analyses for the cyclisation of (1-allylcyclohexyl)
methylamine (0.80 M, 0.5 mL) with **36b** (2 mol%)
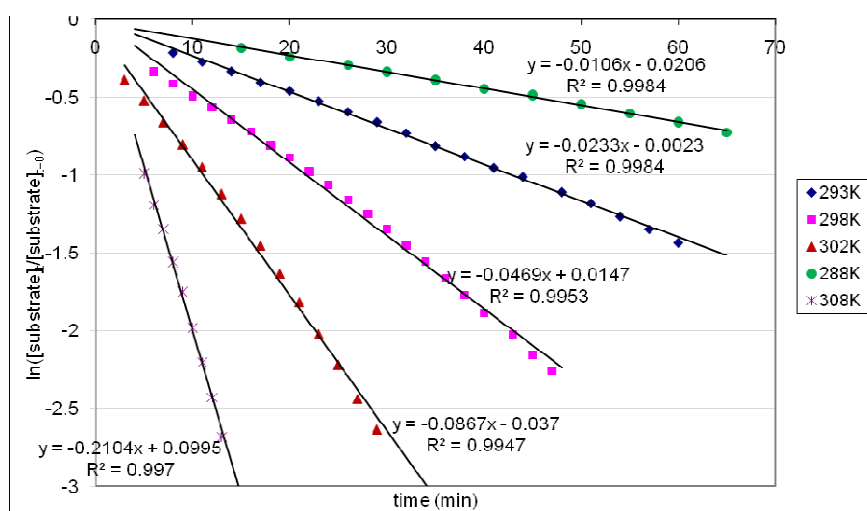
293-308 K: cooling power 5%

Kinetic analyses for the cyclisation of (1-allylcyclohexyl)
methylamine (0.80 M, 0.5 mL) with **36c** (2 mol%)
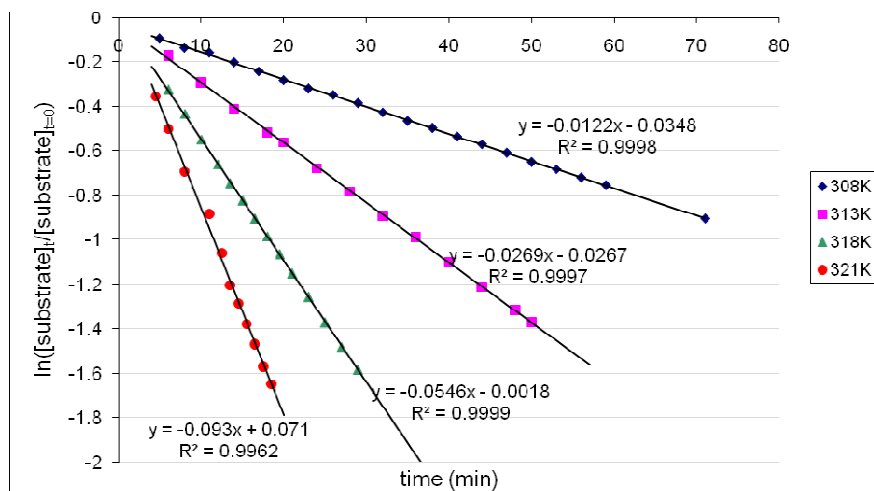
308-321 K: no cooling

Kinetic analyses for the cyclisation of (1-allylcyclohexyl) methylamine (0.80 M, 0.5 mL) with **2** (2 mol%)

$y = -0.0046x - 0.0316$
$R^2 = 0.9984$

$y = -0.0238x - 0.0169$
$R^2 = 0.9994$

$y = -0.0422x - 0.0219$
$R^2 = 0.9991$

$y = -0.0859x - 0.0251$
$R^2 = 0.9991$

Legend: 288K, 283K, 278K, 268K

time (min)
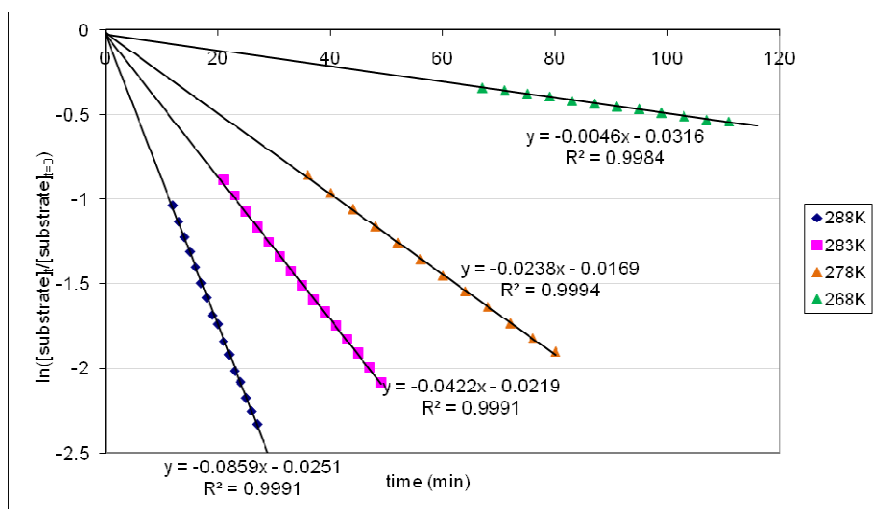
268-288 K: cooling power 5%

Kinetic analyses for the cyclisation of (1-allylcyclohexyl) methylamine (0.80 M, 0.5 mL) with **33** (2 mol%)

$y = -0.0069x - 0.0203$
$R^2 = 0.9995$

$y = -0.0129x - 0.0584$
$R^2 = 0.9998$

$y = -0.0328x - 0.053$
$R^2 = 0.9988$

$y = -0.0785x - 0.0227$
$R^2 = 0.9969$

Legend: 278K, 283K, 238K, 273K

time (min)
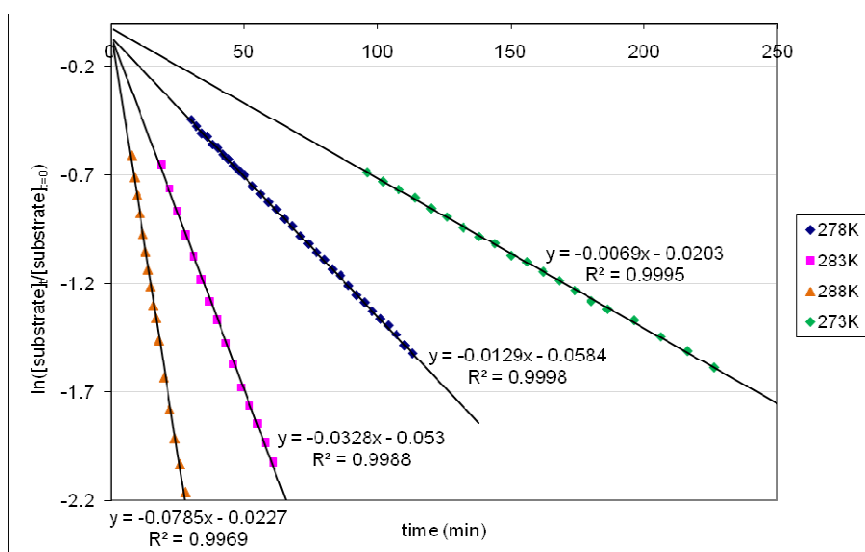
273-288 K: cooling power 5%

Kinetic analyses for the cyclisation of (1-allylcyclohexyl) methylamine (0.80 M, 0.5 mL) with **34** (2 mol%)
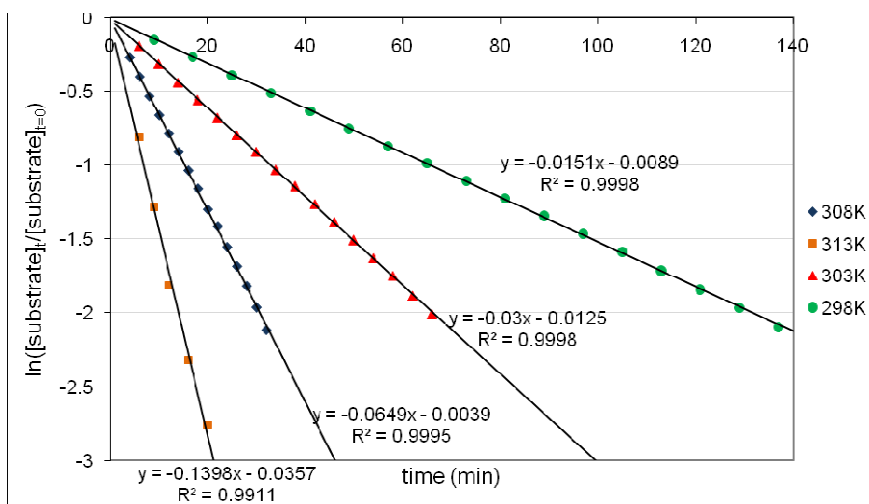
298-313 K: cooling power 5%

Kinetic analyses for the cyclisation of (1-allylcyclohexyl) methylamine (0.56 M, 0.5 mL C_6D_6) with variable concentration of **35b** (298 K)
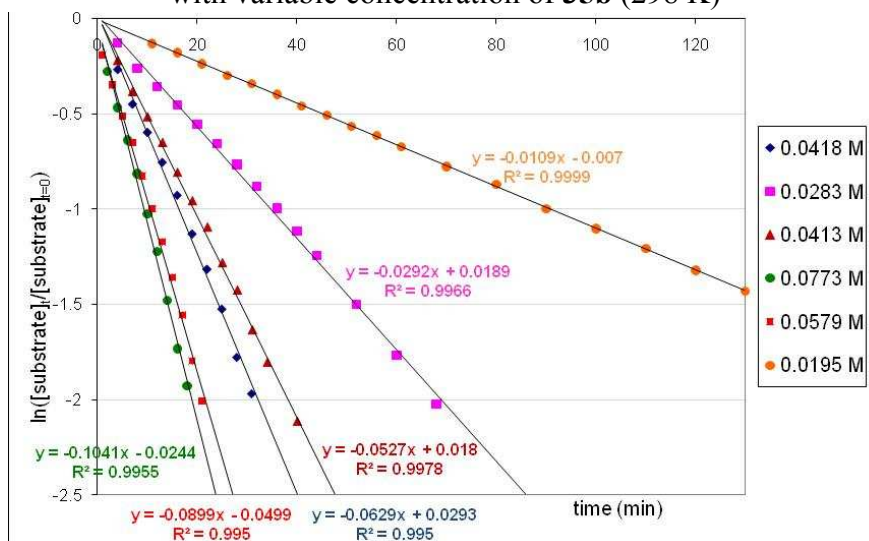
Kinetic analyses for the cyclisation of (1-allylcyclohexyl)
methylamine (0.56 M, 0.5 mL C_6D_6)
with variable concentration of **35c** (313 K)
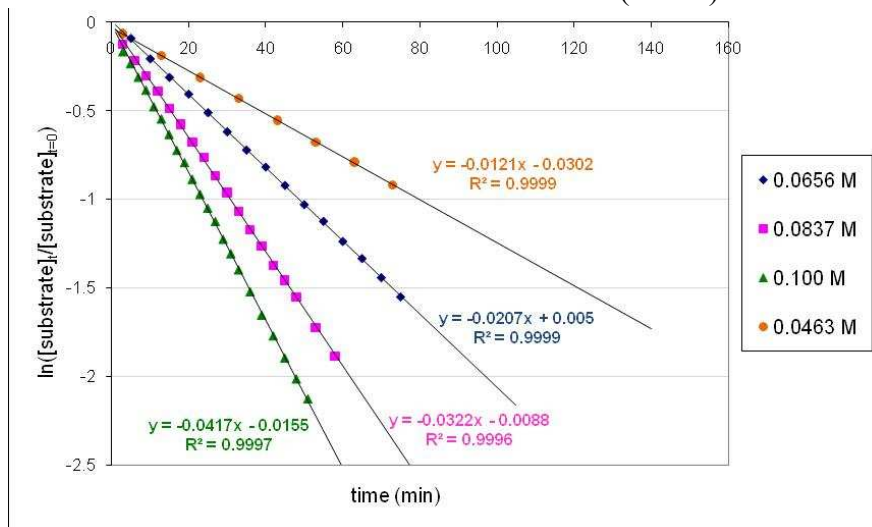
Kinetic analyses for the cyclisation of (1-allylcyclohexyl)
methylamine (0.56 M, 0.5 mL C_6D_6)
with variable concentration of **36b** (293 K)
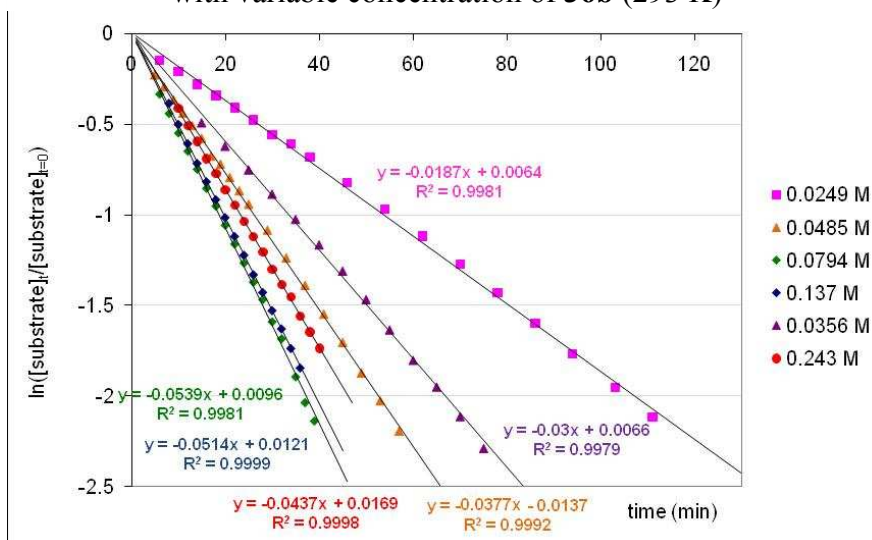
Kinetic analyses for the cyclisation of (1-allylcyclohexyl)
methylamine (0.56 M, 0.5 mL C_6D_6)
with variable concentration of **36c** (293 K)
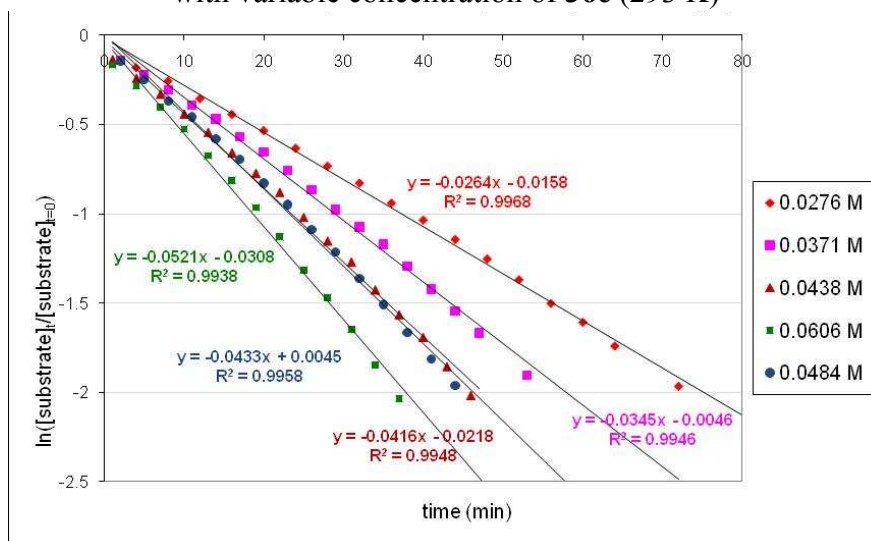
7 References

[1]   M. V. Grignard, *C. R. Hebd. Séances Acad. Sci.***1900**, *T. 130*, 1322-1323.

[2]   G. S. R. Silverman, Phillip E., *Handbook of Grignard Reagents*, Marcel Dekker, Inc., **1996**; H. G. J. Richey, *Grignard reagents - New developments*, Wiley, **2000**; R. G. Hoffmann, *Chem. Soc Rev.* **2003**, *32*, 225-230; J. Garst, M. Soriaga, *Coord. Chem. Rev.* **2004**, 623-652.

[3]   E. Beckmann, *Ber. Deut. Chem. Ges.* **1905**, *38*, 904-906; H. Gilman, F. Schulze, *J. Am. Chem. Soc.* **1926**, *48*, 2463-2467.

[4]   R. Fischer, M. Gartner, H. Gorls, M. Westerhausen, *Organomet.* **2006**, 3496-3500.

[5]   R. Fischer, M. Gartner, H. Gorls, M. Westerhausen, *Angew. Chem. - Int. Ed.* **2006**, 609-612; M. Gartner, H. Gorls, M. Westerhausen, *Synthesis-Stuttgart* **2007**, 725-730; M. Gartner, H. Gorls, M. Westerhausen, *Organomet.* **2007**, *26*, 1077-1083; R. Fischer, M. Gartner, H. Gorls, L. Yu, M. Reiher, M. Westerhausen, *Angew. Chem. - Int. Ed.* **2007**, *46*, 1618-1623.

[6]   R. Shannon, *Acta Cryst. Sect. A* **1976**, 751-767.

[7]   A. Allred, *J. Inorg. & Nucl. Chem* **1961**, 215-221.

[8]   S. Green, C. Jones, A. Stasch, *Science* **2007**, 1754-1757; S. Green, C. Jones, A. Stasch, *Angew. Chem. - Int. Ed.* **2008**, 9079-9083; S. Krieck, H. Gorls, L. Yu, M. Reiher, M. Westerhausen, *J. Am. Chem. Soc.* **2009**, 2977-2985.

[9]   P. Maldivi, L. Petit, C. Adamo, V. Vetere, *C. R. Chim.* **2007**, *10*, 888-896.

[10]   X. G. Zhou, M. Zhu, *J. Organomet. Chem.* **2002**, *647*, 28-49; P. A. Hunt, *Dalton Trans.s* **2007**, 1743-1754.

[11]   G. Molander, *Chem. Rev.* **1992**, 29-68; Z. M. Hou, Y. Wakatsuki, *Coord. Chem. Rev.* **2002**, *231*, 1-22; L. Mei, *Lett. Org. Chem.* **2008**, *5*, 174-190; S. Y. Seo, X. H. Yu, T. J. Marks, *J. Am. Chem. Soc.* **2009**, *131*, 263-276.

[12]   J. Gottfriedsen, F. T. Edelmann, *Coord. Chem. Rev.* **2007**, *251*, 142-202.

[13]   H. Aspinall, *Chem. Rev.* **2002**, 1807-1850; J. Inanaga, H. Furuno, T. Hayano, *Chem. Rev.* **2002**, 2211-2225; K. Mikami, M. Terada, H. Matsuzawa, *Angew. Chem. - Int. Ed.* **2002**, 3555-3571; M. Shibasaki, N. Yoshikawa, *Chem. Rev.* **2002**, 2187-2209.

[14] A. G. M. Barrett, M. R. Crimmin, M. S. Hill, P. A. Procopiou, *Proc. R. Soc. a-Math. Phys. Eng. Sci.* **2010**, *466*, 927-963; S. Harder, *Chem. Rev.* **2010**, *110*, 3852-3876.

[15] CRC, *Handbook of Chemistry and Physics, 77th edition.*

[16] *Sigma-Aldrich catalogue*, **2009-2010**.

[17] U.S. Patent 2891956; U.S. patent 5321188; U.S. Patent 5700754; U.S. Patent 6147246; U.S. patent 7087549; U.S. patent 7563915; Schachte.Y, H. Pines, *J. Catal.* **1968**, *11*, 147-158; G. Zhang, H. Hattori, K. Tanabe, *App. Catal.* **1988**, *36*, 189-197.

[18] F. Buch, S. Harder, *Zeit. Naturforsch. Sect. B-a J. Chem. Sci.* **2008**, *63*, 169-177.

[19] A. G. Avent, M. R. Crimmin, M. S. Hill, P. B. Hitchcock, *Dalton Trans.* **2005**, 278-284.

[20] T. P. Hanusa, *Organomet.* **2002**, *21*, 2559-2571.

[21] M. H. Chisholm, J. C. Gallucci, K. Phomphrai, *Inorg. Chem.* **2004**, *43*, 6717-6725.

[22] S. Nembenna, H. Roesky, S. Nagendran, A. Hofmeister, J. Magull, P. Wilbrandt, M. Hahn, *Angew. Chem. - Int. Ed.* **2007**, 2512-2514; C. Ruspic, S. Harder, *Inorg. Chem.* **2007**, 10426-10433; S. Sarish, H. Roesky, M. John, A. Ringe, J. Magull, *Chem. Commun.* **2009**, 2390-2392.

[23] K. A. Allen, Gowenloc.Bg, W. E. Lindsell, *J. Polym. Sci. Part a- Polym. Chem.* **1974**, *12*, 1131-1133.

[24] Y. F. Li, H. Deng, W. Brittain, M. S. Chisholm, *Polym. Bull.* **1999**, *42*, 635-639.

[25] A. Steffens, H. Schumann, *Macromol. Symp.* **2006**, *236*, 203-208.

[26] A. P. Dove, V. C. Gibson, E. L. Marshall, A. J. P. White, D. J. Williams, *Chem. Commun.* **2002**, 1208-1209.

[27] S. M. Li, I. Rashkov, J. L. Espartero, N. Manolova, M. Vert, *Macromol.* **1996**, *29*, 57-62; I. Rashkov, N. Manolova, S. M. Li, J. L. Espartero, M. Vert, *Macromol.* **1996**, *29*, 50-56.

[28] P. Dobrzynski, J. Kasperczyk, K. Jelonek, M. Ryba, M. Walski, M. Bero, *J. Biomed. Mat. Res. Part A* **2006**, *79A*, 865-873.

[29] Z. Y. Zhong, P. J. Dijkstra, C. Birg, M. Westerhausen, J. Feijen, *Macromol.* **2001**, *34*, 3863-3868; Z. Y. Zhong, M. J. K. Ankone, P. J. Dijkstra, C. Birg, M. Westerhausen, J. Feijen, *Polym. Bull.* **2001**, *46*, 51-57; Z. Y. Zhong, S.

Schneiderbauer, P. J. Dijkstra, M. Westerhausen, J. Feijen, *J. Polym. Env.* **2001**, *9*, 31-38.

[30]   M. Westerhausen, S. Schneiderbauer, A. N. Kneifel, Y. Soltl, P. Mayer, H. Noth, Z. Y. Zhong, P. J. Dijkstra, J. Feijen, *Eur. J. Inorg. Chem.* **2003**, 3432-3439; Z. Y. Zhong, S. Schneiderbauer, P. J. Dijkstra, M. Westerhausen, J. Feijen, *Polym. Bull.* **2003**, *51*, 175-182; Y. Sarazin, R. H. Howard, D. L. Hughes, S. M. Humphrey, M. Bochmann, *Dalton Trans.* **2006**, 340-350; L. H. Piao, J. R. Sun, Z. Y. Zhong, Q. Z. Liang, X. S. Chen, J. H. Kim, X. B. Jing, *J. Appl. Polym. Sci.* **2006**, *102*, 2654-2660; V. Poirier, T. Roisnel, J.-F. Carpentier, Y. Sarazin, *Dalton Trans* **2009**, 9820-9827; S.-M. Ho, C.-S. Hsiao, A. Datta, C.-H. Hung, L.-C. Chang, T.-Y. Lee, J.-H. Huang, *Inorg. Chem.* **2009**, *48*, 8004-8011.

[31]   M. G. Davidson, C. T. O'Hara, M. D. Jones, C. G. Keir, M. F. Mahon, G. Kociok-Köhn, *Inorg. Chem.* **2007**, *46*, 7686-7688.

[32]   D. J. Darensbourg, W. Choi, P. Ganguly, C. P. Richers, *Macromol.* **2006**, *39*, 4374-4379; D. J. Darensbourg, W. Choi, C. P. Richers, *Macromol.* **2007**, *40*, 3521-3523; D. J. Darensbourg, W. Choi, O. Karroonnirun, N. Bhuvanesh, *Macromol.* **2008**, *41*, 3493-3502.

[33]   E. L. Marshall, V. C. Gibson, H. S. Rzepa, *J. Am. Chem. Soc.* **2005**, *127*, 6048-6051.

[34]   M. H. Chisholm, D. Navarro-Llobet, W. J. Simonsick, *Macromol.* **2001**, *34*, 8851-8857; Y. Feng, D. Klee, H. Hocker, *Macromol. Chem. Phys.* **2001**, *202*, 3120-3125.

[35]   Y. L. Xiao, Z. Wang, K. L. Ding, *Macromol.* **2006**, *39*, 128-137; D. F. J. Piesik, S. Range, S. Harder, *Organomet.* **2008**, *27*, 6178-6187.

[36]   M. H. Chisholm, J. Gallucci, K. Phomphrai, *Chem. Commun.* **2003**, 48-49.

[37]   A. Dove, V. Gibson, P. Hormnirun, E. Marshall, J. Segal, A. White, D. Williams, *Dalton Trans.* **2003**, 3088-3097; X. Y. He, J. Morris, B. C. Noll, S. N. Brown, K. W. Henderson, *J. Am. Chem. Soc.* **2006**, *128*, 13599-13610; T. Boyle, B. Hernandez-Sanchez, C. Baros, L. Brewer, M. Rodriguez, *Chem. Mat.* **2007**, 2016-2026; X. Y. He, E. Hurley, B. C. Noll, K. W. Henderson, *Organomet.* **2008**, *27*, 3094-3102.

[38]   C. Ruspic, S. Nembenna, A. Hofmeister, J. Magull, S. Harder, H. Roesky, *J. Am. Chem. Soc.* **2006**, 15000-15004.

[39]   S. Sarish, S. Nembenna, S. Nagendran, H. Roesky, A. Pal, R. Herbst-Irmer, A. Ringe, J. Magull, *Inorg. Chem.* **2008**, 5971-5977.

[40]   V. Arunasalam, D. Mingos, J. Plakatouras, I. Baxter, M. Hursthouse, K. Malik, *Polyhedron* **1995**, 1105-1108; V. Arunasalam, I. Baxter, J. Darr, S. Drake, M. Hursthouse, K. Malik, D. Mingos, *Polyhedron* **1998**, 641-657; I. Bezougli, A. Bashall, M. McPartlin, D. Mingos, *J. Chem. Soc. - Dalton Trans.* **1998**, 2665-2669.

[41]   A. Weeber, S. Harder, H. Brintzinger, K. Knoll, *Organomet.* **2000**, 1325-1332.

[42]   F. Feil, S. Harder, *Organomet.* **2001**, *20*, 4616-4622; S. Harder, F. Feil, A. Weeber, *Organomet.* **2001**, *20*, 1044-1046; F. Feil, C. Muller, S. Harder, *J. Organomet. Chem.* **2003**, *683*, 56-63.

[43]   S. Harder, F. Feil, K. Knoll, *Angew. Chem. - Int. Ed.* **2001**, *40*, 4261-4264; S. Harder, F. Feil, *Organomet.* **2002**, *21*, 2268-2274; F. Feil, S. Harder, *Eur. J. Inorg. Chem.* **2003**, 3401-3408; D. F. J. Piesik, K. Habe, S. Harder, *Eur. J. Inorg. Chem.* **2007**, 5652-5661.

[44]   M. R. Crimmin, A. G. M. Barrett, M. S. Hill, P. A. Procopiou, *Organic Letters* **2007**, *9*, 331-333.

[45]   L. Orzechowski, S. Harder, *Organomet.* **2007**, *26*, 2144-2148.

[46]   A. G. M. Barrett, M. R. Crimmin, M. S. Hill, P. B. Hitchcock, S. L. Lomas, P. A. Procopiou, K. Suntharalingam, *Chem. Commun.* **2009**, 2299-2301.

[47]   C. Bianchini, P. Frediani, D. Masi, M. Peruzzini, F. Zanobini, *Organomet.* **1994**, *13*, 4616-4632; B. M. Trost, M. T. Sorum, C. Chan, A. E. Harms, G. Ruhter, *J. Am. Chem. Soc.* **1997**, *119*, 698-708.

[48]   D. Burkey, T. Hanusa, *Organomet.* **1996**, 4971-4976; D. Green, U. Englich, K. Ruhlandt-Senge, *Angew. Chem. - Int. Ed.* **1999**, 354-357; A. Avent, M. Crimmin, M. Hill, P. Hitchcock, *Organomet.* **2005**, 1184-1188; M. Guino, J. Alexander, M. McKee, H. Hope, U. Englich, K. Ruhlandt-Senge, *Chem. Eur. J.* **2009**, 11842-11852; H. Schumann, A. Steffens, M. Hummert, *Zeit. Anorg. Allg. Chem.* **2009**, 1041-1047; A. Stasch, S. Sarish, H. Roesky, K. Meindl, F. Dall'Antonia, T. Schulz, D. Stalke, *Chem. Asian J.* **2009**, 1451-1457.

[49]   A. Barrett, M. Crimmin, M. Hill, P. Hitchcock, S. Lomas, M. Mahon, P. Procopiou, K. Suntharalingam, *Organomet.* **2008**, *27*, 6300-6306.

[50] H. J. Heeres, J. Nijhoff, J. H. Teuben, R. D. Rogers, *Organomet.* **1993**, *12*, 2609-2617; L. Lee, D. J. Berg, G. W. Bushnell, *Organomet.* **1995**, *14*, 5021-5023.

[51] S. Hong, T. J. Marks, *Acc. Chem. Res.* **2004**, *37*, 673-686.

[52] M. R. Crimmin, I. J. Casely, M. S. Hill, *J. Am. Chem. Soc.* **2005**, *127*, 2042-2043.

[53] M. R. Gagne, C. L. Stern, T. J. Marks, *J. Am. Chem. Soc.* **1992**, *114*, 275-294.

[54] M. Crimmin, M. Arrowsmith, A. Barrett, I. Casely, M. Hill, P. Procopiou, *J. Am. Chem. Soc.* **2009**, *131*, 9670-9685.

[55] A. G. Avent, M. R. Crimmin, M. S. Hill, P. B. Hitchcock, *Dalton Trans.* **2004**, 3166-3169.

[56] A. G. M. Barrett, M. R. Crimmin, M. S. Hill, G. Kociok-Köhn, J. R. Lachs, P. A. Procopiou, *Dalton Trans.* **2008**, 1292-1294.

[57] A. Barrett, I. Casely, M. Crimmin, M. Hill, J. Lachs, M. Mahon, P. Procopiou, *Inorg. Chem.* **2009**, *48*, 4445-4453.

[58] M. Gagne, C. Stern, T. Marks, *J. Am. Chem. Soc.* **1992**, *114*, 275-294.

[59] S. Datta, P. W. Roesky, S. Blechert, *Organomet.* **2007**, *26*, 4392-4394.

[60] S. Datta, M. T. Gamer, P. W. Roesky, *Organomet.* **2008**, *27*, 1207-1213.

[61] A. Barrett, M. Crimmin, M. Hill, P. Hitchcock, G. Kociok-Köhn, P. Procopiou, *Inorg. Chem.* **2008**, *47*, 7366-7376.

[62] X. M. Zhang, T. J. Emge, K. C. Hultzsch, *Organomet.* **2010**, *29*, 5871-5877.

[63] **S. R. Neal**, **A. Ellern**, **A. D. Sadow**, *J. Organomet. Chem.* **2011**, *969*, 228-234.

[64] A. G. M. Barrett, T. C. Boorman, M. R. Crimmin, M. S. Hill, G. Kociok-Köhn, P. A. Procopiou, *Chem. Commun.* **2008**, 5206-5208; J. Lachs, A. Barrett, M. Crimmin, G. Kociok-Köhn, M. Hill, M. Mahon, P. Procopiou, *Eur. J. Inorg. Chem.* **2008**, 4173-4179.

[65] A. Barrett, C. Brinkmann, M. Crimmin, M. Hill, P. Hunt, P. Procopiou, *J. Am. Chem. Soc.* **2009**, *131*, 12906-12907.

[66] M. R. Douglass, C. L. Stern, T. J. Marks, *J. Am. Chem. Soc.* **2001**, *123*, 10221-10238; A. M. Kawaoka, M. R. Douglass, T. J. Marks, *Organomet.* **2003**, *22*, 4630-4632.

[67] K. Takaki, M. Takeda, G. Koshoji, T. Shishido, K. Takehira, *Tet. Lett.* **2001**, *42*, 6357-6360; K. Takaki, G. Koshoji, K. Komeyama, M. Takeda, T. Shishido, A. Kitani, K. Takehira, *J. Org. Chem.* **2003**, *68*, 6554-6565.

[68]   M. R. Crimmin, A. G. M. Barrett, M. S. Hill, P. B. Hitchcock, P. A. Procopiou, *Organomet.* **2007**, *26*, 2953-2956.

[69]   M. Westerhausen, W. Schwarz, *J. Organomet. Chem.* **1993**, 51-63; M. Westerhausen, A. Pfitzner, *J. Organomet. Chem.* **1995**, 187-195; M. Westerhausen, R. Low, W. Schwarz, *J. Organomet. Chem.* **1996**, 213-229; M. Westerhausen, M. Digeser, M. Krofta, N. Wiberg, H. Noth, J. Knizek, W. Ponikwar, T. Seifert, *Eur. J. Inorg. Chem.* **1999**, 743-750; M. Westerhausen, C. Birg, M. Krofta, P. Mayer, T. Seifert, H. Noth, A. Pfitzner, T. Nilges, H. Deiseroth, *Zeit. Anorg. Allg. Chem.* **2000**, 1073-1080; M. Westerhausen, M. Krofta, P. Mayer, *Zeit. Anorg. Allg. Chem.* **2000**, 2307-2312.

[70]   M. Westerhausen, M. Digeser, H. Noth, W. Ponikwar, T. Seifert, K. Polborn, *Inorg. Chem.* **1999**, 3207-3214.

[71]   T. M. A. Al-Shboul, H. Gorls, M. Westerhausen, *Inorg. Chem. Commun.* **2008**, *11*, 1419-1421.

[72]   M. R. Crimmin, A. G. M. Barrett, M. S. Hill, P. B. Hitchcock, P. A. Procopiou, *Organomet.* **2008**, *27*, 497-499.

[73]   T. M. A. Al-Shboul, G. Volland, H. Gorls, M. Westerhausen, *Zeit. Anorg. Allg. Chem.* **2009**, *635*, 1568-1572.

[74]   F. Buch, H. Brettar, S. Harder, *Angew. Chem. Int. Ed.* **2006**, *45*, 2741-2745.

[75]   S. Harder, J. Brettar, *Angew. Chem. Int. Ed.* **2006**, *45*, 3474-3478; S. Bonyhady, C. Jones, S. Nembenna, A. Stasch, A. Edwards, G. McIntyre, *Chem. Eur. J.* **2010**, 938-955.

[76]   M. Arrowsmith, M. Hill, D. MacDougall, M. Mahon, *Angew. Chem. - Int. Ed.* **2009**, 4013-4016.

[77]   J. Spielmann, S. Harder, *Eur. J. Inorg. Chem.* **2008**, 1480-1486.

[78]   J. Spielmann, F. Buch, S. Harder, *Angew. Chem. - Int. Ed.* **2008**, *47*, 9434-9438.

[79]   J. Spielmann, S. Harder, *Chem. Eur. J.* **2007**, 8928-8938.

[80]   M. Niggemann, N. Bisek, *Chem. Eur. J.* **2010**, *16*, 11246-11249.

[81]   Y. Yamada, M. Shibasaki, *Tet. Lett.* **1998**, *39*, 5561-5564.

[82]   T. Suzuki, N. Yamagiwa, Y. Matsuo, S. Sakamoto, K. Yamaguchi, M. Shibasaki, R. Noyori, *Tet. Lett.* **2001**, *42*, 4669-4671.

[83]   A. Yamaguchi, S. Matsunaga, M. Shibasaki, *J. Am. Chem. Soc.* **2009**, *131*, 10842-+.

[84]   G. Kumaraswamy, M. N. V. Sastry, N. Jena, *Tet. Lett.* **2001**, *42*, 8515-8517.

[85] G. Kumaraswamy, N. Jena, M. N. V. Sastry, M. Padmaja, B. Markondaiah, *Adv. Synth. Catal.* **2005**, *347*, 867-871.

[86] M. Agostinho, S. Kobayashi, *J. Am. Chem. Soc.* **2008**, *130*, 2430-2431; S. Kobayashi, M. Yamaguchi, M. Agostinho, U. Schneider, *Chem. Lett.* **2009**, *38*, 296-297.

[87] T. Tsubogo, Y. Yamashita, S. Kobayashi, *Angew. Chem. - Int. Ed.* **2009**, *48*, 9117-9120.

[88] S. Kobayashi, T. Tsubogo, S. Saito, Y. Yamashita, *Org. Lett.* **2008**, *10*, 807-809; T. Tsubogo, S. Saito, K. Seki, Y. Yamashita, S. Kobayashi, *J. Am. Chem. Soc.* **2008**, *130*, 13321-13332; S. Kobayashi, Y. Yamashita, *Acc. Chem. Res.* **2011**, *44*, 58-71; T. Tsubogo, Y. Kano, K. Ikemoto, Y. Yamashita, S. Kobayashi, *Tet. Asymm.* **2010**, *21*, 1221-1225.

[89] T. Poisson, T. Tsubogo, Y. Yamashita, S. Kobayashi, *J. Org. Chem.* **2010**, *75*, 963-965.

[90] S. Saito, T. Tsubogo, S. Kobayashi, *Chem. Commun.* **2007**, 1236-1237; S. Kobayashi, R. Matsubara, *Chem. Eur. J.* **2009**, *15*, 10694-10700.

[91] H. Van Nguyen, R. Matsubara, S. Kobayashi, *Angew. Chem. - Int. Ed.* **2009**, *48*, 5927-5929.

[92] A. Yamaguchi, N. Aoyama, S. Matsunaga, M. Shibasaki, *Org. Lett.* **2007**, *9*, 3387-3390.

[93] F. Buch, S. Harder, *Organomet.* **2007**, *26*, 5132-5135.

[94] J. Spielmann, M. Bolte, S. Harder, *Chem. Commun. (Cambridge)* **2009**, 6934-6936.

[95] J. Spielmann, G. Jansen, H. Bandmann, S. Harder, *Angew. Chem. - Int. Ed.* **2008**, 6290-6295; J. Spielmann, S. Harder, *J. Am. Chem. Soc.* **2009**, *131*, 5064-5065; J. Spielmann, D. F. J. Piesik, S. Harder, *Chemistry* **2010**, *16*, 8307-8318.

[96] D. J. Liptrot, M. S. Hill, M. F. Mahon, D. J. MacDougall, *Chemistry* **2010**, *16*, 8508-8515.

[97] S. A. Lawrence, *Amines: Synthesis, Properties and Applications* **2004**, *Cambridge University Press*.

[98] K. Weissermel, H.-J. Arpe, *Industrial Organic Chemistry* **2003**, *Fourth, completely revised edition*, Wiley-VCH.

[99] D. Steinborn, R. Taube, *Zeit. Chem.* **1986**, *26*, 349-359; J. B. Pedley, R. D. Naylor, S. P. Kirby, *Thermochemical Data of Organic Compounds, Second*

Edition. **1986**, *Chapman and Hall*; T. E. Muller, M. Beller, *Chem. Rev.* **1998**, *98*, 675-703.

[100] H. Fujita, M. Tokuda, M. Nitta, H. Suginome, *Tet. Lett.* **1992**, *33*, 6359-6362.

[101] A. Ates, C. Quinet, *Eur. J. Org. Chem.* **2003**, 1623-1626.

[102] R. Lebeuf, F. Robert, K. Schenk, Y. Landais, *Org. Lett.* **2006**, *8*, 4755-4758; R. Pathak, P. Naicker, W. A. Thompson, M. A. Fernandes, C. B. de Koning, W. A. L. van Otterlo, *Eur. J. Org. Chem.* **2007**, 5337-5345; S. Tsuchida, A. Kaneshige, T. Ogata, H. Baba, Y. Yamamoto, K. Tomioka, *Org. Lett.* **2008**, *10*, 3635-3638; W. Zhang, J. B. Werness, W. P. Tang, *Org. Lett.* **2008**, *10*, 2023-2026.

[103] P. H. Martinez, K. C. Hultzsch, F. Hampel, *Chem. Commun.* **2006**, 2221-2223; T. Ogata, A. Ujihara, S. Tsuchida, T. Shimizu, A. Kaneshige, K. Tomioka, *Tet. Lett.* **2007**, *48*, 6648-6650.

[104] C. Quinet, P. Jourdain, C. Hermans, A. Atest, I. Lucas, I. E. Marko, *Tetrahedron* **2008**, *64*, 1077-1087.

[105] T. E. Muller, A. K. Pleier, *J. Chem. Soc. - Dalton Trans.* **1999**, 583-587; T. E. Muller, M. Grosche, E. Herdtweck, A. K. Pleier, E. Walter, Y. K. Yan, *Organomet.* **2000**, *19*, 170-183; K. C. Hultzsch, *Org. Biomol. Chem.* **2005**, *3*, 1819-1824; K. C. Hultzsch, *Adv. Synth. Catal.* **2005**, *347*, 367-391; S. Burling, L. D. Field, B. A. Messerle, S. L. Rumble, *Organomet.* **2007**, *26*, 4335-4343.

[106] J. Y. Kim, T. Livinghouse, *Org. Lett.* **2005**, *7*, 4391-4393.

[107] H. Kaneko, H. Tsurugi, T. K. Panda, K. Mashima, *Organomet.* **2010**, *29*, 3463-3466.

[108] D. V. Gribkov, K. C. Hultzsch, F. Hampell, *Chem. Eur. J.* **2003**, *9*, 4796-4810; D. V. Gribkov, K. C. Hultzsch, *Chem. Commun.* **2004**, 730-731; K. C. Hultzsch, F. Hampel, T. Wagner, *Organomet.* **2004**, *23*, 2601-2612; K. C. Hultzsch, D. V. Gribkov, F. Hampel, *J. Organomet. Chem.* **2005**, *690*, 4441-4452; J. Y. Kim, T. Livinghouse, *Org. Lett.* **2005**, *7*, 1737-1739; H. Kim, T. Livinghouse, J. H. Shim, S. G. Lee, P. H. Lee, *Adv. Synth. Catal.* **2006**, *348*, 701-704; H. Kim, T. Livinghouse, D. Seomoon, P. H. Lee, *Bull. Kor. Chem. Soc.* **2007**, *28*, 1127-1134; D. Riegert, J. Collin, J. C. Daran, T. Fillebeen, E. Schulz, D. Lyubov, G. Fukin, A. Trifonov, *Eur. J. Inorg. Chem.* **2007**, 1159-1168; S. Z. Ge, A. Meetsma, B. Hessen, *Organomet.* **2008**, *27*, 5339-5346; I. Aillaud, D. Lyubov, J. Collin, R. Guillot, J. Hannedouche, E. Schulz, A. Trifonov, *Organomet.* **2008**,

27, 5929-5936; I. Aillaud, J. Collin, J. Hannedouche, E. Schulz, A. Trifonov, *Tet. Lett.* **2010**, *51*, 4742-4745.

[109] H. Kim, Y. K. Kim, J. H. Shim, M. Kim, M. J. Han, T. Livinghouse, P. H. Lee, *Adv. Synth. Catal.* **2006**, *348*, 2609-2618.

[110] D. Fairfax, M. Stein, T. Livinghouse, M. Jensen, *Organomet.* **1997**, *16*, 1523-1525.

[111] L. Ackermann, R. G. Bergman, *Org. Lett.* **2002**, *4*, 1475-1478; C. Y. Li, R. K. Thomson, B. Gillon, B. O. Patrick, L. L. Schafer, *Chem. Commun.* **2003**, 2462-2463; T. Bytschkov, S. Doye, *Tet. Lett.* **2002**, *43*, 3715-3718; L. Ackermann, R. G. Bergman, R. N. Loy, *J. Am. Chem. Soc.* **2003**, *125*, 11956-11963; J. M. Hoover, J. R. Petersen, J. H. Pikul, A. R. Johnson, *Organomet.* **2004**, *23*, 4614-4620.

[112] P. D. Knight, I. Munslow, P. N. O'Shaughnessy, P. Scott, *Chem. Commun.* **2004**, 894-895; A. L. Gott, G. J. Clarkson, R. J. Deeth, M. L. Hammond, C. Morton, P. Scott, *Dalton Trans.* **2008**, 2983-2990.

[113] D. V. Gribkov, K. C. Hultzsch, *Angew. Chem. - Int. Ed.* **2004**, *43*, 5542-5546; S. Tobisch, *Dalton Trans.* **2006**, 4277-4285.

[114] J. A. Bexrud, J. D. Beard, D. C. Leitch, L. L. Schafer, *Org. Lett.* **2005**, *7*, 1959-1962; R. K. Thomson, J. A. Bexrud, L. L. Schafer, *Organomet.* **2006**, *25*, 4069-4071; J. A. Bexrud, C. Y. Li, L. L. Schafer, *Organomet.* **2007**, *26*, 6366-6372; C. Muller, W. G. Saak, S. Doye, *Eur. J. Org. Chem.* **2008**, 2731-2739; H. Kim, T. Livinghouse, P. H. Lee, *Tetrahedron* **2008**, *64*, 2525-2529; J. A. Bexrud, L. L. Schafer, *Dalton Trans* **2010**, 361-363.

[115] A. L. Gott, A. J. Clarke, G. J. Clarkson, P. Scott, *Organomet.* **2007**, *26*, 1729-1737; L. Xiang, H. B. Song, G. F. Zi, *Eur. J. Inorg. Chem.* **2008**, 1135-1140; A. L. Reznichenko, K. C. Hultzsch, *Organomet.* **2010**, *29*, 24-27; L. Xiang, F. R. Zhang, J. X. Zhang, H. B. Song, G. F. Zi, *Inorg. Chem. Commun.* **2010**, *13*, 666-670; Q. W. Wang, H. B. Song, G. F. Zi, *J. Organomet. Chem.* **2010**, *695*, 1583-1591; G. F. Zi, F. R. Zhang, X. Liu, L. Ai, H. B. Song, *J. Organomet. Chem.* **2010**, *695*, 730-739; G. F. Zi, F. R. Zhang, L. Xiang, Y. Chen, W. H. Fang, H. B. Song, *Dalton Trans.* **2010**, *39*, 4048-4061.

[116] A. L. Gott, A. J. Clarke, G. J. Clarkson, P. Scott, *Chem. Commun.* **2008**, 1422-1424.

[117] S. Majumder, A. L. Odom, *Organomet.* **2008**, *27*, 1174-1177; D. C. Leitch, P. R. Payne, C. R. Dunbar, L. L. Schafer, *J. Am. Chem. Soc.* **2009**, *131*, 18246-18247.

[118] L. L. Ouh, T. E. Muller, Y. K. Yan, *J. Organomet. Chem.* **2005**, *690*, 3774-3782.

[119] K. Komeyama, T. Morimoto, K. Takaki, *Angew. Chem. - Int. Ed.* **2006**, *45*, 2938-2941.

[120] T. Kondo, T. Okada, T. Suzuki, T. Mitsudo, *J. Organomet. Chem.* **2001**, *622*, 149-154; T. Kondo, T. Okada, T. Mitsudo, *J. Am. Chem. Soc.* **2002**, *124*, 186-187.

[121] S. Burling, L. D. Field, B. A. Messerle, *Organomet.* **2000**, *19*, 87-90; S. Burling, L. D. Field, H. L. Li, B. A. Messerle, P. Turner, *Eur. J. Inorg. Chem.* **2003**, 3179-3184; S. Burling, L. D. Field, B. A. Messerle, P. Turner, *Organomet.* **2004**, *23*, 1714-1721; L. D. Field, B. A. Messerle, K. Q. Vuong, P. Turner, *Organomet.* **2005**, *24*, 4241-4250; A. Takemiya, J. F. Hartwig, *J. Am. Chem. Soc.* **2006**, *128*, 6042-6043; L. D. Field, B. A. Messerle, K. Q. Vuong, P. Turner, T. Failes, *Organomet.* **2007**, *26*, 2058-2069; R. Y. Lai, K. Surekha, A. Hayashi, F. Ozawa, Y. H. Liu, S. M. Peng, S. T. Liu, *Organomet.* **2007**, *26*, 1062-1068; Z. Liu, J. F. Hartwig, *J. Am. Chem. Soc.* **2008**, *130*, 1570-1571; S. L. Dabb, J. H. H. Ho, R. Hodgson, B. A. Messerle, J. Wagler, *Dalton Trans* **2009**, 634-642; K. Ogata, T. Nagaya, S. Fukuzawa, *J. Organomet. Chem.* **2010**, *695*, 1675-1681; Y. Kashiwame, S. Kuwata, T. Ikariya, *Chem. Eur. J.* **2010**, *16*, 766-770.

[122] K. D. Hesp, M. Stradiotto, *Org. Lett.* **2009**, *11*, 1449-1452; K. D. Hesp, S. Tobisch, M. Stradiotto, *J. Am. Chem. Soc.* **2010**, *132*, 413-426.

[123] L. S. Hegedus, G. F. Allen, E. L. Waterman, *J. Am. Chem. Soc.* **1976**, *98*, 2674-2676; L. S. Hegedus, G. F. Allen, J. J. Bozell, E. L. Waterman, *J. Am. Chem. Soc.* **1978**, *100*, 5800-5807; M. Meguro, Y. Yamamoto, *Tet. Lett.* **1998**, *39*, 5421-5424; T. E. Muller, *Tet. Lett.* **1998**, *39*, 5961-5962; T. E. Muller, M. Berger, M. Grosche, E. Herdtweck, F. P. Schmidtchen, *Organomet.* **2001**, *20*, 4384-4393; S. R. Fix, J. L. Brice, S. S. Stahl, *Angew. Chem. - Int. Ed.* **2002**, *41*, 164-166; L. M. Lutete, I. Kadota, Y. Yamamoto, *J. Am. Chem. Soc.* **2004**, *126*, 1622-1623; J. Streuff, C. H. Hovelmann, M. Nieger, K. Muniz, *J. Am. Chem. Soc.* **2005**, *127*, 14586-14587; F. E. Michael, B. M. Cochran, *J. Am. Chem. Soc.* **2006**, *128*, 4246-4247; N. T. Patil, L. M. Lutete, H. Y. Wu, N. K. Pahadi, I. D. Gridnev, Y. Yamamoto, *J. Org. Chem.* **2006**, *71*, 4270-4279; A. Minatti, K. Muniz, *Chem. Soc Rev.* **2007**, *36*, 1142-1152; B. M. Cochran, F. E. Michael, *J.*

Am. Chem. Soc. **2008**, *130*, 2786-2792; B. M. Cochran, F. E. Michael, *Org. Lett.* **2008**, *10*, 329-332; M. Narsireddy, Y. Yamamoto, *J. Org. Chem.* **2008**, *73*, 9698-9709.

[124] D. A. Krogstad, J. Cho, A. J. DeBoer, J. A. Klitzke, W. R. Sanow, H. A. Williams, J. A. Halfen, *Inorg. Chim. Acta* **2006**, *359*, 136-148.

[125] J. Ambuehl, P. S. Pregosin, L. M. Venanzi, *J. Organomet. Chem.* **1978**, *160*, 329-335; J. Ambuehl, P. S. Pregosin, L. M. Venanzi, G. Consiglio, F. Bachechi, L. Zambonelli, *J. Organomet. Chem.* **1979**, *181*, 255-269; C. F. Bender, R. A. Widenhoefer, *J. Am. Chem. Soc.* **2005**, *127*, 1070-1071; D. A. Krogstad, S. B. Owens, J. A. Halfen, V. G. Young, *Inorg. Chem. Commun.* **2005**, *8*, 65-69; C. F. Bender, W. B. Hudson, R. A. Widenhoefer, *Organomet.* **2008**, *27*, 2356-2358.

[126] A. Tsuhako, D. Oikawa, K. Sakai, S. Okamoto, *Tet. Lett.* **2008**, *49*, 6529-6532.

[127] N. T. Patil, L. M. Lutete, N. Nishina, Y. Yamamoto, *Tet. Lett.* **2006**, *47*, 4749-4751; R. L. LaLonde, B. D. Sherry, E. J. Kang, F. D. Toste, *J. Am. Chem. Soc.* **2007**, *129*, 2452-2453; Z. B. Zhang, C. F. Bender, R. A. Widenhoefer, *J. Am. Chem. Soc.* **2007**, *129*, 14148-14149; Y. H. Zhang, J. P. Donahue, C. J. Li, *Org. Lett.* **2007**, *9*, 627-630; C. F. Bender, R. A. Widenhoefer, *Chem. Commun.* **2008**, 2741-2743; J. M. Carney, P. J. Donoghue, W. M. Wuest, O. Wiest, P. Helquist, *Org. Lett.* **2008**, *10*, 3903-3906; S. R. Beeren, S. L. Dabb, B. A. Messerle, *J. Organomet. Chem.* **2009**, *694*, 309-312; H. Li, R. A. Widenhoefer, *Org. Lett.* **2009**, *11*, 2671-2674; A. M. Manzo, A. D. Perboni, G. Broggini, M. Rigamonti, *Tet. Lett.* **2009**, *50*, 4696-4699; D. J. Ye, X. Zhang, Y. Zhou, D. Y. Zhang, L. Zhang, H. S. Wang, H. L. Jiang, H. Liu, *Adv. Synth. Catal.* **2009**, *351*, 2770-2778; M. C. P. Yeh, H. F. Pai, Z. J. Lin, B. R. Lee, *Tetrahedron* **2009**, *65*, 4789-4794.

[128] A. Zulys, M. Dochnahl, D. Hollmann, K. Lohnwitz, J. S. Herrmann, P. W. Roesky, S. Blechert, *Angew. Chem. - Int. Ed.* **2005**, *44*, 7794-7798; M. Dochnahl, J. W. Pissarek, S. Blechert, K. Lohnwitz, P. W. Roesky, *Chem. Commun.* **2006**, 3405-3407; N. Meyer, K. Lohnwitz, A. Zulys, P. W. Roesky, M. Dochnahl, S. Blechert, *Organomet.* **2006**, *25*, 3730-3734; M. Dochnahl, K. Lohnwitz, J. W. Pissarek, M. Biyikal, S. R. Schulz, S. Schon, N. Meyer, P. W. Roesky, S. Blechert, *Chem. Eur. J.* **2007**, *13*, 6654-6666; Y. Yin, W. Y. Ma, Z. Chai, G. Zhao, *J. Org. Chem.* **2007**, *72*, 5731-5736; K. Lohnwitz, M. J. Molski,

A. Luhl, P. W. Roesky, M. Dochnahl, S. Blechert, *Eur. J. Inorg. Chem.* **2009**, 1369-1375.

[129] P. Horrillo-Martinez, K. C. Hultzsch, *Tet. Lett.* **2009**, *50*, 2054-2056.

[130] M. R. Gagne, T. J. Marks, *J. Am. Chem. Soc.* **1989**, *111*, 4108-4109; M. R. Gagne, S. P. Nolan, T. J. Marks, *Organomet.* **1990**, *9*, 1716-1718; Y. W. Li, P. F. Fu, T. J. Marks, *Organomet.* **1994**, *13*, 439-440; Y. W. Li, T. J. Marks, *J. Am. Chem. Soc.* **1998**, *120*, 1757-1771; V. M. Arredondo, F. E. McDonald, T. J. Marks, *J. Am. Chem. Soc.* **1998**, *120*, 4871-4872; S. Tian, V. M. Arredondo, C. L. Stern, T. J. Marks, *Organomet.* **1999**, *18*, 2568-2570; V. M. Arredondo, S. Tian, F. E. McDonald, T. J. Marks, *J. Am. Chem. Soc.* **1999**, *121*, 3633-3639; J. S. Ryu, T. J. Marks, F. E. McDonald, *Org. Lett.* **2001**, *3*, 3091-3094; S. W. Hong, T. J. Marks, *J. Am. Chem. Soc.* **2002**, *124*, 7886-7887.

[131] M. R. Gagne, L. Brard, V. P. Conticello, M. A. Giardello, C. L. Stern, T. J. Marks, *Organomet.* **1992**, *11*, 2003-2005; M. A. Giardello, V. P. Conticello, L. Brard, M. R. Gagne, T. J. Marks, *J. Am. Chem. Soc.* **1994**, *116*, 10241-10254; J. Collin, J. C. Daran, E. Schulz, A. Trifonov, *Chem. Commun.* **2003**, 3048-3049; S. W. Hong, S. Tian, M. V. Metz, T. J. Marks, *J. Am. Chem. Soc.* **2003**, *125*, 14768-14783; P. N. O'Shaughnessy, P. Scott, *Tet. Asymm.* **2003**, *14*, 1979-1983; P. N. O'Shaughnessy, P. D. Knight, C. Morton, K. M. Gillespie, P. Scott, *Chem. Commun.* **2003**, 1770-1771; J. Collin, J. C. Daran, O. Jacquet, E. Schulz, A. Trifonov, *Chem. Eur. J.* **2005**, *11*, 3455-3462; N. Meyer, A. Zulys, P. W. Roesky, *Organomet.* **2006**, *25*, 4179-4182; D. Riegert, J. Collin, A. Meddour, E. Schulz, A. Trifonov, *J. Org. Chem.* **2006**, *71*, 2514-2517; X. H. Yu, T. J. Marks, *Organomet.* **2007**, *26*, 365-376; Q. W. Wang, L. Xiang, H. B. Song, G. F. Zi, *Inorg. Chem.* **2008**, *47*, 4319-4328.

[132] Y. W. Li, T. J. Marks, *J. Am. Chem. Soc.* **1996**, *118*, 9295-9306; V. M. Arredondo, F. E. McDonald, T. J. Marks, *Organomet.* **1999**, *18*, 1949-1960; S. Hong, A. M. Kawaoka, T. J. Marks, *J. Am. Chem. Soc.* **2003**, *125*, 15878-15892.

[133] G. A. Molander, E. D. Dowdy, *J. Org. Chem.* **1998**, *63*, 8983-8988; G. A. Molander, E. D. Dowdy, S. K. Pack, *J. Org. Chem.* **2001**, *66*, 4344-4347; Y. K. Kim, T. Livinghouse, J. E. Bercaw, *Tet. Lett.* **2001**, *42*, 2933-2935; Y. K. Kim, T. Livinghouse, *Angew. Chem. - Int. Ed.* **2002**, *41*, 3645-3647; M. R. Douglass, M. Ogasawara, S. Hong, M. V. Metz, T. J. Marks, *Organomet.* **2002**, *21*, 283-292; Y. K. Kim, T. Livinghouse, Y. Horino, *J. Am. Chem. Soc.* **2003**, *125*, 9560-

9561; G. A. Molander, S. K. Pack, *Tetrahedron* **2003**, *59*, 10581-10591; P. W. Roesky, *Zeit. Anorg. Allg. Chem.* **2003**, *629*, 1881-1894; G. A. Molander, S. K. Pack, *J. Org. Chem.* **2003**, *68*, 9214-9220; D. V. Gribkov, F. Hampel, K. C. Hultzsch, *Eur. J. Inorg. Chem.* **2004**, 4091-4101; G. A. Molander, H. Hasegawa, *Heterocycles* **2004**, *64*, 467-474; A. M. Seyam, B. D. Stubbert, T. R. Jensen, J. J. O'Donnell, C. L. Stern, T. J. Marks, *Inorg. Chim. Acta* **2004**, *357*, 4029-4035; A. Zulys, T. K. Panda, M. T. Gamer, P. W. Roesky, *Chem. Commun.* **2004**, 2584-2585; T. K. Panda, A. Zulys, M. T. Gamer, P. W. Roesky, *J. Organomet. Chem.* **2005**, *690*, 5078-5089; T. K. Panda, A. Zulys, M. T. Gainer, P. W. Roesky, *Organomet.* **2005**, *24*, 2197-2202; D. V. Gribkov, K. C. Hultzsch, F. Hampel, *J. Am. Chem. Soc.* **2006**, *128*, 3748-3759; M. Rastatter, A. Zulys, P. W. Roesky, *Chem. Commun.* **2006**, 874-876; L. Xiang, Q. W. Wang, H. B. Song, G. F. Zi, *Organomet.* **2007**, *26*, 5323-5329; M. Rastatter, A. Zulys, P. W. Roesky, *Chem. Eur. J.* **2007**, *13*, 3606-3616; T. K. Panda, C. G. Hrib, P. G. Jones, J. Jenter, P. W. Roesky, M. Tamm, *Eur. J. Inorg. Chem.* **2008**, 4270-4279; H. F. Yuen, T. J. Marks, *Organomet.* **2008**, *27*, 155-158; H. F. Yuen, T. J. Marks, *Organomet.* **2009**, *28*, 2423-2440.

[134] J. S. Ryu, T. J. Marks, F. E. McDonald, *J. Org. Chem.* **2004**, *69*, 1038-1052.

[135] I. Aillaud, J. Collin, C. Duhayon, R. Guillot, D. Lyubov, E. Schulz, A. Trifonov, *Chem. Eur. J.* **2008**, *14*, 2189-2200.

[136] B. D. Stubbert, T. J. Marks, *J. Am. Chem. Soc.* **2007**, *129*, 4253-4271.

[137] B. D. Stubbert, T. J. Marks, *J. Am. Chem. Soc.* **2007**, *129*, 6149-6167.

[138] S. Tobisch, *J. Am. Chem. Soc.* **2005**, *127*, 11979-11988; A. Motta, I. L. Fragala, T. J. Marks, *Organomet.* **2006**, *25*, 5533-5539; S. Tobisch, *Chem. Eur. J.* **2007**, *13*, 9127-9136.

[139] S. Tobisch, *Chem. Eur. J.* **2010**, *16*, 3441-3458.

[140] S. Tobisch, *Chem. Eur. J.* **2008**, *14*, 8590-8602.

[141] M. R. Crimmin, M. S. Hill, P. B. Hitchcock, M. F. Mahon, *New J. Chem.* **2010**, *34*, 1572-1578.

[142] M. Westerhausen, *Inorg. Chem.* **1991**, *30*, 96-101.

[143] P. B. Hitchcock, M. F. Lappert, G. A. Lawless, B. Royo, *J. Chem. Soc. - Chem. Commun.* **1990**, 1141-1142; Y. J. Tang, L. N. Zakharov, W. S. Kassel, A. L. Rheingold, R. A. Kemp, *Inorg. Chim. Acta* **2005**, *358*, 2014-2022.

[144] M. Crimmin, A. Barrett, M. Hill, D. MacDougall, M. Mahon, P. Procopiou, *Chem. Eur. J.* **2008**, *14*, 11292-11295.

[145] P. B. Hitchcock, J. A. K. Howard, M. F. Lappert, W. P. Leung, S. A. Mason, *J. Chem. Soc. - Chem. Commun.* **1990**, 847-849.

[146] A. G. Avent, C. F. Caro, P. B. Hitchcock, M. F. Lappert, Z. N. Li, X. H. Wei, *Dalton Trans.* **2004**, 1567-1577.

[147] S. S. Aljuaid, C. Eaborn, P. B. Hitchcock, C. A. McGeary, J. D. Smith, *J. Chem. Soc. - Chem. Commun.* **1989**, 273-274.

[148] J. E. Baldwin, *J. Chem. Soc. - Chem. Commun.* **1976**, 734-736.

[149] A. W. Addison, T. N. Rao, J. Reedijk, J. Vanrijn, G. C. Verschoor, *J. Chem. Soc. - Dalton Trans.* **1984**, 1349-1356.

[150] W. J. Teng, M. Guino-O, J. Hitzbleck, U. Englich, K. Ruhlandt-Senge, *Inorg. Chem.* **2006**, *45*, 9531-9539.

[151] J. W. Park, J. T. Kim, S. M. Koo, C. G. Kim, Y. S. Kim, *Polyhedron* **2000**, *19*, 2547-2555.

[152] X. Zhang, T. J. Emge, K. C. Hultzsch, *Organomet.* **2010**, *29*, 5871-5877.

[153] J. Feldman, S. J. McLain, A. Parthasarathy, W. J. Marshall, J. C. Calabrese, S. D. Arthur, *Organomet.* **1997**, *16*, 1514-1516.

[154] S. Harder, *Angew. Chem. - Int. Ed.* **2003**, 3430-3434.

[155] M. Crimmin, A. Barrett, M. Hill, D. MacDougall, M. Mahon, P. Procopiou, *Dalton Trans.* **2009**, 9715-9717.

[156] G. Berthon-Gelloz, M. A. Siegler, A. L. Spek, B. Tinant, J. N. H. Reek, I. E. Marko, *Dalton Trans.* **2010**, *39*, 1444-1446.

[157] M. Chisholm, J. Gallucci, G. Yaman, *Chem. Commun.* **2006**, 1872-1874.

[158] A. P. Dove, V. C. Gibson, E. L. Marshall, A. J. P. White, D. J. Williams, *Dalton Trans.* **2004**, 570-578; J. M. Fritsch, K. A. Thoreson, K. McNeill, *Dalton Trans.* **2006**, 4814-4820.

[159] H. M. El-Kaderi, M. J. Heeg, C. H. Winter, *Polyhedron* **2006**, *25*, 224-234.

[160] P. O. Oguadinma, F. Schaper, *Organomet.* **2009**, *28*, 4089-4097; F. Drouin, P. O. Oguadinma, T. J. J. Whitehorne, R. E. Prud'homme, F. Schaper, *Organomet.* **2010**, *29*, 2139-2147; I. El-Zoghbi, S. Latreche, F. Schaper, *Organomet.* **2010**, *29*, 1551-1559.

[161] K. Ofele, *J. Organomet. Chem.* **1968**, *12*, P42-P43.

[162] H. W. Wanzlick, E. Schikora, *Angew. Chem. - Int. Ed.* **1960**, *72*, 494-494; H. W. Wanzlick, H. J. Kleiner, *Angew. Chem. - Int. Ed.* **1961**, *73*, 493; H. W. Wanzlick, E. Schikora, *Chem. Ber. Rec.* **1961**, *94*, 2389-2393; H. W. Wanzlick, *Angew. Chem. - Int. Ed.* **1962**, *74*, 129-134; H. W. Wanzlick, H. J. Schonher, *Angew. Chem. - Int. Ed.* **1968**, *7*, 141-142.

[163] D. J. Cardin, Cetinkay.B, M. F. Lappert, *Chem. Rev.* **1972**, *72*, 545-574; D. J. Cardin, Cetinkay.B, M. J. Doyle, M. F. Lappert, *Chem. Soc Rev.* **1973**, *2*, 99-144; M. F. Lappert, *J. Organomet. Chem.* **1988**, *358*, 185-214.

[164] A. J. Arduengo, R. L. Harlow, M. Kline, *J. Am. Chem. Soc.* **1991**, *113*, 361-363.

[165] W. A. Herrmann, M. Elison, J. Fischer, C. Kocher, G. R. J. Artus, *Angew. Chem. - Int. Ed. Eng.* **1995**, *34*, 2371-2374.

[166] W. A. Herrmann, *Angew. Chem. - Int. Ed.* **2002**, *41*, 1290-1309.

[167] M. C. Perry, K. Burgess, *Tet. Asymm.* **2003**, *14*, 951-961; V. Cesar, S. Bellemin-Laponnaz, L. H. Gade, *Chem. Soc Rev.* **2004**, *33*, 619-636; E. Peris, R. H. Crabtree, *Coord. Chem. Rev.* **2004**, *248*, 2239-2246; L. H. Gade, S. Bellemin-Laponnaz, *Coord. Chem. Rev.* **2007**, *251*, 718-725; J. A. Mata, M. Poyatos, E. Peris, *Coord. Chem. Rev.* **2007**, *251*, 841-859; A. T. Normand, K. J. Cavell, *Eur. J. Inorg. Chem.* **2008**, 2781-2800; S. Diez-Gonzalez, N. Marion, S. P. Nolan, *Chem. Rev.* **2009**, *109*, 3612-3676; H. Richter, H. Schwertfeger, P. R. Schreiner, R. Frohlich, F. Glorius, *Synlett* **2009**, 193-197; R. Corberan, E. Mas-Marza, E. Peris, *Eur. J. Inorg. Chem.* **2009**, 1700-1716; M. Poyatos, J. A. Mata, E. Peris, *Chem. Rev.* **2009**, *109*, 3677-3707; C. Samojlowicz, M. Bieniek, K. Grela, *Chem. Rev.* **2009**, *109*, 3708-3742.

[168] T. M. Trnka, R. H. Grubbs, *Acc. Chem. Res.* **2001**, *34*, 18-29; T. M. Trnka, J. P. Morgan, M. S. Sanford, T. E. Wilhelm, M. Scholl, T. L. Choi, S. Ding, M. W. Day, R. H. Grubbs, *J. Am. Chem. Soc.* **2003**, *125*, 2546-2558.

[169] R. H. Grubbs, *Tetrahedron* **2004**, *60*, 7117-7140; R. H. Grubbs, *Angew. Chem. - Int. Ed.* **2006**, *45*, 3760-3765.

[170] D. Enders, T. Balensiefer, *Acc. Chem. Res.* **2004**, *37*, 534-541; D. Enders, O. Niemeier, A. Henseler, *Chem. Rev.* **2007**, *107*, 5606-5655; T. Boddaert, Y. Coquerel, J. Rodriguez, *Adv. Synth. Catal.* **2009**, *351*, 1744-1748; Y. Kayaki, M. Yamamoto, T. Ikariya, *Angew. Chem. - Int. Ed.* **2009**, *48*, 4194-4197; N. Li, W. J. Liu, L. Z. Gong, *Prog. Chem.* **2010**, *22*, 1362-1379; J. L. Moore, T. Rovis,

Asymm. Organocat. **2010**, *291*, 77-144; J. Raynaud, C. Absalon, Y. Gnanou, D. Taton, *Macromol.* **2010**, *43*, 2814-2823.

[171] J. C. Green, R. G. Scurr, P. L. Arnold, F. G. N. Cloke, *Chem. Commun.* **1997**, 1963-1964; K. Ofele, W. A. Herrmann, D. Mihalios, M. Elison, E. Herdtweck, W. Scherer, J. Mink, *J. Organomet. Chem.* **1993**, *459*, 177-184; W. A. Herrmann, M. Elison, J. Fischer, C. Kocher, G. R. J. Artus, *Chem. Eur. J.* **1996**, *2*, 772-780.

[172] D. Bourissou, O. Guerret, F. P. Gabbai, G. Bertrand, *Chem. Rev.* **2000**, *100*, 39-91; G. Frenking, M. Sola, S. F. Vyboishchikov, *J. Organomet. Chem.* **2005**, *690*, 6178-6204; N. M. Scott, S. P. Nolan, *Eur. J. Inorg. Chem.* **2005**, 1815-1828; U. Radius, F. M. Bickelhaupt, *Coord. Chem. Rev.* **2009**, *253*, 678-686; H. Jacobsen, A. Correa, A. Poater, C. Costabile, L. Cavallo, *Coord. Chem. Rev.* **2009**, *253*, 2784-2784.

[173] R. Dorta, E. D. Stevens, N. M. Scott, C. Costabile, L. Cavallo, C. D. Hoff, S. P. Nolan, *J. Am. Chem. Soc.* **2005**, *127*, 2485-2495.

[174] A. Furstner, H. Krause, *Adv. Synth. Catal.* **2001**, *343*, 343-350; R. Jackstell, M. G. Andreu, A. Frisch, K. Selvakumar, A. Zapf, H. Klein, A. Spannenberg, D. Rottger, O. Briel, R. Karch, M. Beller, *Angew. Chem. - Int. Ed.* **2002**, *41*, 986-989; C. W. Gao, X. C. Tao, Y. L. Qian, J. L. Huang, *Chem. Commun.* **2003**, 1444-1445; J. Ramirez, R. Corberan, M. Sanau, E. Peris, E. Fernandez, *Chem. Commun.* **2005**, 3056-3058; T. Yamagami, R. Shintani, E. Shirakawa, T. Hayashi, *Org. Lett.* **2007**, *9*, 1045-1048; T. Kobayashi, H. Ohmiya, H. Yorimitsu, K. Oshima, *J. Am. Chem. Soc.* **2008**, *130*, 11276-11277; L. Zhang, J. Wu, *Adv. Synth. Catal.* **2008**, *350*, 2409-2413; R. H. Crabtree, *J. Organomet. Chem.* **2005**, *690*, 5451-5457.

[175] W. A. Herrmann, C. P. Reisinger, M. Spiegler, *J. Organomet. Chem.* **1998**, *557*, 93-96; C. M. Zhang, J. K. Huang, M. L. Trudell, S. P. Nolan, *J. Org. Chem.* **1999**, *64*, 3804-3805; W. A. Herrmann, V. P. W. Bohm, C. W. K. Gstottmayr, M. Grosche, C. P. Reisinger, T. Weskamp, *J. Organomet. Chem.* **2001**, *617*, 616-628; A. Furstner, A. Leitner, *Synlett* **2001**, 290-292; M. Eckhardt, G. C. Fu, *J. Am. Chem. Soc.* **2003**, *125*, 13642-13643; A. C. Frisch, F. Rataboul, A. Zapf, M. Beller, *J. Organomet. Chem.* **2003**, *687*, 403-409; G. Altenhoff, R. Goddard, C. W. Lehmann, F. Glorius, *Angew. Chem. - Int. Ed.* **2003**, *42*, 3690-3693.

[176] Y. J. Kim, A. Streitwieser, *J. Am. Chem. Soc.* **2002**, *124*, 5757-5761; A. M. Magill, K. J. Cavell, B. F. Yates, *J. Am. Chem. Soc.* **2004**, *126*, 8717-8724.

[177] A. C. Hillier, W. J. Sommer, B. S. Yong, J. L. Petersen, L. Cavallo, S. P. Nolan, *Organomet.* **2003**, *22*, 4322-4326; S. Diez-Gonzalez, S. P. Nolan, *Coord. Chem. Rev.* **2007**, *251*, 874-883; L. Cavallo, A. Correa, C. Costabile, H. Jacobsen, *J. Organomet. Chem.* **2005**, *690*, 5407-5413; H. Clavier, S. P. Nolan, *Chem. Commun.* **2010**, *46*, 841-861; C. C. Scarborough, B. V. Popp, I. A. Guzei, S. S. Stahl, *J. Organomet. Chem.* **2005**, *690*, 6143-6155.

[178] C. Heinemann, T. Muller, Y. Apeloig, H. Schwarz, *J. Am. Chem. Soc.* **1996**, *118*, 2023-2038; J. F. Lehmann, S. G. Urquhart, L. E. Ennis, A. P. Hitchcock, K. Hatano, S. Gupta, M. K. Denk, *Organomet.* **1999**, *18*, 1862-1872.

[179] A. A. D. Tulloch, A. A. Danopoulos, S. Kleinhenz, M. E. Light, M. B. Hursthouse, G. Eastham, *Organomet.* **2001**, *20*, 2027-2031; J. C. Garrison, R. S. Simons, W. G. Kofron, C. A. Tessier, W. J. Youngs, *Chem. Commun.* **2001**, 1780-1781; X. L. Hu, Y. J. Tang, P. Gantzel, K. Meyer, *Organomet.* **2003**, *22*, 612-614; D. Nemcsok, K. Wichmann, G. Frenking, *Organomet.* **2004**, *23*, 3640-3646; H. Nakai, X. L. Hu, L. N. Zakharov, A. L. Rheingold, K. Meyer, *Inorg. Chem.* **2004**, *43*, 855-857.

[180] N. M. Scott, R. Dorta, E. D. Stevens, A. Correa, L. Cavallo, S. P. Nolan, *J. Am. Chem. Soc.* **2005**, *127*, 3516-3526.

[181] S. A. Mungur, S. T. Liddle, C. Wilson, M. J. Sarsfield, P. L. Arnold, *Chem. Commun.* **2004**, 2738-2739.

[182] P. L. Arnold, I. J. Casely, *Chem. Rev.* **2009**, *109*, 3599-3611.

[183] H. Schumann, M. Glanz, J. Winterfeld, H. Hemling, N. Kuhn, T. Kratz, *Angew. Chem. - Int. Ed. Eng.* **1994**, *33*, 1733-1734.

[184] A. J. Arduengo, M. Tamm, S. J. McLain, J. C. Calabrese, F. Davidson, W. J. Marshall, *J. Am. Chem. Soc.* **1994**, *116*, 7927-7928.

[185] L. Maron, D. Bourissou, *Organomet.* **2007**, *26*, 1100-1103.

[186] L. Maron, D. Bourissou, *Organomet.* **2009**, *28*, 3686-3690.

[187] S. T. Liddle, I. S. Edworthy, P. L. Arnold, *Chem. Soc Rev.* **2007**, *36*, 1732-1744.

[188] D. Patel, S. T. Liddle, S. A. Mungur, M. Rodden, A. J. Blake, P. L. Arnold, *Chem. Commun.* **2006**, 1124-1126.

[189] B. L. Wang, D. Wang, D. M. Cui, W. Gao, T. Tang, X. S. Chen, X. B. Jing, *Organomet.* **2007**, *26*, 3167-3172.

[190] B. L. Wang, D. M. Cui, K. Lv, *Macromol.* **2008**, *41*, 1983-1988.

[191] K. Lv, D. M. Cui, *Organomet.* **2010**, *29*, 2987-2993.

[192] R. W. Alder, M. E. Blake, C. Bortolotti, S. Bufali, C. P. Butts, E. Linehan, J. M. Oliva, A. G. Orpen, M. J. Quayle, *Chem. Commun.* **1999**, 241-242; A. J. Arduengo, M. Tamm, J. C. Calabrese, F. Davidson, W. J. Marshall, *Chem. Lett.* **1999**, 1021-1022; R. Frankell, C. Birg, U. Kernbach, T. Habereder, H. Noth, W. P. Fehlhammer, *Angew. Chem. - Int. Ed.* **2001**, *40*, 1907-1910; P. L. Arnold, M. Rodden, K. M. Davis, A. C. Scarisbrick, A. J. Blake, C. Wilson, *Chem. Commun.* **2004**, 1612-1613; P. L. Arnold, M. Rodden, C. Wilson, *Chem. Commun.* **2005**, 1743-1745; I. S. Edworthy, A. J. Blake, C. Wilson, P. L. Arnold, *Organomet.* **2007**, *26*, 3684-3689; P. L. Arnold, C. Wilson, *Inorg. Chim. Acta* **2007**, *360*, 190-196; I. V. Shishkov, F. Rominger, P. Hofmann, *Organomet.* **2009**, *28*, 3532-3536.

[193] A. J. Arduengo, H. V. R. Dias, F. Davidson, R. L. Harlow, *J. Organomet. Chem.* **1993**, *462*, 13-18.

[194] W. A. Herrmann, O. Runte, G. Artus, *J. Organomet. Chem.* **1995**, *501*, C1-C4.

[195] A. Arduengo, F. Davidson, R. Krafczyk, W. Marshall, M. Tamm, *Organomet.* **1998**, *17*, 3375-3382.

[196] H. Schumann, J. Gottfriedsen, M. Glanz, S. Dechert, J. Demtschuk, *J. Organomet. Chem.* **2001**, *617*, 588-600.

[197] A. G. M. Barrett, M. R. Crimmin, M. S. Hill, G. Kociok-Köhn, D. J. MacDougall, M. F. Mahon, P. A. Procopiou, *Organomet.* **2008**, *27*, 3939-3946.

[198] P. L. Arnold, I. S. Edworthy, C. D. Carmichael, A. J. Blake, C. Wilson, *Dalton Trans.* **2008**, 3739-3746.

[199] P. L. Arnold, I. J. Casely, Z. R. Turner, R. Bellabarba, R. B. Tooze, *Dalton Trans* **2009**, 7236-7247.

[200] S. Trofimenko, *J. Am. Chem. Soc.* **1966**, *88*, 1842-1844.

[201] K. Niedenzu, S. Trofimenko, *Top. Curr. Chem.* **1986**, *131*, 1-37; S. Trofimenko, *Chem. Rev.* **1993**, *93*, 943-980; S. Trofimenko, *Polyhedron* **2004**, *23*, 197-203; S. Trofimenko, *J. Chem. Edu.* **2005**, *82*, 1715-1720.

[202] S. Trofimenko, *Scorpionates. The Coordination Chemistry of Polypyrazolylborate Ligands* **1999**, *Imperial College Press*.

[203] J. Smith, *Comm. Inorg. Chem.* **2008**, *29*, 189-233; A. Otero, J. Fernandez-Baeza, A. Lara-Sanchez, J. Tejeda, L. F. Sanchez-Barba, *Eur. J. Inorg. Chem.* **2008**, 5309-5326; M. D. Spicer, J. Reglinski, *Eur. J. Inorg. Chem.* **2009**, 1553-1574.

[204] M. Chisholm, J. Gallucci, G. Yaman, T. Young, *Chem. Commun.* **2009**, 1828-1830.

[205] U. Kernbach, M. Ramm, P. Luger, W. P. Fehlhammer, *Angew. Chem. - Int. Ed. Eng.* **1996**, *35*, 310-312.

[206] R. Frankel, J. Kniczek, W. Ponikwar, H. Noth, K. Polborn, W. P. Fehlhammer, *Inorg. Chim. Acta* **2001**, *312*, 23-39; R. Frankel, U. Kernbach, M. Bakola-Christianopoulou, U. Plaia, M. Suter, W. Ponikwar, H. Noth, C. Moinet, W. P. Fehlhammer, *J. Organomet. Chem.* **2001**, *617*, 530-545; R. E. Cowley, R. P. Bontchev, J. Sorrell, O. Sarracino, Y. H. Feng, H. B. Wang, J. M. Smith, *J. Am. Chem. Soc.* **2007**, *129*, 2424-2425; A. P. Forshaw, R. P. Bontchev, J. M. Smith, *Inorg. Chem.* **2007**, *46*, 3792-3794; A. Biffis, G. G. Lobbia, G. Papini, M. Pellei, C. Santini, E. Scattolin, C. Tubaro, *J. Organomet. Chem.* **2008**, *693*, 3760-3766; I. Nieto, F. Ding, R. P. Bontchev, H. B. Wang, J. M. Smith, *J. Am. Chem. Soc.* **2008**, *130*, 2716-2717; J. J. Scepaniak, M. D. Fulton, R. P. Bontchev, E. N. Duesler, M. L. Kirk, J. M. Smith, *J. Am. Chem. Soc.* **2008**, *130*, 10515-10517; J. J. Scepaniak, J. A. Young, R. P. Bontchev, J. M. Smith, *Angew. Chem. - Int. Ed.* **2009**, *48*, 3158-3160; C. Tubaro, A. Biffis, E. Scattolin, M. Basato, *Tetrahedron* **2008**, *64*, 4187-4195; A. Biffis, C. Tubaro, E. Scattolin, M. Basato, G. Papini, C. Santini, E. Alvarez, S. Conejero, *Dalton Trans* **2009**, 7223-7229.

[207] I. Nieto, F. Cervantes-Lee, J. M. Smith, *Chem. Commun.* **2005**, 3811-3813.

[208] R. E. Cowley, R. P. Bontchev, E. N. Duesler, J. M. Smith, *Inorg. Chem.* **2006**, *45*, 9771-9779.

[209] I. Nieto, R. P. Bontchev, A. Ozarowski, D. Smirnov, J. Krzystek, J. Telser, J. M. Smith, *Inorg. Chim. Acta* **2009**, *362*, 4449-4460.

[210] I. Nieto, R. P. Bontchev, J. M. Smith, *Eur. J. Inorg. Chem.* **2008**, 2476-2480.

[211] M. Arrowsmith, M. S. Hill, G. Kociok-Köhn, *Organomet.* **2009**, *28*, 1730-1738.

[212] P. A. Fox, S. T. Griffin, W. M. Reichert, E. A. Salter, A. B. Smith, M. D. Tickell, B. F. Wicker, E. A. Cioffi, J. H. Davis, R. D. Rogers, A. Wierzbicki, *Chem. Commun.* **2005**, 3679-3681; M. D. Soutullo, C. I. Odom, A. B. Smith, D. R. McCreary, R. E. Sykora, E. A. Salter, A. Wierzbicki, J. H. Davis, *Inorg. Chim. Acta* **2007**, *360*, 3099-3102.

[213] A. Barrett, M. Crimmin, M. Hill, G. Kociok-Köhn, D. MacDougall, M. Mahon, P. Procopiou, *Organomet.* **2008**, *27*, 3939-3946.

[214] T. R. Belderrain, M. Paneque, E. Carmona, E. Gutierrez-Puebla, M. A. Monge, C. Ruiz-Valero, *Inorg. Chem.* **2002**, *41*, 425-428.

[215] M. Bremer, H. Noth, M. Thomann, M. Schmidt, *Chemische Berichte* **1995**, *128*, 455-460.

[216] K. Izod, C. Wills, W. Clegg, R. W. Harrington, *Inorg. Chem.* **2007**, *46*, 4320-4325.

[217] L. Orzechowski, G. Jansen, S. Harder, *J. Am. Chem. Soc.* **2006**, *128*, 14676-14684.

[218] A. Barrett, M. Crimmin, M. Hill, P. Hitchcock, P. Procopiou, *Organomet.* **2007**, 4076-4079.

[219] J. Liu, J. Chen, J. Zhao, Y. Zhao, L. Li, H. Zhang, *Synthesis-Stuttgart* **2003**, 2661-2666.

[220] M. J. Frisch, G. W. Trucks, H. B. Schlegel, G. E. Scuseria, M. A. Robb, J. R. Cheeseman, J. A. J. Montgomery, T. Vreven, K. N. Kudin, J. C. Burant, J. M. Millam, S. S. Iyengar, J. Tomasi, V. Barone, B. Mennucci, M. Cossi, G. Scalmani, N. Rega, G. A. Petersson, H. Nakatsuji, M. Hada, M. Ehara, K. Toyota, R. Fukuda, J. Hasegawa, M. Ishida, T. Nakajima, Y. Honda, O. Kitao, H. Nakai, M. Klene, X. Li, J. E. Knox, H. P. Hratchian, J. B. Cross, C. Adamo, J. Jaramillo, R. Gomperts, R. E. Stratmann, O. Yazyev, A. J. Austin, R. Cammi, C. Pomelli, J. W. Ochterski, P. Y. Ayala, K. Morokuma, G. A. Voth, P. Salvador, J. J. Dannenberg, V. G. Zakrzewski, S. Dapprich, A. D. Daniels, M. C. Strain, O. Farkas, D. K. Malick, A. D. Rabuck, K. Raghavachari, J. B. Foresman, J. V. Ortiz, Q. Cui, A. G. Baboul, S. Clifford, J. Cioslowski, B. B. Stefanov, G. Liu, A. Liashenko, P. Piskorz, I. Komaromi, R. L. Martin, D. J. Fox, T. Keith, M. A. Al-Laham, C. Y. Peng, A. Nanayakkara, M. Challacombe, P. M. W. Gill, B. Johnson, W. Chen, M. W. Wong, C. Gonzalez, J. A. Pople, *Gaussian 03, revision C.02* **2004**, *Gaussian, Inc.: Wallingford, CT*.

[221] M. Arrowsmith, A. Heath, M. S. Hill, P. B. Hitchcock, G. Kociok-Köhn, *Organomet.* **2009**, *28*, 4550-4559.

[222] S. Datta, M. Gamer, P. Roesky, *Dalton Trans.* **2008**, 2839-2843.

[223] M. Gartner, H. Gorls, M. Westerhausen, *J. Organomet. Chem.* **2008**, *693*, 221-227.

253

[224] D. Harding, H. Adams, T. Tuntulani, *Acta Cryst. Sect. C- Cryst. Struc. Commun.* **2005**, *61*, M301-M303.

[225] O. Graziani, L. Toupet, J.-R. Hamon, M. Tilset*, Inorg. Chim. Acta* **2002**, *341*, 127-131.

[226] Z. R. Bell, G. R. Motson, J. C. Jeffery, J. A. McCleverty, M. D. Ward, *Polyhedron* **2001**, *20*, 2045-2053; A. Domingos, M. R. J. Elsegood, A. C. Hillier, G. Y. Lin, S. Y. Liu, I. Lopes, N. Marques, G. H. Maunder, R. McDonald, A. Sella, J. W. Steed, J. Takats, *Inorg. Chem.* **2002**, *41*, 6761-6768.

[227] M. Moser, B. Wucher, D. Kunz, F. Rominger, *Organomet.* **2007**, *26*, 1024-1030; K. Lv, D. M. Cui, *Organomet.* **2008**, *27*, 5438-5440; A. R. Chianese, A. Mo, N. L. Lampland, R. L. Swartz, P. T. Bremer, *Organomet.* **2010**, *29*, 3019-3026.

[228] M. Arrowsmith, M. S. Hill, G. Kociok-Köhn, *Organomet.* **2010**, *29*, 4203-4206.

[229] G. J. P. Britovsek, V. C. Gibson, D. F. Wass, *Angew. Chem. - Int. Ed.* **1999**, *38*, 428-447; V. C. Gibson, S. K. Spitzmesser, *Chem. Rev.* **2003**, *103*, 283-315; K. C. Gupta, A. K. Sutar, *Coord. Chem. Rev.* **2008**, *252*, 1420-1450; D. Takeuchi, *Dalton Trans.* **2010**, *39*, 311-328.

[230] B. L. Small, M. Brookhart, *J. Am. Chem. Soc.* **1998**, *120*, 7143-7144; B. L. Small, M. Brookhart, A. M. A. Bennett, *J. Am. Chem. Soc.* **1998**, *120*, 4049-4050; G. J. P. Britovsek, V. C. Gibson, B. S. Kimberley, P. J. Maddox, S. J. McTavish, G. A. Solan, A. J. P. White, D. J. Williams, *Chem. Commun.* **1998**, 849-850; B. L. Small, M. Brookhart, *Macromol.* **1999**, *32*, 2120-2130; A. M. A. Bennett, *Chemtech* **1999**, *29*, 24-28; G. J. P. Britovsek, M. Bruce, V. C. Gibson, B. S. Kimberley, P. J. Maddox, S. Mastroianni, S. J. McTavish, C. Redshaw, G. A. Solan, S. Stromberg, A. J. P. White, D. J. Williams, *J. Am. Chem. Soc.* **1999**, *121*, 8728-8740.

[231] V. C. Gibson, M. J. Humphries, K. P. Tellmann, D. F. Wass, A. J. P. White, D. J. Williams, *Chem. Commun.* **2001**, 2252-2253; G. J. P. Britovsek, V. C. Gibson, S. K. Spitzmesser, K. P. Tellmann, A. J. P. White, D. J. Williams, *J. Chem. Soc. - Dalton Trans.* **2002**, 1159-1171; V. C. Gibson, K. P. Tellmann, M. J. Humphries, D. F. Wass, *Chem. Commun.* **2002**, 2316-2317; G. J. P. Britovsek, V. C. Gibson, O. D. Hoarau, S. K. Spitzmesser, A. J. P. White, D. J. Williams, *Inorg. Chem.* **2003**, *42*, 3454-3465; M. J. Humphries, K. P. Tellmann, V. C. Gibson, A. J. P. White, D. J. Williams, *Organomet.* **2005**, *24*, 2039-2050; F. Pelascini, F. Peruch, P. J. Lutz, M. Wesolek, J. Kress, *Eur. Polym. J.* **2005**, *41*, 1288-1295; K. P.

Tellmann, V. C. Gibson, A. J. P. White, D. J. Williams, *Organomet.* **2005**, *24*, 280-286; V. C. Gibson, N. J. Long, P. J. Oxford, A. J. P. White, D. J. Williams, *Organomet.* **2006**, *25*, 1932-1939; C. Gorl, H. G. Alt, *J. Organomet. Chem.* **2007**, *692*, 4580-4592; F. A. R. Kaul, G. T. Puchta, G. D. Frey, E. Herdtweck, W. A. Herrmann, *Organomet.* **2007**, *26*, 988-999; I. E. Soshnikov, N. V. Semikolenova, A. N. Bushmelev, K. P. Bryliakov, O. V. Lyakin, C. Redshaw, V. A. Zakharov, E. P. Talsi, *Organomet.* **2009**, *28*, 6003-6013; K. Tenza, M. J. Hanton, A. M. Z. Slawin, *Organomet.* **2009**, *28*, 4852-4867; C. Bianchini, G. Giambastiani, L. Luconi, A. Meli, *Coord. Chem. Rev.* **2010**, *254*, 431-455; B. Y. Su, G. X. Feng, *Polym. Int.* **2010**, *59*, 1058-1063.

[232] I. Kim, B. Han, J. Kim, C. S. Ha, *Catal. Lett.* **2005**, *101*, 249-253; R. B. Huang, N. Kukalyekar, C. E. Koning, J. C. Chadwick, *J. Molec. Catal. a- Chem.* **2006**, *260*, 135-143; S. S. Ivanchev, N. I. Ivanchev, S. Y. Khaikin, E. V. Sviridova, D. G. Rogozin, *Polym. Sci. Ser. A* **2006**, *48*, 251-256; H. Kurokawa, M. Matsuda, K. Fujii, Y. Ishihama, T. Sakuragi, M. A. Ohshima, H. Miura, *Chem. Lett.* **2007**, *36*, 1004-1005; M. Seitz, W. Milius, H. G. Alt, *J. Molec. Catal. a- Chem.* **2007**, *261*, 246-253.

[233] E. A. H. Griffiths, G. J. P. Britovsek, V. C. Gibson, I. R. Gould, *Chem. Commun.* **1999**, 1333-1334; P. Margl, L. Q. Deng, T. Ziegler, *Organomet.* **1999**, *18*, 5701-5708; K. F. Tellmann, M. J. Humphries, H. S. Rzepa, V. C. Gibson, *Organomet.* **2004**, *23*, 5503-5513; R. Raucoules, T. de Bruin, P. Raybaud, C. Adamo, *Organomet.* **2008**, *27*, 3368-3377; V. L. Cruz, J. Ramos, J. Martinez-Salazar, S. Gutierrez-Oliva, A. Toro-Labbe, *Organomet.* **2009**, *28*, 5889-5895; G. Fayet, P. Raybaud, H. Toulhoat, T. de Bruin, *J. Molec. Struc. - Theochem.* **2009**, *903*, 100-107.

[234] B. Cetinkaya, E. Cetinkaya, M. Brookhart, P. S. White, *J. Molec. Catal. a- Chem.* **1999**, *142*, 101-112.

[235] C. Bianchini, H. M. Lee, *Organomet.* **2000**, *19*, 1833-1840.

[236] A. M. Archer, M. W. Bouwkamp, M. P. Cortez, E. Lobkovsky, P. J. Chirik, *Organomet.* **2006**, *25*, 4269-4278; S. C. Bart, E. Lobkovsky, P. J. Chirik, *J. Am. Chem. Soc.* **2004**, *126*, 13794-13807; S. C. Bart, E. Lobkovsky, E. Bill, P. J. Chirik, *J. Am. Chem. Soc.* **2006**, *128*, 5302-5303; A. M. Tondreau, E. Lobkovsky, P. J. Chirik, *Org. Lett.* **2008**, *10*, 2789-2792; R. J. Trovitch, E. Lobkovsky, E. Bill, P. J. Chirik, *Organomet.* **2008**, *27*, 1470-1478; R. J.

Trovitch, E. Lobkovsky, M. W. Bouwkamp, P. J. Chirik, *Organomet.* **2008**, *27*, 6264-6278; A. M. Tondreau, J. M. Darmon, B. M. Wile, S. K. Floyd, E. Lobkovsky, P. J. Chirik, *Organomet.* **2009**, *28*, 3928-3940.

[237] M. W. Bouwkamp, A. C. Bowman, E. Lobkovsky, P. J. Chirik, *J. Am. Chem. Soc.* **2006**, *128*, 13340-13341; K. T. Sylvester, P. J. Chirik, *J. Am. Chem. Soc.* **2009**, *131*, 8772-8774.

[238] V. C. Gibson, C. Redshaw, G. A. Solan, *Chem. Rev.* **2007**, *107*, 1745-1776.

[239] D. Reardon, G. Aharonian, S. Gambarotta, G. P. A. Yap, *Organomet.* **2002**, *21*, 786-788; H. Sugiyama, G. Aharonian, S. Gambarotta, G. P. A. Yap, P. H. M. Budzelaar, *J. Am. Chem. Soc.* **2002**, *124*, 12268-12274; H. Sugiyama, S. Gambarotta, G. P. A. Yap, D. R. Wilson, S. K. H. Thiele, *Organomet.* **2004**, *23*, 5054-5061; T. M. Kooistra, D. G. H. Hetterscheid, E. Schwartz, Q. Knijnenburg, P. H. M. Budzelaar, A. W. Gal, *Inorg. Chim. Acta* **2004**, *357*, 2945-2952; I. Vidyaratne, S. Gambarotta, I. Korobkov, P. H. M. Budzelaar, *Inorg. Chem.* **2005**, *44*, 1187-1189; M. W. Bouwkamp, E. Lobkovsky, P. J. Chirik, *Inorg. Chem.* **2006**, *45*, 2-4; G. Reeske, A. H. Cowley, *Chem. Commun.* **2006**, 4856-4858; I. Vidyaratne, J. Scott, S. Gambarotta, P. H. M. Budzelaar, *Inorg. Chem.* **2007**, *46*, 7040-7049; I. Vidyaratne, J. Scott, S. Gambarotta, R. Duchateau, *Organomet.* **2007**, *26*, 3201-3211; J. Scott, I. Vidyaratne, I. Korobkov, S. Gambarotta, P. H. M. Budzelaar, *Inorg. Chem.* **2008**, *47*, 896-911; A. C. Bowman, C. Milsmann, C. C. H. Atienza, E. Lobkovsky, K. Wieghardt, P. J. Chirik, *J. Am. Chem. Soc.* **2010**, *132*, 1676-1684.

[240] H. Sugiyama, I. Korobkov, S. Gambarotta, A. Moller, P. H. M. Budzelaar, *Inorg. Chem.* **2004**, *43*, 5771-5779.

[241] M. Bruce, V. C. Gibson, C. Redshaw, G. A. Solan, A. J. P. White, D. J. Williams, *Chem. Commun.* **1998**, 2523-2524; G. K. B. Clentsmith, V. C. Gibson, P. B. Hitchcock, B. S. Kimberley, C. W. Rees, *Chem. Commun.* **2002**, 1498-1499; J. Scott, S. Gambarotta, I. Korobkov, P. H. M. Budzelaar, *J. Am. Chem. Soc.* **2005**, *127*, 13019-13029; I. Fernandez, R. J. Trovitch, E. Lobkovsky, P. J. Chirik, *Organomet.* **2008**, *27*, 109-118; M. Gallagher, N. L. Wieder, V. K. Dioumaev, P. J. Carroll, D. H. Berry, *Organomet.* **2010**, *29*, 591-603; N. L. Wieder, M. Gallagher, P. J. Carroll, D. H. Berry, *J. Am. Chem. Soc.* **2010**, *132*, 4107-4109.

[242] I. J. Blackmore, V. C. Gibson, P. B. Hitchcock, C. W. Rees, D. J. Williams, A. J. P. White, *J. Am. Chem. Soc.* **2005**, *127*, 6012-6020.

[243] Q. Knijnenburg, J. M. M. Smits, P. H. M. Budzelaar, *Organomet.* **2006**, *25*, 1036-1046.

[244] D. Reardon, F. Conan, S. Gambarotta, G. Yap, Q. Y. Wang, *J. Am. Chem. Soc.* **1999**, *121*, 9318-9325.

[245] I. Khorobkov, S. Gambarotta, G. P. A. Yap, P. H. M. Budzelaar, *Organomet.* **2002**, *21*, 3088-3090.

[246] N. Kleigrewe, W. Steffen, T. Blomker, G. Kehr, R. Frohlich, B. Wibbeling, G. Erker, J. C. Wasilke, G. Wu, G. C. Bazan, *J. Am. Chem. Soc.* **2005**, *127*, 13955-13968.

[247] D. J. Nielsen, K. J. Cavell, B. W. Skelton, A. H. White, *Inorg. Chim. Acta* **2002**, *327*, 116-125; M. Poyatos, J. A. Mata, E. Falomir, R. H. Crabtree, E. Peris, *Organomet.* **2003**, *22*, 1110-1114.

[248] G. Desimoni, G. Faita, P. Quadrelli, *Chem. Rev.* **2003**, *103*, 3119-3154; L. Q. Zhong, R. R. Tang, Q. Yang, *Prog. Chem.* **2007**, *19*, 902-910; P. K. Singh, V. K. Singh, *Pure Appl. Chem.* **2010**, *82*, 1845-1853.

[249] M. Dvolaitzky, *C. R. Séances Acad. Sci. Ser. C: Sci. Chim.* **1969**, *268*, 1811-1813.

[250] A. Paulovicova, U. El-Ayaan, K. Shibayama, T. Morita, Y. Fukuda, *Eur. J. Inorg. Chem.* **2001**, 2641-2646; F. Ragaini, S. Cenini, S. Tollari, G. Tummolillo, R. Beltrami, *Organomet.* **1999**, *18*, 928-942; F. Ragaini, S. Cenini, E. Borsani, M. Dompe, E. Gallo, M. Moret, *Organomet.* **2001**, *20*, 3390-3398; A. Paulovicova, U. El-Ayaan, K. Umezawa, C. Vithana, Y. Ohashi, Y. Fukuda, *Inorg. Chim. Acta* **2002**, *339*, 209-214; M. Gasperini, F. Ragaini, S. Cenini, *Organomet.* **2002**, *21*, 2950-2957; U. El-Ayaan, A. Paulovicova, Y. Fukuda, *J. Molec. Struc.* **2003**, *645*, 205-212; M. Gasperini, F. Ragaini, *Organomet.* **2004**, *23*, 995-1001; M. Gasperini, F. Ragaini, E. Gazzola, A. Caselli, P. Macchi, *Dalton Trans.* **2004**, 3376-3382; F. Ragaini, S. Cenini, F. Turra, A. Caselli, *Tetrahedron* **2004**, *60*, 4989-4994; D. N. Coventry, A. S. Batsanov, A. E. Goeta, J. A. K. Howard, T. B. Marder, *Polyhedron* **2004**, *23*, 2789-2795; U. El-Ayaan, A. A. M. Abdel-Aziz, *Eur. J. Med. Chem.* **2005**, *40*, 1214-1221; F. Ragaini, M. Gasperini, P. Parma, E. Gallo, N. Casati, P. Macchi, *New J. Chem.* **2006**, *30*, 1046-1057; M. M. Khusniyarov, K. Harms, O. Burghaus, J. Sundermeyer, *Eur.*

J. Inorg. Chem. **2006**, 2985-2996; I. L. Fedushkin, A. A. Skatova, S. Y. Ketkov, O. V. Eremenko, A. V. Piskunov, G. K. Fukin, *Angew. Chem. - Int. Ed.* **2007**, *46*, 4302-4305; I. L. Fedushkin, V. M. Makarov, V. G. Sokolov, G. K. Fukin, *Dalton Trans.* **2009**, 8047-8053; I. L. Fedushkin, O. V. Eremenko, A. A. Skatova, A. V. Piskunov, G. K. Fukin, S. Y. Ketkov, E. Irran, H. Schumann, *Organomet.* **2009**, *28*, 3863-3868.

[251] U. El-Ayaan, A. Paulovicova, S. Yamada, Y. Fukuda, *J. Coord. Chem.* **2003**, *56*, 373-381.

[252] R. Vanasselt, C. J. Elsevier, *Organomet.* **1992**, *11*, 1999-2001; R. Vanasselt, C. J. Elsevier, *Tetrahedron* **1994**, *50*, 323-334; R. Vanasselt, C. J. Elsevier, W. J. J. Smeets, A. L. Spek, *Inorg. Chem.* **1994**, *33*, 1521-1531; R. Vanasselt, K. Vrieze, C. J. Elsevier, *J. Organomet. Chem.* **1994**, *480*, 27-40; C. J. Elsevier, *Coord. Chem. Rev.* **1999**, *185-6*, 809-822; J. W. Sprengers, M. de Greef, M. A. Duin, C. J. Elsevier, *Eur. J. Inorg. Chem.* **2003**, 3811-3819; A. M. Kluwer, T. S. Koblenz, T. Jonischkeit, K. Woelk, C. J. Elsevier, *J. Am. Chem. Soc.* **2005**, *127*, 15470-15480; H. Guo, Z. L. Zheng, F. Yu, S. M. Ma, A. Holuigue, D. S. Tromp, C. J. Elsevier, Y. H. Yu, *Angew. Chem. - Int. Ed.* **2006**, *45*, 4997-5000; A. Scarel, M. R. Axet, F. Amoroso, F. Ragaini, C. J. Elsevier, A. Holuigue, C. Carfagna, L. Mosca, B. Milani, *Organomet.* **2008**, *27*, 1486-1494.

[253] C. M. Killian, D. J. Tempel, L. K. Johnson, M. Brookhart, *J. Am. Chem. Soc.* **1996**, *118*, 11664-11665; C. M. Killian, L. K. Johnson, M. Brookhart, *Organomet.* **1997**, *16*, 2005-2007; S. Mecking, L. K. Johnson, L. Wang, M. Brookhart, *J. Am. Chem. Soc.* **1998**, *120*, 888-899; S. A. Svejda, M. Brookhart, *Organomet.* **1999**, *18*, 65-74; D. J. Tempel, L. K. Johnson, R. L. Huff, P. S. White, M. Brookhart, *J. Am. Chem. Soc.* **2000**, *122*, 6686-6700; A. C. Gottfried, M. Brookhart, *Macromol.* **2001**, *34*, 1140-1142; A. C. Gottfried, M. Brookhart, *Macromol.* **2003**, *36*, 3085-3100; M. D. Leatherman, S. A. Svejda, L. K. Johnson, M. Brookhart, *J. Am. Chem. Soc.* **2003**, *125*, 3068-3081; W. J. Liu, M. Brookhart, *Organomet.* **2004**, *23*, 6099-6107; M. Shiotsuki, P. S. White, M. Brookhart, J. L. Templeton, *J. Am. Chem. Soc.* **2007**, *129*, 4058-4067.

[254] A. E. Cherian, J. M. Rose, E. B. Lobkovsky, G. W. Coates, *J. Am. Chem. Soc.* **2005**, *127*, 13770-13771; J. M. Rose, A. E. Cherian, G. W. Coates, *J. Am. Chem. Soc.* **2006**, *128*, 4186-4187; J. M. Rose, F. Deplace, N. A. Lynd, Z. G. Wang, A.

Hotta, E. B. Lobkovsky, E. J. Kramer, G. W. Coates, *Macromol.* **2008**, *41*, 9548-9555.

[255] I. L. Fedushkin, A. A. Skatova, V. A. Chudakova, V. K. Cherkasov, G. K. Fukin, M. A. Lopatin, *Eur. J. Inorg. Chem.* **2004**, 388-393.

[256] L. L. Fedushkin, N. M. Khvoinova, A. V. Piskunov, G. K. Fukin, M. Hummert, H. Schumann, *Russ. Chem. Bull.* **2006**, *55*, 722-730.

[257] K. V. Vasudevan, I. Vargas-Baca, A. H. Cowley, *Angew. Chem. - Int. Ed.* **2009**, *48*, 8369-8371.

[258] I. L. Fedushkin, V. A. Chudakova, A. A. Skatova, G. K. Fukin, *Heteroat. Chem.* **2005**, *16*, 663-670.

[259] I. L. Fedushkin, A. A. Skatova, V. A. Chudakova, G. K. Fukin, S. Dechert, H. Schumann, *Eur. J. Inorg. Chem.* **2003**, 3336-3346; I. L. Fedushkin, V. A. Chudakova, A. A. Skatova, N. M. Khvoinova, Y. A. Kurskii, T. A. Glukhova, G. K. Fukin, S. Dechert, M. Hummert, H. Schumann, *Zeit. Anorg. Allg. Chem.* **2004**, *630*, 501-507.

[260] I. L. Fedushkin, A. A. Skatova, V. A. Chudakova, V. K. Cherkasov, S. Dechert, H. Schumann, *Russ. Chem. Bull.* **2004**, *53*, 2142-2147.

[261] H. Schumann, M. Hummert, A. N. Lukoyanov, V. A. Chudakova, I. L. Fedushkin, *Zeit. Naturforsch. Sect. B-a J. Chem. Sci.* **2007**, *62*, 1107-1111.

[262] I. L. Fedushkin, A. G. Morozov, M. Hummert, H. Schumann, *Eur. J. Inorg. Chem.* **2008**, 1584-1588; I. L. Fedushkin, A. G. Morozov, V. A. Chudakova, G. K. Fukin, V. K. Cherkasov, *Eur. J. Inorg. Chem.* **2009**, 4995-5003.

[263] I. L. Fedushkin, A. S. Nikipelov, A. A. Skatova, O. V. Maslova, A. N. Lukoyanov, G. K. Fukin, A. V. Cherkasov, *Eur. J. Inorg. Chem.* **2009**, 3742-3749.

[264] I. L. Fedushkin, N. M. Khvoinova, A. Y. Baurin, G. K. Fukin, V. K. Cherkasov, M. P. Bubnov, *Inorg. Chem.* **2004**, *43*, 7807-7815; I. L. Fedushkin, A. A. Skatova, V. A. Chudakova, N. M. Khvoinova, A. Y. Baurin, S. Deckert, M. Hummert, H. Schumann, *Organomet.* **2004**, *23*, 3714-3718; R. J. Baker, C. Jones, M. Kloth, D. P. Mills, *New J. Chem.* **2004**, *28*, 207-213; H. Schumann, M. Hummert, A. N. Lukoyanov, I. L. Fedushkin, *Organomet.* **2005**, *24*, 3891-3896; I. L. Fedushkin, N. M. Khvoinova, A. Y. Baurin, V. A. Chudakova, A. A. Skatova, V. K. Cherkasov, G. K. Fukin, E. V. Baranov, *Russ. Chem. Bull.* **2006**, *55*, 74-83; N. J. Hill, G. Reeske, J. A. Moore, A. H. Cowley, *Dalton Trans.* **2006**,

4838-4844; H. Schumann, M. Hummert, A. N. Lukoyanov, I. L. Fedushkin, *Chem. Eur. J.* **2007**, *13*, 4216-4222; I. L. Fedushkin, A. N. Lukoyanov, S. Y. Ketkov, M. Hummert, H. Schumann, *Chem. Eur. J.* **2007**, *13*, 7050-7056; I. L. Fedushkin, A. N. Lukoyanov, M. Hummert, H. Schumann, *Zeit. Anorg. Allg. Chem.* **2008**, *634*, 357-361; I. L. Fedushkin, A. N. Lukoyanov, A. N. Tishkina, G. K. Fukin, K. A. Lyssenko, M. Hummert, *Chem. Eur. J.* **2010**, *16*, 7563-7571.

[265] I. L. Fedushkin, O. V. Maslova, E. V. Baranov, A. S. Shavyrin, *Inorg. Chem.* **2009**, *48*, 2355-2357; K. Vasudevan, A. H. Cowley, *Chem. Commun.* **2007**, 3464-3466.

[266] I. L. Fedushkin, A. A. Skatova, V. K. Cherkasov, V. A. Chudakova, S. Dechert, M. Hummert, H. Schumann, *Chem. Eur. J.* **2003**, *9*, 5778-5783.

[267] I. L. Fedushkin, A. A. Skatova, A. N. Lukoyanova, V. A. Chudakova, S. Dechert, M. Hummert, H. Schumann, *Russ. Chem. Bull.* **2004**, *53*, 2751-2762.

[268] I. L. Fedushkin, A. A. Skatova, G. K. Fukin, M. Hummert, H. Schumann, *Eur. J. Inorg. Chem.* **2005**, 2332-2338.

[269] I. L. Fedushkin, N. M. Khvoinova, A. A. Skatova, G. K. Fukin, *Angew. Chem. - Int. Ed.* **2003**, *42*, 5223-5226.

[270] I. L. Fedushkin, A. G. Morozov, O. V. Rassadin, G. K. Fukin, *Chem. Eur. J.* **2005**, *11*, 5749-5757.

[271] I. L. Fedushkin, V. M. Makarov, E. C. E. Rosenthal, G. K. Fukin, *Eur. J. Inorg. Chem.* **2006**, 827-832.

[272] I. L. Fedushkin, M. Hummert, H. Schumann, *Eur. J. Inorg. Chem.* **2006**, 3266-3273.

[273] A. N. Tishkina, A. N. Lukoyanov, A. G. Morozov, G. K. Fukin, K. A. Lyssenko, I. L. Fedushkin, *Russ. Chem. Bull., Int. Ed.* **2009**, *58*, 2250-2257.

[274] M. R. Crimmin, A. G. M. Barrett, M. S. Hill, P. B. Hitchcock, P. A. Procopiou, *Inorg. Chem.* **2007**, *46*, 10410-10415; M. Gartner, R. Fischer, J. Langer, H. Gorls, D. Walther, M. Westerhausen, *Inorg. Chem.* **2007**, 5118-5124.

[275] S. Harder, *Organomet.* **2002**, *21*, 3782-3787.

[276] A. E. Cherian, E. B. Lobkovsky, G. W. Coates, *Chem. Commun.* **2003**, 2566-2567; A. E. Cherian, G. J. Domski, J. M. Rose, E. B. Lobkovsky, G. W. Coates, *Org. Lett.* **2005**, *7*, 5135-5137.

[277] M. Hagar, F. Ragaini, E. Monticelli, A. Caselli, P. Macchi, N. Casati, *Chem. Commun.* **2010**, *46*, 6153-6155.

[278] K. C. Jantunen, B. L. Scott, P. J. Hay, J. C. Gordon, J. L. Kiplinger, *J. Am. Chem. Soc.* **2006**, *128*, 6322-6323; J. D. Masuda, K. C. Jantunen, B. L. Scott, J. L. Kiplinger, *Organomet.* **2008**, *27*, 803-806.

[279] P. Jochmann, T. S. Dols, T. P. Spaniol, L. Perrin, L. Maron, J. Okuda, *Angew Chem Int Ed Engl* **2010**, *49*, 7795-7798.

[280] M. S. Hill, D. J. MacDougall, M. F. Mahon, *Dalton Trans* **2010**, *39*, 11129-11131.

[281] Z. Otwinowski, W. Minor, *Processing of X-ray Diffraction Data Collected in Oscillation Mode.* **1997**, *Methods in Enzymology, Vol. 276, Macromolecular Crystallography, part A*, Carter, C. W., Jr., Sweet, R. M., Eds.; Academic Press: New York, 1307-1326.

[282] L. J. Farrugia, *J. Appl. Cryst.* **1999**, *32*, 837-838.

[283] M. A. Mathur, G. E. Ryschkewitsch, B. F. Swicker, F. S. C., J. C. Carter, *Inorg. Synth.* **1975**, *12*, 118-126.

[284] M. A. Mathur, D. A. Moore, R. E. Popham, H. H. Sisler, *Inorg. Synth.* **1992**, *29*, 51-107.

[285] W. Haubold, J. Herdtle, W. Gollinger, W. Einholz, *J. Organomet. Chem.* **1986**, *315*, 1-8.

[286] R. Q. Fan, D. S. Zhu, Y. Mu, G. H. Li, Y. L. Yang, Q. Su, S. H. Feng, *Eur. J. Inorg. Chem.* **2004**, 4891-4897.

[287] G. Lente, I. Fabian, A. J. Poe, *New J. Chem.* **2005**, *29*, 759-760.

[288] M. Veith, Barnigha.H, *Acta Cryst. Sect. B- Struc. Sci.* **1974**, *B 30*, 1806-1813.